

STUDY OF POLY(PHENYLENE ETHYNYLENE)S, DENDRITIC QUENCHERS,
AND MOLECULAR BEACONS TOWARDS THE APPLICATION OF A
POLY(PHENYLENE ETHYNYLENE)-BASED BIOSENSOR

by

GHISLAINE CAROLINE BAILEY

B. Sc. Honours Chemistry
McGill University, 2000

Submitted to the Department of Chemistry
in Partial Fulfillment of the Requirements for the Degree of

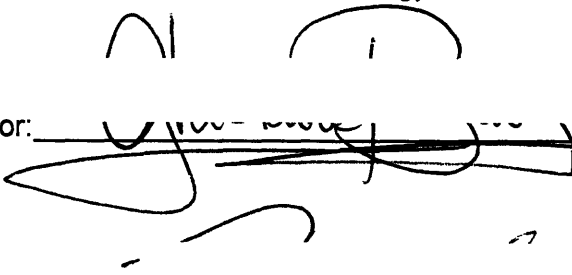
DOCTOR OF PHILOSOPHY

at the

MASSACHUSETTS INSTITUTE OF TECHNOLOGY

February, 2007

© Massachusetts Institute of Technology, 2006. All rights reserved.

Signature of Author: 

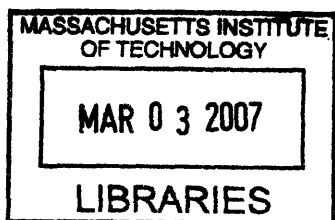
Department of Chemistry
September 7, 2006

Certified by: 

Timothy M. Swager
Professor of Chemistry
Thesis Supervisor


Accepted by: _____

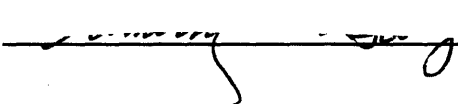
Robert W. Field
Chairman, Departmental Committee on Graduate Studies

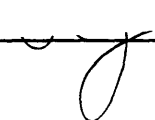


ARCHIVES

This doctoral thesis has been examined by a Committee of the Department of Chemistry as follows:

Professor Barbara Imperiali:  _____ Thesis Chair

Professor Timothy M. Swager:  _____ Thesis Supervisor

Professor Timothy F. Jamison:  _____

*dedicated to my family
for their unwavering support, patience, and above all, love*

*first and foremost,
my parents,*

Raja and Mark Bailey,

my sisters,

Nawel and Soraya Bailey

my husband,

Curtis Berlinguette

STUDY OF POLY(PHENYLENE ETHYNYLENE)S, DENDRITIC QUENCHERS, AND
MOLECULAR BEACONS TOWARDS THE APPLICATION OF A POLY(PHENYLENE
ETHYNYLENE)-BASED BIOSENSOR

By

Ghislaine Caroline Bailey

Submitted to the Department of Chemistry on September 7, 2006 in
Partial Fulfillment of the Requirements for the Degree of
Doctor of Philosophy in Chemistry

ABSTRACT

Poly(*para*-phenylene ethynylene)s (PPE)s are highly emissive conjugated polymers that are easily quenched by target analytes. As a result, they have been increasingly incorporated into sensing platforms, both as chemosensors and as biosensors. This thesis describes the three components necessary for a MB-based PPE biosensor, as well as preliminary work towards assembly of the components. A sensor system composed of three parts is presented: (1) a PPE with masked pendent maleimide groups for bioconjugation, (2) a dendritic quencher (DQ) that will be crucial for signal transduction, and (3) a DNA sequence known as a molecular beacon (MB) selective for *Escherichia coli* O157:H7.

In order to continue expanding the scope of PPEs in sensor applications, new handles are required with which to manipulate the polymers. These handles should be designed so as to tether small molecules, cross-linkers, and biomolecules, such as DNA, to the polymer. To this end, a PPE containing pendent maleimide units has been designed and synthesized. The maleimide group was protected as the Diels-Alder adduct with furan to prevent the maleimide from interfering with polymer synthesis. The maleimide group was then revealed post-polymerization under relatively mild thermal conditions and monitored using thermogravimetric analysis. The ability of this group to bind compounds to the polymer was investigated using a thiol-containing dye.

A family of dendritic quenchers (DQs) was designed and prepared. The quenching properties of these compounds were investigated, both in aqueous buffers and in DMF, as well as with PPE-coated microspheres. With the microspheres, amplified quenching was observed with increasing DQ generation.

In collaboration with the US Army Solider Systems Center (Natick, MA), a MB sequence selective for *E. coli* O157:H7 was designed. The performance of the MB in buffers, its melting profile, and its selectivity for *E. coli* targets was investigated.

Thesis Supervisor: Timothy M. Swager
Title: Professor of Chemistry

TABLE OF CONTENTS

LIST OF ABBREVIATIONS	8
LIST OF FIGURES	10
LIST OF SCHEMES	13
LIST OF TABLES	15
CHAPTER 1: INTRODUCTION	16
1.1 Introduction to Sensors	17
1.2 Sensor Design	19
1.3 Conjugated Polymers	22
1.4 Conjugated Polymer Sensors	24
1.5 Synthesis of Conjugated Polymers	27
1.6 Fluorescence and Energy Transfer	28
1.7 Fluorescence Quenching	32
1.8 Conclusion	33
1.9 References	34
CHAPTER 2: MASKED MICHAEL ACCEPTORS IN POLY(<i>p</i>-PHENYLENEETHYNYLENE)S	40
2.1 Introduction	41
2.2 Synthesis of Masked-Maleimide Containing Polymer	42
2.3 Removing the Mask	47
2.4 Application of Revealed Maleimide as Tethering Point	50
2.5 Further Exploration of Applications – Use of Maleimide Group for Crosslinking	54
2.6 Conclusion and Discussion	57
2.7 Experimental	58

2.8 References	84
CHAPTER 3: DENDRITIC QUENCHERS	87
3.1 Introduction	88
3.2 Dendritic Quencher Synthesis	89
3.2.1 PAMAM Dendrimers	89
3.2.2 DQ Core with Peptide Linkages	95
3.3. Quenching Effects of DQ on Solution and Solid-state PPEs	101
3.3.1 DQ Extinction Coefficients	101
3.3.2 Quenching Studies in Solution	101
3.3.3 Quenching of PPE-Coated Microspheres	106
3.4 Discussion	107
3.5 Conclusion	108
3.6 Experimental Section	109
3.7 References	130
CHAPTER 4: MOLECULAR BEACON SEQUENCE AND PROPERTIES	135
4.1 Brief Introduction to DNA	136
4.2 Molecular Beacons	137
4.3 Molecular Beacon Sequence	140
4.3.1 Conjugating MBs Using Terminal Amine Groups	143
4.3.2 Complement Sequences for Ecmb	144
4.4 Determination of Optimal Hybridization Conditions for MB	145
4.4.1 Buffer Selection	145
4.4.2 MB Response Without Prior Annealing Cycle	150
4.5 Detection Limit of MJ Opticon Real Time PCR Instrument	152
4.6 Conclusions	153
4.7 Experimental	154
4.7.1 Buffer Selection	154
4.7.3 Detection Limit of MJ Opticon Real Time PCR	155
4.8 References	156

CHAPTER 5: INITIAL EXPLORATIONS INTO CONJUGATING DNA TO PPEs	159
5.1 Introduction	160
5.2 Coupling DNA to Carboxylic Acid-PPEs	160
5.2.1 Determination of Extinction Coefficients for P-7 and EcmbT	161
5.2.2 Coupling Conditions	163
5.2.3 Determination of DNA Loading	167
5.3 New Approach to Conjugating DNA to PPEs	171
5.3.1 Preparation and Application of Furan-Containing Beads	173
5.3.2 Interaction of EcmbT3 and B-3	181
5.3.3 Solid-phase Conjugation of EcmbT3 onto P-8	181
5.4 Conclusion	184
5.5 Experimental	185
5.6 References	190
Curriculum Vitae	192
Acknowledgment	194
Appendix 1: NMR Spectra for Chapter 2	197
Appendix 2: NMR Spectra for Chapter 3	218

List of Abbreviations

56FAM	5-(and-6)-carboxyfluorescein
A	acceptor
aCHC	a-cyano-4-hydroxy cinnamic acid
BHQ1	black hole quencher 1
D	donor
DABCYL	4-dimethylamino)phenylazo)benzoic acid
DHB	2,5-dihydroxybenzoic acid
DMF	dimethylformamide
DNA	deoxyribonucleic acid
DNP	dinitrophenyl
DP	degree of polymerization
DQ	dendritic quencher
DTT	dithiothreitol
E. coli	Escherichia coli
Ecmb	E. coli molecular beacon
EDAC	N-(3-Dimethylaminopropyl)-N_-ethylcarbodiimide hydrochloride
FRET	fluorescence energy transfer
FTIR	Fourier-transform infra-red spectroscopy
GPC	gel permeation chromatography
HABA	2-(4'-hydroxyphenylazobenzoic acid)
HBTU	O-(Benzotriazol-1-yl)-N,N,N_,N_-tetramethyluronium hexafluorophosphate
HMDS	hexamethyl disilazane
HOBt	1-Hydroxybenzotriazole
HOMO	highest occupied molecular orbital
HPLC	high performance liquid chromatography
LUMO	lowest unoccupied molecular orbital
MALDI-ToF	matrix-assisted laser desorption ionization time of flight mass spectroscopy
MB	molecular beacon
MeOH	methanol
MES	4-morpholineethanesulfonic acid
Mn	number-average molecular weight
MWCO	molecular weight cut-off
NHS	N-hydroxysuccinimide
NMM	N-methylmorpholine
NMP	1-Methyl-2-pyrrolidinone
NMR	nuclear magnetic resonance spectroscopy
PAMAM	polyamidoamine dendrimer
PCR	polymerase chain reaction, also buffer for polymerase chain reaction
PEG	polyethylene glycol

PNA	peptide nucleic acid
PPE	poly(phenylene ethynylene)
PPV	poly(phenylene vinylene)
RET	resonance energy transfer
RNA	ribonucleic acid
ROX	carboxy-X-rhodamine
ROX,SE	carboxy-X-rhodamine, succinimidyl ester
TBS	Tris buffered saline
TGA	thermal gravimetric analysis
TGA-MS	thermal gravimetric analysis-mas spectroscopy
THF	tetrahydrofuran
TNT	trinitrotoluene
Tris	Triethanolamine hydrochloride
UV/Vis	ultra-violet and visible spectroscopy

List of Figures

CHAPTER 1

- Figure 1** Sensor design: A PPE modified with a MB - DQ complex would be in an “off” state in the absence of any target DNA. In the presence of a complementary strand, the loop would be opened removing the quencher from the PPE, thereby turning “on” fluorescence. _____ 20
- Figure 2** Absorption of a photon in a small molecule results in an electron being promoted from the HOMO to the LUMO. In a conjugated polymer, absorption of a photon results in electron-hole pair being formed with the electron in the conduction band and the hole in the valence band. _____ 24
- Figure 3** Top, A turn-off sensor: excitons are quenched through electron transfer to an acceptor resulting in amplified quenching. Bottom, A turn-off sensor: selective recombination of excitons occur at local minima introduced by the analyte, leading to emission of red-shifted light and amplified wavelength shifts. _____ 26
- Figure 4** Jablonski energy diagram. _____ 30

CHAPTER 2

- Figure 1** A: TGA-MS for 7b; monitoring at 68 for furan and at 39 for a known furan fragment. (Ramp rate: 5°C/min to 300°C.) B: Thermogravimetric analysis for P-1, P-3, and 12a. (Ramp rate: 0.1°C/min to 300°C.) _____ 49
- Figure 2** (A) Normalized absorbance and emission spectra for P-5 after exposure in THF to thiolated-ROX dye, 15 with excitation at both 410 and 500 nm. (B) Normalized GPC trace for polymers P-2 and P-5, monitoring at 410 nm and 570 nm (absorption at 570 nm scaled 75×). _____ 54

CHAPTER 3

- Figure 1** MALDI-ToF spectrum for G0-3Q in DHB-Fucose. _____ 94
- Figure 2** Stern-Volmer quenching constants obtained in Tris, TBS, PCR (G0 and G1 only) and DMF for G0, G1₂, G1₃, G2₄, and G2₆ grouped by quencher. 104
- Figure 3** Stern-Volmer quenching constants obtained in Tris, TBS, PCR (G0 and G1 only) and DMF for G0, G1₂, G1₃, G2₄, and G2₆ grouped by buffer/solvent. _____ 105
- Figure 4** Quenching with DQ of PPE-coated microspheres. _____ 107

CHAPTER 4

- Figure 1** Molecular beacon response to the presence of complementary target. _____ 138
- Figure 2** Typical molecular beacon melting profile. _____ 140
- Figure 3** Normalized absorbance spectra for the modified Ecmb sequences and P-7. _____ 143
- Figure 4** The fluorescence response of EcmbT2 in the presence of the true complement CompEcmb (Avg C) and no complement (Avg No Comp) in buffers P1, P2, and P3 are plotted. The sample was first heated to 90 °C, the fluorescence data were then collected over the first cooling ramp (decreasing temperature) and then over a second heating ramp (increasing temperature). _____ 147
- Figure 5** The fluorescence response of EcmbT2 in the presence of the true complement CompEcmb (Avg C) and the complement sequence with one mismatch Ecmb1mm (Avg 1mm) in buffers P1, P2, and P3 are plotted. The sample was first heated to 90 °C, the fluorescence data were then collected over the first cooling ramp (decreasing temperature) and then over the second heating ramp (increasing temperature). **Error! Bookmark not defined.**
- Figure 6** The fluorescence response of EcmbT2 in the presence of the true complement CompEcmb (Avg C) and a complement with two mismatches Ecmb2mm (Avg 2mm) in buffers P1, P2, and P3 are plotted. The sample was first heated to 90 °C, the fluorescence data were collected on the first cooling ramp (decreasing temperature) and then over a second heating ramp (increasing temperature). _____ 149
- Figure 7** The fluorescence response of EcmbT2 in the presence of the true complement CompEcmb (Avg C) and the completely scrambled sequence EcmbSc (Avg Sc) in buffers P1, P2, and P3 are plotted. The sample was first heated to 90 °C, the fluorescence data were then collected over the first cooling ramp (decreasing temperature) and then over the second heating ramp (increasing temperature). _____ 150
- Figure 8** The response of the MB EcmbT2 to CompEcmb, Ecmb1mm, Ecmb2mm, and EcmbSc without an initial annealing step. The background response of a blank sample composed of P1 buffer is included for comparison. _____ 151
- Figure 9** The response of 50 nM EcmbT2 to CompEcmb with concentrations varying from 300 nM to 500 pM are plotted over a heating and then cooling cycle, without a prior annealing cycle. _____ 152

CHAPTER 5

- Figure 1** (A) Absorption spectra of aliquots of EcmbT added to P1 buffer. (B) Determination of ϵ_{548} for the Cy3 dye on EcmbT. Error! Bookmark not defined.
- Figure 2** Determination of ϵ_{460} for **P-7**. _____ 163
- Figure 3** Absorbance and fluorescence spectra obtained for Experiments 7-9, 11, 13, 15, and 16, with excitation of the polymer at 460 nm and the dye at 540 nm. _____ 168
- Figure 4** The binding and subsequent release of Rhodamine Red C2 maleimide from **B-3** by a retro-Diels-Alder mechanism. _____ 176
- Figure 5** The binding and subsequent release of **P-8** maleimide from **B-3**. Heating the beads and **P-8** results in yellow beads and a colourless solution. In the presence of the unfunctionalized silica, labeled Bromo silica, **P-8** remains largely in solution. Heating the **B-3/P-8** beads releases the polymer into solution. _____ 178
- Figure 6** FTIR for **B-3** and **P-8** (KBr pellets). (A) Beads **B-3** (black) and the bromo silica (green); (B) Polymer **P-8**; (C) Result from control reaction of bromo-silica and **P-8**; (D) Result from reaction of **B-3** and **P-8**. _____ 180
- Figure 7** (A)-(C) Fluorescence results for Exp 1-3 with excitation of both the polymer at 410 nm and the dye at 530 nm. Inset: Dye fluorescence upon direct excitation at 530 nm. _____ 183

List of Schemes

CHAPTER 1

Scheme 1 Common conjugated polymers. _____ 22

Scheme 2 Palladium catalyzed cross-coupling mechanism for the production of PPEs. _____ 28

CHAPTER 2

Scheme 1 (A): (a) K_2CO_3 , RBr, acetone; (b) I_2 , KIO_3 , H_2SO_4 , AcOH, H_2O ; (c) *t*-BuSH, NaH, DMF; (d) K_2CO_3 , $BrCH_2(CH_2)_nCH_2Br$, acetone; (e) K_2CO_3 , acetone. For synthesis of **6** please see Section 2.8 Experimental. (B): (f) I_2 , KIO_3 , H_2SO_4 , AcOH, H_2O ; (g) BBr_3 , CH_2Cl_2 , $-78^\circ C$, quench with water; (h) 1 eq. NaH, DMF, ROTs; (i) 1,3-dibromopropane, K_2CO_3 , refluxing acetone; (j) K_2CO_3 , DMF. (C): (k) Catalytic $Pd(PPh_3)_4$ and CuI, toluene, diisopropylamine, 1-methyl-2-pyrrolidinone, room temperature 5 days, ($M_n=11,000$); (l) Catalytic $Pd(PPh_3)_4$ and CuI, toluene, diisopropylamine, room temperature 7 days ($M_n=8,000$). _____ 45

Scheme 2 (a) $65^\circ C$; (b) 15, DTT, $65^\circ C$. _____ 51

Scheme 3 Preparation of di-furan crosslinker for use with maleimide-PPEs. _ 55

Scheme 4 Removal of the mask and subsequent introduction of the cross-linker. _____ 56

CHAPTER 3

Scheme 1 Synthesis of PAMAM dendrimers. _____ 89

Scheme 2 Modification of terminal amines to DNP groups to form DQ. _____ 90

Scheme 3 Synthesis of **G0-3Q** and structure of **G1-7Q**. _____ 93

Scheme 4 New DQ family: Structures of **G0**, **G1₂**, **G1₃**, **G2₄**, **G2₆**, and **G2₉**. ___ 96

Scheme 5 Preparation of linking and quenching branches, as well as the preparation of **G0**. _____ 98

Scheme 6 Preparation of branching compounds and first generation DQ. ___ 99

Scheme 7 Preparation of second generation DQ. _____ 100

Scheme 8 Carboxylic acid-PPE, P-7. _____	102
---	------------

CHAPTER 4

Scheme 1 (A) Building a nucleotide from a sugar. (B) The four DNA bases. (C) The DNA polymer. (D) Hydrogen bonding between bases in DNA. _____	137
---	------------

Scheme 2 Structures of DNA labels and modifications. _____	142
---	------------

Scheme 3 Tethering of amine containing molecules, in this case DNA, to a carboxy-PPE via activation with EDAC/NHS. _____	144
---	------------

CHAPTER 5

Scheme 1 Initial activation of carboxylic acid groups with NHS and EDAC, followed by coupling of an amine-containing compound. _____	161
---	------------

Scheme 2 Conjugation of EcmbT to P-7. _____	164
--	------------

Scheme 3 Synthesis of P-8. _____	172
---	------------

Scheme 4 Immobilization of P-8 on a furan-bead, followed by DNA conjugation and removal of the DNA-P-8 conjugate under thermal conditions. _____	173
---	------------

Scheme 5 Preparation of furan-containing beads. _____	174
--	------------

Scheme 6 Structure of Rhodamine Red C2 maleimide. _____	174
--	------------

Scheme 7 Preparation of a furan-containing silica bead. _____	175
--	------------

List of Tables

CHAPTER 3

Table 1 Extinction values determined for DQ in DMF at 357 nm. _____ 101

Table 2 Quenching constants obtained in solution for DQ family. _____ 106

CHAPTER 4

Table 1 MB sequences and melting temperatures.^a _____ 142

Table 2 Absorbance and emission maxima for dyes used with Ecmb. _____ 143

Table 3 Complementary target sequences and melting temperatures.^a _____ 145

CHAPTER 5

Table 1 Experimental conditions that were explored using EDAC/NHS as activating agents and dialysis for purification. _____ 166

Table 2 Ratio of DNA to P-7 repeat units. _____ 170

Table 3 Reaction matrix for the solid-phase conjugation of EcmbT3 to P-8. _ 182

Chapter 1:
Introduction

1.1 Introduction to Sensors

From their very first days, children are taught about their five senses: sight, smell, taste, touch, and hearing. These senses give us our bearings in relation to the physical world around us. In addition, they provide basic and vital information that keeps our bodies safe from harm, from the bitter taste of poisonous plants to the burning heat of boiling water. Our sense of smell is quite sensitive and can discriminate volatile compounds with great accuracy,¹ and in some cases in the parts per trillion levels, as with *tert*-butyl mercaptan, the tracer used in natural gas.

The advantage of our senses is their accurate response in real-time. Their disadvantage is that they are quite limited in scope and ability. The world today contains risks and dangers that our senses are not equipped to detect, such as explosives in buried landmines or bacterial contamination in drinking water. In order to properly protect ourselves from these dangers, and a multitude of others, we have had to design and develop a broad range of sensors, including, but not limited to, chemo- and biosensors.

A chemosensor is a device or molecule designed to detect and report a specific analyte, while a biosensor is further defined as either detecting biomolecules or incorporating biomolecules in the detection or transduction components. An ideal chemosensor will bind its target with great specificity and

have little interference, and the binding event must be easily converted to a measurable signal. Artificial or man-made sensors have become increasingly important to the wellbeing of society. These can be designed to sense a range of phenomena from mechanical stress that can result in structure failure in buildings, to particles in a smoke detector. Sensors can be broken down into two elements: a recognition event and a transduction event. A strip of pH paper can be considered the most simple of chemosensors. The dyes coated on the strip change in colour in response to the concentration of protons in a solution, the combination of which allows one to determine the pH. A more elaborate chemosensor is one developed in our group to detect the presence of the explosive trinitrotoluene (TNT).²⁻⁵

Since the first biosensor was developed in 1967 to monitor glucose levels,⁶ a broad range of biosensors with high selectivity and sensitivity has been developed. Biosensors generally involve a bio-recognition event and the corresponding visualization of the event. The bio-recognition event may involve sugars, proteins, antibodies, enzymes, nucleic acids, cell components, and any derivatives thereof. These events can be coupled with any number of transduction mechanisms, including electrochemical, optical, and changes in mass.

In recent years, there has been a veritable explosion in the investigation of and development of biosensors, with reviews available on, but

not limited to, such narrow subjects as biosensors for the environmental monitoring of endocrine disruptors,⁷ for the detection of food and water-borne pathogens,⁸ for the detection of biological warfare agents,⁹ and biosensors that employ solely optical detection mechanisms.¹⁰

1.2 Sensor Design

Our goal is to incorporate a conjugated polymer, and more specifically, a poly(*para*-phenyleneethynylene) (PPE), into a biosensor. The platform is designed to be modular and will combine three components: 1) a PPE as a reporter or transducer; 2) a specially designed DNA strand to recognize the target; and 3) a dendritic quencher that will be responsible for turning on and off the polymer fluorescence (Figure 1). This project will require the design and synthesis of a PPE capable of conjugating biomolecules such as DNA, and could also be used with peptides, antibodies, and enzymes. A dendritic quencher (DQ) will be designed, synthesized, and explored based on a dendrimer core and an outer shell of quenching units, and will be further discussed in Chapter 3. The DNA strand used will be self-complementary, allowing it to fold into a stem-loop or hairpin structure, and is known as a molecular beacon (MB).¹¹ This strand of DNA will be bound to the PPE at one end and modified at the other with the quencher. The loop portion of the molecular beacon will be specific for *Escherichia coli* O157:H7, but can be tailored to any desired toxin. The specific sequence used is described in Chapter 4 and was developed in collaboration

with the US Army Soldier Systems Center (Natick, MA). In the presence of a sequence complementary to the loop portion, the hairpin is opened removing the two ends of the strand from each other, and in this case, the DQ from the PPE.

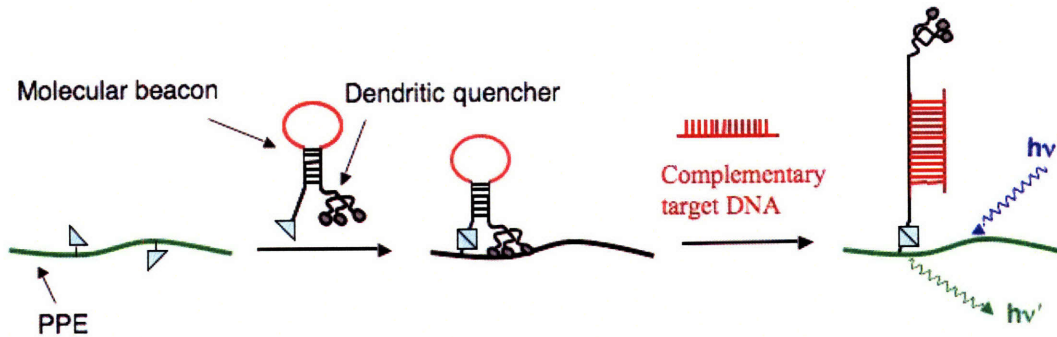


Figure 1 Sensor design: A PPE modified with a MB - DQ complex would be in an “off” state in the absence of any target DNA. In the presence of a complementary strand, the loop would be opened removing the quencher from the PPE, thereby turning “on” fluorescence.

The robustness, selectivity, and reliability of MBs has resulted in their incorporation in a broad range of applications including: quantifying the polymerase chain reaction,¹² determining their sensing ability while immobilized on surfaces,^{13, 14} probing the permeability of DNA across thin films,¹⁵ detecting the human immunodeficiency virus,¹⁶ and measuring DNA and RNA hybridization in living cells.¹⁷

A molecular beacon modified with fluorescein at one terminus and a “superquencher” at the other consisting of three 4-(dimethylamino)phenylazo)benzoic acid (DABCYL) groups was recently

reported.¹⁸ The authors observed an increase in quenching efficiency attributed to two factors: an increase in the overall extinction coefficients of the superquenchers and the increased dipole-dipole interactions between fluorescein and the superquencher. In addition, the stability of the hairpin structure increased, granting greater selectivity in discerning strands with single base pair mismatches.

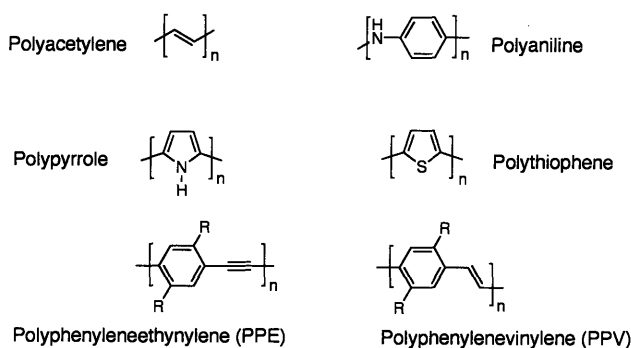
Combining PPEs and DNA into a biosensor has been explored,¹⁹ as has the combination of poly(phenylenevinylene) (PPV) and DNA.²⁰ Most recently, peptide nucleic acids (PNAs) have also been investigated in conjunction with conducting polymers.²¹ In these cases, however, the DNA is not bound to the polymer but the two are brought together through electrostatic interactions or as a result of conformational changes in the DNA, causing a signal to be elicited from the polymer.

A brief introduction to conjugated polymers and their synthesis, conjugated polymer sensors, energy transfer, and quenching is outlined here. Detailed explanations on dendrimers, molecular beacons, and DNA are given in the relevant chapters.

1.3 Conjugated Polymers

Intense interest in the field of conjugated polymers began nearly thirty years ago with the discovery that an organic polymer could conduct electricity as well as a metal.²² Conjugated polymers can now be customized to suit the electrical, mechanical, and optical needs of many applications.^{17, 23} Most relevant to this thesis, these materials absorb electromagnetic radiation strongly and can be highly luminescent. The absorption and emission maxima are influenced by the side-chain substituents attached directly to the conjugated backbone, producing bathochromic shifts. A few well-studied conjugated polymers are illustrated in Scheme 1.

Scheme 1 Common conjugated polymers.



PPEs are conjugated polymers with a backbone consisting of alternating phenyl and alkyne linkers. PPEs in their neutral state are wide band gap semiconductors with direct optical band gaps.^{24, 25} The conjugated polymer band gap is largely determined by the local electronic structure of the constituent

monomers and is determined at very low degrees of polymerization.²⁶ This is evidenced by the fact that absorption and emission spectra are independent of molecular weight when the polymers are longer than short oligomers.²

In small molecules, absorption of a photon results in an excited state where an electron has been promoted from the highest occupied molecular orbital (HOMO) to the lowest unoccupied molecular orbital (LUMO) as illustrated in Figure 2. As small molecule monomer units are combined to form polymers, the individual HOMO levels are mixed to form the valence band, while the LUMO levels combine to form the conduction band. When the polymer absorbs a photon of light, an electron is excited from the valence band to the conduction band forming a mobile electron-hole pair.

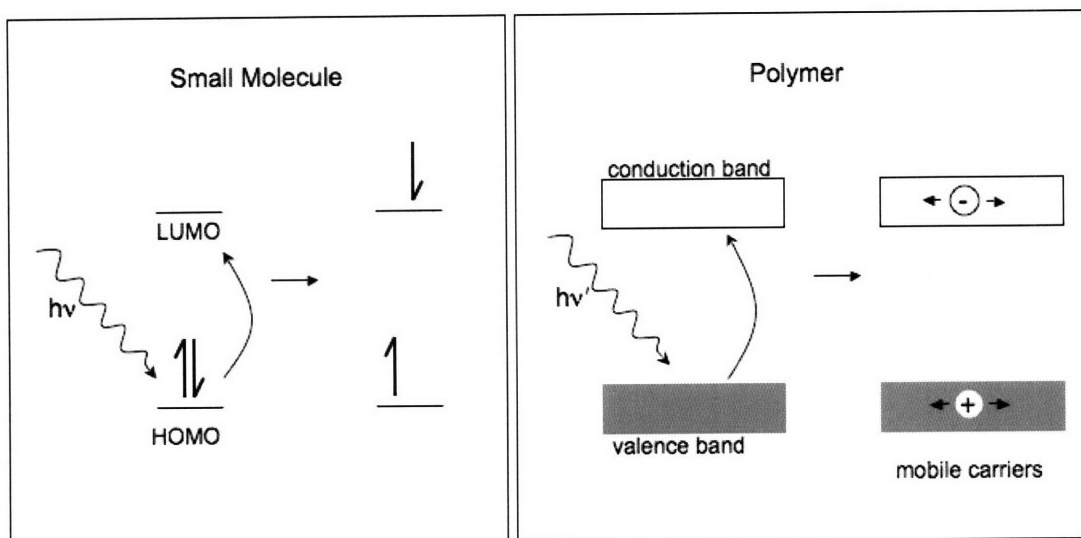


Figure 2 Absorption of a photon in a small molecule results in an electron being promoted from the HOMO to the LUMO. In a conjugated polymer, absorption of a photon results in an electron-hole pair being formed with the electron in the conduction band and the hole in the valence band.

While PPEs would appear to have a rigid linear structure, in solution these materials are loosely coiled and have persistence lengths of approximately 15 nm.²⁷ As a result, they have highly anisotropic properties relative to most polymers which have much lower persistence lengths.

1.4 Conjugated Polymer Sensors

Conjugated polymers can be categorized into several classifications including conductometric, potentiometric, colorimetric, and fluorescent.¹⁷ To summarize the first three categories briefly: conductometric sensors measure the

change in current or resistivity when exposed to an analyte or dopant, potentiometric sensors use analyte-induced changes in the system's chemical potential and have the advantage of requiring only a voltage measurement between a working and reference electrode, and a colorimetric sensor monitors changes in absorption properties upon exposure to an analyte. The fourth category, fluorescence based sensors, offer perhaps the most diverse transduction processes based upon changes in intensity, energy transfer, excitation and emission wavelengths, and excited state lifetimes. The sensors discussed in this thesis are based on the production and quenching of a fluorescence signal.

Sensors, and more specifically, chemosensors, are composed of two components: a receptor and a reporter. Real-time sensors can be developed when the binding equilibrium between the target and receptor is rapid. Ideally, the response obtained varies with the concentration of the target present. An equally important factor for determining the level of sensitivity, in addition to the binding selectivity, is the transduction method employed.

Conducting polymers composed from monomers containing sensors are essentially chemosensors wired in series, and this architecture has been shown to produce signal amplification.² In a "turn-off" sensor, binding of a single analyte to a polymer introduces a new state in the band gap and electron transfer can occur, quenching the polymer's fluorescence (Figure 3, top). A "turn-on" sensor

occurs when the binding of a target causes a localized reduced band-gap that can trap the mobile excited states, resulting in red-shifted emission (Figure 3, bottom). A turn-on sensor can also be designed whereby a quencher is removed due to the presence of a target and is essentially the reverse of the turn-off sensor.

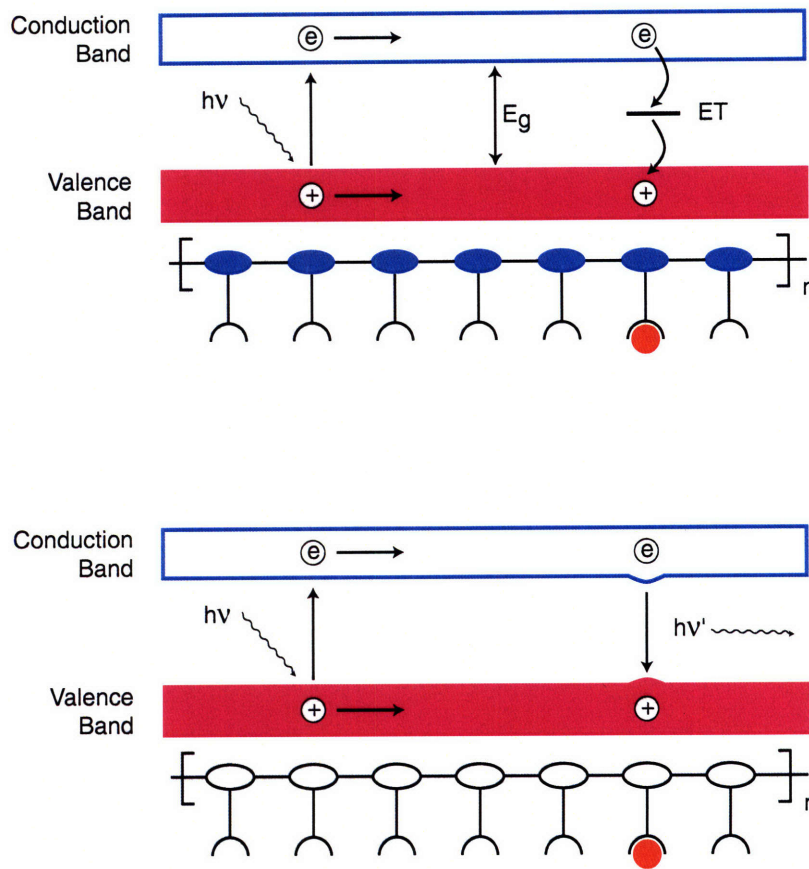


Figure 3 Top, A turn-off sensor: excitons are quenched through electron transfer to an acceptor resulting in amplified quenching. Bottom, A turn-off sensor: selective recombination of excitons occur at local minima introduced by the analyte, leading to emission of red-shifted light and amplified wavelength shifts.

1.5 Synthesis of Conjugated Polymers

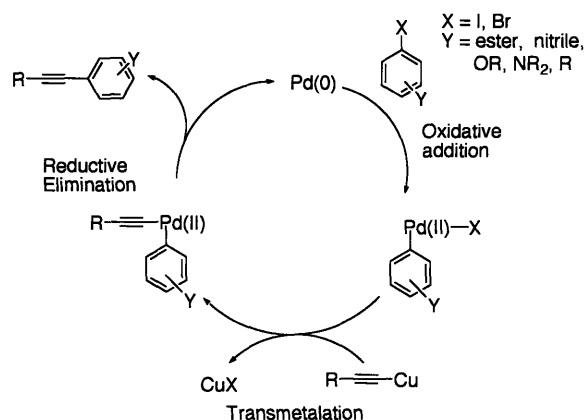
PPEs are produced by the stepwise addition of monomers with two functional groups and the mechanism is known as step-growth polymerization. Each reaction is independent of the previous one and a polymer is obtained from high yielding reactions that connect the monomers in series. As a result, producing high molecular weight polymers requires extremely clean starting materials and quantitative chemistries.

Metal-catalyzed coupling reactions are powerful tools for the synthesis of step-growth polymers, especially for the preparation of unsaturated polymers such as PPEs. Yamamoto *et al.* first demonstrated the use of a metal-catalyzed cross-coupling reaction in the synthesis of polyphenylenes,²⁸ which was later followed by the synthesis of poly(aryleneethynylene)s.²⁹ The development of a number of cross-coupling reactions³⁰⁻³² with high yields and high functional group tolerance has allowed greater freedom and the ability to synthesize a broad range of conjugated polymers.

PPEs are prepared using a palladium catalyzed Sonogashira-Hagihara cross-coupling reaction of an aryl dihalide and an aryl diacetylene.³³⁻³⁵ Aryl iodides have generally yielded better results than aryl bromides. This coupling is performed in the presence of a palladium catalyst, a copper (I) co-catalyst, and amine base under anaerobic conditions. A slight excess of the aryl dialkyne is

used to compensate for the formation of dialkyne linkages, which are formed in the presence of trace amounts of oxygen.²

Scheme 2 Palladium catalyzed cross-coupling mechanism for the production of PPEs.



1.6 Fluorescence and Energy Transfer

Luminescence, the emission of light from a substance, can be subdivided into three categories: chemiluminescence, fluorescence, and phosphorescence. Chemiluminescence is the emission of light as a product of a chemical reaction and will not be treated further here. Fluorescence and phosphorescence are both the result of emission from electronically excited states (singlet and triplet states respectively) as a molecule relaxes to the ground state after the absorption of a photon. The processes that occur between absorption and emission are illustrated in what is commonly known as a Jablonski energy diagram (Figure 4). Absorption of the photon results in promotion of an electron

into a higher energy level, which relaxes through internal conversion to the lowest vibronic level of the excited state. The ground state and excited state electrons in most conjugated polymers retain their respective spins and therefore remain paired, the two states are referred to as the singlet excited state (S_1) and the singlet ground state (S_0). Fluorescence occurs when a photon is emitted upon relaxation from the S_1 state to the S_0 state. The paired spin allows for rapid relaxation to the ground state, with excited state lifetimes often on the order of nanoseconds. When intersystem crossing from the S_1 state occurs, the excited state electron spin can be reversed and the electron relaxes to the T_1 excited state. Relaxation from a triplet excited state orbital to a singlet ground state orbital is spin forbidden, resulting in much longer excited state lifetimes on the order of milliseconds to seconds. The excited state electron must reverse its spin once more before relaxing to the S_0 state. When this occurs with the emission of a photon, it is designated as phosphorescence.³⁶

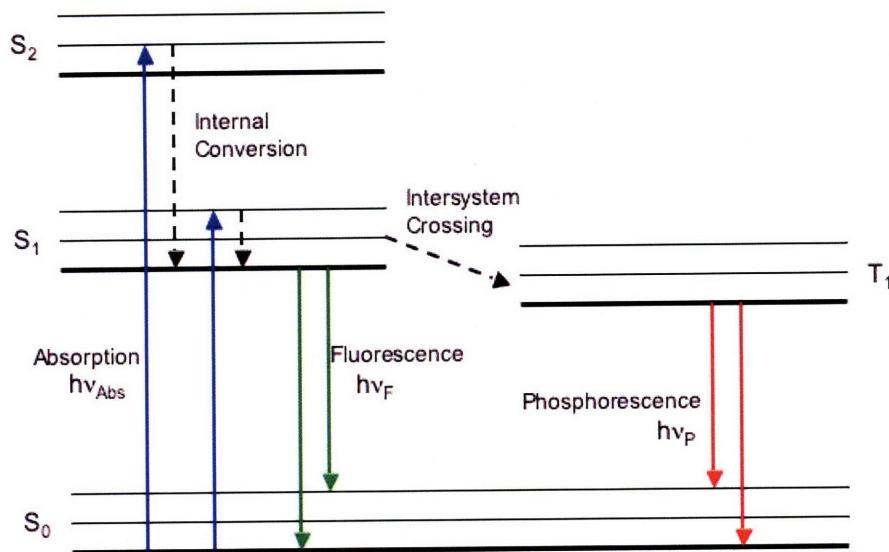


Figure 4 Jablonski energy diagram.

If the emission spectrum of a fluorophore overlaps with the absorption spectrum of a second fluorophore, energy transfer is possible from the excited donor (D*), to the ground state acceptor (A). The end result is a ground state donor (D) and an excited acceptor (A*). Energy transfer occurs without the emission and absorption of a photon due to the dipole-dipole interactions between the two molecules. The term resonance energy transfer (RET) is used because of the lack of an intermediate photon. In the case when fluorescence is the source of energy transfer from the donor, fluorescence resonance energy transfer (FRET) is specified. The rate of energy transfer is dependent on the extent of spectral overlap, the relative orientation of the donor and acceptor transition dipoles, and the distance between the two molecules. The distance at which RET is 50% efficient is known as the Förster distance or radius.³⁷ The rate of energy transfer is given by the equation³⁶

$$k_T = (1/\tau_D)(R_0/r)^6 \quad \text{Eq. (1)}$$

where τ_D is the donor decay time in the absence of the acceptor, R_0 the Förster radius, and r the D-A distance. The rate of RET is strongly dependent on distance between the two molecules as it is inversely proportionate to r^6 . Typically, FRET is used as a “spectroscopic ruler” to measure D-A distances in biological macromolecules by measuring the extent of donor quenching.^{38, 39}

In addition to energy transfer via dipole-dipole interactions, a second mechanism is also possible and is known as Dexter or electron exchange energy transfer. This method requires orbital overlap or collision between the donor and acceptor. During collisions, significant overlap of electron clouds occurs and electron exchange may take place in the region of overlap. The rate constant of energy transfer is described by the equation⁴⁰

$$k_{ET} = K \cdot J \cdot e^{(-2R_{DA}/L)} \quad \text{Eq. (2)}$$

where K is a constant that represents specific orbital interactions, J is the spectral overlap integral normalized to ϵ_A (the extinction coefficient of the acceptor), R_{DA} is the D-A separation, and L their van der Waals radii. The rate of energy transfer decreases sharply as R_{DA} increases and at distances greater

than 5 – 10 Å the rate becomes negligible. In contrast to the Förster mechanism, the rate is independent of the oscillator strength of the $D^*\gamma D$ and $A\gamma A^*$ transitions.

1.7 Fluorescence Quenching

Quenching decreases fluorescence intensity and can occur by different mechanisms. Both static and dynamic or collisional quenching require molecular contact between the fluorophore and quencher. Collisional quenching occurs when an excited state fluorophore is deactivated upon contact with another molecule and requires that the quencher diffuse to the fluorophore during the excited state lifetime. Examples of collisional quenchers include molecular oxygen,⁴¹ halogens,⁴² amines, and electron deficient molecules, such as acrylamide. A second method is static quenching whereby a non-fluorescent complex is formed between the fluorophore and the quencher. In this case, quenching occurs in the ground state and does not rely on diffusion or molecular collisions.

For collisional quenching, the decrease in fluorescence intensity is described by the Stern-Volmer equation⁴³

$$F_0/F = 1 + k_q\tau_0[Q] \quad \text{Eq. (3a)}$$

$$= 1 + K_D[Q] \quad \text{Eq. (3b)}$$

where F_0 and F are, respectively, the fluorescence intensities in the absence and presence of the quencher, k_q is the bimolecular quenching constant, τ_0 the excited state lifetime in the absence of the quencher, and $[Q]$ the quencher concentration. The Stern-Volmer constant is identified as K_D if quenching is known to be dynamic, and K_{SV} in other cases.

1.8 Conclusion

A sensor should recognize its target quickly, selectively, sensitively, and ideally, reversibly. The sensing platform presented here incorporates three components that can be independently modified and tailored to a particular target.

The synthesis and investigation of a polymer capable of binding biological molecules will be discussed in Chapter 2. A dendritic quencher will be designed, synthesized, and its quenching abilities explored in Chapter 3. The sequences and responses of the molecular beacon and the corresponding complements will be outlined in Chapter 4. In Chapter 5, the initial explorations into the conjugation of the molecular beacon to the polymer, a crucial step in the development of this sensor, will be detailed.

1.9 References

1. Firestein, S., "How the olfactory system makes sense of scents," *Nature* **2001**, *413*, 211-218.
2. Zhou, Q.; Swager, T. M., "Fluorescent chemosensors based on energy migration in conjugated polymers: The molecular wire approach to increased sensitivity," *J. Am. Chem. Soc.* **1995**, *117*, 12593-12602.
3. Swager, T. M., "The molecular wire approach to sensory signal amplification," *Acc. Chem. Res.* **1998**, *31*, 201-207.
4. Yang, J.-S.; Swager, T. M., "Porous Shape Persistent Fluorescent Polymer Films: An Approach to TNT Sensory Materials," *J. Am. Chem. Soc.* **1998**, *120*, 5321-5322.
5. Yang, J. S.; Swager, T. M., "Fluorescent porous polymer films as TNT chemosensors: Electronic and structural effects," *J. Am. Chem. Soc.* **1998**, *120*, 11864-11873.
6. Updike, S. J.; Hicks, G. P., "The Enzyme Electrode," *Nature* **1967**, *214*, 986.
7. Rodriguez-Mozaz, S.; Marco, M. P.; de Alda, M. J. L.; Barcelo, D., "Biosensors for environmental monitoring of endocrine disruptors: a review article," *Anal. Bioanal. Chem.* **2004**, *378*, 588-598.
8. Leonard, P.; Hearty, S.; Brennan, J.; Dunne, L.; Quinn, J.; Chakraborty, T.; O'Kennedy, R., "Advances in biosensors for detection of pathogens in food and water," *Enzyme Microb. Technol.* **2003**, *32*, 3-13.

9. Gooding, J. J., "Biosensor technology for detecting biological warfare agents: Recent progress and future trends," *Anal. Chim. Acta* **2006**, *559*, 137-151.
10. Rich, R. L.; Myszka, D. G., "Survey of the year 2004 commercial optical biosensor literature," *J. Molec. Recogn.* **2005**, *18*, 431-478.
11. Tyagi, S.; Kramer, F. R., "Molecular Beacons: Probes that Fluoresce upon Hybridization," *Nat. Biotechnol.* **1996**, *14*, 303-308.
12. Ma, C. B.; Tang, Z. W.; Wang, K. M.; Tan, W. H.; Li, J.; Li, W.; Li, Z. H.; Yang, X. H.; Li, H. M.; Liu, L. F., "Real-time monitoring of DNA polymerase activity using molecular beacon," *Anal. Biochem.* **2006**, *353*, 141-143.
13. Fang, X. H.; Liu, X. J.; Schuster, S.; Tan, W. H., "Designing a novel molecular beacon for surface-immobilized DNA hybridization studies," *J. Am. Chem. Soc.* **1999**, *121*, 2921-2922.
14. Du, H.; Strohsahl, C. M.; Camera, J.; Miller, B. L.; Krauss, T. D., "Sensitivity and specificity of metal surface-immobilized "molecular beacon" biosensors," *J. Am. Chem. Soc.* **2005**, *127*, 7932-7940.
15. Johnston, A. P. R.; Caruso, F., "A molecular beacon approach to measuring the DNA permeability of thin films," *J. Am. Chem. Soc.* **2005**, *127*, 10014-10015.
16. McClernon, D. R.; Vavro, C.; Clair, M. S., "Evaluation of a real-time nucleic acid sequence-based amplification assay using molecular beacons for detection of human immunodeficiency virus type 1," *J. Clin. Microbiol.* **2006**, *44*, 2280-2282.

17. Sokol, D. L.; Zhang, X. L.; Lu, P. Z.; Gewitz, A. M., "Real time detection of DNA RNA hybridization in living cells," *Proc. Natl. Acad. Sci. U.S.A.* **1998**, *95*, 11538-11543.
18. Yang, C. Y. J.; Lin, H.; Tan, W. H., "Molecular assembly of superquenchers in signaling molecular interactions," *J. Am. Chem. Soc.* **2005**, *127*, 12772-12773.
19. Wang, S.; Gaylord, B. S.; Bazan, G. C., "Fluorescein provides a resonance gate for FRET from conjugated polymers to DNA intercalated dyes," *J. Am. Chem. Soc.* **2004**, *126*, 5446-5451.
20. Lv, W.; Li, N.; Li, Y.; Li, Y.; Xia, A., "Shape-Specific Detection Based on Fluorescence Resonance Energy Transfer Using a Flexible Water-Soluble Conjugated Polymer," *J. Am. Chem. Soc.* **2006**, *126*, 10281-10287.
21. Baker, E. S.; Hong, J. W.; Gaylord, B. S.; Bazan, G. C.; Bowers, M. T., "PNA/dsDNA complexes: Site specific binding and dsDNA biosensor applications," *J. Am. Chem. Soc.* **2006**, *128*, 8484-8492.
22. Chiang, C. K.; Fincher, C. R.; Park, Y. W.; Heeger, A. J.; Shirakawa, H.; Louis, E. J.; Gau, S. C.; Macdiarmid, A. G., "Electrical-Conductivity in Doped Polyacetylene," *Phys. Rev. Lett.* **1977**, *39*, 1098-1101.
23. Bunz, U. H. F., "Poly(Arylene Ethynylene)s: from Synthesis to Application," *Adv. Polym. Sci.* **2005**, *177*, 1-52.
24. Samuel, I. D. W.; Rumbles, G.; Collison, C. J.; Friend, R. H.; Moratti, S. C.; Holmes, A. B., "Picosecond Time-Resolved Photoluminescence of PPV Derivatives," *Synth. Met.* **1997**, *84*.

25. Smilowitz, L.; Hays, A.; Heeger, A. J.; Wang, G.; Bowers, J. E., "Time-resolved photoluminescence from poly[2-methoxy, 5-(2'-ethyl-hexyloxy)-*p*-phenylene-vinylene]: Solutions, gels, films, and blends," *J. Chem. Phys.* **1993**, *98*, 6504-6509.
26. Thienpont, H.; Rikken, G.; Meijer, E. W.; Tenhoeve, W.; Wynberg, H., "Saturation of the Hyperpolarizability of Oligothiophenes," *Phys. Rev. Lett.* **1990**, *65*, 2141-2144.
27. Cotts, P. M.; Swager, T. M.; Zhou, Q., "Equilibrium Flexibility of a Rigid Linear Conjugated Polymer," *Macromolecules* **1996**, *29*, 7323-7328.
28. Yamamoto, T.; Hayashi, Y.; Yamamoto, A., "Novel Type of Polycondensation Utilizing Transition Metal-Catalyzed C-C Coupling .1. Preparation of Thermostable Polyphenylene Type Polymers," *Bull. Chem. Soc. Jpn.* **1978**, *51*, 2091-2097.
29. Sanechika, K.; Yamamoto, T.; Yamamoto, A., "Palladium Catalyzed C-C Coupling for Synthesis of π -Conjugated Polymers Composed of Arylene and Ethynylene Units," *Bull. Chem. Soc. Jpn.* **1984**, *57*, 752-755.
30. Stille, J. K., "The Palladium-Catalyzed Cross-Coupling Reactions of Organotin Reagents with Organic Electrophiles," *Angew. Chem. Int. Ed.* **1986**, *25*, 508-523.
31. Kumada, M., "Nickel and Palladium Complex Catalyzed Cross-Coupling Reactions of Organometallic Reagents with Organic Halides," *Pure Appl. Chem.* **1980**, *52*, 669-679.

32. Heck, R., *Palladium reagents in organic syntheses*. Academic Press: London; Orlando [Fla.], 1985.
33. Sonogashira, K.; Tohda, Y.; Hagihara, N., "Convenient synthesis of acetylenes. Catalytic substitutions of acetylenic hydrogen with bromo alkenes, iodo arenes, and bromopyridines," *Tetrahedron Lett.* **1975**, *16*, 4467.
34. Neenan, T. X.; Whitesides, G. M., "Synthesis of High-Carbon Materials from Acetylenic Precursors - Preparation of Aromatic Monomers Bearing Multiple Ethynyl Groups," *J. Org. Chem.* **1988**, *53*, 2489-2496.
35. Stille, J. K., "The Palladium-Catalyzed Cross-Coupling Reactions of Organotin Reagents with Organic Electrophiles," *Angewandte Chemie-International Edition in English* **1986**, *25*, 508-523.
36. Lakowicz, J. R., *Principles of Fluorescence Spectroscopy*. 2 ed.; Kluwer Academic/Plenum Publishers: New York, 1999.
37. Förster, T., "Intermolecular energy transference and fluorescence," *Ann. Physik* **1948**, *2*, 55-75.
38. Stryer, L., "Fluorescence Energy-Transfer as a Spectroscopic Ruler," *Ann. Rev. Biochem.* **1978**, *47*, 819-846.
39. Steinberg, I. Z., "Long-range nonradiative transfer of electronic excitation energy in proteins and polypeptides," *Ann. Rev. Biochem.* **1971**, *40*, 83-114.
40. Turro, N. J., *Modern Molecular Photochemistry*. University Science Books: Sausalito, CA, 1991.
41. Kautsky, H., "Quenching of luminescence by oxygen," *Trans. Faraday Soc.* **1939**, *35*, 216-219.

42. Kasha, M., "Collisional perturbation of spin-orbit coupling and the mechanism of fluorescence quenching. A visual demonstration of perturbation," *J. Chem. Phys.* **1952**, *20*, 71-74.
43. Stern, O.; Volmer, M., "Über die Abklingungszeit der Fluoreszenz," *Physik. Zeitschr.* **1919**, *20*, 183-188.

Chapter 2:

Masked Michael Acceptors in Poly(*p*-phenylene ethynylene)s

Reproduced in part with permission from Bailey, G. C.; Swager, T. M. *Macromolecules*, **2006**, *39*, 2815-2818. Copyright 2006 American Chemical Society.

2.1 Introduction

The ability of poly(*p*-phenylene ethynylene)s (PPEs) to transport and funnel energy has resulted in their utilization as chemosensors both in solution and in the solid state.¹ Conjugated polymers have successfully been developed to sense nitroaromatics, such as TNT, and quinones via photoinduced electron transfer from the polymer excited state to the bound analyte, resulting in a turn-off sensor from the nonradiative recombination of electron-hole pairs.^{2, 3} Biological binding events have also been successfully detected via fluorescent labeling and Förster energy transfer processes.⁴⁻⁷ In order to expand the scope and sensory applications of PPEs, we have been interested in developing methods for their conjugation to biomolecules. The most commonly used methods for the conjugation of biomolecules to surfaces or other molecules generally involve addition and substitution reactions with the amine of lysine or the thiol of cysteine.⁸ The Swager group recently reported reactions with lysine residues in the context of protease detection.⁹ The thiol functionality, however, presents greater challenges as typical polymerization methodologies are incompatible with conventional thiol-acceptors, which generally have reactive alkenes and halides. Cysteine conjugation reactions most often employ maleimides, vinyl sulfones, iodoacetamides, and orthopyridyl disulfide units.¹⁰ We have targeted the maleimide group due to the facile conjugate addition of thiols across the electron-deficient double bond.

An additional attribute is the excellent dienophile character of the maleimide group; it readily participates in reversible [4+2] Diels-Alder reactions under relatively mild thermal conditions.^{11, 12} This reversibility has additional utility for producing reversibly cross-linked elastomers and plastics¹³ and thermally “re-mendable” cross-linked polymeric materials.^{14, 15} Early work utilizing the Diels-Alder reaction with maleimides was carried out by Stille and coworkers to polymerize bis(maleimide)s and bis(cyclopentadiene)s.¹⁶ Herein we report a polymer bearing masked Michael acceptors that can be thermally unveiled, thereby allowing thiol addition reactions or Diels-Alder chemistries.

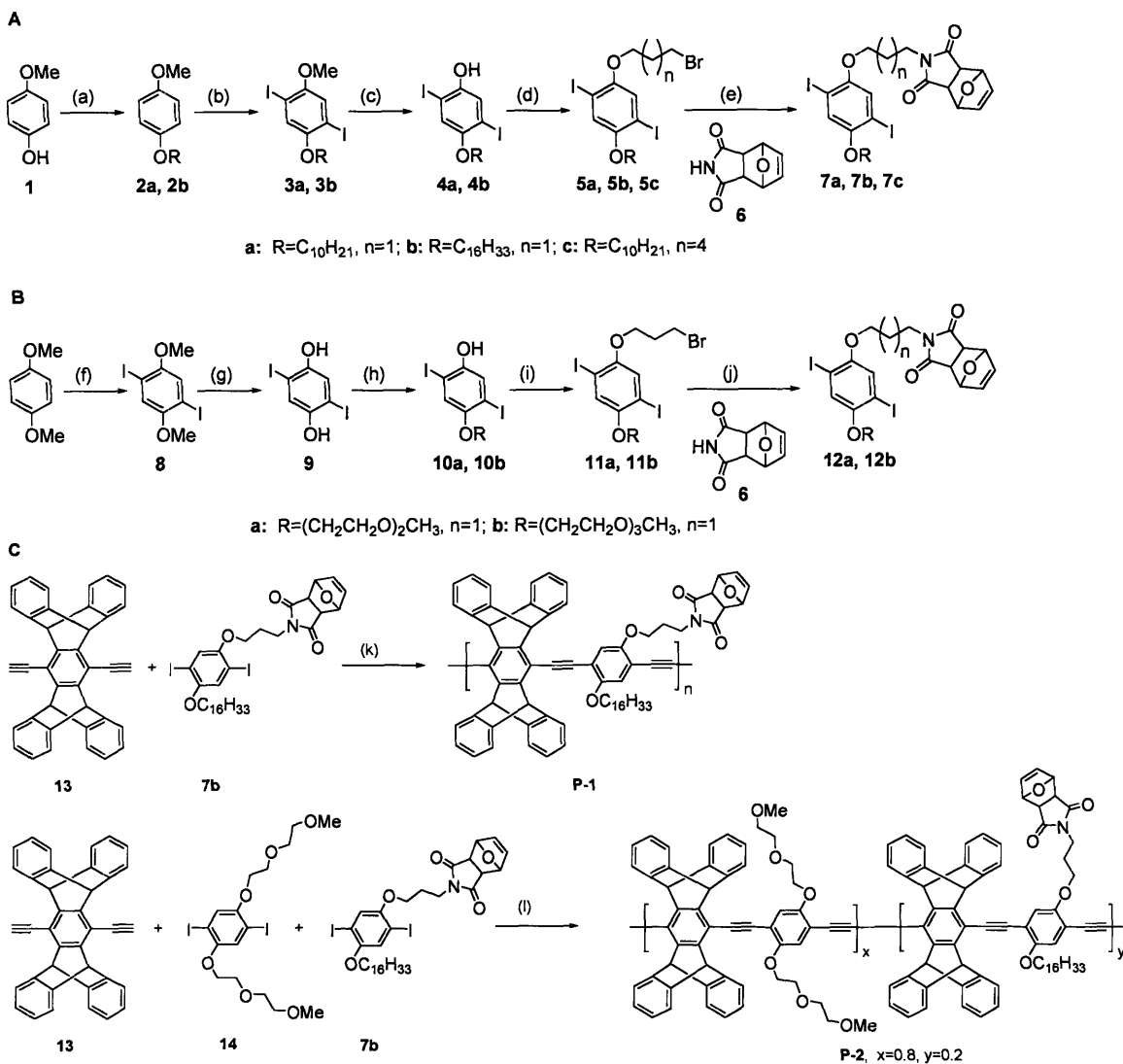
2.2 Synthesis of Masked-Maleimide Containing Polymer

PPEs are typically prepared by palladium catalyzed Sonogashira-Hagihara cross-coupling of 2,5-dialkoxy-1,4-diiodobenzenes with aryl dialkynes. Having targeted PPEs with pendent maleimides, we initially investigated the compatibility of this group with the Sonogashira-Hagihara reaction conditions.¹⁷ When maleimide groups were present during polymerization, only low molecular weight oligomers ($M_n \sim 3000$, $DP \sim 4$) were obtained, which is suggestive of Heck-type side-reactions.¹⁸ It was therefore necessary to protect the maleimide during polymerization so that the reactive double bond is only revealed when needed. We took advantage of the facility with which maleimide partakes in Diels-Alder reactions and used these reactions with furan to mask the maleimide.

Two separate synthetic pathways were developed for masked-maleimide containing aryl diiodide monomers as shown in Scheme 1. For the preparation of alkoxy-containing monomers the first step is alkylation of methoxyhydroquinone to yield **2**, which can be iodinated under acidic conditions to give **3** in 73% yield (Scheme 1A). During our investigations, it was discovered that *tert*-butylmercaptan, *t*-BuSH, in the presence of base will selectively react with aryl methoxy groups without interfering with longer chain primary aryl alkoxy groups to yield the corresponding phenolic groups via an S_N2 reaction. Using these conditions, **4a** was obtained in 80 % yield and **4b** in 87 % yield. Williamson ether synthesis with an excess of the alkyl dibromide affords **5a-c** in yields ranging from 52 % yield for **5a** and 85 % yield for **5b**. Compound **6** is synthesized quantitatively from maleimide in neat furan, yielding ~ 2:1 ratio of endo:exo isomers at room temperature; alkylation of this furan-protected maleimide yields **7** (**7a**, 82 %; **7b**, 58 %; **7c**, 72%).¹⁹ The alternative two-step approach of initially attaching the maleimide moiety, with subsequent addition of furan led to lower yields than the direct introduction of the masked maleimide **6**. The isomers of **6** were separated, however, the mixture of endo and exo adduct isomers of **7** produced polymers with greater solubility.

As a deprotecting agent, *t*-BuSH is not selective for the removal of methyl groups in the presence of 2-[2-(2-methoxyethoxy)ethoxy]ethoxy or the shorter 2-(2-methoxyethoxy)ethoxy chains. Therefore, an alternative synthetic route was developed for monomers containing these groups (Scheme 1B). Compound **9** is

synthesized in nearly quantitative yield in two steps from 1,4-diiodo-2,5-dimethoxybenzene using boron tribromide to remove both methyl groups from **8**. Monoalkylation of the hydroquinone occurs in relatively low isolated yields to generate **10a** (14 % yield) and **10b** (23 % yield). Subsequent alkylation with a dibromide yields **11a** (62% yield) and **11b** (58 % yield), to which **6** is added in the presence of base to produce **12a** in 68 % yield and **12b** in 42 % yield.



Scheme 1 (A): (a) K₂CO₃, RBr, acetone; (b) I₂, KIO₃, H₂SO₄, AcOH, H₂O; (c) *t*-BuSH, NaOH, DMF; (d) K₂CO₃, BrCH₂(CH₂)_nCH₂Br, acetone; (e) K₂CO₃, acetone. For synthesis of **6** please see Section 2.8 Experimental. (B): (f) I₂, KIO₃, H₂SO₄, AcOH, H₂O; (g) BBr₃, CH₂Cl₂, -78°C, quench with water; (h) 1 eq. NaH, DMF, ROTs; (i) 1,3-dibromopropane, K₂CO₃, refluxing acetone; (j) K₂CO₃, DMF. (C): (k) Catalytic Pd(PPh₃)₄ and CuI, toluene, diisopropylamine, 1-methyl-2-pyrrolidinone, room temperature 5 days, (M_n=11,000); (l) Catalytic Pd(PPh₃)₄ and CuI, toluene, diisopropylamine, room temperature 7 days (M_n=8,000).

Among the many advantages of this design is that the solubility of the polymer can be tailored by changing the R group, i.e. alkyl vs. 2-methoxyethoxy chains. In addition, the distance of the maleimide group from the polymer backbone can be controlled by introducing different chain lengths of the dibromide in the synthesis of **5** or **11**. This linkage can also be varied to influence polymer solubility.

Polymers were prepared by step-growth polymerization using the Sonogashira-Hagihara cross-coupling reaction depicted in Scheme 1C.¹⁷ All dialkyne (**13**, **14**) monomers were prepared using established literature procedures.^{20, 21} The pentiptycene dialkyne comonomer was used for the superior physical properties that it produces in the resulting polymer for incorporation into chemosensors, such as improved fluorescence in thin films, greater solubility, and the ability to prevent chain aggregation. The aryl diiodide and a slight excess (1-2 %) of the aryl dialkynes in the presence of catalytic amounts of palladium tetrakis(triphenylphosphine) and copper iodide are dissolved in a suitable solvent with an amine base and stirred for five to seven days. The polymerization is conducted at room temperature to prevent the Diels-Alder adduct from undergoing cycloreversion. The polymers were precipitated and dried *in vacuo* overnight. The diiodide monomer **14** was introduced to form statistical copolymer **P-2** (x=0.8, y=0.2) thereby reducing the loading of masked maleimide along the polymer backbone. In addition, polymer **P-3** (x=1.0, y=0) was prepared with no masked maleimide units. The polymers obtained varied in

molecular weight from 8,000 to 11,000. For NMR spectrum of **P-2**, please refer to the supplemental information. Due to solubility limitations, a suitable NMR spectrum could not be obtained for **P-1**, however, its optical properties were in complete accord with the assigned structure.

2.3 Removing the Mask

The thermal decomposition of polymers and monomers were monitored by TGA and TGA-MS, and representative data is presented in Figure 1. The monomers each displayed a distinct two-step loss attributed to loss of one isomer of the Diels-Alder adduct (exo or endo) at ~ 70 °C followed by loss of the other at ~ 140 °C. TGA-MS data were obtained for monomers and **P-2**; data for monomer **7b** are presented in Figure 1A. Two masses were monitored: 68 for furan and 39 for a furan fragment. Loss of furan clearly coincides with each of the two-step losses of mass. TGA data for compound **12a**, which has a $\sim 1:2$ endo:exo ratio, indicate initial loss is from the endo isomer (Figure 1B). The expected weight loss for **12a** was 10.2 %, and an experimental loss of 11.0 % is observed. The two-step loss pattern was also observed for all of the polymers containing the masked maleimide groups. The TGA analysis showed that for all polymers, the observed weight losses were consistently lower than predicted. For instance, the predicted weight loss from cycloreversion is 6.7 % for **P-1**, however, only 3.6 % was observed experimentally. This discrepancy is rationalized as the result of a broad range of local environments experienced in the solid state by the adducts.

Unmasking of monomers in solution is quantitative as monitored by proton NMR and the temperatures required to remove furan were considerably milder (60 - 70 °C). In addition, **P-2** was monitored by FTIR before and after heating in the solid state under an inert atmosphere. Three bands attributed to cyclic ether stretches disappeared after heating: 1105 cm⁻¹, 1023 cm⁻¹, and 754 cm⁻¹.

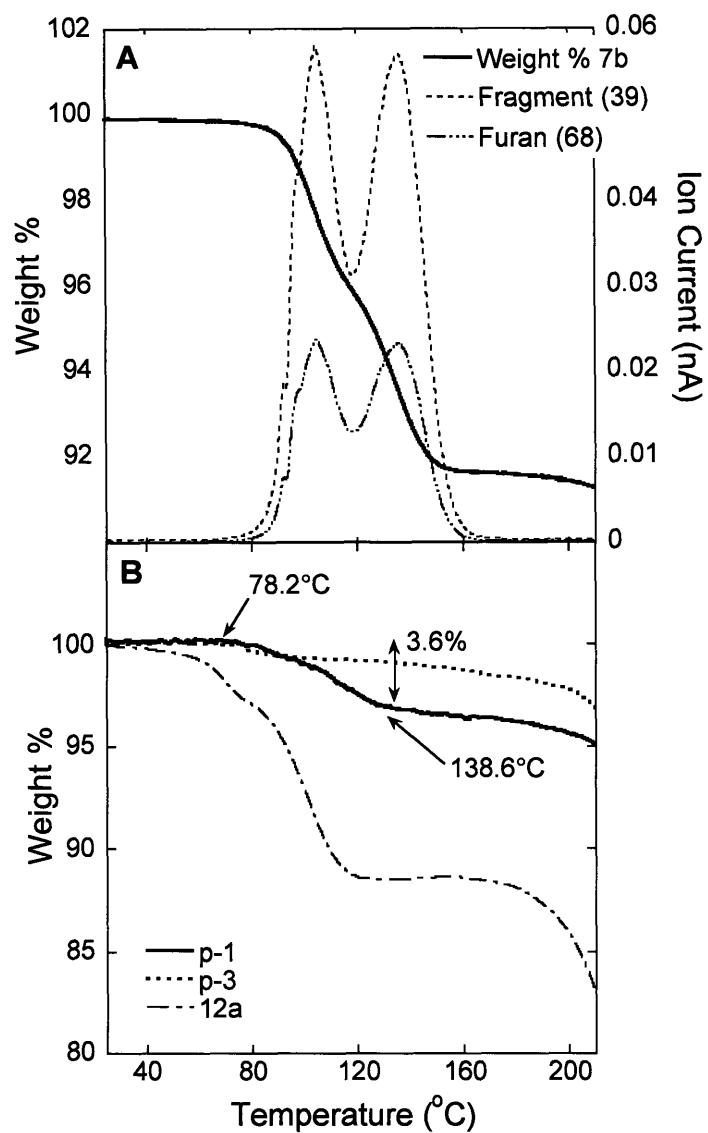
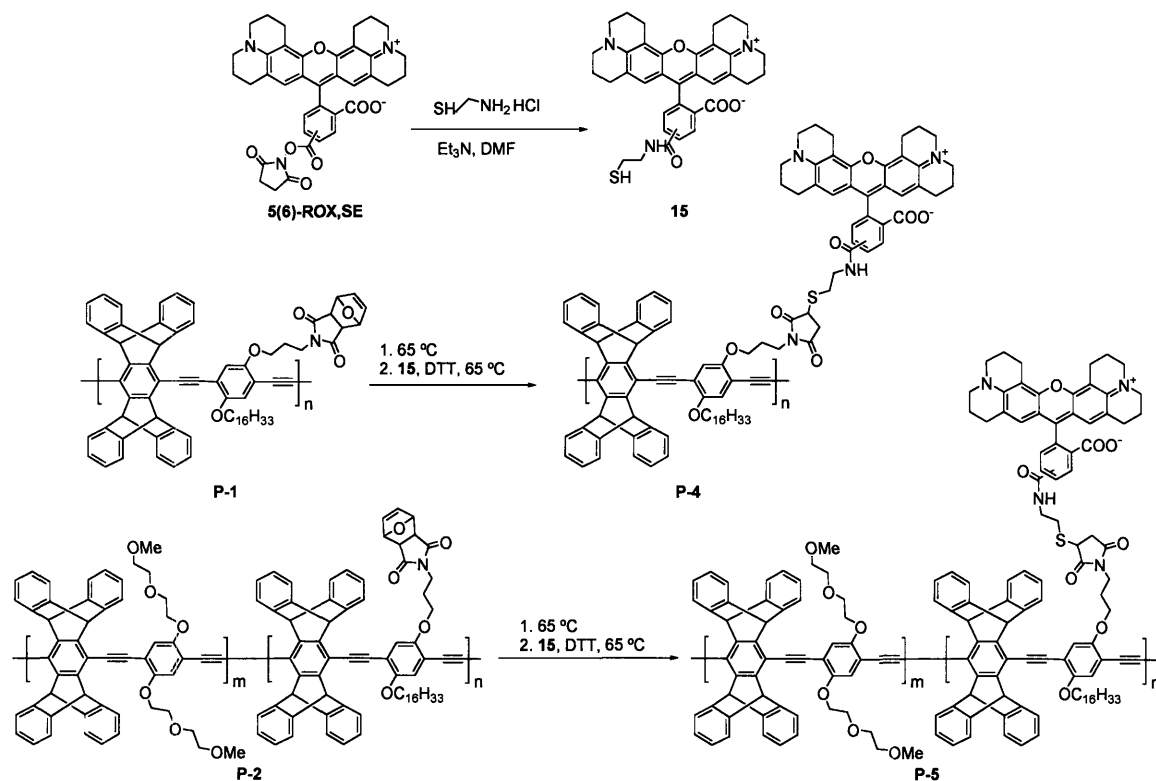


Figure 1 A: TGA-MS for 7b; monitoring at 68 for furan and at 39 for a known furan fragment. (Ramp rate: 5°C/min to 300°C.) **B:** Thermogravimetric analysis for P-1, P-3, and 12a. (Ramp rate: 0.1°C/min to 300°C.)

2.4 Application of Revealed Maleimide as Tethering Point

To explore the ability of tethering thiols to the polymers, a carboxy-X-rhodamine (ROX) dye with a free sulfhydryl group, **15** was synthesized (Scheme 2). Polymers **P-1** and **P-2** were refluxed in tetrahydrofuran (THF), followed by the introduction of a methanol/THF solution of **15** and dithiothreitol (DTT), which is needed to reduce any disulfide linkages present. Due to the partial solubility of the resulting polymers in methanol, precipitation was not possible and so the polymers were purified by preparative GPC. The change in solubility is thought to be the result of addition of a large number of methanol-soluble dyes to the polymers.

Scheme 2 Labeling unmasked maleimides with ROX dye.



The progress of the reaction of thiolated ROX dye **15** with **P-2** was monitored by absorbance and fluorescence spectra, as well as GPC analysis (Figure 3). In Figure 3A the absorbance and fluorescence spectra for the addition of the dye in THF are shown. The characteristic double peak absorbance of ROX at 500 and 540 nm is clearly visible in addition to the absorption maximum of **P-2** at 348 nm. The emission of the ROX dye at 538 nm and 580 nm is observed upon direct excitation of the dye at 500 nm and also upon excitation of the polymer at 410 nm. The latter is a signature of light harvesting by the polymer and energy transfer to the dye. Repeated attempts at determining the extent of dye loading by NMR failed due to the inability to produce samples

concentrated enough to obtain suitable spectra and overlapping signals. The chemical shifts for these protons occur in regions with a high density of peaks from the polymer, namely from 2 to 4 ppm and 6 to 8 ppm. As a result, the peaks for protons resulting from the conjugate addition of dye were not observed. Attempts at analyzing this process by FTIR spectroscopy were limited due to the weakness of the C-S stretch.

The GPC chromatograms of polymers **P-2** and **P-5** are shown in Figure 3B. The UV-Vis absorption signal of the dye and the polymer occur simultaneously in the chromatogram, indicating that the dye is bound to the polymer. The absorption at 570 nm is significantly weaker due to a lower concentration of the dye relative to the polymer. The ROX dye-polymer conjugate elutes at minute 23, while the free dye elutes at minute 30. The difference in shape of the chromatograms when monitoring at 410 nm and 570 nm is attributed to the fact that the dye is likely non-uniformly distributed as a function of the molecular weight of **P-5**. High molecular-weight polymers may also undergo an aggregation process that is molecular-weight dependent and distorts the chromatogram.

Extent of loading of the dye was determined from the relative absorbance of the polymer and the dye in GPC chromatograms. The absorbance at 450 nm for the polymer and 570 nm for the dye were compared and normalized using the extinction coefficients at the two respective wavelengths. Loadings of 1–8.5%

dye/polymer ratios were observed for polymer **P-5** over multiple experiments, which correlates to 5–42 % of maleimide groups modified with the dye. The extinction coefficient in THF of the succinimidyl ester of ROX (ROX,SE) at 570 nm and **P-2** at 450 nm are $10.3 \text{ mL} \cdot \text{mg}^{-1} \cdot \text{cm}^{-1}$ and $17.2 \text{ mL} \cdot \text{mg}^{-1} \cdot \text{cm}^{-1}$. The chromatograms were corrected to ensure a baseline of zero absorbance. In one case, the relative area of the polymer absorption at 450 nm (while the polymer is eluting) was found to be 76.7 while the dye absorption area at 570 nm was found to be 3.9. Taking into consideration the extinction coefficients, the loading percentage as a function of mass is 8.5 %. **P-2** has 20 % maleimide monomers, and a loading ratio of 8.5% dye to polymer corresponds to 42.6% of the maleimide groups modified with the dye. The lower loadings were observed at lower temperatures and in the absence of methanol, which was added to increase the solubility of the dye.

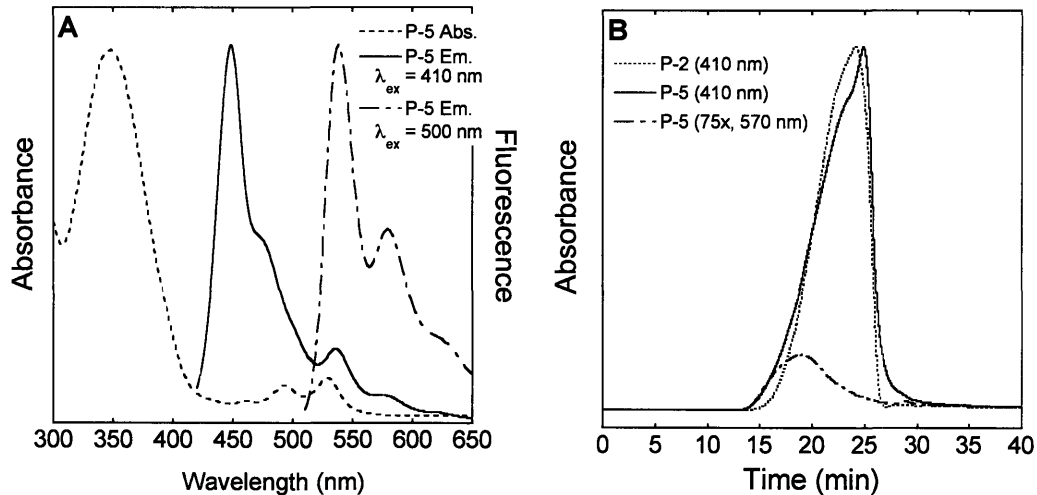


Figure 2 (A) Normalized absorbance and emission spectra for P-5 after exposure in THF to thiolated-ROX dye, **15** with excitation at both 410 and 500 nm. (B) Normalized GPC trace for polymers P-2 and P-5, monitoring at 410 nm and 570 nm (absorption at 570 nm scaled 75×).

2.5 Further Exploration of Applications – Use of Maleimide Group for Crosslinking

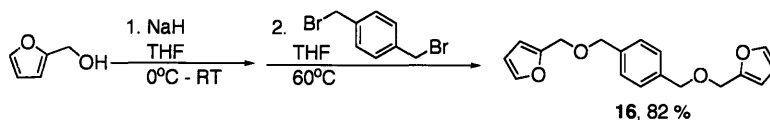
Crosslinking provides anchoring points for polymer chains, restraining excessive movement and maintaining the position of the chain in the network. When a sample is crosslinked several properties of the polymer are affected; the dimensional stability is improved, the creep rate is lowered, the resistance to solvents is increased, and it becomes less prone to heat distortion because the

glass transition temperature (T_g) is raised. All of these effects are intensified with increased crosslink density.²²

When dithiol cross linkers were used, the polymer fluorescence decreased sharply, most likely due to a side reaction wherein the thiol adds across the triple bond contained in the polymer backbone.

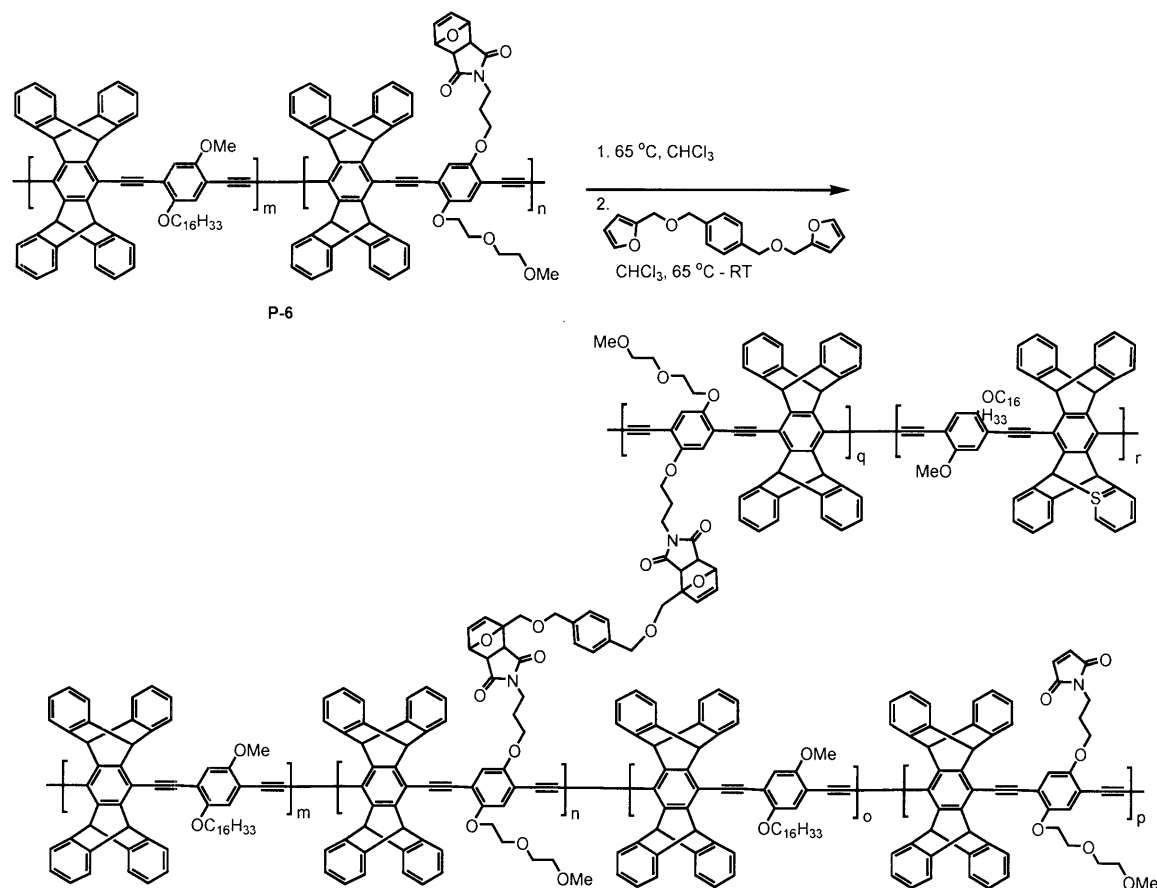
To further investigate the ability of the maleimide units to act as anchoring points for crosslinking, a di-furan compound, **16**, was prepared in two steps from furfuryl alcohol (Scheme 3).

Scheme 3 Preparation of di-furan crosslinker for use with maleimide-PPEs.



Polymer **P6** was heated in chloroform at 65 °C under inert atmosphere for 8 hours, at which point a chloroform solution of **16** was added so that the final ratio of maleimide to crosslinker was 10:1. This solution was stirred for a further 12 hours at 65 °C and then cooled to room temperature (Scheme 3).

Scheme 4 Removal of the mask and subsequent introduction of the cross-linker.



The molecular weight (M_n) of the resulting polymer, **P-7**, was obtained by GPC (THF eluent) and increased by 24% from 1.01×10^4 to 1.24×10^4 . In addition, the polydispersity index decreased from 2.5 to 2. The polymer fluorescence was not noticeably affected by the addition of the crosslinker throughout this reaction. We suspect that some dimer formation is occurring, however, accurate comparisons of molecular weights obtained by GPC is difficult given that molecules of different shapes are being compared relative to polystyrene, a polymer that itself has different structural properties from PPEs.

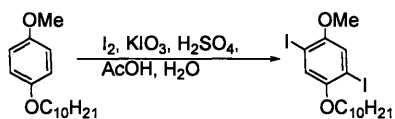
2.6 Conclusion and Discussion

PPEs containing masked maleimide groups capable of partaking in Michael addition and Diels-Alder chemistries have been synthesized. The furan protecting group for the maleimide moiety must be present during polymerization to prevent it from participating in side reactions. Furan can be removed quantitatively post-polymerization in solution under relatively mild thermal conditions via cycloreversion. The resulting unmasked polymer can be generated *in situ* and then functionalized with a compound containing a thiol or diene. This was demonstrated by the grafting of a thiolated dye to a maleimide-PPE with maleimide loading efficiencies up to 42 %. The versatility of the maleimide unit can be expanded through the use of heterobifunctional linkers to bind a host of molecules to PPEs, including amines. Homobifunctional compounds could be used to form cross-linked PPE networks.

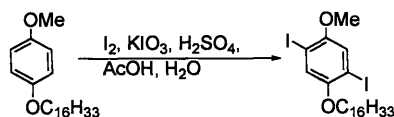
The ability to incorporate a dieneophile within a polymer network opens the door to a wide range of applications. As a result of the modularity of PPE synthesis, a large library of PPEs can be synthesized and incorporated into a broad spectrum of uses, including, but not limited to, biosensors and chemosensors.

2.7 Experimental

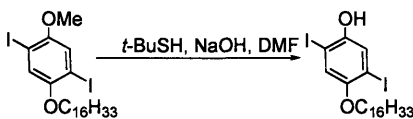
Synthetic manipulations were performed under an argon atmosphere using standard Schlenk techniques when necessary. NMR spectra were recorded on either a Varian 300 MHz or a Varian 500 MHz spectrometer. Polymer molecular weights were determined by gel-permeation chromatography (GPC) using an HP series 1100 GPC system running at 1.0 mL/min in THF or DMF equipped with a diode array detector (254 nm and 450 nm) and a refractive index detector. Molecular weights are reported relative to polystyrene standards. UV/Vis spectra were recorded on an Agilent 8453 diode-array spectrophotometer and corrected for background signal with a solvent-filled cuvette. Emission spectra were acquired on a SPEX Fluorolog- τ 3 fluorometer (model FL-321, 450 W Xenon lamp) using right angle detection. The absorbance of all samples was kept to 0.1 au in order to minimize artifacts. Thermogravimetric analyses were obtained on a TA Instruments Q50 under a nitrogen atmosphere.



3a: To a stirred 1:10:100 solution of H₂SO₄:H₂O:acetic acid were added **2a** (2.5 g, 9.6 mmol), I₂ (2.5 g, 10 mmol), KIO₃ (1.04 g, 4.88 mmol) and the mixture was left to reflux overnight. The reaction was quenched by pouring over 50 mL water and a fine brown powder was collected by vacuum filtration and washed with 20 mL 1.0 N NaOH. The powder was dissolved in acetone and hot filtered to remove insoluble materials. The solvent was removed, the product dissolved in DCM and filtered through a bed of silica. Quantitative yield. ¹H NMR (CDCl₃, ppm, 500 MHz): 0.89 (t, 3H, *J*= 6.3 Hz), 1.28 (broad, 12H), 1.50 (m, 2H, *J*= 7.8 Hz), 1.81 (quintet, 2H, *J*= 6.6 Hz), 3.83 (s, 3H), 3.94 (t, 2H, *J*= 6.6 Hz), 7.19 (s, 1H), 7.19 (s, 1H). ¹³C NMR (CDCl₃, ppm, 125 MHz): 14.36, 22.91, 26.23, 29.49, 29.54, 29.75, 29.77, 32.12, 57.36, 70.55, 85.59, 86.54, 121.60, 123.06, 153.12, 153.37. HRMS: *m/z* 538.9916 (calc'd [C₁₇H₂₆I₂O₂+Na]⁺, 538.992).

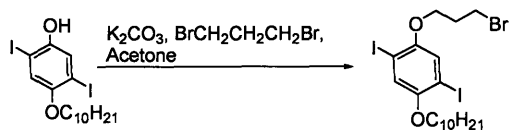


3b: To a stirred 1:10:100 solution of H₂SO₄:H₂O:acetic acid were added **2b** (5.0 g, 14.9 mmol), I₂ (3.8 g, 15.2 mmol), KIO₃ (1.60 g, 7.5 mmol) and was left to reflux overnight. The reaction was quenched by pouring over 100 mL water and a fine brown powder was collected by vacuum filtration, which was then washed with 40 mL 1.0 N NaOH. The powder was dissolved in acetone and hot filtered to remove insoluble materials. 73% yield. ¹H NMR (CDCl₃, ppm, 500 MHz): 0.88 (t, 3H, *J*= 7Hz), 1.25 (broad, 24H), 1.50 (quintet, 2H, 7.5Hz), 1.80 (quintet, 2H, 7Hz), 3.83 (s, 3H), 3.94 (t, 2H, 6.5Hz), 7.19 (s, 1H), 7.19 (s, 1H). ¹³C NMR (CDCl₃, ppm, 125 MHz): 14.36, 22.92, 26.23, multiple aliphatic peaks 29.59-29.92, 32.15, 57.36, 70.56, 85.59, 86.55, 121.61, 123.07, 153.14, 153.38. HRMS: *m/z* 1223.1957 (calc'd [2(C₂₃H₃₈I₂O₂)+Na]⁺, 1223.182).

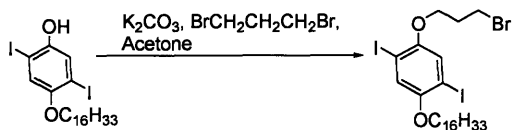


4b: Ground NaOH (0.68 g, 16.9 mmol) and **3b** (2.02 g, 3.37 mmol) were dissolved in 100 mL DMF and stirred at 100°C, followed by addition of *t*-butylmercaptan. Upon completion of reaction (approximately 2 hours), the reaction mixture poured over 10% HCl in ice. The yellow compound was extracted into ether, dried over anhydrous MgSO₄, and the solvent and excess *t*-BuSH were removed by short-path distillation. The product was separated from starting material by extraction with 0.3 M KOH in 1:10 H₂O:MeOH. This solution was neutralized with 10% HCl in water. MeOH was removed under vacuum and additional water was added to precipitate the product. The yellow compound was collected by filtration. The product was finally extracted into CHCl₃ and washed with brine. The organic phase was dried over anhydrous MgSO₄ and the solvent was removed to obtain a pale yellow powder, 87% yield. ¹H NMR (CDCl₃, ppm, 300 MHz): 0.88 (t, 3H, 7.2Hz), 1.26 (broad, 24H), 1.45 (m, 2H), 1.81 (m, 2H), 3.92 (t, 2H, 6.3 Hz), 4.94 (s, 1H), 7.03 (s, 1H), 7.42 (s, 1H). ¹³C NMR (CDCl₃, ppm, 125 MHz): 14.36, 22.92, 26.93, multiple aliphatic peaks 29.31-29.92, 31.14, 70.54, 84.60, 87.79, 121.03, 124.99, 149.98, 152.82. HRMS: *m/z* 609.0700 (calc'd [C₂₂H₃₆I₂O₂+Na]⁺, 609.0702).

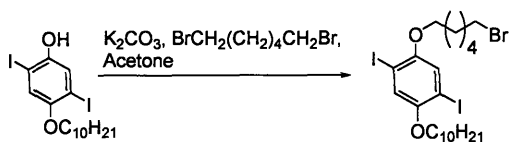
4a: Similar procedure used as for **4b**.



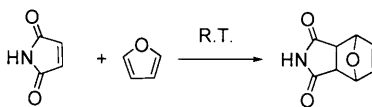
5a: 1,3-dibromopropane (1.05 g, 5.2 mmol) and K₂CO₃ (1.37 g, 9.9 mmol) were added to a round bottom flask and stirred while refluxing in 15 mL acetone. Compound **4a** (0.16 g, 0.32 mmol) was dissolved in 10 mL acetone and added by syringe pump at a rate of 0.3 mL/hr. Upon completion, the solvent was removed *in vacuo* and the residue dissolved in CHCl₃. The organic phase was washed with brine and dried over anhydrous MgSO₄. Excess 1,3-dibromopropane was removed by short-path distillation. 76% yield. ¹H NMR (CDCl₃, ppm, 300 MHz): 0.89 (t, 3H, 6.9 Hz), 1.29 (broad, 12H), 1.49 (m, 2H), 1.81 (quintet, 2H, 7.8 Hz), 2.34 (quintet, 2H, 6 Hz), 3.70 (t, 2H, 6.6 Hz), 3.94 (t, 2H, 6.6 Hz), 4.09 (t, 2H, 5.7 Hz), 7.17 (s, 1H), 7.22 (s, 1H). ¹³C NMR (CDCl₃, ppm, 500 MHz): 14.37, 22.91, 26.23, 29.32, 29.49, 29.55, 29.76, 29.78, 30.43, 32.13, 32.48, 67.73, 70.52, 86.47, 86.52, 122.80, 123.16, 152.42, 152.41. HRMS: *m/z* 644.9349 (calc'd [C₁₉H₂₉BrI₂O₂+Na]⁺, 644.9338).



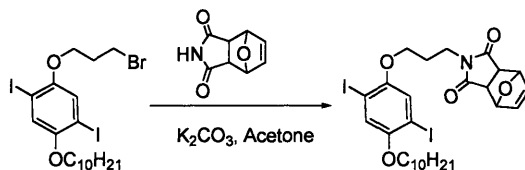
5b: 1,3-Dibromopropane (1.7 g, 8.6 mmol) and K_2CO_3 (0.60 g 4.3 mmol) were added to 20 mL acetone and stirred while refluxing. Compound **4b** was dissolved in 10 mL acetone and added via syringe pump at a rate of 0.6 mL/hr to the refluxing solution. Upon completion, the solvent was removed *in vacuo* and the residue dissolved in $CHCl_3$. The organic phase was washed with brine and dried over anhydrous $MgSO_4$. Excess 1,3-dibromopropane was removed by short-path distillation. 85% yield. 1H NMR ($CDCl_3$, ppm, 500 MHz): 0.89 (t, 3H, 6.6 Hz), 1.26 (broad, 22H), 1.51 (m, 2H), 1.81 (m, 2H), 2.37 (quintet, 2H, 6 Hz), 3.57 (t, 2H, 6.3 Hz), 3.70 (t, 2H, 6.3 Hz), 3.94 (t, 2H, 6.3 Hz), 4.09 (t, 2H, 5.4 Hz), 7.17 (s, 1H), 7.22 (s, 1H). ^{13}C NMR ($CDCl_3$, ppm, 500 MHz): 14.37, 22.92, 26.23, multiple aliphatic peaks 22.92-30.41, 32.14, 32.48, 67.72, 70.51, 86.47, 86.52, 122.79, 123.14, 152.42, 153.41. HRMS: m/z 729.0259 (calc'd $[C_{25}H_{41}BrI_2O_2+Na]^+$, 729.0277).



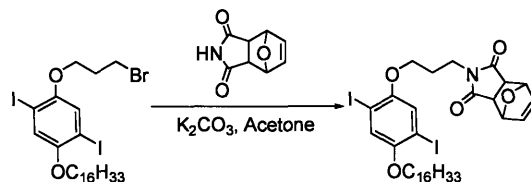
5c: Similar procedures used for this compound as with **5a** and **5b**. 1H NMR ($CDCl_3$, ppm, 300 MHz): 0.89 (t, 3H, 6.6 Hz), 1.28 (broad, 12H), 1.50-1.56 (m, 6H), 1.76-1.97 (m, 6H), 3.46 (t, 2H, 6.9 Hz), 3.94 (m, 4H), 7.17 (s, 1H), 7.22 (s, 1H). ^{13}C NMR ($CDCl_3$, ppm, 500 MHz): 14.34, 22.87, 25, 47, 26.20, 27.99, multiple peaks due to aliphatic chains from 29.12 to 29.74, 32.08, 32.84, 34.01, 70.16, 70.47, 86.48, 122.83, 122.88, 152.83, 153.05. HRMS: m/z 686.9786 (calc'd $[C_{22}H_{35}BrI_2O_2+Na]^+$, 686.9808).



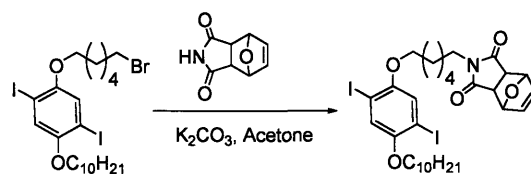
6: Chilled furan (75mL, 1.03 mol) was added to maleimide (10.1 g, 0.104 mol) and the solution stirred at room temperature overnight. Excess furan was removed *in vacuo*, leaving white solid. 96% yield of a mixture of endo and exo adducts. ^1H NMR (CDCl_3 , ppm, 300 MHz): 2.91 (s, exo adduct, 2H), 3.58 (m, endo adduct, 2H), 5.32 (s, exo adduct, 2H), 5.35 (m, endo adduct, 2H), 6.52 (m, both adducts, 2H), 8.03 (broad s from amine, 1H), 8.45 (broad s from amine, 1H). ^{13}C NMR (CDCl_3 , ppm, 125 MHz): 47.60, 48.92, 79.60, 81.17, 134.82, 136.78, 175.20, 176.53. HRMS: m/z 188.0319 (calc'd $[\text{C}_8\text{H}_7\text{NO}_3+\text{Na}]^+$, 188.0324).



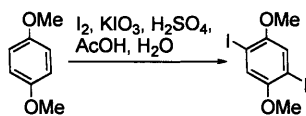
7a: The masked maleimide **6** (0.13 g, 0.77 mmol) and K_2CO_3 (0.34 g, 2.5 mmol) were dissolved in 15 mL DMF under an inert atmosphere. Compound **5a** (0.15 g, 0.24 mmol) was added and the solution stirred while refluxing overnight. The solvent was removed by short-path distillation followed by an aqueous work-up and extraction into chloroform. The product was purified by flash column chromatography on silica gel with 4:6 hexane:ethyl acetate as the eluent. The endo and exo fractions were combined to give 82% yield. 1H NMR ($CDCl_3$, ppm, 500 MHz): 0.89 (t, 3H, 6.6 Hz), 1.28 (broad, 10H), 1.49 (m, 2H), 1.80 (quintet, 2H, 6.6 Hz), 1.97 (endo isomer, quintet, 2H, 6.6 Hz), 2.09 (exo isomer, quintet, 2H, 6.6 Hz), 2.87 (s, 2H), 3.54 (m, 2H), 3.59 (endo isomer, t, 2H, 6.9 Hz), 3.76 (exo isomer, t, 2H, 6.9 Hz), 3.87-3.94 (m, 2H), 5.27-5.34 (endo and exo isomers, 2H), 6.42-6.52 (endo and exo isomers, 2H), 7.149 (s, 1H), 7.159 (s, 1H). ^{13}C NMR ($CDCl_3$, ppm, 125 MHz): 14.35, 22.90, 26.22, 27.70, 29.30, 29.47, 29.53, 29.75, 29.76, 32.11, 36.25, 36.58, 46.24, 47.69, 67.87, 68.12, 70.46, 79.59, 81.14, 86.50, 122.80, 123.06, 123.19, 134.70, 136.73, 152.50, 153.42, 175.07, 176.40. HRMS: m/z 730.0497 (calc'd $[C_{27}H_{35}I_2NO_5+Na]^+$, 730.0502).



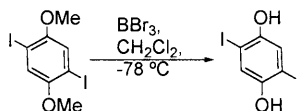
7b: Similar procedure used as for **7a**, save for use of acetone as solvent, 60 % yield. ^1H NMR (CDCl_3 , ppm, 300 MHz): 0.89 (t, 3H, 6.3 Hz), 1.26 (broad s, 24H), 1.50 (m, 2H), 1.80 (m, 2H), 1.97 (endo isomer, m, 2H), 2.09 (exo isomer, m, 2H), 2.87 (exo isomer, s, 2H), 3.55 (endo isomer, m, 2H), 3.60 (endo isomer, t, 2H), 3.76 (exo isomer, t, 2H, 6.6 Hz), 3.91 (m, 2H), 5.27 (exo isomer, s, 2H), 5.33 (endo isomer, m, 2H), 6.42 (endo isomer, s, 2H), 6.52 (exo isomer, s, 2H), 7.150 (endo isomer, s, 1H), 7.154 (exo isomer, s, 1H), 7.16 (s, 1H). ^{13}C NMR (CDCl_3 , ppm, 125 MHz, mix of endo and exo isomers): 14.36, 22.91, 26.23, 27.71, 29.33, 29.49, 29.58, 29.77, 29.80, 29.87, 29.91, 32.14, 36.26, 36.58, 46.25, 47.70, 67.88, 68.13, 70.47, 76.98, 77.23, 77.49, 79.60, 81.14, 86.46, 86.49, 122.81, 123.19, 134.70, 136.72, 152.51, 152.58, 153.30, 153.43, 175.06, 176.38. HRMS: m/z 814.1411 (calc'd $[\text{C}_{33}\text{H}_{47}\text{I}_2\text{NO}_5+\text{Na}]^+$, 814.1441).



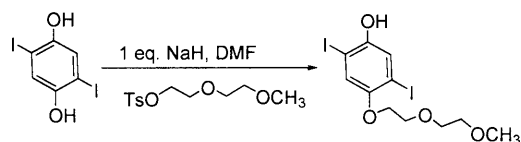
7c: Similar procedure used as for **7a**. 42% yield. ^1H NMR (CDCl_3 , ppm, 300 MHz): 0.89 (t, 3H, 7.0 Hz), 1.28 (broad, 14H), 1.36 (m, 2H), 1.49 (m, 2H), 1.61 (m, 2H), 1.80 (m, 2H), 2.84 (s, 2H), 3.50 (t, 2H, 7.0 Hz), 3.54 (t, 2H, 7.0 Hz), 3.92 (m, 4H), 5.27 (s, 2H), 6.51 (s, 2H), 7.15 (s, 1H), 7.17 (s, 1H). ^{13}C NMR (CDCl_3 , ppm, 125 MHz): 14.35, 22.90, 25.79, 25.86, 26.22, 26.48, 26.63, 27.70, 28.70, 29.12, 29.17, 29.33, 29.48, 29.53, 29.74, 29.76, 32.11, 38.01, 39.09, 46.13, 47.59, 70.22, 70.24, 70.52, 79.60, 81.10, 86.47, 122.87, 122.92, 134.25, 136.72, 152.90, 152.93, 153.03, 171.07, 176.49. HRMS: m/z 772.0942 (calc'd $[\text{C}_{36}\text{H}_{53}\text{I}_2\text{NO}_5+\text{Na}]^+$, 772.0972).



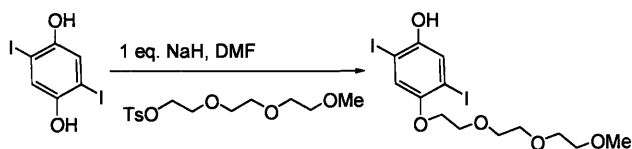
8: 1,4-Dimethoxybenzene (50.03 g, 0.362 mol), I₂ (94.04 g, 0.370 mol), and KIO₃ (38.83 g, 0.181 mol) were added to a 2 L stirred solution of 1:10:100 of H₂SO₄:H₂O:AcOH. This solution was refluxed for 7 hours and then cooled to room temperature. The reaction mixture was poured over 1 L deionized water and the precipitate was collected and washed with ~400 mL 1 N NaOH. The precipitate was recrystallized from acetone. 78% yield. ¹H NMR (CDCl₃, ppm, 500 MHz): 3.84 (s, 6H), 7.20 (s, 4H). ¹³C NMR (CDCl₃, ppm, 125 MHz): 57.36, 85.64, 121.71, 153.44. HRMS: *m/z* 412.8519 (calc'd [C₈H₈I₂O₂+Na]⁺, 412.8511).



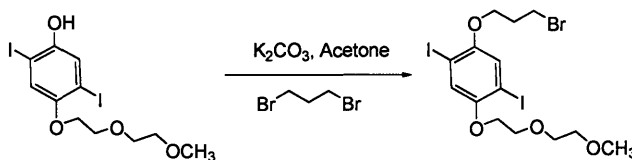
9: Compound **8** (30.461 g, 0.0781 mol) was measured into a thoroughly dried flask. Under an Ar atmosphere, dichloromethane was added and the solution cooled to -78°C. BBr₃ (22 mL, 0.237 mol) was then added and the solution left to stir 24 hours. The bright orange solution was poured over 500 mL ice-water. A cream-coloured precipitate was formed, collected, and dried *in vacuo*. Quantitative yield. ¹H NMR (Acetone-d₆, ppm): 7.29 (s, 2H), 8.73 (s, 2H). ¹³C NMR (CDCl₃): 84.60, 125.22, 151.87. HRMS: *m/z* 361.8295 (calc'd [C₆H₄I₂O₂], 361.8301).



10a: Compound **9** (10.012 g, 27.6 mmol) was dissolved in 150 mL dried DMF under Ar atmosphere and cooled to 0°C. NaH (60 % suspension in mineral oil, 0.6668 g, 27.78 mmol) was added and the solution stirred for 20 minutes. 1-(*p*-Tolylsulfonyl)-3,6-dioxoheptane²³ was added and the solution stirred overnight at 50°C. The solvent was removed by short-path distillation and the crude product was dissolved in dichloromethane and washed first with 10% HCl, then with saturated NH₄Cl, and finally with water. The organic phase was dried over anhydrous MgSO₄, concentrated *in vacuo*. The crude product was purified by flash column chromatography (eluent: 5% MeOH in CH₂Cl₂). The product was further purified by recrystallization from hot ethanol, 10-25% yield. ¹H NMR (CDCl₃, ppm): 3.42 (s, 3H), 3.61 (m, 2H), 3.80 (m, 2H), 3.90 (m, 2H), 4.09 (m, 2H), 5.41 (broad s, 1H), 7.09 (s, 1H), 7.37 (s, 1H). ¹³C NMR (CDCl₃, ppm, 125 MHz): 59.35, 69.81, 70.50, 71.27, 72.25, 84.37, 87.53, 121.93, 124.85, 150.66, 152.34. HRMS: *m/z* 486.8886 (calc'd [C₁₁H₁₄I₂O₄+Na]⁺, 486.8879).

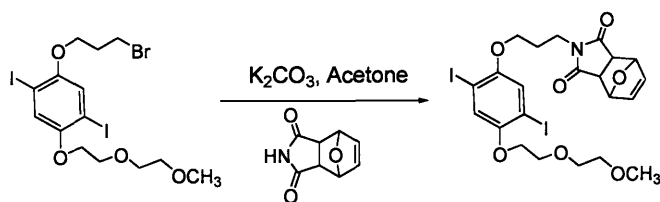


10b: Similar procedure as **10a**, except that 1-(*p*-tolylsulfonyl)-3,6,9-trioxodecane was used rather than 1-(*p*-tolylsulfonyl)-3,6-dioxoheptane. The product was purified by flash column chromatography with silica gel and 1:2 hexane:ethylacetate as the eluent, 24% yield. ^1H NMR (CDCl_3 , ppm, 300 MHz): 3.40 (s, 3H), 3.59 (m, 2H), 3.67-3.83 (multiple peaks, 6H), 3.90 (t, 2H, 4.8 Hz), 4.10 (t, 2H, 4.2 Hz), 5.23 (broad s, 1H), 7.10 (s, 1H), 7.40 (s, 1H). HRMS: m/z 530.9141 (calc'd $[\text{C}_{13}\text{H}_{18}\text{I}_2\text{O}_5+\text{Na}]^+$, 530.9141).

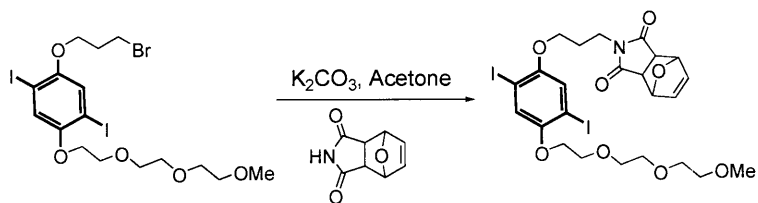


11a: Compound **10a** (2.51 g, 5.41 mmol) was dissolved in 20 mL acetone and added by syringe pump at a rate of 0.34 mL/hr to a refluxing acetone solution of 1,3-dibromopropane (5.439 g, 26.94 mmol) and K_2CO_3 (1.880 g, 13.61 mmol). The solvent was removed *in vacuo* and excess 1,3-dibromopropane removed by short-path distillation. The crude product was purified by flash column chromatography (eluent 1:1 hexane:ethylacetate), 58% yield. 1H NMR ($CDCl_3$, ppm, 500 MHz): 2.35 (m, 2H), 3.42 (s, 3H), 3.56-3.62 (m, 2H), 3.70 (t, 2H, $J=6Hz$), 3.79 (m, 2H), 3.91 (t, 2H, $J=4.5Hz$), 4.08 (t, 2H, 6Hz), 4.12 (t, 2H, $J=4.5Hz$), 7.20 (s, 1H), 7.25 (s, 1H). ^{13}C NMR ($CDCl_3$, ppm, 125 MHz): 30.38, 32.43, 59.36, 67.64, 69.81, 70.53, 71.26, 72.24, 86.39, 86.68, 122.94, 123.69, 152.78, 153.26. HRMS: m/z 606.8456 (calc'd $[C_{14}H_{19}BrI_2O_4+Na]^+$, 606.8454).

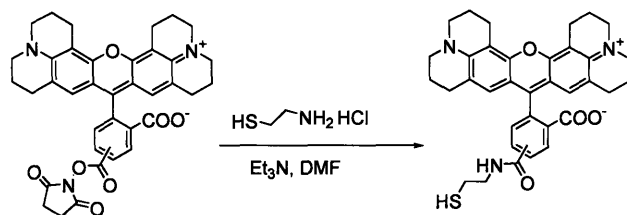
11b: Similar procedure as **11a**, save for the use of 1:5 hexane:ethylacetate as eluent for flash chromatography. 41% yield.



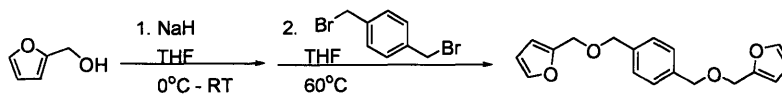
12a: Compound **11a** (1.51 g, 2.58 mmol), **6** (2.12 g, 12.8 mmol), NaI (0.386 g, 2.58 mmol), and K_2CO_3 (3.547 g, 25.7 mmol) were dissolved in 30 mL acetone and stirred at room temperature for 24 hours. The solvent was removed *in vacuo*, followed by an aqueous work-up in dichloromethane. The crude product was purified by flash chromatography on silica gel (1:3 hexane:ethylacetate eluant), 70% yield, mixture of endo and exo isomers. 1H NMR ($CDCl_3$, ppm, 300 MHz): 2.08 (m, 2H, $J=6.5Hz$), 2.87 (s, 2H), 3.40 (s, 3H), 3.58 (m, 2H) 3.73-3.78 (m, 4H), 3.89(t, 2H, $J=4.5Hz$), 3.92 (t, 2H, 6Hz), 4.11 (t, 2H, $J=5.5Hz$), 5.27 (exo isomer, s, 2H), 5.30 (endo isomer, m, 2H), 6.42 (endo isomer, s, 2H), 6.51 (exo isomer, s, 2H), 7.13 (s, 1H), 7.24 (s, 1H). ^{13}C NMR ($CDCl_3$, ppm, 125 MHz): 27.64, 36.52, 46.21, 47.66, 48.87, 59.32, 67.79, 69.77, 70.47, 71.22, 72.21, 79.55, 81.10, 81.14, 86.40, 86.62, 122.83, 123.66, 134.38, 134.66, 136.69, 136.73, 152.92, 153.11, 176.36. HRMS: m/z 691.9615 (calc'd $[C_{22}H_{25}I_2NO_7+Na]^+$, 691.9618).



12b: A similar procedure was used as for **12a**, 42% yield. 1H NMR ($CDCl_3$, ppm, 300 MHz): 1.97 (endo isomer, m, 2H), 2.20 (exo isomer, m, 2H), 2.87 (exo isomer, s, 2H), 3.37 (s, 3H), 3.54-3.61 (m, 4H), 3.66-3.71 (m, 4H), 3.87-3.91 (m, 2H), 4.10 (t, 2H, 4.5 Hz), 5.26 (endo isomer, s, 2H), 5.33 (exo isomer, m, 2H), 6.41 (endo isomer, s, 2H), 6.51 (exo isomer, s, 2H), 7.122 (endo isomer, s, 1H), 7.125 (exo isomer, s, 1H), 7.23 (s, 1H). HRMS: m/z 735.9880 (calc'd $[C_{24}H_{29}I_2NO_8+Na]^+$, 735.9880).

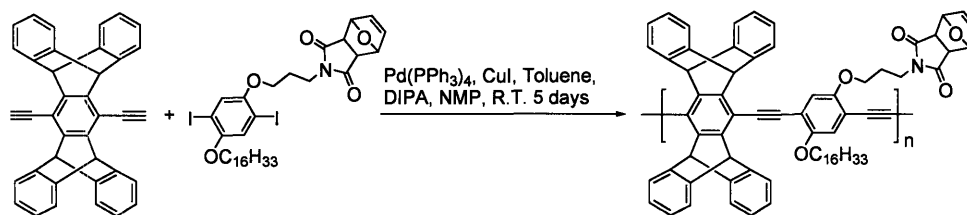


15: The dye 5(6)-ROX,SE (10.64 mg, 0.017 mmol) and cysteamine hydrochloride (4.74 mg, 0.042 mmol) were added to 2 mL DMF, followed by the addition of 9 μ L Et₃N. This solution was stirred for 24 hours and the product was purified by reverse-phase HPLC (C18 column, 10% acetonitrile in methanol). ~60% yield. HRMS: *m/z* 616.2143 (calc'd [C₃₅H₃₅N₃O₄S+Na]⁺, 616.2246).

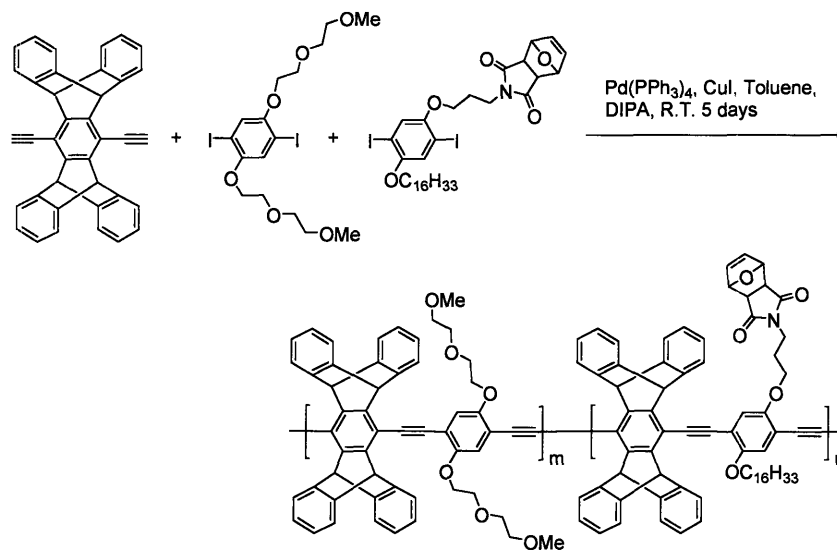


16: NaH (60 % dispersion in oil, 1.04 g, 43.4 mmol) was added to 15 mL dry THF in 250 mL round bottom flask and cooled to 0 °C. Furfuryl alcohol (2.6 mL, 30.1 mmol) was mixed with 7 mL dry THF first, then slowly added to the NaH solution by use of an addition funnel. This solution was warmed to room temperature and stirred for 2 hours. α,α' -Dibromo-*p*-xylene (3.1717 g, 12.02 mmol) was dissolved in 20 mL THF and slowly added to the furfuryl solution. This solution was heated to 60 °C overnight. The reaction was quenched over ice and the solvent removed *in vacuo*. The resulting aqueous solution was extracted twice with diethyl ether. The organic phase was washed twice with brine, dried over anhydrous magnesium sulfate, and concentrated *in vacuo*. The product was purified by column chromatography (silica gel, 3:1 hexanes:ethyl acetate). The second fraction was collected and combined: 2.94 g, 82 % yield. $^1\text{H NMR}$ (CDCl_3 , ppm, 300 MHz): 4.49 (s, 4H), 4.56 (s, 4H), 6.33 (d, 2H), 6.37 (dd, 2H), 7.36 (s, 4H), 7.44 (m, 2H). HRMS: m/z 321.1098 (calc'd $[\text{C}_{18}\text{H}_{18}\text{O}_4 + \text{Na}]^+$, 321.1097).

Polymer Synthesis.



P-1: Compounds **13** (12.32 mg, 0.026 mmol) and **7b** (19.88 mg, 0.025 mmol) were measured into a Schlenck flask. Under an inert atmosphere, a catalytic amount of palladium tetrakis(triphenyl)phosphine, Pd(PPh₃)₄, and copper iodide were added and the contents dissolved in thoroughly degassed 1:4 diisopropylamine:toluene. The solution was left to stir at room temperature for seven days. The resulting solution was washed with deionized water and the polymer precipitated in methanol. The yellow polymer was dried under vacuum.

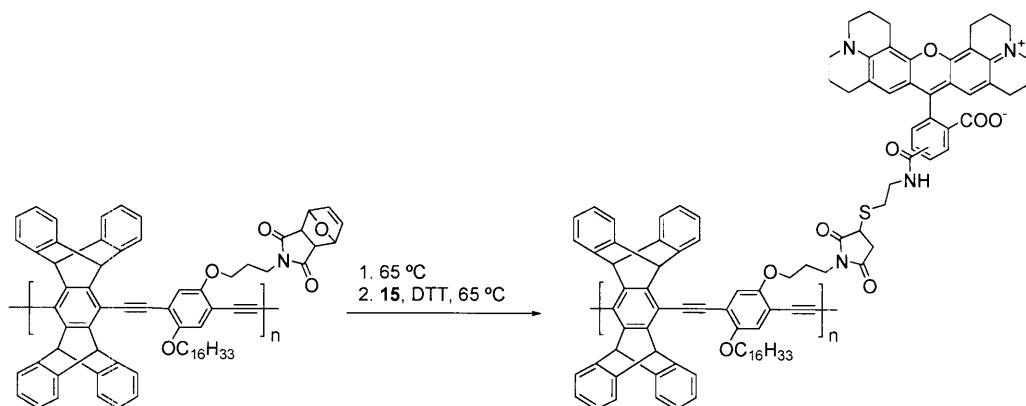


P-2: Compounds **7a** (10.35 mg, 0.0146 mmol), **13** (35.74 mg, 0.0747 mmol), and 1,4-diiodo-2,5-bis[2-(2-methoxyethoxy)ethoxy]benzene (33.11 mg, 0.0585 mmol) were placed into a Schlenk flask. Under an inert atmosphere, a catalytic amount of Pd(PPh₃)₄ and CuI were added and the contents dissolved in thoroughly degassed 1:4:5 diisopropylamine:toluene:*N*-methylpyrrolidinone. The solution was left to stir at room temperature for five days. The resulting solution was washed with deionized water and the polymer precipitated in acetone. The yellow polymer was dried under vacuum. ¹H NMR obtained at 50°C in d₈-THF on 500MHz NMR. 0.90 (br), 1.23 (br), 1.40, 1.52, 1.73, 2.32, 3.21 (br), 3.45 (m), 3.52 (br), 3.68 (m), 3.78 (br), 3.78 (m), 3.95 (m), 4.26 (br), 4.32 (m), 4.49 (m), 4.55 (br), 4.84 (m), 5.92, 6.09-6.24 (m), 6.92-6.99 (m), 7.36-7.71 (m).

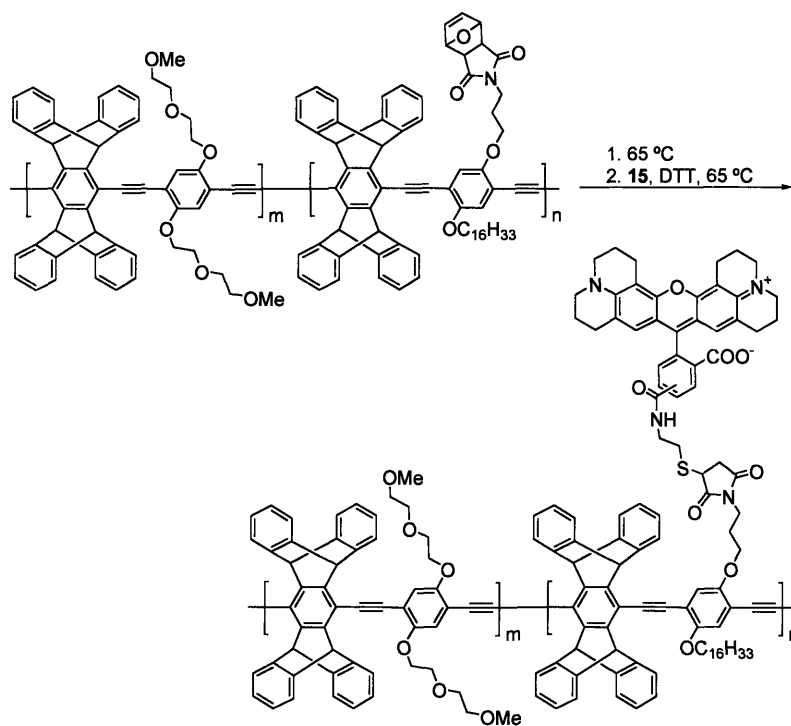
P-2 was monitored by FTIR spectroscopy before and after heating in the solid state. Three bands attributed to cyclic ether stretches disappeared after heating:

1105 cm^{-1} (C-O-C stretch), 1023 cm^{-1} ($\text{R}_{\text{alkyl}}\text{-C-O}$ stretch), and 754 cm^{-1} (vinylidene C-H).

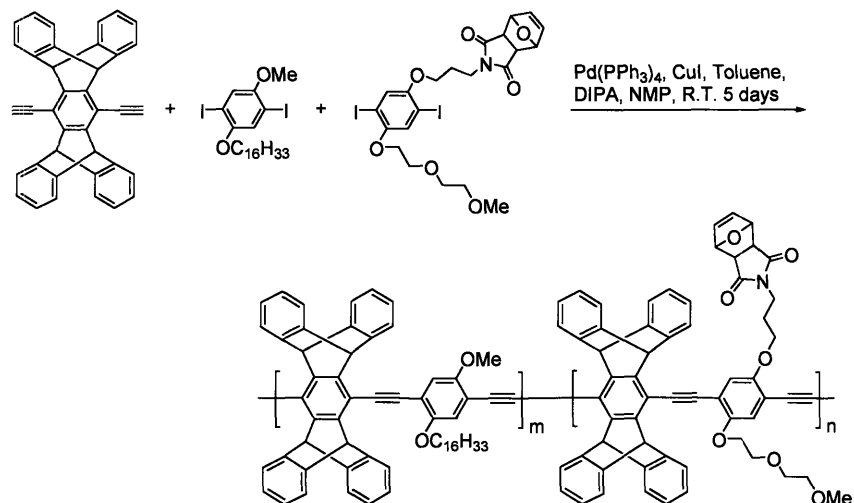
P-3: Same procedure as for **P-1**.



P-4: Polymer **P-1** (0.684 mg) was dissolved in 5 mL dry degassed THF and stirred at 65 °C overnight. Compound **15** (1.186 mg) was dissolved in 0.54 mL THF and added to the polymer solution, followed by 55 μ L of 0.1 M DTT/THF solution. This solution was heated at 65°C overnight. The resulting polymer was purified by preparative GPC using THF as the eluent.



P-5: Polymer **P-2** (1.058 mg) was dissolved in 5 mL dry degassed THF and heated while stirring to 65 °C overnight. Compound **15** (0.390 mg) was dissolved in 0.54 mL THF and added to the polymer solution, followed by 55 μ L of 0.1 M DTT solution. This solution was heated at 65°C overnight. The resulting polymer was purified by preparative GPC using THF as the eluent.



P-6: Compounds **13** (50.53 mg, 0.106 mmol), **3b** (29.55 mg, 0.049 mmol), and **12b** (34.96 mg, 0.058 mmol) were placed into a Schlenk flask. Under an inert atmosphere, a catalytic amount of Pd(PPh₃)₄ and CuI were added and the contents were dissolved in 4.25 mL of thoroughly degassed 1:4:5 diisopropylamine:toluene:NMP. The solution was stirred at room temperature for seven days. The resulting solution was washed with deionized water and saturated NH₄Cl. The polymer (29.4 mg) was precipitated in acetone. The yellow polymer was collected by centrifuge and dried under vacuum. Mn (GPC, THF eluent, polystyrene standards): 1.01 × 10⁴.

2.8 References

1. Swager, T. M., "The molecular wire approach to sensory signal amplification," *Acc. Chem. Res.* **1998**, *31*, 201-207.
2. Yang, J.-S.; Swager, T. M., "Porous Shape Persistent Fluorescent Polymer Films: An Approach to TNT Sensory Materials," *J. Am. Chem. Soc.* **1998**, *120*, 5321-5322.
3. Yang, J. S.; Swager, T. M., "Fluorescent Porous Polymer Films as TNT Chemosensors: Electronic and Structural Effects," *J. Am. Chem. Soc.* **1998**, *120*, 11864-11873.
4. McQuade, D. T.; Hegedus, A. H.; Swager, T. M., "Signal Amplification of a "Turn-On" Sensor: Harvesting the Light Captured by a Conjugated Polymer," *J. Am. Chem. Soc.* **2000**, *122*, 12389-12390.
5. Liu, B.; Gaylord, B. S.; Wang, S.; Bazan, G. C., "Effect of Chromophore-Charge Distance on the Energy Transfer Properties of Water-Soluble Conjugated Oligomers," *J. Am. Chem. Soc.* **2003**, *125*, 6705-6714.
6. Disney, M. D.; Zheng, J.; Swager, T. M.; Seeberger, P. H., "Detection of Bacteria with Carbohydrate-Functionalized Fluorescent Polymers," *J. Am. Chem. Soc.* **2004**, *126*, 13343-13346.
7. Doré, K.; Dubus, S.; Ho, H.-A.; Lévesque, I.; Brunetter, M.; Corbeil, G.; Boissinot, G.; Bergeron, M. G.; Bourdreau, D.; Leclerc, M., "Fluorescent Polymeric Transducer for the Rapid, Simple, and Specific Detection of Nucleic Acids at the Zeptomole Level," *J. Am. Chem. Soc.* **2004**, *126*, 4240-4244.

8. Aslam, M.; Dent, A., *Bioconjugation: Protein Coupling Techniques for the Biomedical Sciences*. Macmillan: London, 1999.
9. Wosnick, J. H.; Mello, C. M.; Swager, T. M., "Synthesis and Application of Poly(phenylene Ethynylene)s for Bioconjugation: A Conjugated Polymer-Based Fluorogenic Probe for Proteases," *J. Am. Chem. Soc.* **2005**, *127*, 3400-3405.
10. Roberts, M. J.; Bently, M. D.; Harris, J. M., "Chemistry for peptide and protein PEGylation," *Adv. Drug. Delivery Rev.* **2002**, *54*, 459-476.
11. Kwart, H.; King, K., "The Reversible Diels-Alder or Retrodiene Reaction," *Chem. Rev.* **1968**, *68*, 415-447.
12. Goussé, C.; Gandini, A.; Hodge, P., "Application of the Diels-Alder Reaction to Polymers Bearing Furan Moieties. 2. Diels-Alder and Retro-Diels-Alder Reactions Involving Furan Rings in Some Styrene Copolymers," *Macromolecules* **1998**, *31*, 314-321.
13. Gheneim, R.; Perez-Berumen, C.; Gandini, A., "Diels-Alder Reactions with Novel Polymeric Dienes and Dienophiles: Synthesis of Reversibly Cross-Linked Elastomers," *Macromolecules* **2002**, *35*, 7246.
14. Chen, X.; Dam, M.; Ono, K.; Mal, A.; Shen, H.; Nutt, S.; Sheran, K.; Wudl, F., "A Thermally Re-mendable Cross-Linked Polymeric Material," *Science* **2002**, *295*, 1698-1702.
15. Chen, X.; Wudl, F.; Mal, A.; Shen, H.; Nutt, S., "New Thermally Remendable Highly Cross-Linked Polymeric Materials," *Macromolecules* **2003**, *36*, 1802-1807.

16. Stille, J.; Plummer, L., "Polymerization by the Diels-Alder Reaction," *J. Org. Chem.* **1961**, *26*, 4026.
17. Sonogashira, K.; Tohda, Y.; Hagihara, N., "Convenient synthesis of acetylenes. Catalytic substitutions of acetylenic hydrogen with bromo alkenes, iodo arenes, and bromopyridines. *Tetrahedron Lett.* **1975**, *16*, 4467.
18. Heck, R. F., "Palladium-Catalyzed Vinylation of Organic Halides," *Organic Reactions* **1982**, *27*, 345-390.
19. Flitsch, W.; Schindler, S. R., "Alkenylation of Imides and Activated Amides," *Synthesis* **1975**, *11*, 685-700.
20. Swager, T. M.; Gil, C. J.; Wrighton, M. S., "Fluorescence Studies of Poly(*p*-phenyleneethynylene)s: The Effect of Anthracene Substitution," *J. Phys. Chem.* **1995**, *99*, 4886-4893.
21. McQuade, D. T.; Pullen, A. E.; Swager, T. M., "Conjugated polymer-based chemical sensors," *Chem. Rev.* **2000**, *100*, 2537-2574.
22. Cowie, J. M. G., *Polymers: Chemistry & Physics of Modern Materials*. 2nd ed.; Blackie Academic & Professional; Chapman & Hall: London, 1997.
23. Snow, A. W.; Foos, E. E., "Conversion of Alcohols to Thiols via Tosylate Intermediates," *Synthesis* **2003**, 509-512.

Chapter 3:

Dendritic Quenchers

3.1 Introduction

Dendrimers^{1, 2} are unique synthetic macromolecules having a broad range of applications in the physical, chemical, and biological sciences. Branched and tree-like, dendrimers are formed when stitching together layers of highly regular branched monomers from a central core molecule. The synthesis of dendrimers can be carried out in a convergent³ or divergent⁴ fashion. Each successive addition of a monomer layer results in a new “generation” of the polymer. Dendrimers of a few generations have molecular weights resembling those of step-growth polymers, and thus, along with the presence of an identifiable repeat unit, higher generation dendrimers are considered polymers. The outermost generation contains the peripheral or terminal groups. The branching functionality of the core and the monomers can differ, thereby allowing for the formation of a diverse range of polymers.⁵⁻⁷ The flexibility afforded in the design of dendrimers has resulted in their incorporation into many varied applications that include catalysis,^{8, 9} chromatography,¹⁰ and for use as nanoscopic containers.¹¹ The primary interest in dendrimers, however, has been in the biological fields, and more specifically, in drug delivery.¹²⁻²⁰

The exponential growth of terminal groups with each additional generation presents an opportunity to produce a polyfunctional fluorescence quenching molecule to be used in sensor schemes. Our interest in these possibilities leads to a key question: how will different generations of a dendrimer family containing terminal quenching groups affect PPE emission? To address this question, a

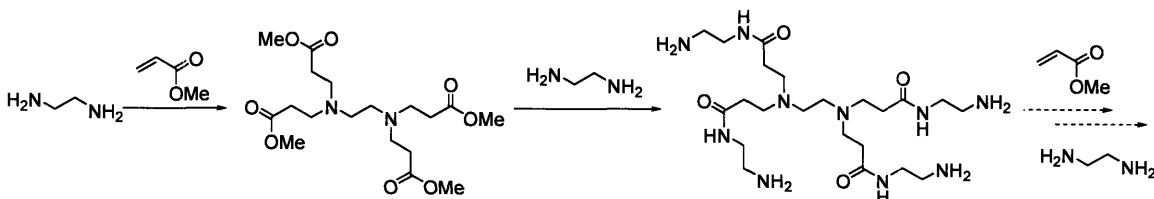
series of dendritic quenchers (DQ) was prepared and the Stern-Volmer quenching constants were obtained both in solution and as coatings on particles. Our interest in dendrimers is to modify the outer generation into compounds capable of quenching polymers, thereby forming a dendritic quencher.

3.2 Dendritic Quencher Synthesis

3.2.1 PAMAM Dendrimers

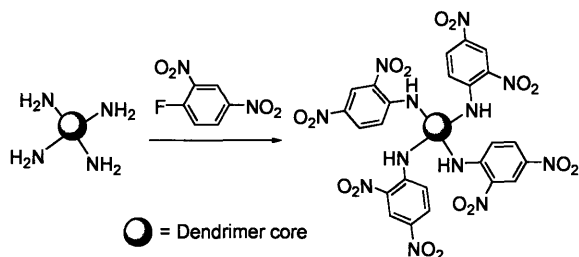
The first DQ target was based on the polyamidoamine (PAMAM) dendrimer as the core. PAMAM dendrimers, also known as starburst dendrimers, are highly structured oligomeric and polymeric compounds produced using a divergent approach by reacting a core molecule, such as ethylenediamine, with branches, such as methyl acrylate. This is followed by exhaustive amidation of the terminal esters with ethylenediamine, resulting in an outer shell of amines. Each amine, in turn, can react with two methyl acrylates to produce a branch, and repeating this processes builds additional dendrimer generations as illustrated in Scheme 1.

Scheme 1 Synthesis of PAMAM dendrimers.



The outer shell of amine groups can be easily functionalized with 2,4-dinitrophenyl (DNP) groups via a S_NAr reaction by addition of the Sanger reagent, 2,4-dinitrofluorobenzene (Scheme 2). DNP is a well-established quenching agent which has been studied extensively in our group.²¹ It quenches through an electron transfer quenching mechanism through static interactions as explained in Chapter 1.

Scheme 2 Modification of terminal amines to DNP groups to form DQ.



To broaden the applications for which these DQ could be used, a handle is needed on the molecule in order to affix it to surfaces, targets, and tethers, including those of biological relevance such as DNA. This requires leaving one terminal amine group unfunctionalized while modifying the remaining groups into quenchers. Differentiating between identical surface groups poses a definite challenge in conventional solution chemistry.

We implemented a strategy that takes advantage of site localization by immobilizing the dendrimers on solid supports. The relative size of the beads used in this method and the dendrimers, as well as the loading of the amine

reactive functional groups on the beads, can limit the number of terminal groups from one molecule that can bind to the bead. The beads selected contained aldehyde moieties that readily react with the terminal amine groups of PAMAM dendrimers. Once the dendrimer was affixed to the bead and after addition of the Sanger reagent to all of the free amines, the modified dendrimer could be cleaved from the bead under relatively mild acidic conditions. The beads used for all the work with PAMAM dendrimers were 4-benzyloxybenzaldehyde polystyrene (200-400 mesh) with a 3.2 mmol/g loading of aldehyde groups (Novabiochem #01-64-0182).

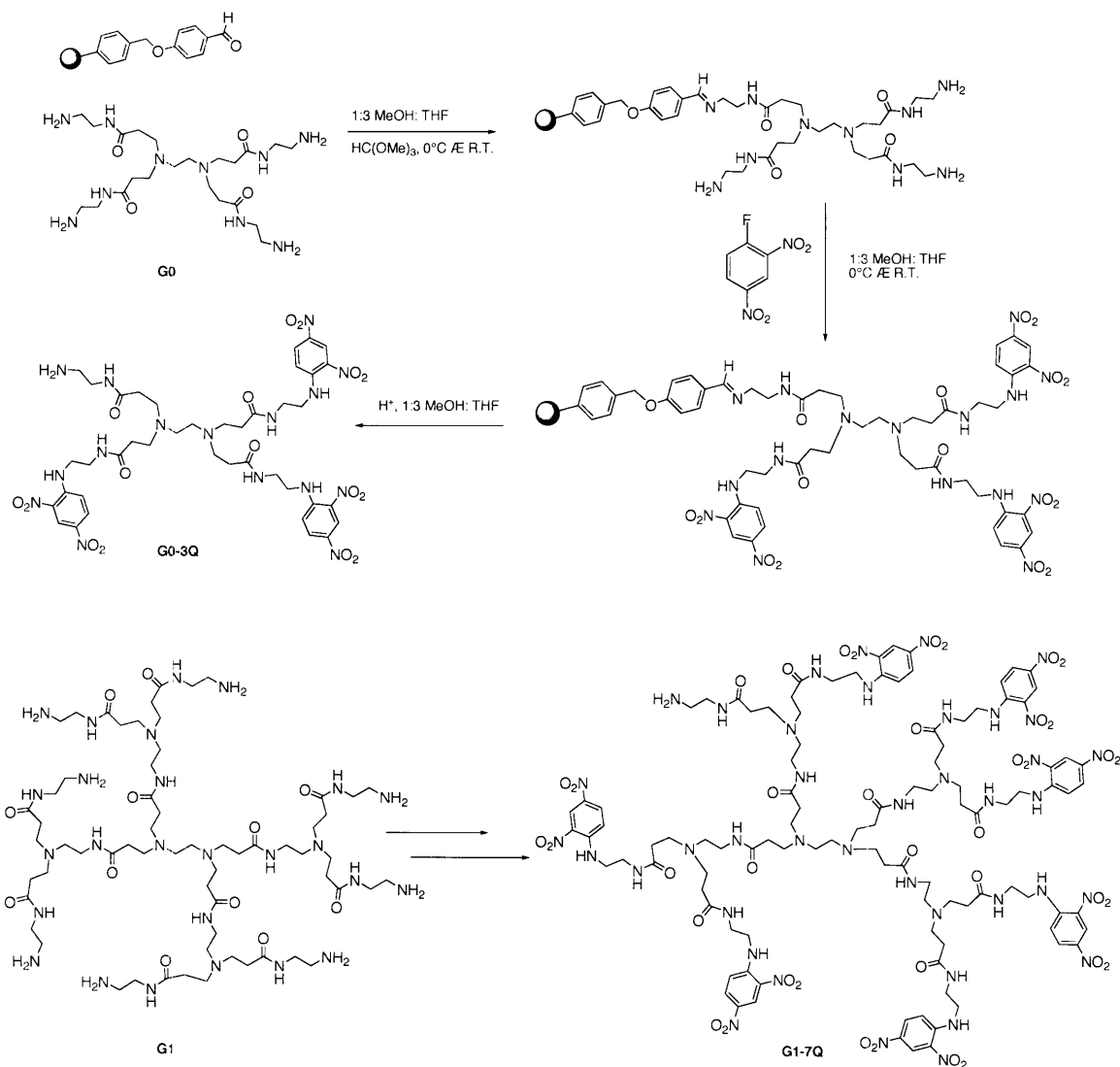
Several conditions were explored to optimize this process, namely reaction temperatures, solvent ratios, and the acid used, until the target was finally obtained (Scheme 3). The beads were swollen in a 1:3 MeOH:THF mixture for 4 hours, cooled to 0 °C, followed by the addition of PAMAM-G0 or PAMAM-G1 solution (20 % weight solution) and trimethylorthoformate as a dehydrating agent²² to promote immobilization of the dendrimers onto the beads. The beads were then washed repeatedly with mixtures of MeOH and THF until the solution no longer tested positive for amines using picrylsulfonic acid.

The beads were then suspended again in 1:3 MeOH:THF and then 2,4-dinitrofluorobenzene was introduced (2 equivalents/free amine) with pyridine as a base. The solution turned an intense yellow-orange color immediately upon addition of the Sanger reagent. The reaction mixture was then stirred for 16

hours, and the resultant reddish-orange beads were washed with copious amounts of cooled 1:3 MeOH:THF until the solution was colorless. Trifluoroacetic acid was added to the beads in 1:3 MeOH:THF to cleave the dendrimers from the solid support and stirred at room temperature for an additional 16 hours.

The solution collected for **G0** contained a mixture of compounds. This included the desired target with one free amine and three DNP (Q) groups (**G0-3Q**) mixed with compounds with two DNP groups (**G0-2Q**), one DNP group (**G0-1Q**), and the completely unmodified **G0**, as determined by electrospray ionization mass spectrometry. These impurities were removed by reverse phase HPLC with a gradient of 10% acetonitrile in 0.1 % trifluoroacetic acid/H₂O to 50 % acetonitrile. The last peak to elute was identified as G0-3Q and it was isolated by lyophilization. The target compound of **G1-7Q** was never isolated, only dendrimers with less than 7 DNP units were observed from **G1-1Q** to **G1-5Q**. The crude sample was purified by reverse phase HPLC, and several peaks corresponded to fragments of **G1**, indicating the relative instability of the compound.

Scheme 3 Synthesis of G0-3Q and structure of G1-7Q.



The purified samples were studied by matrix assisted laser desorption ionization-time of flight mass spectrometry (MALDI-ToF). Initial studies utilizing the matrices α -cyano-4-hydroxy cinnamic acid (α CHC) or 2,5-dihydroxybenzoic acid (DHB) resulted in significant fragmentation of the dendrimers. In order to circumvent this and improve resolution, fucose was included with DHB to form a “cold-matrix”.²³⁻²⁵ While the matrix α CHC did not show any improvement, after

the addition of fucose, positive results were obtained with DHB-fucose. The MALDI-ToF spectrum obtained for purified **G0-3Q** in DHB-fucose, (Figure 1), shows the parent compound at 1015 g/mol and the two fragmentation halves at 438 g/mol and 576 g/mol as indicated. The step-wise loss of oxygen from the nitro groups of DNP is the reason for the peaks observed decreasing by 16 g/mol from the parent peaks.²⁶

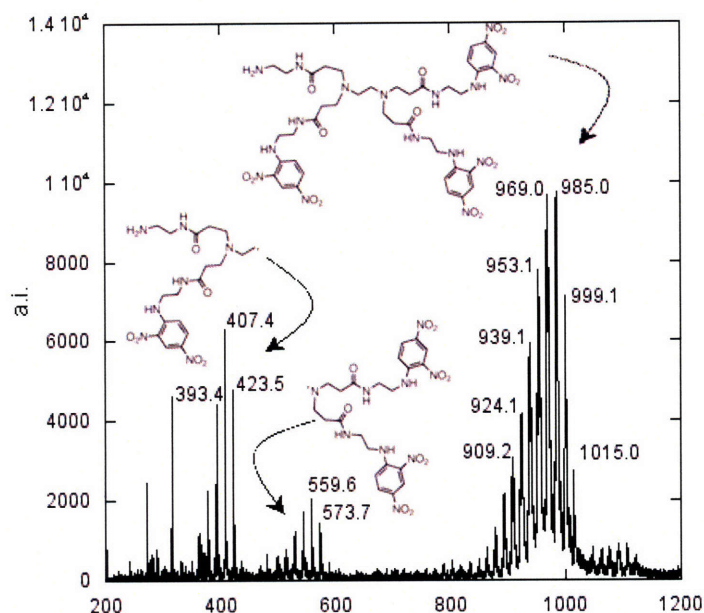


Figure 1 MALDI-ToF spectrum for G0-3Q in DHB-Fucose.

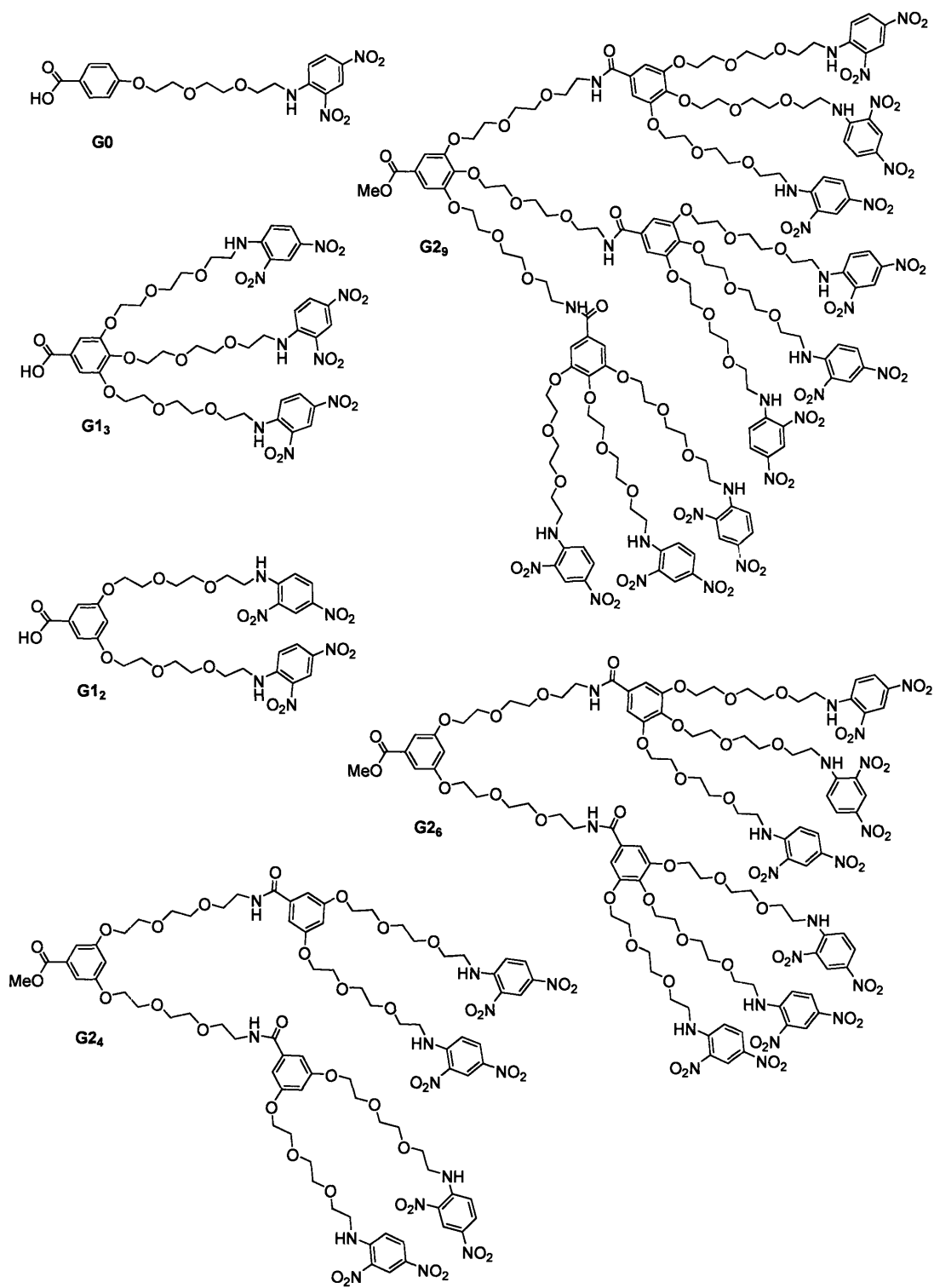
In further exploring matrices, it was discovered that 2-(4'-hydroxyphenylazo)benzoic acid (HABA) performed well without the need to include fucose. For all subsequent MALDI-ToF obtained, HABA was used as the matrix without any additives.

During the course of preparing and purifying the PAMAM-based dendrimers, it became apparent that these compounds were not stable unless kept below 4 °C. At elevated temperatures, branches of the dendrimer would fragment off, undergoing a reverse Michael addition. If these dendritic quenchers are to be incorporated into real-world sensors, increased thermal stability is needed to ensure long-term stability of a device. In combination with the fact that these compounds were difficult to isolate in high yields, a new DQ core was devised.

3.2.2 DQ Core with Peptide Linkages

In order to overcome the instability and relative difficulty of isolating the PAMAM-based dendritic quenchers, a new DQ family was devised inspired by the convergent synthesis of amino acid based dendrimers (Scheme 4).²⁷ The dendrimers are built with 3,4,5-trihydroxybenzoic acid or 3,5-dihydroxybenzoic acid as branching points and 2-[2-(2-aminoethoxy)ethoxy]ethanol as branches, all connected by amide linkages. The terminal groups are functionalized to DNP groups. The model compound, **G0**, contains only one branch and one quencher unit. The first and second generations are labeled with a subscript indicating the total number of branches in the outer shell. Hence, **G1₃** contains 3 terminal quencher units, while **G1₂** only two.

Scheme 4 New DQ family: Structures of **G0**, **G1₂**, **G1₃**, **G2₄**, **G2₆**, and **G2₉**.



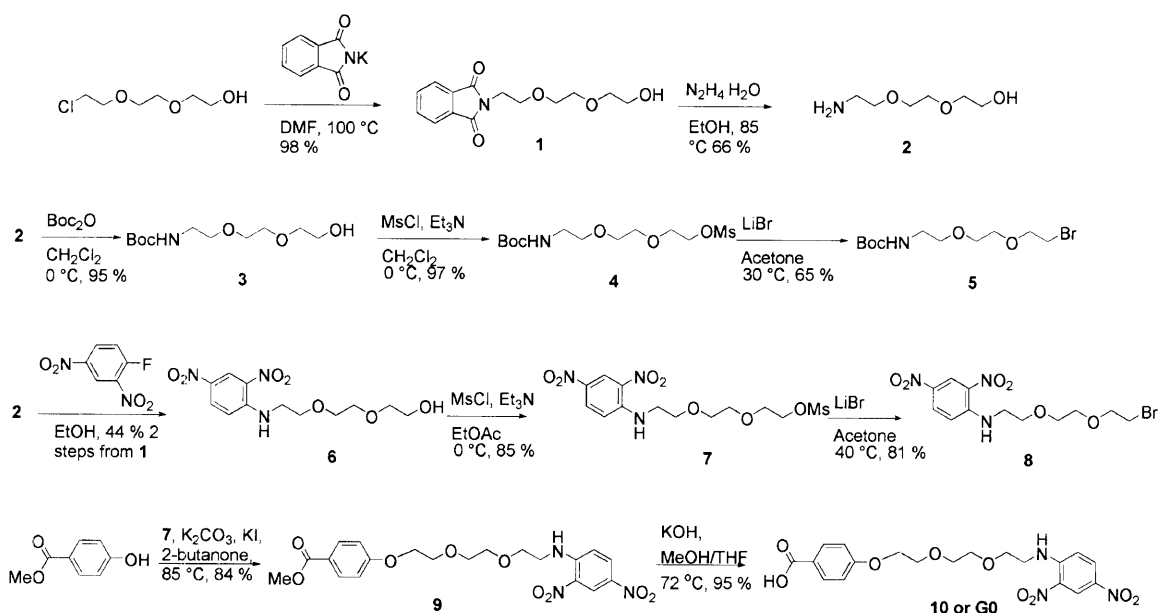
The convergent synthesis of these compounds is illustrated in Schemes 5-7. Compound **1** was prepared from potassium phthalimide and 2-[2-(2-chloroethoxy)ethoxy]ethanol in DMF. This was subsequently reduced with hydrazine to form 2-[2-(2-aminoethoxy)ethoxy]ethanol, **2**. This short chain was then modified to be either a terminal quenching group or the amine protected to be used later as a linking group. For branching molecules, the amine group was protected by introducing di-*tert*-butyl dicarbonate, Boc₂O, to a solution of **2** in methylene chloride to yield **3**.²⁸ The terminal hydroxyl group was converted to the bromide, **5**, by way of the mesylate, **4**. To form 1-to-3 and 1-to-2 branching units, Williamson ether synthesis with methyl-3,4,5-trihydroxybenzoate and **5** affords **11**, while the use of methyl-3,5-dihydroxybenzoate and **5** yields **15** (Scheme 6). These can then be converted to the amine form (**12** and **16**) in ether saturated with gaseous hydrochloric acid.

The introduction of 2,4-dinitrofluorobenzene to **2** results in the formation of **6** (Scheme 5). This is converted to the bromide, **8**, again by way of the mesylate, **7**.

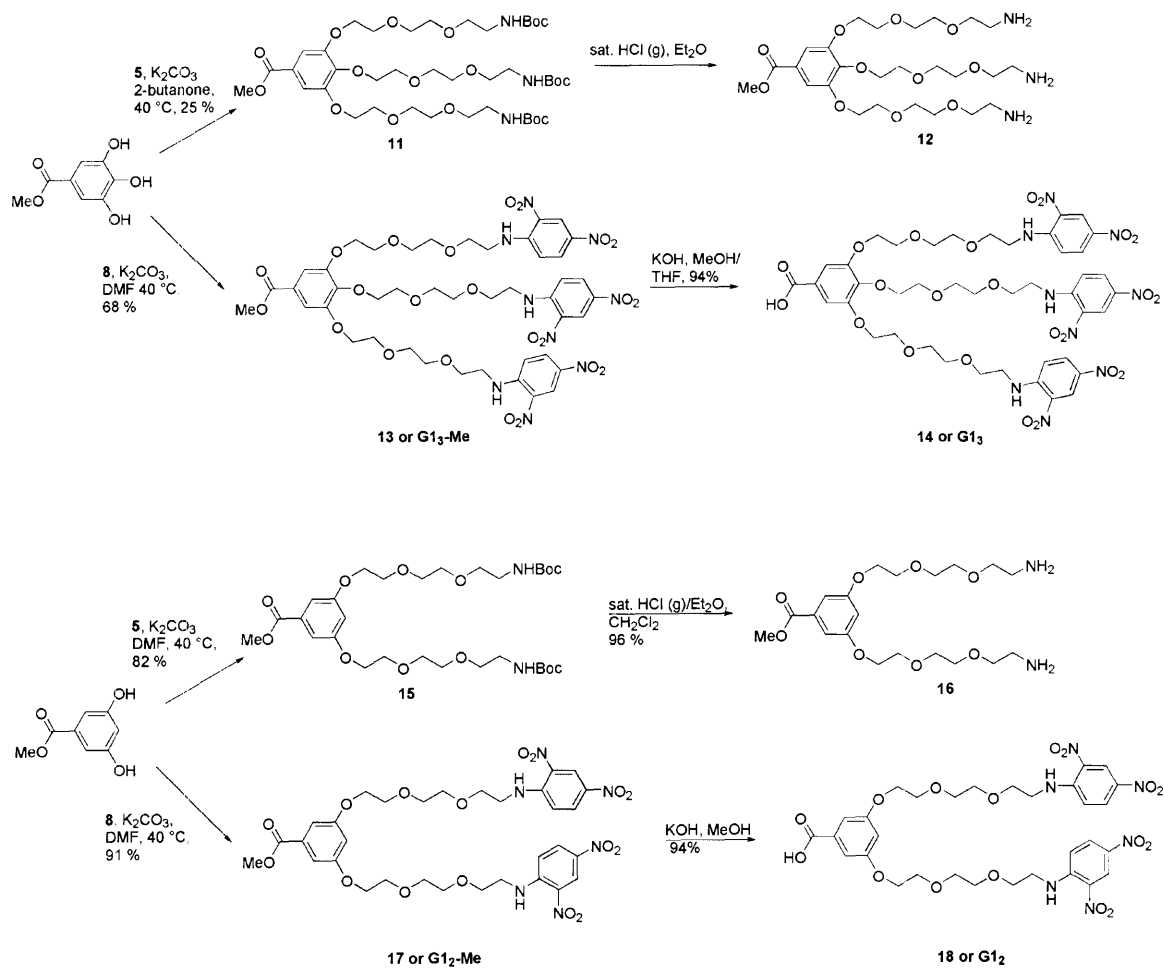
G0, **G1₂**, and **G1₃** are all prepared by Williamson ether synthesis in the presence of potassium carbonate in DMF between **8** and methyl-4-hydroxybenzoate, methyl-3,5-dihydroxybenzoate, and methyl-3,4,5-trihydroxybenzoate, respectively. The second generation compounds (Scheme 7) were prepared by mixing the 1-to-2 and 1-to-3 units in the presence of

coupling agents *O*-(Benzotriazol-1-yl)-*N,N,N,N*-tetramethyluronium hexafluorophosphate (HBTU), 1-hydroxybenzotriazole (HOBt), and an amine base to obtain **G24**, **G26**, and **G29**. Compound **G29** was not obtained in sufficient yields for complete characterization; the main product contained only two of the three branches. The inability to form the compound may reflect the more sterically demanding steric bulk of nine DNP groups. **G0**, **G12**, and **G13** were saponified to the acid from the methyl ester to increase solubility in aqueous environments. Compounds **G24** and **G26** were used directly as the methyl esters in all quenching experiments.

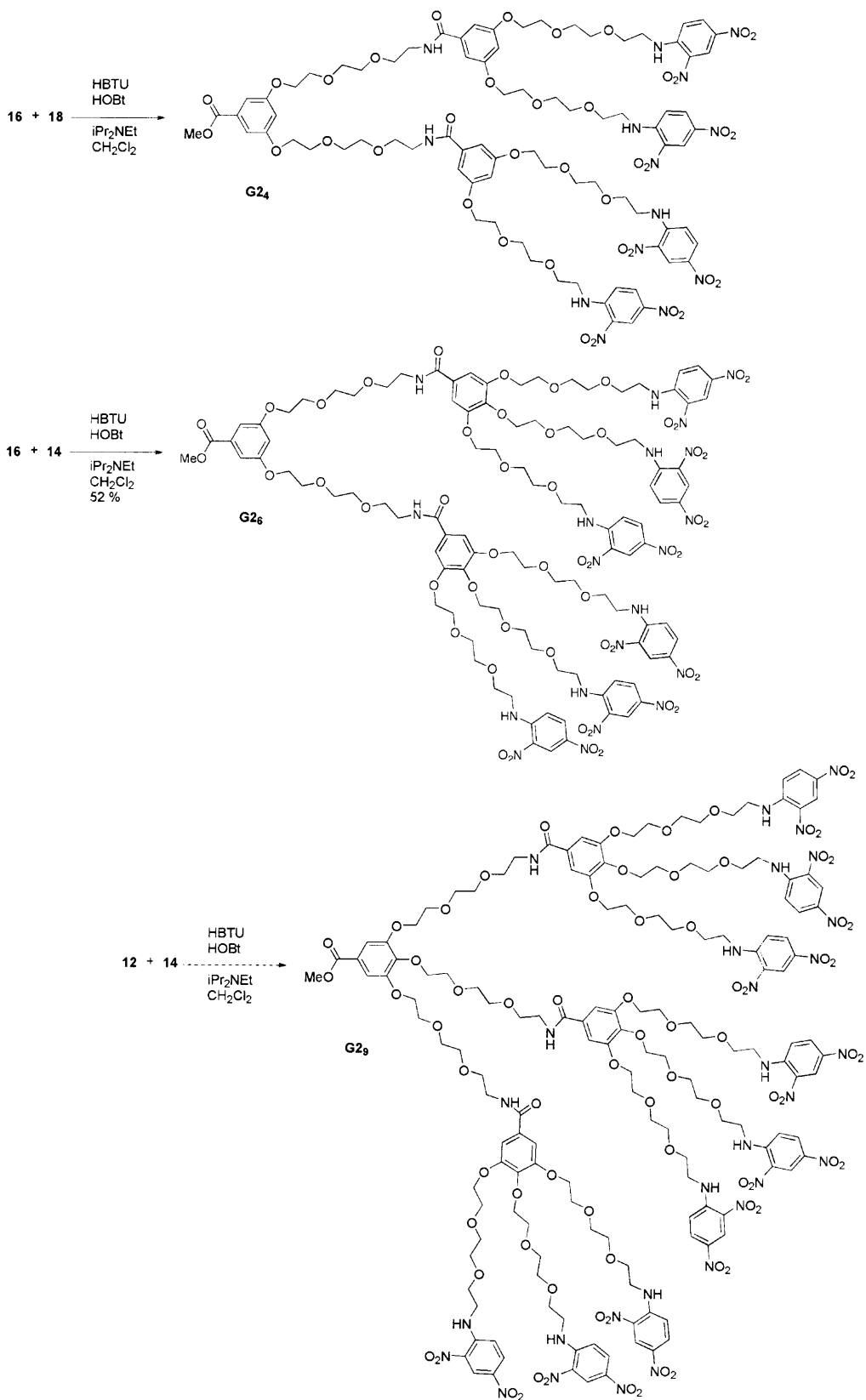
Scheme 5 Preparation of linking and quenching branches, as well as the preparation of **G0**.



Scheme 6 Preparation of branching compounds and first generation DQ.



Scheme 7 Preparation of second generation DQ.



3.3. Quenching Effects of DQ on Solution and Solid-state PPEs

3.3.1 DQ Extinction Coefficients

The extinction coefficients for the quenchers were obtained in triplicate in DMF at 357 nm and the average values are tabulated below.

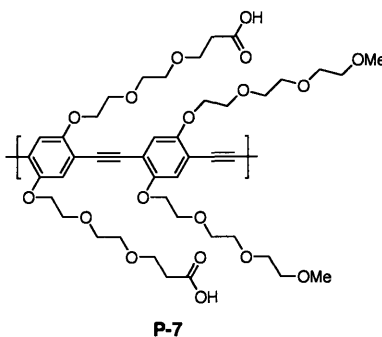
Table 1 Extinction values determined for DQ in DMF at 357 nm.

Dendrimer	MW (g·mol ⁻¹)	ϵ_{357} (DMF, L·mol ⁻¹ ·cm ⁻¹)
G0	435.38	17,160 ± 20
G1₂	748.65	31,630 ± 170
G1₃	1061.91	42,800 ± 190
G2₄	1891.76	57,180 ± 180
G2₆	2518.29	159,630 ± 230

3.3.2 Quenching Studies in Solution

The quenching effects of the dendritic quenchers on polymer **P-7** were determined in solution using three separate buffers and in DMF (Scheme 8). The buffers selected were tris(hydroxymethyl)aminomethane (Tris: 20 mM Tris pH 7.4), tris-buffered saline (TBS: 20 mM Tris pH 7.4, 150 mM NaCl, 5 mM CaCl₂), and a common buffer used for real-time polymerase chain reactions (PCR: 50 mM KCl, 1.5 mM MgCl₂, 10 mM Tris pH 8.3).

Scheme 8 Carboxylic acid-PPE, P-7.



Initially, the dendrimers were added directly to the buffers to prepare stock quencher solutions. Unfortunately, this required excessive sonication and heat to coax the dendrimers into solution and compromised the accuracy of the stock solution concentration. Even the addition of up to 5% THF or DMF did not eliminate all DQ precipitate from solution. To overcome this, stock DMF solutions with concentrations of 0.5 mM of each quencher were used in the preparation of all subsequent stock solutions. A stock **P-7** solution was prepared in each buffer and in DMF with a polymer concentration that corresponded to a maximum absorption intensity for the polymer of approximately 0.1 au. The two solutions were then used to prepare a final DQ/**P-7** solution with a [DQ] of 0.01 mM and 2 % DMF. The DQ solution was prepared with the **P-7** solution to ensure that any decreases in fluorescence intensity were not due to dilution from DQ aliquots added. The absorbance and fluorescence spectra were recorded after the addition of each aliquot and each experiment was repeated a minimum of three times.

In order to ensure that any reductions in fluorescence were in fact due to quenching and not from an inner filter effect since the DQ are strongly absorbant, changes in absorbance at the polymer excitation wavelength were monitored. If the absorbance changed by greater than 10%, a correction was used to determine the actual fluorescence intensity.²⁹ The final quencher concentrations were generally sufficiently dilute so that this was not needed. To determine K_{SV} , the Stern-Volmer quenching constants, F_0/F were plotted against the DQ concentration. The K_{SV} values were determined from the linear portions of the plots. At high quencher concentrations, the values of F_0/F reach saturation, as no increased quenching is observed with further additions of DQ. The values obtained are shown below in Figure 2 as a function of quencher and Figure 3 as a function of buffer/solvent. The Stern-Volmer constants are listed in Table 2. Quenching constants could not be determined in PCR buffer for the second generation dendrimers due to poor solubility.

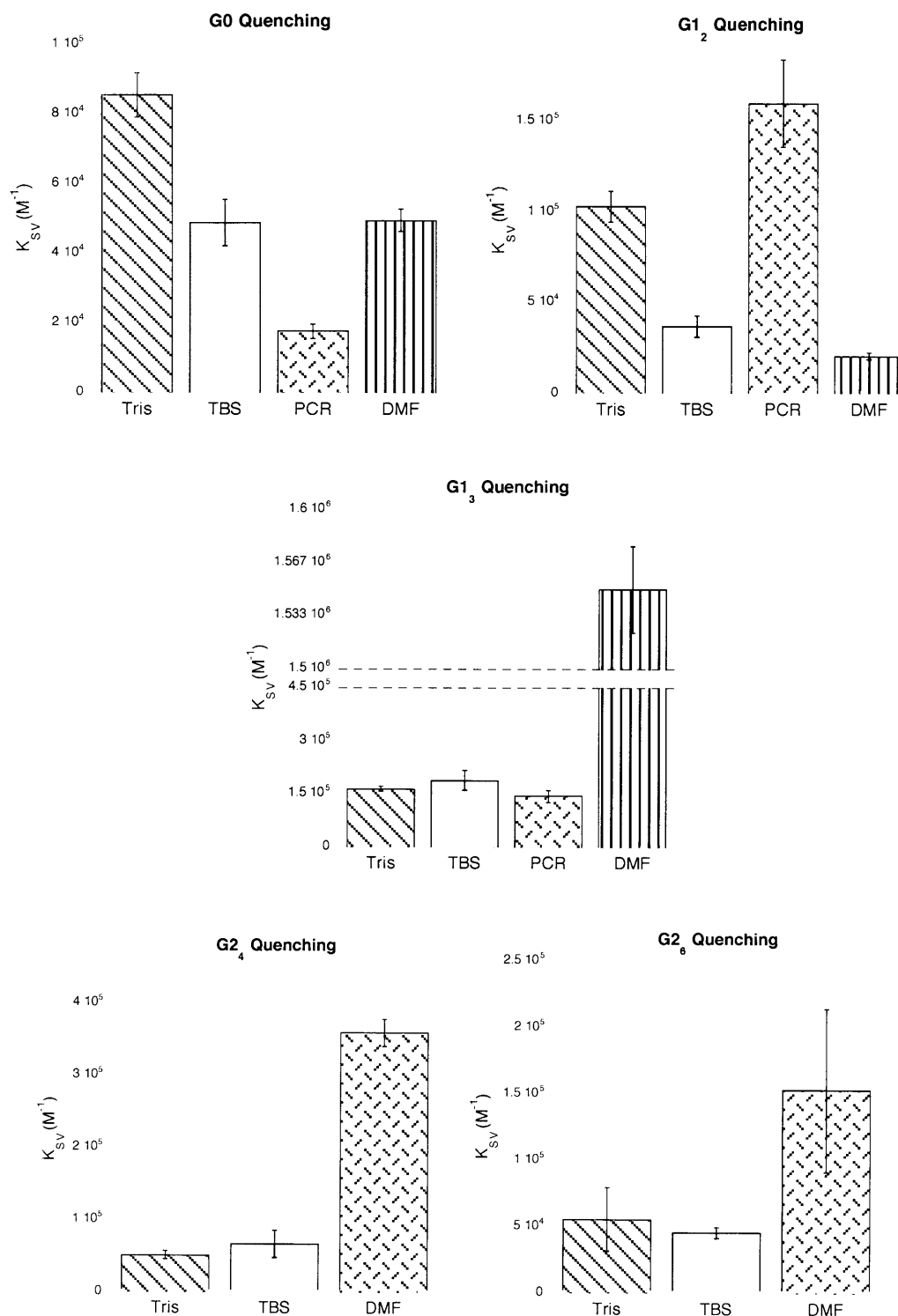


Figure 2 Stern-Volmer quenching constants obtained in Tris, TBS, PCR (**G0** and **G1** only) and DMF for **G0**, **G1₂**, **G1₃**, **G2₄**, and **G2₆** grouped by quencher.

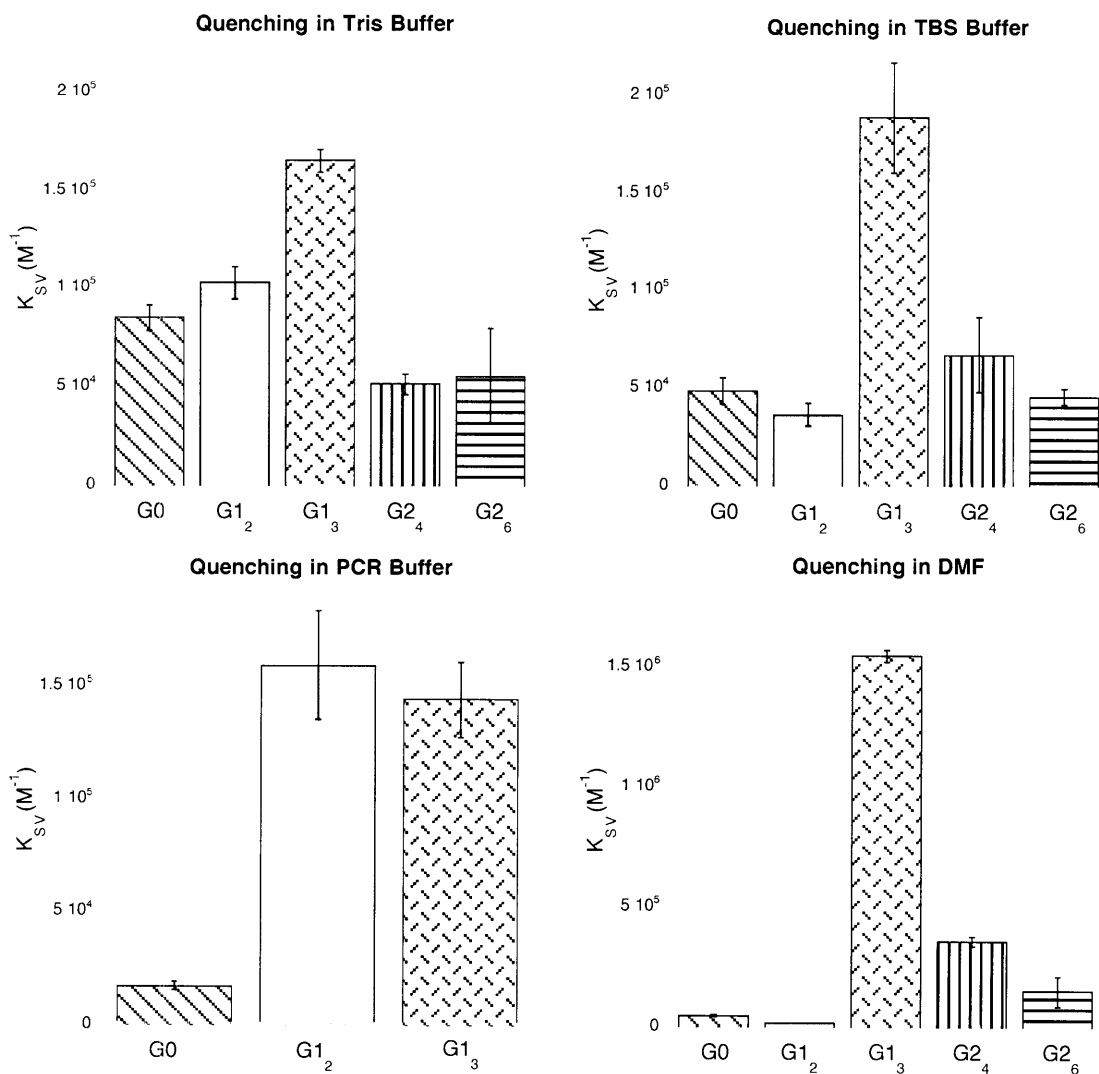


Figure 3 Stern-Volmer quenching constants obtained in Tris, TBS, PCR (G0 and G1 only) and DMF for G0, G1₂, G1₃, G2₄, and G2₆ grouped by buffer/solvent.

Table 2 Quenching constants obtained in solution for DQ family.

Dendrimer	Buffer/Solvent	$K_{SV} (M^{-1})$
G0	Tris	$(8.6 \pm 0.6) \times 10^4$
	TBS	$(4.9 \pm 0.2) \times 10^4$
	PCR	$(1.8 \pm 0.2) \times 10^4$
	DMF	$(5.0 \pm 0.3) \times 10^4$
G1₂	Tris	$(10.3 \pm 0.8) \times 10^4$
	TBS	$(3.7 \pm 0.6) \times 10^4$
	PCR	$(1.6 \pm 0.2) \times 10^5$
	DMF	$(2.1 \pm 0.2) \times 10^4$
G1₃	Tris	$(16.5 \pm 0.6) \times 10^4$
	TBS	$(18.9 \pm 0.3) \times 10^4$
	PCR	$(1.4 \pm 0.2) \times 10^5$
	DMF	$(1.6 \pm 0.5) \times 10^6$
G2₄	Tris	$(5.2 \pm 0.5) \times 10^4$
	TBS	$(6.7 \pm 0.4) \times 10^4$
	DMF	$(3.6 \pm 0.2) \times 10^5$
G2₆	Tris	$(5.6 \pm 0.7) \times 10^4$
	TBS	$(4.6 \pm 0.4) \times 10^4$
	DMF	$(1.5 \pm 0.6) \times 10^5$

3.3.3 Quenching of PPE-Coated Microspheres

Initial studies into the quenching ability of the DQ family with polymers in the solid-state have been investigated in collaboration with another group member, Ms. Jessica Liao. This method uses Europium(III)-polystyrene microspheres, wherein the Eu^{+3} emission is used as an internal reference. These spheres were coated with a carboxylic acid-PPE and the corresponding quenching response as a result of aliquot addition was monitored (Figure 4). The preliminary results were promising, revealing a distinct trend with increasing quencher units per molecule, as well as amplified quenching. Furthermore, the quenching appears to follow an exponential relationship with the number of DNP groups per molecule.

The DQ clearly provide amplified quenching, and in conjunction with the amplified response obtained with PPEs, the overall sensitivity of a sensor system based on these elements will be increased. In addition, fewer DQ groups will be needed to elicit a dramatic response.

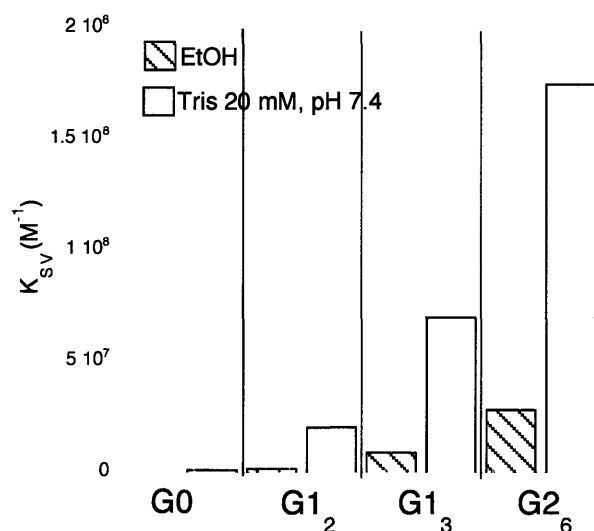


Figure 4 Quenching with DQ of PPE-coated microspheres.

3.4 Discussion

The synthesis of the second family of DQ was straightforward and its modularity allows for a broad range of DQs to be prepared. The DQs were soluble in aqueous buffer after an initial DMF stock solution was prepared. One unexpected trend was the observation that solution quenching appears to peak with **G1₃** and then decreases with **G2₄** and **G2₆**. It is interesting to note that in some cases, the fluorescence intensity increased slightly with the initial aliquots before quenching began. This indicates that two competing forces are possibly at play, quenching and solubility. The addition of the dendrimers, while

quenching fluorescence, may also be increasing the solubility of the polymer strands in solution. The lack of this observation with the particle quenching experiments where polymer solubility is not an issue, lends credence to this theory. Another explanation for the drop in value for K_{SV} for **G 2₄** and **G 2₆** compared with **G 1₃** is that in solution, no advantage is gained from increasing the number of quenchers beyond three per molecule. The sphere of quenching perhaps begins to overlap with larger molecules.

Ultimately, any sensing platform would have the polymers in the solid-phase for practical reasons, and so the response observed with the microspheres is extremely encouraging. The amplified quenching response in the solid state also indicates that fewer quenchers would be required to gain a response. For example, with the molecular beacon-PPE system, fewer strands of DNA modified at one terminus with a DQ would need to be grafted to a PPE, simplifying production and also reducing overall cost.

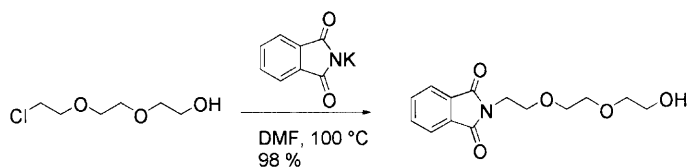
3.5 Conclusion

A dendritic quencher family was designed initially using PAMAM dendrimers as the core. These molecules proved difficult to isolate and were unstable over long periods of time and with exposure to heat. A second DQ family was devised using more stable peptide linkages between the generations. These compounds were prepared and their quenching properties with PPEs both in solution and in the solid phase were investigated, with the particle quenching

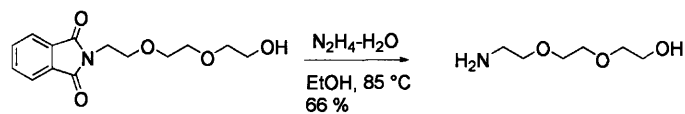
showing much promise for incorporation into a sensing device.

3.6 Experimental Section

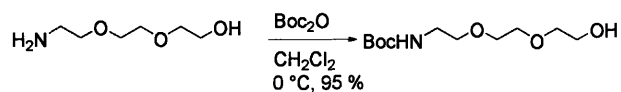
All solvents and chemicals were used as received, unless otherwise noted. NMR spectra were recorded on either a Varian 300 MHz or a Varian 500 MHz spectrometer. UV/Vis spectra were recorded on an Agilent 8453 diode-array spectrophotometer and corrected for background signal with a solvent-filled cuvette. Emission spectra were acquired on a SPEX Fluorolog- τ 3 fluorometer (model FL-321, 450 W Xenon lamp) using right angle detection. The absorbance of all samples was kept to 0.1 au in order minimize artifacts. All buffers were prepared using Millipore water.



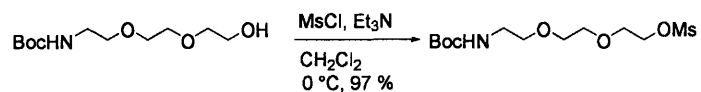
1: 2-[2-(2-chloroethoxy)ethoxy]ethanol (10.56 g, 62.6 mmol) and potassium phthalate (12.76 g, 68.9 mmol) were stirred at 100 °C in DMF for 2 days. The reaction mixture was cooled and the white precipitate removed by filtration, followed by removal of DMF. The oily residue was dissolved in DCM and washed repeatedly with water. The organic phase was dried over anhydrous MgSO_4 and concentrated *in vacuo* to yield a yellow oil that slowly solidified. 97 % yield. ^1H NMR (CDCl_3 , 500 MHz, ppm): 2.22 (br, 1H), 3.53 (m, 2H), 3.60 (m, 2H), 3.66 (m, 4H), 3.76 (t, 2H), 3.91 (t, 2H), 7.71 (m, 2H), 7.85 (m, 2H); ^{13}C NMR (CDCl_3 , 125 MHz, ppm): 37.33, 61.89, 68.08, 70.12, 70.50, 72.59, 123.44, 132.21, 134.15, 168.53. HRMS: m/z 302.10088 (calc'd $[\text{C}_{14}\text{H}_{17}\text{NO}_5+\text{Na}]^+$, 302.09989).



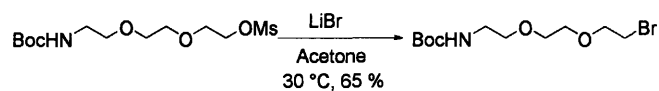
2: Compound **1** (16.81 g, 60.2 mmol) was dissolved in 280 mL ethanol. Hydrazine monohydrate (3.2 mL, 66.0 mmol) was added and the solution was stirred at 85 °C. The reaction mixture was cooled to room temperature and the white precipitate removed by filtration. The solution was concentrated and the residue dissolved in DCM and washed with water. The organic phase was dried over anhydrous MgSO₄ and concentrated *in vacuo* to yield a yellow oil. A second extraction was performed with diethyl ether to remove phthalate salts. ~65 % yield. This compound was difficult to purify and was used directly in subsequent reactions. ¹H NMR (CDCl₃, 500 MHz, ppm): 1.22 (t, 1 H), 2.71 (br), 2.89 (t, 2H), 3.55 (t, 2H), 3.60 (m 2H), 3.63 (m, 2H), 3.66 (m, 2H), 3.72 (m, 2H). HRMS: *m/z* 150.11210 (calc'd [C₆H₁₅NO₃+H]⁺, 150.11247).



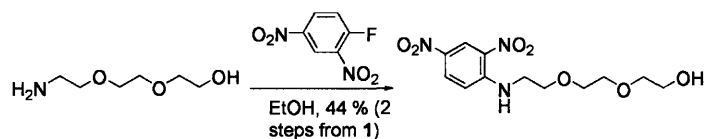
3: Compound **2** (4.04 g, 27.1 mmol) was dissolved in 15 mL DCM and cooled to 0 °C. Di-*t*-butyl dicarbonate, Boc₂O (6.20 g, 28.4 mmol) was dissolved in 20 mL DCM and slowly added to the cooled stirring solution of **2**. The solution was then allowed to warm to room temperature. The reaction mixture was washed with water. A white precipitate formed in the aqueous fraction, which was isolated and washed with DCM. This was combined with the original DCM fraction and dried over anhydrous MgSO₄. The solution was dried *in vacuo* to yield a yellow oil. 83 % yield. ¹H NMR (CDCl₃, 500 MHz, ppm): 1.43 (s, 9H), 3.32 (m, 2H), 3.55 (m, 2H), 3.59-3.65 (m, 6H), 3.74 (m, 2H), 5.15 (br, 1H). HRMS: *m/z* 272.14693 (calc'd [C₁₁H₂₃NO₅+Na]⁺ 272.14684).



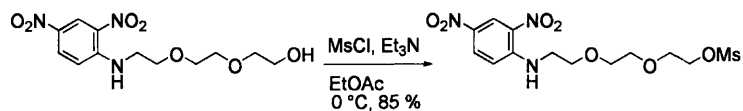
4: Compound **3** (9.11 g, 36.5 mmol) and triethylamine, TEA (5.0 mL, 35.9 mmol) were added to 400 mL DCM and cooled to 0 °C and sparged with argon. To this solution was slowly added a solution of methylsulfonylchloride, MsCl (2.8 mL, 36.1 mmol) under an Ar atmosphere. The reaction mixture was warmed to room temperature and stirred overnight. The reaction mixture was washed repeatedly with water. The organic phase was dried over anhydrous MgSO₄ and concentrated *in vacuo* to obtain a yellow oil. 97 % yield. ¹H NMR (CDCl₃, 300 MHz, ppm): 1.47 (s, 9H), 3.07 (s, 3H), 3.40 (q, 2H), 3.52 (t, 3H), 3.60-3.67 (m, 4H), 3.77 (m, 2H), 4.38 (m, 2H), 4.95 (br, 1 H); ¹³C NMR (CDCl₃, 125 MHz, ppm): 27.60, 28.60, 37.87, 40.49, 69.25, 69.28, 70.35, 70.45, 70.79. HRMS: *m/z* 350.12345 (calc'd [C₁₂H₂₅NO₇S+Na]⁺, 350.12439).



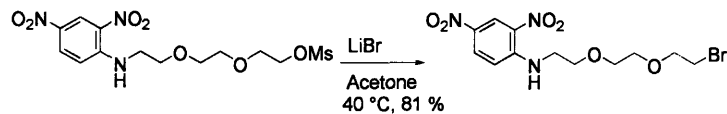
5: Lithium bromide (12.27 g, 141.28 mmol) and **3** (11.49 g, 35.10 mmol) were stirred in 135 mL acetone at 30 °C and the reaction monitored. Upon completion, the solvent was removed *in vacuo*. The residue was dissolved in EtOAc and the cloudy solution washed with water repeatedly. The organic phase was dried over anhydrous MgSO₄ and concentrated *in vacuo* to obtain a cloudy yellow oil. The product was purified by column chromatography (ethyl acetate eluant). 65 % yield. ¹H NMR (CDCl₃, 500 MHz, ppm): 1.43 (s, 9H), 3.32 (m, 2H), 3.47 (t, 2H), 3.54 (t, 2H), 3.61-3.66 (m, 4H), 3.80 (t, 2H), 5.00 (br, 1H). ¹³C NMR (CDCl₃, 125 MHz, ppm): 28.60, 30.4, 40.50, 70.34, 70.46, 70.60, 71.35, 79.40. HRMS: *m/z* 334.06161 (calc'd [C₁₁H₂₂BrNO₄+Na]⁺, 334.06299).



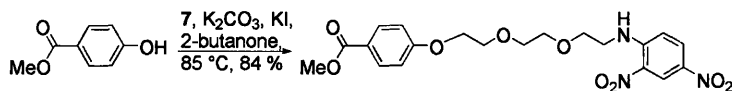
6: Crude **2** (3 g scale) was dissolved in a cooled 50 mL ethanol. 1 equivalent of 2,4-dinitrofluorobenzene (1.4 mL, 11.1 mmol) was slowly added. The solution initially turned yellow, but gradually went a dark orange. After one hour, the solution was filtered and the product loaded onto a silica column and eluted with ethyl acetate. The last fraction was collected and concentrated to yield a vibrant yellow oil. 44 %, over two steps from **1**. ^1H NMR (CDCl_3 , 500 MHz, ppm): 2.35 (br, 1H), 3.61 (m, 4H), 3.69-3.75 (m, 6H), 3.83 (t, 2H), 6.93 (d, 1H), 8.25 (dd, 1H), 8.83 (br, 1H), 9.11 (d, 1H). ^{13}C NMR (CDCl_3 , 125 MHz, ppm): 43.34, 61.95, 68.61, 70.52, 70.95, 72.74, 114.22, 124.47, 130.48, 130.80, 136.25, 148.53. HRMS: m/z 338.09529 (calc'd $[\text{C}_{12}\text{H}_{17}\text{N}_3\text{O}_7+\text{Na}]^+$, 338.09587).



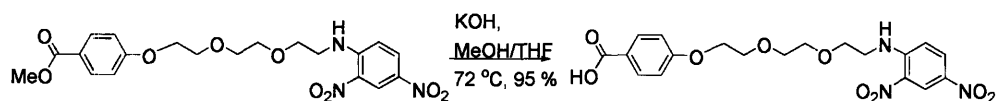
7: A solution of **6** (1.4511 g, 4.6 mmol) and TEA (5.0 mL, 36 mmol) in 25 mL ethyl acetate was cooled to 0 °C. MsCl (1.8 mL, 23.3 mmol) was slowly added and the reaction warmed to room temperature. Remove solvent, load onto silica column, and elute with ethyl acetate. Second fraction is concentrated to yield product. 85 % yield. ¹H NMR (CDCl₃, 500 MHz): 3.06 (s, 3H), 3.60 (q, 2H), 3.73, (br, 4H), 3.79 (m, 2H), 3.84 (t, 2H), 4.39 (m, 2H), 6.94 (d, 1H), 8.28 (dd, 1H), 8.81 (br, 1H), 9.14 (d, 1H). ¹³C NMR (CDCl₃, 125 MHz, ppm): 37.80, 43.42, 68.75, 69.29, 69.35, 70.87, 70.95, 114.21, 124.56, 130.55, 148.56. HRMS: *m/z* 394.08961 (calc'd [C₁₁H₂₂BrNO₄+H]⁺, 394.0842).



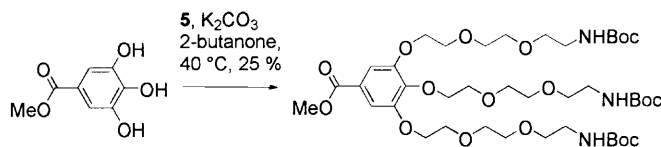
8: Compound **7** (0.1012 g, 0.26 mmol) in 1.64 mL acetone was stirred with LiBr (0.0702 g, 0.808 mmol) and stirred at 30 °C overnight. Additional LiBr (3.1274 g total, 36.0 mmol total) needed to push reaction to completion. Remove solvent *in vacuo* and residue dissolved in EtOAc and washed with water and brine. Organic phase dried over anhydrous MgSO₄ and concentrated. Crude product clean and used as is in all subsequent steps. 81 %. ¹H NMR (CDCl₃, 500 MHz): 3.49 (t, 2H), 3.61 (q, 2H), 3.71-3.75 (m, 4H), 3.83 (t, 2H), 3.86 (t, 2H), 6.95 (d, 1H), 8.27 (dd, 1H), 8.82 (br, 1H), 9.15 (d, 1H). ¹³C NMR (CDCl₃, 125 MHz, ppm): 30.72, 43.48, 68.88, 70.82, 70.91, 71.46, 114.22, 124.56, 130.50, 136.31, 148.60. HRMS: *m/z* 400.0115 (calc'd [C₁₂H₁₆BrN₃O₆+Na]⁺, 400.0120).



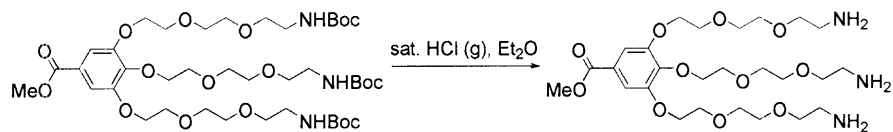
9: Methyl-4-hydroxybenzoate (0.487 g, 3.20 mmol), **7** (0.257 g, 0.652 mmol), potassium carbonate (0.890 g, 6.44 mmol), potassium iodide (0.090 g, 0.55 mmol) were stirred at 85 °C in 20 mL 2-butanone for 48 hours. The reaction mixture was cooled to room temperature and the solution concentrated. The residue was dissolved in EtOAc, washed with water and brine, dried over anhydrous MgSO₄, and concentrated. The product was purified by column chromatography (silica gel, EtOAc eluent). 84% yield. ¹H NMR (CDCl₃, 500 MHz, ppm): 3.57 (q, 2H), 3.74-3.79 (m, 4H), 3.85 (t, 2H), 3.88 (s, 3H), 3.90 (t, 2H), 4.20 (t, 2H), 6.89-6.92 (m, 2H+1H), 7.95 (dd, 2H), 8.25 (dd, 1H), 8.80 (br, 1H), 9.11 (d, 1H). ¹³C NMR (CDCl₃, 125 MHz, ppm): 43.41, 52.10, 67.68, 68.71, 69.87, 70.94, 71.12, 114.16, 114.29, 115.37, 122.90, 125.50, 130.44, 131.71, 132.03, 148.51, 162.66, 166.97. HRMS: *m/z* 472.1332 (calc'd [C₂₀H₂₃N₃O₉+Na]⁺, 472.1327).



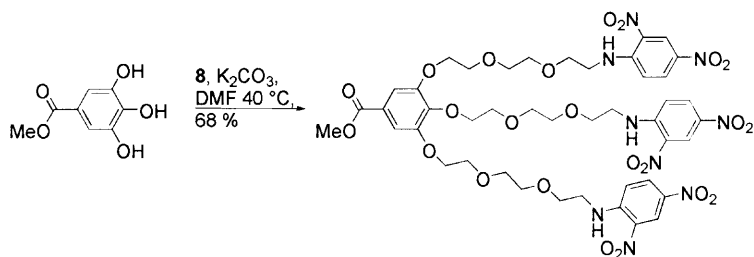
10 or G0: Compound **9** (0.2203 g, 0.490 mmol) was dissolved in 50 mL 1:1 MeOH:THF. 2 mL 1.0 N KOH was added and the solution stirred at 72 °C. The red reaction mixture was monitored until only product present in solution. Solvent removed *in vacuo* and the residue dissolved in DCM. Water added and 1.2 M HCl added to neutralize the suspension, changing the solution from red (under basic conditions) to yellow (under neutral and acidic conditions). ¹H NMR (CDCl₃, 500 MHz, ppm): 3.55 (q, 2H), 3.73-3.78 (m, 4H), 3.83 (t, 2H), 3.90 (t, 2H), 4.20 (t, 2H), 6.88-6.92 (m, 2H+1H), 7.99 (d, 2H), 8.21 (dd, 1H), 8.78 (br, 1H), 9.07 (d, 1H). ¹³C NMR (CDCl₃, 125 MHz, ppm): 43.36, 67.73, 68.67, 69.80, 70.87, 71.06, 114.20, 114.42, 121.91, 124.42, 130.41, 130.56, 132.39, 136.17, 148.50, 163.37, 171.78. HRMS: *m/z* 458.11557 (calc'd [C₁₉H₂₁N₃O₉+Na]⁺, 458.11700).



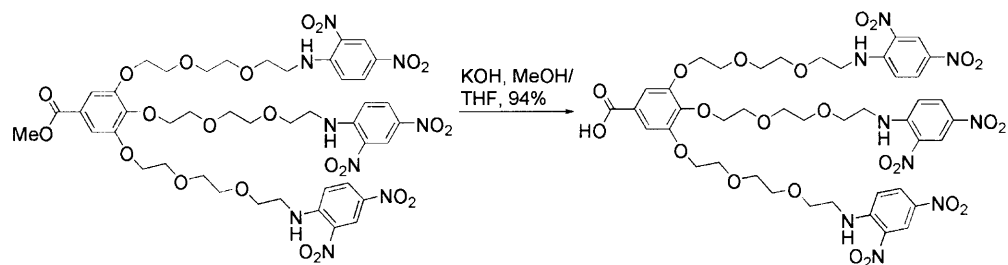
11: Methyl-3,4,5-trihydroxybenzoate (0.2809 g, 1.65 mmol), **5** (1.8200 g, 5.83 mmol), potassium carbonate (1.1588 g, 8.38 mmol) were dissolved in 2-butanone and stirred at 40 °C for five days. The reaction mixture was then concentrated and the crude product dissolved in EtOAc, washed with water and brine, dried over anhydrous $MgSO_4$, and concentrated *in vacuo*. The product was purified by column chromatography (silica gel, EtOAc eluent). 25 %. 1H NMR ($CDCl_3$, 500 MHz, ppm): 1.40 (s, 2H), 3.30 (m, 6H), 3.52 (m, 6H), 3.60 (m, 6H), 3.69 (m, 6H), 3.78 (t, 2H), 3.84 (m, 3H+4H), 4.20 (m, 6H), 7.28 (2H, s). ^{13}C NMR ($CDCl_3$, 125 MHz, ppm): 28.56, 40.49, 52.22, 52.38, 68.40, 68.95, 69.66, 69.76, 70.43, 70.46, 70.52, 70.62, 70.75, 70.81, 70.90, 70.96, 72.59, 73.09, 79.28, 106.28, 109.08, 111.60, 125.18, 126.29, 142.58, 150.65, 150.65, 152.41, 156.15, 166.70. HRMS: m/z 900.4656 (calc'd $[C_{41}H_{71}N_3O_{17}+Na]^+$, 900.4676).



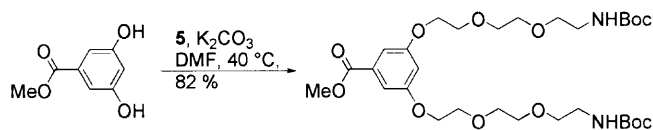
12: A solution of diethyl ether saturated with HCl (g) was first prepared. Compound **11** was dissolved in 1 mL HCl(g)/Et₂O and stirred at room temperature. The solution went from clear to opaque. Solvent was removed *in vacuo* and the residue dried over KOH *in vacuo*. Quantitative. NMR signals are very broad due to extensive hydrogen bonding; ¹H NMR (CD₂Cl₂, 500 MHz, ppm): 3.19 (4H+2H), 3.65-3.85 (br, 3H+24H), 4.25 (4H), 4.32 (2H), 7.27 (2H), 7.96 (1H), 8.05 (2H). ¹³C NMR (CD₂Cl₂, 125 MHz, ppm): 39.78, 67.17, 68.42, 69.63, 69.77, 69.94, 70.21, 70.66, 70.76, 100.35, 108.01, 126.39, 152.57. HRMS: *m/z* 578.3280 (calc'd [C₂₆H₄₇N₃O₁₁+H]⁺, 578.3283).



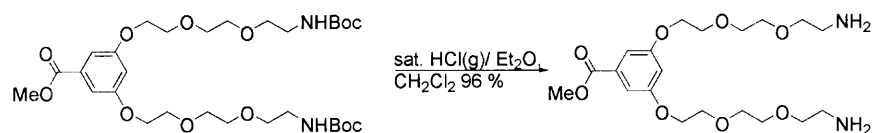
13: Methyl-3,4,5-trihydroxybenzoate (0.5334 g, 2.90 mmol, purified before use), **8** (5.80 g, 15.3 mmol), potassium carbonate (4.0604 g, 29.4 mmol) were dissolved in DMF and stirred at 40 °C for seven days. Solution concentrated, the product dissolved in EtOAc and washed with water and brine, dried over anhydrous MgSO₄. Product purified by column chromatography (silica gel, EtOAc eluent). ¹H NMR (CDCl₃, 500 MHz, ppm): 3.56-3.63 (m, 4H+2H), 3.69-3.87 (m, 3H+24H), 4.15-4.19 (m, 4H+2H), 6.90-6.95 (m, 2H+1H), 7.21 (s, 2H), 8.21 (dd, 2H), 8.26 (dd, 1H), 8.78 (br, 2H), 8.84 (br, 1H), 9.07 (d, 2H), 9.14 (d, 1H). ¹³C NMR (CDCl₃, 125 MHz, ppm): 24.81, 31.17, 31.66, 31.79, 31.84, 43.42, 52.46, 68.70, 68.76, 68.93, 69.92, 70.57, 70.79, 70.96, 71.11, 72.59, 72.76, 108.92, 114.27, 124.44, 124.54, 125.16, 130.41, 130.57, 136.17, 148.55, 152.33, 166.62. HRMS: *m/z* 1098.3163 (calc'd [C₄₄H₅₃N₉O₂₃+Na]⁺, 1098.3147).



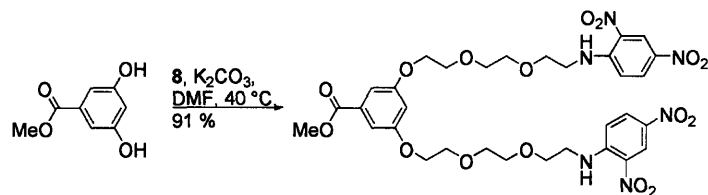
14 or **G1₃**: Compound **13** (14.6 mg, 0.0136 mmol) was dissolved in 3.0 mL 1:1 MeOH:THF. 50 μ L 1.0 N KOH was added and the solution stirred at 72 $^{\circ}$ C. The reaction mixture was monitored until only product present in solution. Solvent removed *in vacuo* and the residue dissolved in DCM. Water added and 1.2 M HCl added to neutralize the suspension, changing the solution from red (under basic conditions) to yellow (under neutral and acidic conditions). 94 %. ^1H NMR (CD_2Cl_2 , 500 MHz, ppm): 3.59-3.88 (overlapping q, m, m, q, t, t), 4.18 (t, 4H), 4.21 (t, 2H), 6.96 (d, 3H), 7.27 (s, 2H), 8.21 (m, 3H), 8.76 (br, 3H), 9.02 (m, 3H). ^{13}C NMR (CD_2Cl_2 , 125 MHz, ppm): 30.22, 30.53, 30.59, 43.81, 69.00, 69.21, 69.29, 70.22, 71.07, 71.20, 71.22, 71.32, 71.35, 72.96, 109.46, 114.85, 124.31, 124.54, 130.61, 130.63, 136.40, 148.99, 152.77, 170.69. HRMS: m/z 1084.2970 (calc'd $[\text{C}_{43}\text{H}_{51}\text{N}_9\text{O}_{23}+\text{Na}]^+$, 1084.2990).



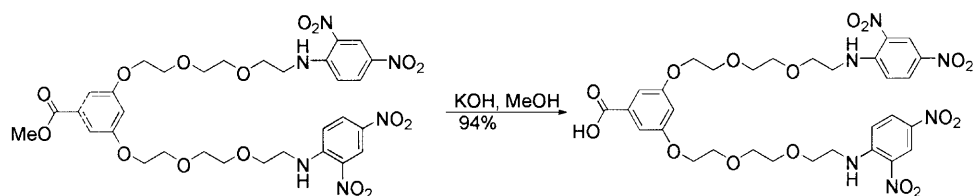
15: Methyl-3,5-dihydroxybenzoate (0.4902 g, 2.92 mmol, purified before use), **5** (2.0114 g, 6.44 mmol), and potassium carbonate (1.4533 g, 10.52 mmol) were dissolved in 4.4 mL DMF and stirred at $40\text{ }^\circ\text{C}$ for four days. The solution was then concentrated, the product dissolved in EtOAc, washed with water and brine. The organic phase was dried over anhydrous $MgSO_4$, concentrated, and the product purified by column chromatography (silica gel, EtOAc eluent). 82%. ^1H NMR ($CDCl_3$, 500 MHz, ppm): 1.42 (s, 18H) 3.32 (m, 4H), 3.54 (t, 4H), 3.64 (m, 4H), 3.71 (m, 4H), 3.85 (t, 4H), 3.89 (s, 3H), 4.15 (t, 4H), 6.70 (t, 1H), 7.19 (d, 2H). ^{13}C NMR ($CDCl_3$, 125 MHz, ppm): 14.41, 28.61, 40.55, 52.47, 60.61, 67.90, 69.81, 70.50, 70.96, 107.19, 108.20, 130.77, 132.09, 159.89, 159.90.



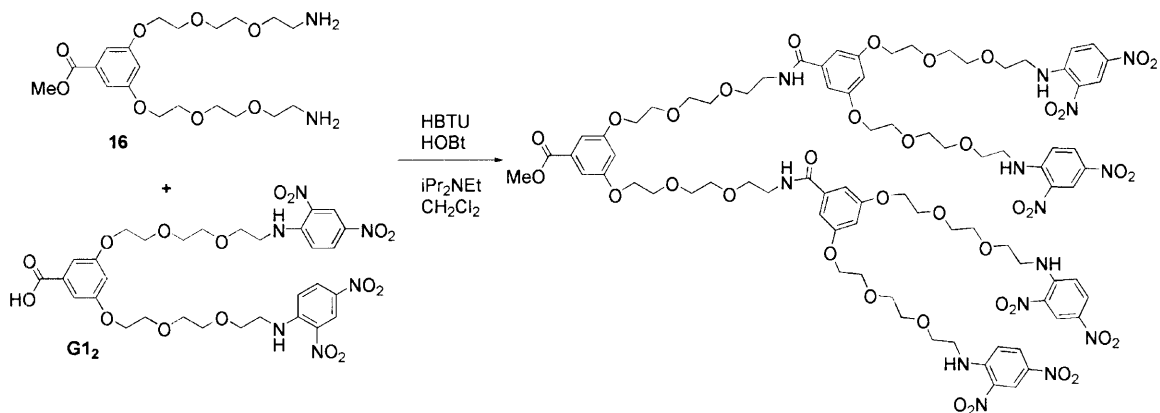
16: A solution of saturated HCl(g)/Et₂O was first prepared. Compound **15** (0.5284 g, 0.838 mmol) was dissolved in 1.5 mL dry DCM. HCl(g)/Et₂O (1.5 mL) was then added. The solution produced bubbles until it became opaque with a white precipitate. The solvent was removed and the residue dried over KOH pellets. ¹H NMR (CDCl₃, 500 MHz, ppm): 3.19 (s, 4H), 3.67 (s, 8H), 3.81-3.86 (m, 3H+8H), 4.20 (m, 4H), 7.08 (t, 1H), 7.18 (d, 2H), 8.27 (br, 6H). ¹³C NMR (CDCl₃, 125 MHz, ppm): 39.43, 52.45, 66.67, 67.46, 69.47, 69.63, 70.61, 107.82, 109.03, 132.15, 159.55, 166.79. HRMS: *m/z* 431.2383 (calc'd [C₂₀H₃₄N₂O₈+H]⁺, 431.2388).



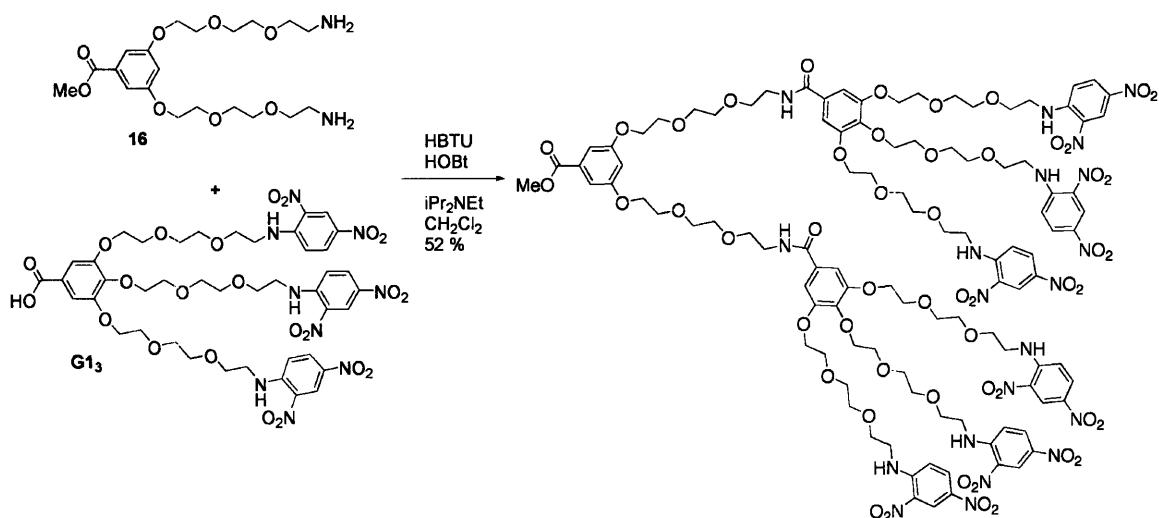
17: Methyl-3,5-dihydroxybenzoate (0.2541 g, 1.51 mmol, purified before use), **8** (2.2943 g, 6.07 mmol), and potassium carbonate (0.8329 g, 6.03 mmol) were dissolved in 5.0 mL DMF and stirred at $40\text{ }^\circ\text{C}$ for six days. The reaction mixture was then concentrated and the contents dissolved in EtOAc, washed with water and brine. The organic phase was dried over anhydrous $MgSO_4$, concentrated and the product purified by column chromatography (silica gel, EtOAc eluent with up to 2 % MeOH added to speed elution). 91 % yield. ^1H NMR ($CDCl_3$, 500 MHz, ppm): 3.55 (q, 4H), 3.72 (m, 3H+8H), 3.82 (m, 8H), 4.09 (m, 4H), 6.58 (t, 1H), 6.88 (d, 2H), 7.05 (d, 2H), 8.17 (dd, 2H), 8.76 (br, 2H), 9.01 (d, 2H). ^{13}C NMR ($CDCl_3$, 125 MHz, ppm): 43.34, 52.36, 67.78, 68.64, 69.76, 70.82, 71.00, 106.59, 107.98, 114.23, 124.28, 130.26, 130.42, 131.89, 136.00, 148.47, 159.77, 166.67. HRMS: m/z 763.2408 (calc'd $[C_{32}H_{38}N_6O_{16}+H]^+$: 763.2417).



18 or **G1₂**: Compound **17** was dissolved in 23 mL MeOH, to which was added 1 mL 1.0 N KOH. This solution was stirred at 72 °C for 8 hours. Compound **17** is not particularly soluble in MeOH, but dissolves with heating. The solution is concentrated and the product extracted into EtOAc and neutralized with 1.2 M HCl. The organic phase was washed with water and brine, dried over anhydrous MgSO₄ and concentrated *in vacuo*. Quantitative yield. ¹H NMR (CDCl₃, 500 MHz, ppm): 3.57 (q, 4H), 3.74-3.79 (m, 8H), 3.85-3.89 (m, 8H), 4.13 (m, 4H), 6.65 (t, 1H), 6.90 (d, 2H), 7.13 (d, 2H), 8.21 (dd, 2H), 8.79 (m, 2H), 9.07 (d, 2H). ¹³C NMR (CDCl₃, 125 MHz, ppm): 29.92, 43.47, 67.90, 68.76, 69.91, 70.91, 71.17, 108.66, 114.25, 124.47, 130.43, 130.59, 131.05, 136.17, 148.57, 159.95. HRMS: *m/z* 747.2082 (calc'd [C₃₁H₃₆N₆O₁₆-H], 747.2115).



G24: Compounds **16** (49.427 mg, 0.098 mmol), **18** (0.2872 g, 0.377 mmol), *N,N,N,N*-Tetramethyl-*O*-(1*H*-benzotriazol-1-yl)uronium hexafluorophosphate (HBTU, 171.40 mg, 0.452 mmol), 1-hydroxybenzotriazole (HOBt, 61.81 mg, 0.457 mmol), diisopropylethylamine (DIPEA, 230 μL , 1.32 mmol) were dissolved and stirred at room temperature in 30 mL dry DCM for seven days. The reaction was concentrated *in vacuo*, the product dissolved in EtOAc, washed with water and brine, and dried over anhydrous MgSO_4 . The product was purified twice by column chromatography (silica gel, EtOAc eluent). ^1H NMR (CDCl_3 , 500 MHz, ppm): 3.56 (q, 8H), 3.62 (m, 4H), 3.68 (m, 8H), 3.71-3.76 (m, 20H), 3.83 (m, 16H), 3.86 (s, 4H), 4.08 (m, 12H), 6.50 (t, 2H), 6.58 (t, 1H), 6.80 (t, 2H), 6.86 (d, 2H), 6.90 (d, 4H), 7.08 (d, 2H), 8.21 (dd, 4H), 8.78 (br, 4H), 9.05 (d, 4H). ^{13}C NMR (CDCl_3 , 125 MHz, ppm): 30.61, 40.13, 43.52, 44.34, 67.90, 67.96, 68.83, 69.99, 70.11, 70.56, 71.02, 71.14, 100.09, 104.62, 106.07, 114.34, 124.54, 130.51, 130.87, 148.66, 160.10, 167.38. HRMS: m/z 1913.6380 (calc'd [$\text{C}_{82}\text{H}_{102}\text{N}_{14}\text{O}_{38}+\text{Na}$] $^+$, 1913.6372).



G2₆: Compounds **16** (1.797 mg, 3.57 μ mol), **14** (15.188 mg, 14.30 μ mol), *N,N,N,N*-Tetramethyl-*O*-(1*H*-benzotriazol-1-yl)uronium hexafluorophosphate (HBTU, 6.678 mg, 17.61 μ mol), 1-hydroxybenzotriazole (HOBt, 2.525 mg, 18.69 μ mol), diisopropylethylamine (DIPEA, 8.7 μ L, 50 μ mol) were dissolved and stirred at room temperature in 30 mL dry DCM for seven days. The reaction was monitored by MALDI-ToF (HABA matrix). The reaction was concentrated *in vacuo*, the product dissolved in EtOAc, washed with water and brine, and dried over anhydrous $MgSO_4$. The product was purified twice by column chromatography (silica gel, EtOAc eluent). 52 %. Low quantity obtained, high molecular weight, strong hydrogen bonding, and low solubility precluded the ability to obtain 1H NMR with sufficient resolution. HRMS: m/z 1259.4248 (calc'd [$C_{106}H_{132}N_{20}O_{52}+2H$] $^{2+}$, 1259.4222).

P-7: Prepared as previously reported by Dr. Juan Zheng.³⁰

3.7 References

1. Tomalia, D. A.; Baker, H.; Dewald, J.; Hall, M.; Kallos, G.; Martin, S.; Roeck, J.; Ryder, J.; Smith, P., "Dendritic macromolecules: synthesis of starburst dendrimers," *Macromolecules* **1986**, *19*, 2466-2468.
2. Tomalia, D. A.; Naylor, A. M.; Goddard, W. A., "Starburst Dendrimers - Molecular-level control of size, shape, surface-chemistry, topology, and flexibility from atoms to macroscopic matter," *Angew. Chem. Int. Ed.* **1990**, *29*, 138-175.
3. Hawker, C. J.; Fréchet, J. M. J., "A new convergent approach to dendritic macromolecules," *J. Am. Chem. Soc.* **1990**, *112*, 7638-7647.
4. Tomalia, D. A., "Starburst dendrimers - nanoscopic supermolecules according to dendritic rules and principles," *Macromol. Symp.* **1996**, *101*, 243-255.
5. Roovers, J.; Comanita, B., "Dendrimers and Dendrimer-Polymer Hybrids," *Adv. Poly. Sci.* **1999**, *142*, 179-228.
6. Svenson, S.; Tomalia, D. A., "Dendrimers in biomedical applications - reflections on the field," *Adv. Drug Del. Rev.* **2005**, *57*, 2106-2129.
7. Al-Jamal, K. T.; Ramaswamy, C.; Florence, A. T., "Supramolecular structures from dendrons and dendrimers," *Adv. Drug Del. Rev.* **2005**, *57*, 2238-2270.
8. Goetheer, E. L. V.; Baars, M.; van den Broeke, L. J. P.; Meijer, E. W.; Keurentjes, J. T. F., "Functionalized poly(propylene imine) dendrimers as novel

phase transfer catalysts in supercritical carbon dioxide," *Industrial & Engineering Chemistry Research* **2000**, *39*, 4634-4640.

9. Piotti, M. E.; Rivera, F.; Bond, R.; Hawker, C. J.; Frechet, J. M. J., "Synthesis and catalytic activity of unimolecular dendritic reverse micelles with "internal" functional groups," *Journal of the American Chemical Society* **1999**, *121*, 9471-9472.

10. Kuzdzal, S. A.; Monnig, C. A.; Newkome, G. R.; Moorefield, C. N., "A study of dendrimer-solute interactions via electrokinetic chromatography," *Journal of the American Chemical Society* **1997**, *119*, 2255-2261.

11. Aulenta, F.; Hayes, W.; Rannard, S., "Dendrimers: a new class of nanoscopic containers and delivery devices," *European Polymer Journal* **2003**, *39*, 1741-1771.

12. Gillies, E. R.; Jonsson, T. B.; Frechet, J. M. J., "Stimuli-responsive supramolecular assemblies of linear-dendritic copolymers," *Journal of the American Chemical Society* **2004**, *126*, 11936-11943.

13. Sideratou, Z.; Tsiourvas, D.; Paleos, C. M., "Quaternized poly(propylene imine) dendrimers as novel pH-sensitive controlled-release systems," *Langmuir* **2000**, *16*, 1766-1769.

14. Nigavekar, S. S.; Sung, L. Y.; Llanes, M.; El-Jawahri, A.; Lawrence, T. S.; Becker, C. W.; Balogh, L.; Khan, M. K., "H-3 dendrimer nanoparticle organ/tumor distribution," *Pharmaceutical Research* **2004**, *21*, 476-483.

15. Sakthivel, T.; Toth, I.; Florence, A. T., "Distribution of a lipidic 2.5 nm diameter dendrimer carrier after oral administration," *International Journal of Pharmaceutics* **1999**, *183*, 51-55.
16. Jevprasesphant, R.; Penny, J.; Attwood, D.; D'Emanuele, A., "Transport of dendrimer nanocarriers through epithelial cells via the transcellular route," *Journal of Controlled Release* **2004**, *97*, 259-267.
17. Krishna, T. R.; Jayaraman, N., "Synthesis of poly(propyl ether imine) dendrimers and evaluation of their cytotoxic properties," *Journal of Organic Chemistry* **2003**, *68*, 9694-9704.
18. Maszewska, M.; Leclaire, J.; Cieslak, M.; Nawrot, B.; Okruszek, A.; Caminade, A. M.; Majoral, J. P., "Water-soluble polycationic dendrimers with a phosphoramidothioate backbone: Preliminary studies of cytotoxicity and oligonucleotide/plasmid delivery in human cell culture," *Oligonucleotides* **2003**, *13*, 193-205.
19. Fuchs, S.; Kapp, T.; Otto, H.; Schoneberg, T.; Franke, P.; Gust, R.; Schluter, A. D., "A surface-modified dendrimer set for potential application as drug delivery vehicles: Synthesis, in vitro toxicity, and intracellular localization," *Chemistry-a European Journal* **2004**, *10*, 1167-1192.
20. Svenson, S.; Tomalia, D. A., "Commentary - Dendrimers in biomedical applications - reflections on the field," *Advanced Drug Delivery Reviews* **2005**, *57*, 2106-2129.

21. Wosnick, J. H.; Mello, C. M.; Swager, T. M., "Synthesis and Application of Poly(phenylene Ethynylene)s for Bioconjugation: A Conjugated Polymer-Based Fluorogenic Probe for Proteases," *J. Am. Chem. Soc.* **2005**, *127*, 3400-3405.
22. Look, G. C.; Murphy, M. M.; Campbell, D. A.; Gallop, M. A., "Trimethylorthoformate: A Mild and Effective Dehydrating Reagent for Solution and Solid Phase Imine Formation," *Tetrahedron Lett.* **1995**, *36*, 2937-2940.
23. Billeci, T. M.; Stults, J. T., "Tryptic Mapping of Recombinant Proteins by Matrix-Assisted Laser-Desorption Ionization Mass-Spectrometry," *Analytical Chemistry* **1993**, *65*, 1709-1716.
24. Gusev, A. I.; Wilkinson, W. R.; Proctor, A.; Hercules, D. M., "Improvement of Signal Reproducibility and Matrix/Comatrix Effects in Maldi Analysis," *Analytical Chemistry* **1995**, *67*, 1034-1041.
25. Peterson, J.; Allikmaa, V.; Subbi, J.; Pehk, T.; Lopp, M., "Structural deviations in poly(amidoamine) dendrimers: a MALDI-TOF MS analysis," *European Polymer Journal* **2003**, *39*, 33-42.
26. Sarver, A.; Scheffler, N. K.; Shetlar, M. D.; Gibson, B. W., "Analysis of Peptides and Proteins Containing Nitrotyrosine by Matrix-Assisted Laser Desorption/Ionization mass Spectrometry," *J. Am. Soc. Mass. Spectrom.* **2001**, *12*, 439-448.
27. Brouwer, A. J.; Mulders, S. J. E.; Liskamp, R. M. J., "Convergent synthesis and diversity of amino acid based dendrimers," *Eur. J. Org. Chem.* **2001**, 1903-1915.

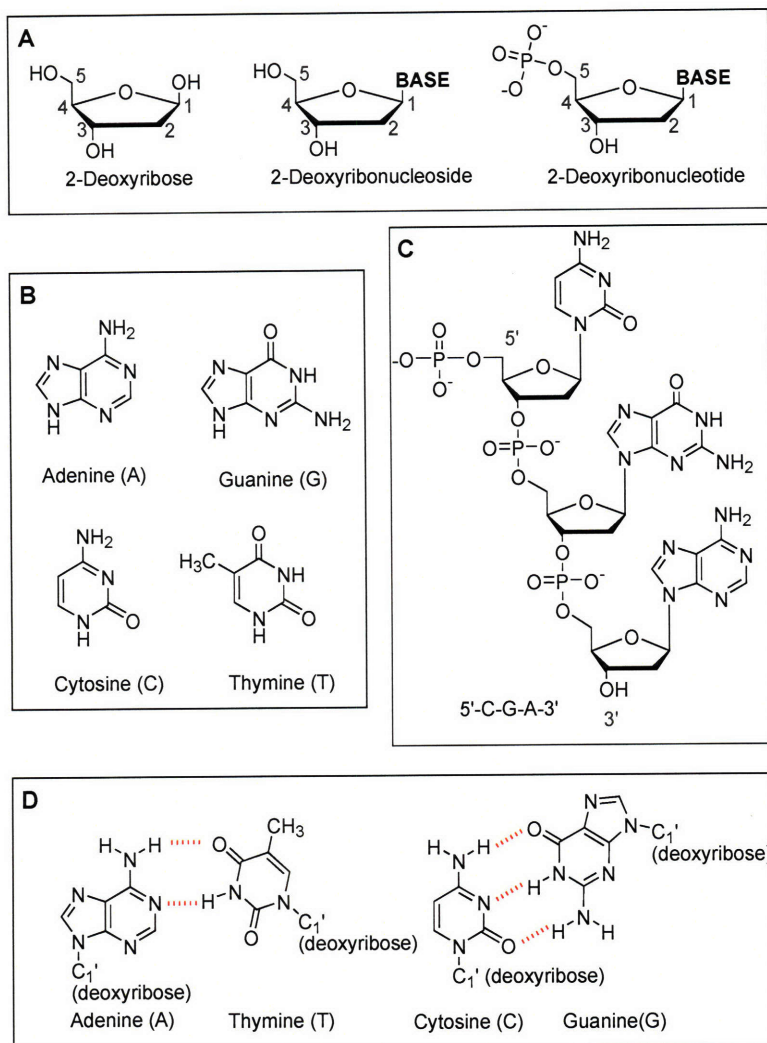
28. Kim, Y.-S.; Kim, K. M.; Song, R.; Jun, M. J.; Sohn, Y. S., "Synthesis, characterization and antitumor activity of quinolone-platinum (II) conjugates," *J. Inorg. Biochem.* **2001**, *87*, 157-163.
29. Zheng, M.; Bai, F.; Li, F.; Li, Y.; Zhu, D., "The Interaction Between Conjugated Polymer and Fullerenes," *J. Appl. Polym. Sci.* **1998**, *70*, 599-603.
30. Disney, M. D.; Zheng, J.; Swager, T. M.; Seeberger, P. H., "Detection of Bacteria with Carbohydrate-Functionalized Fluorescent Polymers," *J. Am. Chem. Soc.* **2004**, *126*, 13343-13346.

Chapter 4:
Molecular Beacon Sequence and
Properties

4.1 Brief Introduction to DNA

Deoxyribonucleic acid (DNA) is a polymer composed of nucleotide monomers (Scheme 2). Nucleotides are phosphorylated nucleosides, which in turn are β -glycosides formed between a sugar and heterocyclic molecules, known as the bases (Scheme 1A). DNA has two purine bases: adenine (A) and guanine (G), and two pyrimidine bases: cytosine (C) and thiamine (T) (Scheme 1B). In these polymers, the sugars are linked through phosphoric acid groups attached to the 5' position of one sugar and the 3' position of the other, while the base is attached at the 1' position (Scheme 1C). The structures of the bases allow hydrogen bonding to occur between adenine and thiamine and between guanine and cytosine (Scheme 1D). Two nucleic acid chains are held together by the hydrogen bonds between base pairs on opposite strands and are complementary as a result of this specific base pairing.

Scheme 1 (A) Building a nucleotide from a sugar. (B) The four DNA bases. (C) The DNA polymer. (D) Hydrogen bonding between bases in DNA.



4.2 Molecular Beacons

Molecular beacons (MB) are short single-stranded hybridization probes most commonly used to monitor the polymerase chain reaction (PCR) in real time.^{1, 2} PCR was first developed to amplify rare DNA sequences by using short primers and the polymerase enzyme.³ In the absence of their target, MBs fold to

form “stem-loop” or “hairpin” structures (Figure 1). The stem portion is formed by the annealing of the complementary arm sequences located on each terminus of the probe sequence. By placing a fluorophore and an acceptor at either end of the sequence, the scheme takes advantage of the distance dependence of fluorescence resonance energy transfer (FRET). Generally, the acceptor used is a non-radiative acceptor, or quencher. Thus, in the absence of a target sequence the MB is in the closed stem-loop form, the fluorophore and quencher are in close proximity, and fluorescence is turned-off. Upon exposure to the target, the loop sequence will bind to the complementary strand and open the stem-hybrid. This removes the quencher from the fluorophore, thereby allowing fluorescence to occur upon excitation.

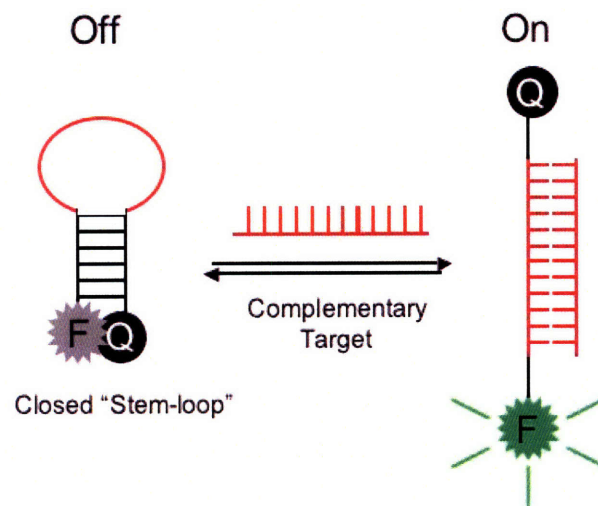


Figure 1 Molecular beacon response to the presence of complementary target.

The loop or probe sequence of a MB is highly specific to a target and can selectively bind to its complementary strand even in the presence of a large

excess of other strands. The key factors that must be taken into consideration when designing a MB are the length of the arm sequences, the length of the probe, and the GC content of the arm sequences. These must all be optimized to ensure that the probe-target hybrid is more stable than the stem hybrid, and that the stem hybrid, in turn, is more stable than the complex formed between the probe and a non-complementary strand.

The overall probe must be long enough to ensure that in the open form, the fluorophore and quencher are at a sufficient distance to allow fluorescence to occur. In addition, sequences of length 15, 25, or 35 nucleotides will place the open arms in a *trans* configuration with respect to the probe-target helix.¹ The probe, however, cannot be so long that the stem portion will not be stable enough to hold the structure in the stem-loop form in the absence of any target because this will result in false positive signals. The length of the stem must therefore be balanced against the length of the probe. Generally, the stem is 5 to 8 bases long and has a high GC content. In the event of a one base-pair mismatch, the stem helix should be more stable, thus ensuring that the MB will be specific enough to discriminate between the correct sequence and incorrect sequences with single-nucleotide polymorphisms.

Molecular beacons are characterized by their melting profiles (Figure 2). In the absence of a target (red line), the MB is in the folded form and the fluorescence is in an off state. As the sample is heated, the stem helix will melt

and the fluorescence will increase. In the presence of the target (green line), the MB is open as the probe-target hybrid is formed. The fluorescence signal is at its greatest at this point. As the sample is heated, the probe-target hybrid dissociates and the fluorescence decreases as the stem helix forms. With continued heating, the stem helix melts and the fluorescence again increases. The fluorescence signal observed at elevated temperatures is never as great as that observed initially in the presence of the target at lower temperatures due to the random conformations in the dissociated beacons that bring the fluorophore and quencher within the Förster radius of the donor-acceptor pair.

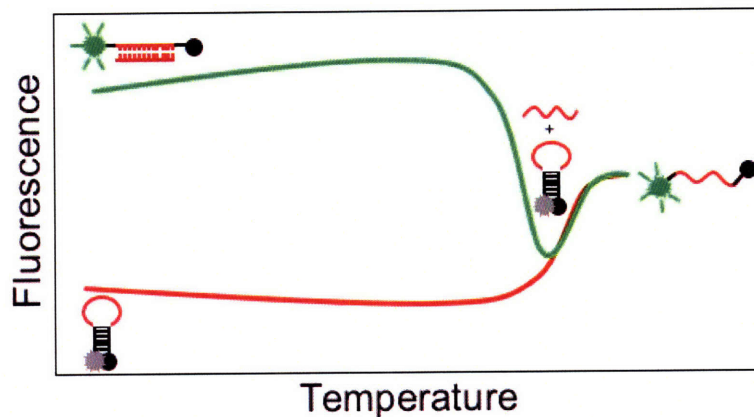


Figure 2 Characteristic molecular beacon melting profile.

4.3 Molecular Beacon Sequence

The molecular beacon sequence selected for the experiments herein was taken from the solved genome sequence of enterohaemorrhagic *Escherichia coli* O157:H7,⁴ and developed in collaboration with the US Army Soldier Systems

Center (Natick, Massachusetts). The bacterium *Escherichia coli* O157:H7 (*E. coli* O157:H7) is a foodborne pathogen of immense importance to public health, and is responsible for 73,000 cases of infection and 61 deaths each year in the United States alone.⁵ It was only after a wide-spread outbreak of illness associated with contaminated hamburger in 1982 that *E. coli* was connected with human disease.⁶ Its primary mechanism for toxicity is the production of one or more bacteriophage-encoded⁷ Shiga-like toxins.⁸⁻¹⁰ These toxins bind to the intestinal mucosa “by an attaching and effacing mechanism”.^{9, 11}

The loop portion of our beacon contains 15 bases that correspond to the sequence between position 1,352,546 and 1,352,560 of the genome of *E. coli* O157:H7 EDL933, and is found within the region that codes for the Shiga-like toxin II A subunit. The two self-complementary arms contain 5 bases, resulting in a MB, labeled as Ecmb, composed of 25 bases.

5'-CCTAG TTAGCCATCTTCGTC CTAGG-3'

123 14444244443 123

stem loop stem

Ecmb can be modified at both the 5'- or 3'-terminal. Sequences used in experiments described below are modified with a six-carbon chain with a terminal amino group or a fluorescein dye at the 5'-terminus. At the opposite end, the 3'-terminus, a Cy3 dye or black hole quencher-1 (BHQ1TM) quencher is attached. The MBs used in experiments are listed in Table 1. The absorbance spectra obtained for the MBs are shown in Figure 3, along with the absorbance of **P-7**.

The absorbance and emission maxima for the dyes used are tabulated in Table 2. The structure for Cy3 unit that is bound via a five-carbon chain is provided below in Scheme 2.

Table 1 MB sequences and melting temperatures.^a

Name	MW (g/mol)	T _m (°C)	Sequence (5'—3') ^b
EcmbL	7,763.1	58.1	/AminoC6/-CCT AGT TGA CCA TCT TCG TCC TAG G
EcmbQ	8,317.6	58.1	/AminoC6/-CCT AGT TGA CCA TCT TCG TCC TAG G- /BHQ1/
EcmbT	5,260.7	44.6	/AminoC6/-TTG ACC ATC TTC GTC-/Cy3/
EcmbT2	8,675.9	58.1	/5,6-Fluorescein/-CCT AGT TGA CCA TCT TCG TCC TAG G-/BHQ1/
EcmbT3	8,407.8	58.1	/AminoC6/-CCT AGT TGA CCA TCT TCG TCC TAG G- /Cy3/

^a Melting temperatures obtained in 50 mM NaCl and provided with samples.

^b Modifications: /AminoC6/- six carbon chain spacer; /BHQ1/- BHQ1TM quencher; 5,6-Fluorescein, both isomers used; /Cy3/- Cy3 dye.

Scheme 2 Structures of DNA labels and modifications.

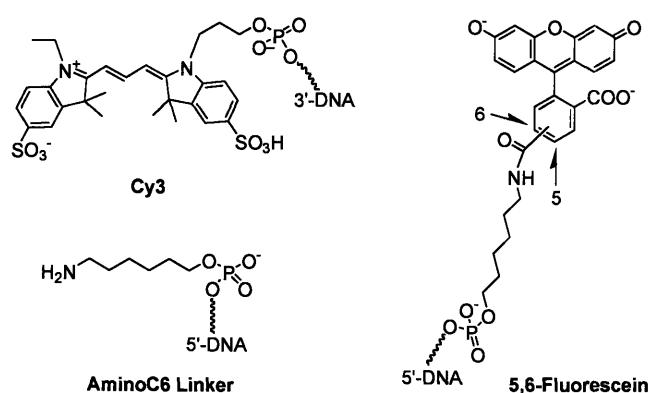


Table 2 Absorbance and emission maxima for dyes used with Ecmb.

Compound	Absorbance λ_{max}	Emission λ_{max}
Cy3 TM	550 nm	564 nm

56FAM	495 nm	530 nm
BHQ1™	534 nm	—

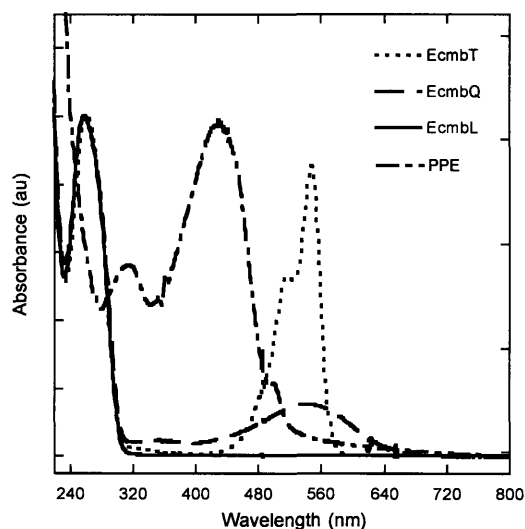
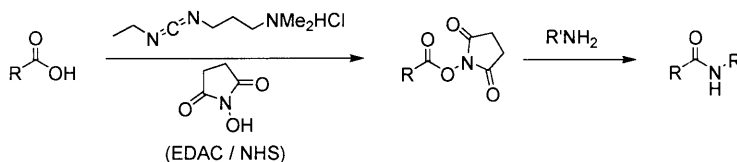


Figure 3 Normalized absorbance spectra for the modified Ecmb sequences and P-7.

4.3.1 Conjugating MBs Using Terminal Amine Groups

EcmbL with the 5'-amino group can be bound to carboxylic acids (Scheme 3). This process requires initial activation of the carboxylic acid groups with 1-ethyl-3-[3-dimethylaminopropyl]carbodiimide hydrochloride (EDAC) to yield an amine-reactive *O*-acylisourea intermediate. In the absence of an amine, this group will react with water to regenerate the carboxylic acid. By introducing *N*-hydroxysuccinimide (NHS), however, an NHS-ester intermediate is formed that is slightly more resistant to hydrolysis, yet readily reacts with amines and improves the efficiency of EDAC-mediated coupling reactions.¹²⁻¹⁴

Scheme 3 Tethering of amine containing molecules, in this case DNA, to a carboxy-PPE via activation with EDAC/NHS.



4.3.2 Complement Sequences for Ecmb

Investigations into the selectivity of Ecmb and its ability to discriminate one mismatch were carried out with the sequences in listed in Table 3. The perfect complement without errors is labeled as CompEcmb. Sequences with one mismatch and two mismatches are labeled Ecmb1mm and Ecmb2mm, respectively. The mismatched base(s) are indicated in bold. A purely scrambled target is EcmbSc.

Table 3 Complementary target sequences and melting temperatures.^a

Name	MW (g/mol)	T_m (°C)	Sequence (5'—3')
CompEcmb	4,650.1	44.6	GAC GAA GAT GGT CAA
Ecmb1mm	4,625.1	41.8	GAC GAA GAT TGT CAA
Ecmb2mm	4,665.1	41.0	GAG GAA GAT TGT CAA
EcmbSc	4,524.0	37.6	GCT TCT TAC TTA TGT

^a Melting temperatures obtained in 50 mM NaCl and provided with samples.

4.4 Determination of Optimal Hybridization Conditions for MB

4.4.1 Buffer Selection

Two common buffers used in PCR were initially investigated for use with Ecmb; the first contained 50 mM KCl, 10 mM Tris pH 8.3, and 1.5 mM MgCl₂ (buffer P1) and the second had 50 mM KCl, 20 mM Tris pH 7.6 and 10 mM MgCl₂. The second buffer did not perform well and was therefore abandoned. Magnesium salts are known to influence DNA hybridization¹⁵ and so the next two buffers had modified MgCl₂ concentrations of 2.5 mM (buffer P2) and 5 mM (buffer P3). The molecular beacon used for these experiments, EcmbT2, was modified at the 5'-end with fluorescein and with BHQ1 at its 3'-end. The MB was tested in the presence and absence of the complements listed in Table 3. The strands were first annealed by heating to 90°C. The fluorescence was measured every degree as the solution was cooled to 20 °C and reheated to 90 °C.

The fluorescence data obtained for the EcmbT2 in the presence of CompEcmb, Ecmb1mm, Ecmb2mm, EcmbSc, or no complement on the first cooling ramp and second heating ramp are shown in Figures 4-7. The

experiments were repeated in triplicate and the average response is shown. The results quickly eliminated the viability of buffer P2 as a useful solvent due to the non-ideal response produced in all cases. At elevated temperatures, the fluorescence signal obtained in the absence of any target, correct or incorrect, was greater than that in the presence of a target. Both buffer P1 and P3 behaved reasonably well. It is important that the MB be able to distinguish between the correct sequence from one with one mismatch. In order to establish which buffer demonstrated superior performance, the response of EcmbT2 relative to Ecmb1mm was examined. A greater difference between the “on” state with CompEcmb and the “off” state with Ecmb1mm occurs in buffer P1. This indicates that P1 is a better system for this application.

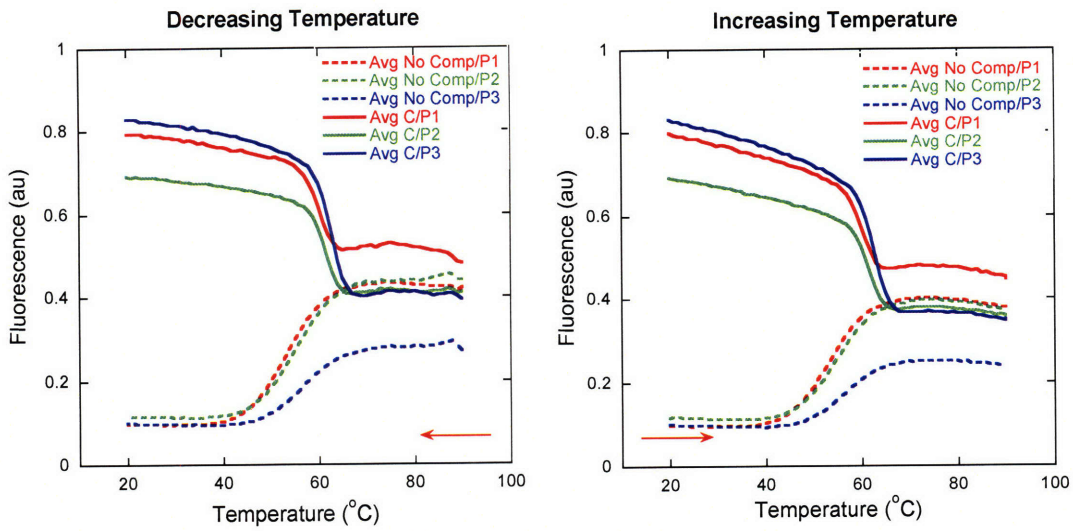


Figure 4 The fluorescence response of EcmbT2 in the presence of the true complement CompEcmb (Avg C) and no complement (Avg No Comp) in buffers P1, P2, and P3 are plotted. The sample was first heated to 90 °C, the fluorescence data were then collected over the first cooling ramp (decreasing temperature) and then over a second heating ramp (increasing temperature).

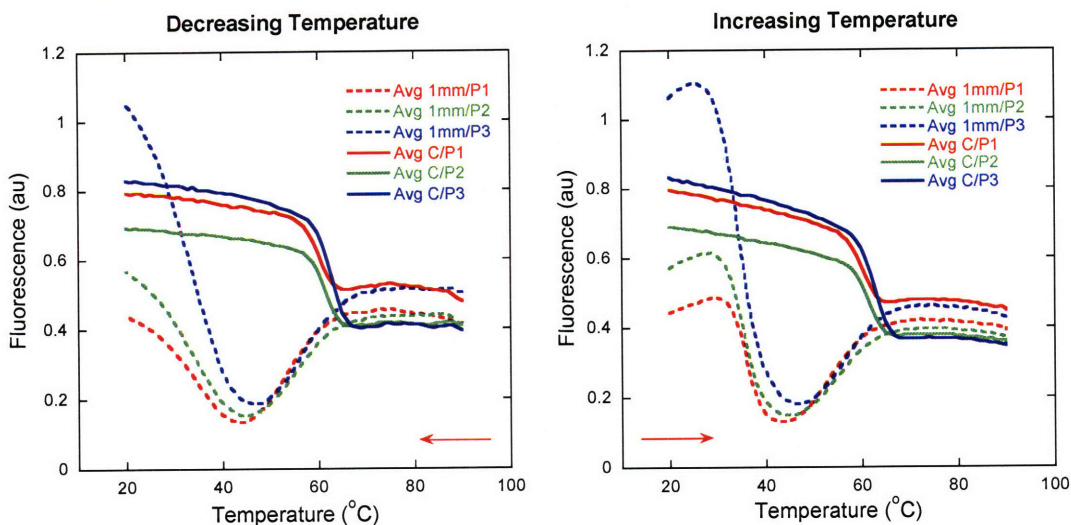


Figure 5 The fluorescence response of EcmbT2 in the presence of the true complement CompEcmb (Avg C) and the complement sequence with one mismatch Ecmb1mm (Avg 1mm) in buffers P1, P2, and P3 are plotted. The sample was first heated to 90 °C, the fluorescence data were then collected over the first cooling ramp (decreasing temperature) and then over the second heating ramp (increasing temperature).

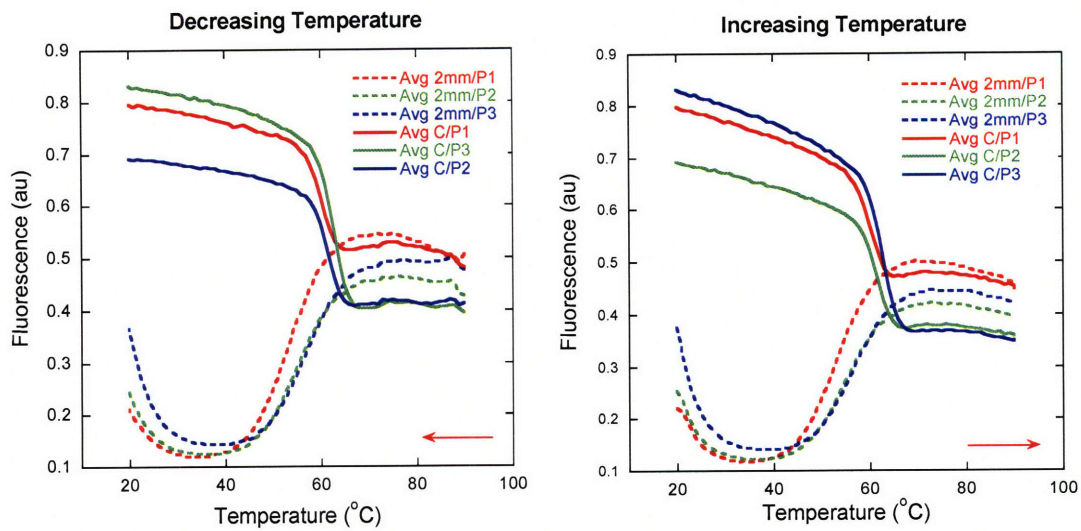


Figure 6 The fluorescence response of EcmB2 in the presence of the true complement CompEcmB (Avg C) and a complement with two mismatches EcmB2mm (Avg 2mm) in buffers P1, P2, and P3 are plotted. The sample was first heated to 90 °C, the fluorescence data were collected on the first cooling ramp (decreasing temperature) and then over a second heating ramp (increasing temperature).

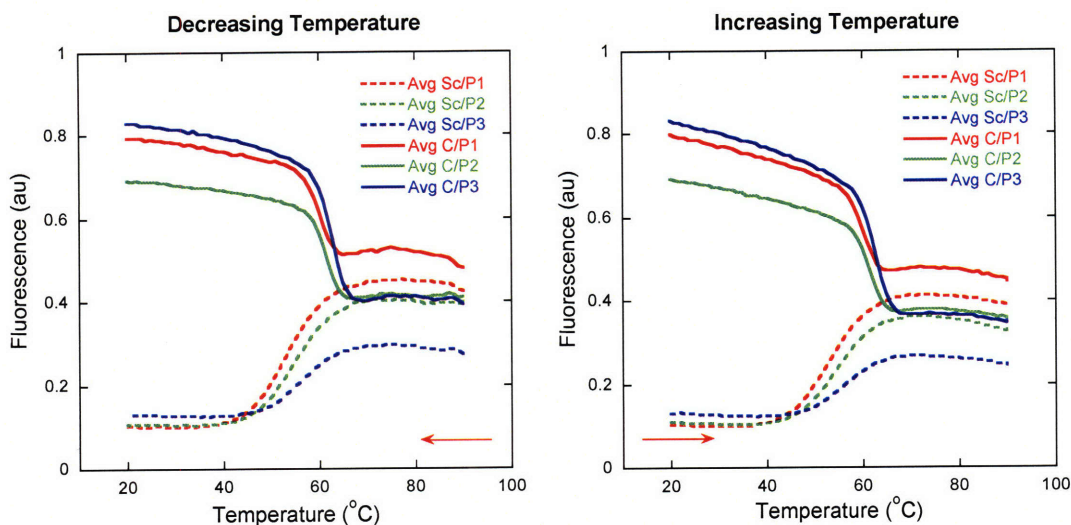


Figure 7 The fluorescence response of EcmbT2 in the presence of the true complement CompEcmb (Avg C) and the completely scrambled sequence EcmbSc (Avg Sc) in buffers P1, P2, and P3 are plotted. The sample was first heated to 90 °C, the fluorescence data were then collected over the first cooling ramp (decreasing temperature) and then over the second heating ramp (increasing temperature).

4.4.2 MB Response Without Prior Annealing Cycle

Ultimately, when the MB is incorporated into a sensor, it would be desirable to reduce the number of steps required between the introduction of a sample to be probed and the final read-out. To this end, the response of the MB without a prior annealing step was probed. The fluorescence response of EcmbT2 was then followed as a function of temperature (1 °C increments) by heating from 25 °C to 55 °C, then cooling back down to 25 °C in the presence and absence of the various complement sequences (CompEcmb, Ecmb1mm,

Ecmb2mm, EcmbSc). The fluorescence response of the first heating ramp and the subsequent cooling ramp are illustrated in Figure 8 (average of triplicate runs shown). These results were extremely encouraging as the molecular beacon behaved well under these conditions, easily distinguishing between the true complement, CompEcmb, and the complement with one base pair mismatch, Ecmb1mm. From these data, one could design a sensor system to read the signal at 40 °C, and so would require only a short heating ramp from room temperature to 40 °C. The subsequent cooling ramp shows much greater discrimination between CompEcmb and Ecmb1mm, and indicates that should an initial heating ultimately be needed, heating to 90 °C would not be necessary because heating to 55 °C would suffice.

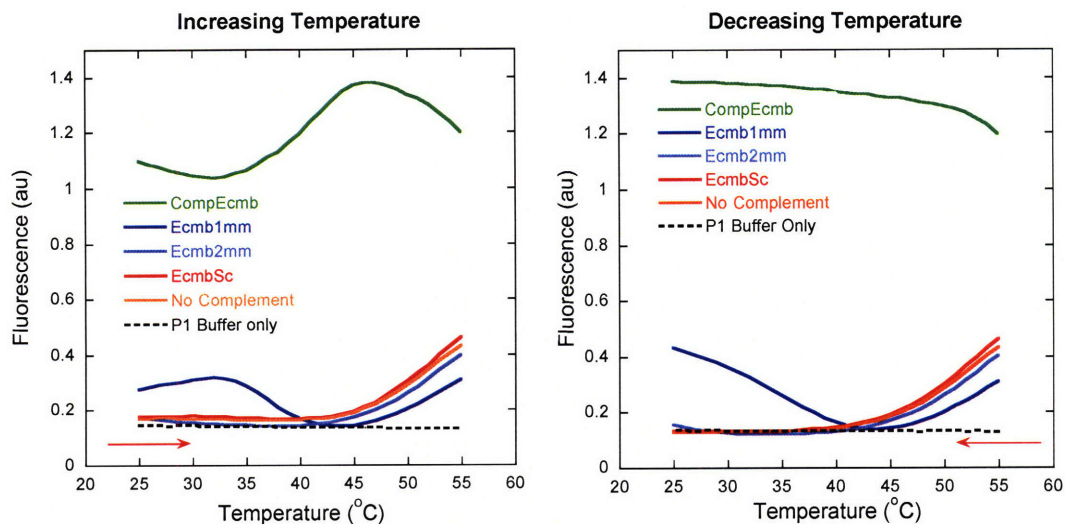


Figure 8 The response of the MB EcmbT2 to CompEcmb, Ecmb1mm, Ecmb2mm, and EcmbSc without an initial annealing step. The background response of a blank sample composed of P1 buffer is included for comparison.

4.5 Detection Limit of MJ Opticon Real Time PCR Instrument

In order to determine the detection limits of the current system, the response of EcmbT2 to varying concentrations of the complement, CompEcmb, as a function of temperature in P1 buffer was investigated. EcmbT2 (50 nM) was exposed to 300 nM, 150 nM, 75 nM, 50 nM, 25 nM, 12.5 nM, 500 pM, and 0 M CompEcmb. Without an initial annealing cycle, the fluorescence was recorded as the temperature was increased from 25 °C to 55 °C at a rate of 1 °C/min, then decreased at the same rate back to 25 °C. The response at each concentration was obtained in triplicate and the average values are shown below in Figure 9.

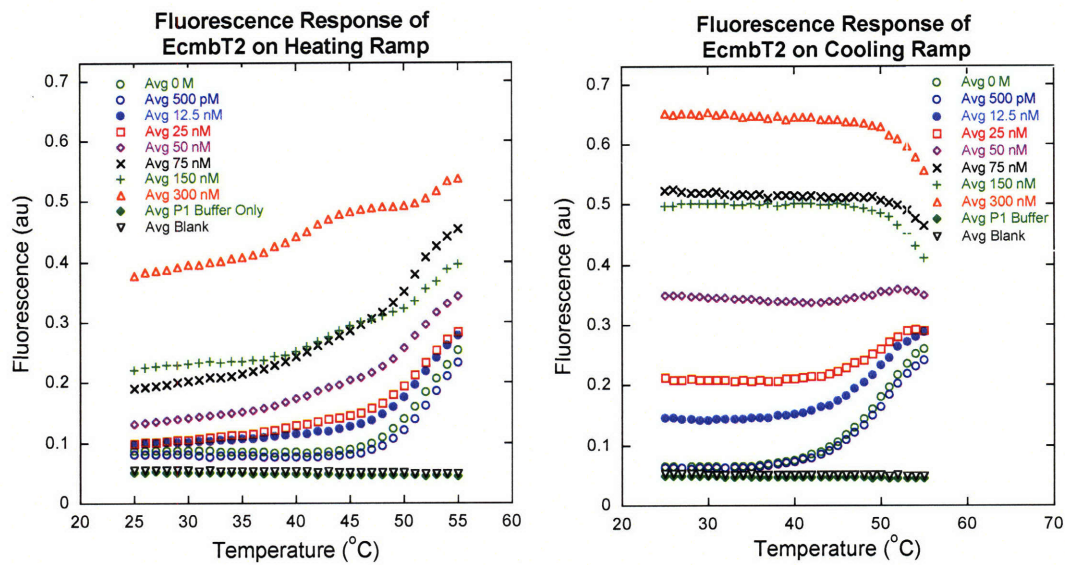


Figure 9 The response of 50 nM EcmbT2 to CompEcmb with concentrations varying from 300 nM to 500 pM are plotted over a heating and then cooling cycle, without a prior annealing cycle.

As expected, the fluorescence response between the heating and cooling ramps indicate that results are more uniform on the cooling ramp after an initial annealing ramp. The signal obtained with a complement concentration of 500 pM is essentially identical to that of 0 nM, and from the 12.5 nM data we estimate the limit of detection for the MJ Opticon is on the order of 10 nM.

4.6 Conclusions

A sequence specific for the Shiga-like toxin II subunit of *E. coli* O157:H7 EDL933 was selected and modified to be a molecular beacon with self-complementary ends. Target sequences to probe Ecmb were designed that contained no errors (CompEcmb), one mismatch (Ecmb1mm), two mismatches (Ecmb2mm), or a purely scrambled sequence (EcmbSc). Several buffers were investigated and buffer P1 (50 mM KCl, 20 mM Tris pH 8.3, 1.5 mM MgCl₂) was determined to yield the highest reproducibility. Furthermore, it was found that no prior annealing step is required as the molecular beacon behaved well when heating directly to 40 °C. The limit of detection for this current molecular beacon system was found to be on the order of 10 nM. The results gained in these studies indicate that this MB will be successful when incorporated into a MB-PPE based sensing system.

4.7 Experimental

All DNA sequences were obtained from Integrated DNA Technologies (Coralville, IA) purified by HPLC and used as received. DNA was resuspended in Millipore water to have a final stock concentration of 1 nmol/ 10 μ L. All buffers used were prepared using Millipore purified water. Sterile 96 well plates were used for these experiments with an MJ Opticon Real Time PCR Instrument (formally MJ Research, now Bio-Rad). The 6FAM filter was selected with an excitation of 495 nm and collection of emission data at 520 nm. Experiments were done in triplicate and the results averaged.

4.7.1 Buffer Selection

The first two buffers investigated were (1) 50 mM KCl, 10 mM Tris pH 8.3, 1.5 mM MgCl₂ (buffer P1) and (2) 50 mM KCl, 20 mM Tris pH 7.6 and 10 mM MgCl₂. Variations of P1 were then investigated with modified concentrations of Mg²⁺: 2.5mM (buffer P2) and 5mM (buffer P3). EcmbT2 (50 nM) was loaded into wells of a sterile 96-well plate along with 300 nM of either EcmbComp, Ecmb1mm, Ecmb2mm, EcmbSc or no complement, and 5x buffer and water to bring the final buffer concentration to that listed above and a final volume of 100 μ L.

The samples were heated to 90 °C from room temperature at 1 °C/min. The fluorescence reading (excitation: 495 nm, emission: 520 nm) was collected

during the cooling ramp (1 °C/min to 20 °C) and again during the second heating ramp (1 °C/min to 90 °C).

4.7.2 MB Response Without Annealing

A sterile 96-well plate was used and wells were loaded with 100 µL P1 buffer containing 50 nM EcmbT2 and 300 nM EcmbComp, Ecmb1mm, Ecmb2mm, EcmbSc or no complement. The fluorescence reading (excitation: 495 nm, emission: 520 nm) was collected on the first heating ramp from 25 °C to 50 °C (1 °C/min), and again on the cooling ramp.

4.7.3 Detection Limit of MJ Opticon Real Time PCR

A sterile 96-well plate was used and wells were loaded with 100 µL P1 buffer containing 50 nM EcmbT and 0 M, 500 pM, 12.5 nM, 25 nM, 50 nM, 75 nM, 150 nM, 300 nM CompEcmb. The fluorescence reading (excitation: 495 nm, emission: 520 nm) was collected on the first heating ramp from 25 °C to 50 °C (1 °C/min), and again on the cooling ramp.

4.8 References

1. Tyagi, S.; Kramer, F. R., "Molecular beacons: Probes that fluoresce upon hybridization," *Nat. Biotechnol.* **1996**, *14*, 303-308.
2. Ma, C. B.; Tang, Z. W.; Wang, K. M.; Tan, W. H.; Li, J.; Li, W.; Li, Z. H.; Yang, X. H.; Li, H. M.; Liu, L. F., "Real-time monitoring of DNA polymerase activity using molecular beacon," *Anal. Biochem.* **2006**, *353*, 141-143.
3. Saiki, R. K.; Scharf, S.; Faloona, F.; Mullis, K. B.; Horn, G. T.; Erlich, H. A.; Arnheim, N., "Enzymatic Amplification of Beta-Globin Genomic Sequences and Restriction Site Analysis for Diagnosis of Sickle-Cell Anemia," *Science* **1985**, *230*, 1350-1354.
4. Perna, N. T.; Plunkett, G.; Burland, V.; Mau, B.; Glasner, J. D.; Rose, D. J.; Mayhew, G. F.; Evans, P. S.; Gregor, J.; Kirkpatrick, H. A.; Posfai, G.; Hackett, J.; Klink, S.; Boutin, A.; Shao, Y.; Miller, L.; Grotbeck, E. J.; Davis, N. W.; Limk, A.; Dimalanta, E. T.; Potamousis, K. D.; Apodaca, J.; Anantharaman, T. S.; Lin, J. Y.; Yen, G.; Schwartz, D. C.; Welch, R. A.; Blattner, F. R., "Genome sequence of enterohaemorrhagic *Escherichia coli* O157 : H7," *Nature* **2001**, *409*, 529-533.
5. Centers for Disease Control, www.cdc.gov.
6. Riley, L. W.; Remis, R. S.; Helgerson, S. D.; McGee, H. B.; Wells, J. G.; Davis, B. R.; Hebert, R. J.; Olcott, E. S.; Johnson, L. M.; Hargrett, N. T.; Blake, P. A.; Cohen, M. L., "Hemorrhagic Colitis Associated with a Rare *Escherichia-Coli* Serotype," *New England Journal of Medicine* **1983**, *308*, 681-685.

7. A bacteriophage is a virus that infects bacteria.
8. Plunkett, G.; Rose, D. J.; Durfee, T. J.; Blattner, F. R., "Sequence of Shiga Toxin 2 Phage 933W from *Escherichia coli* O157:H7: Shiga Toxin as a Phage Late-Gene Product," *Journal of Bacteriology* **1999**, *181*, 1767-1778.
9. Fratamico, P. M.; Sackitey, S., K.; Wiedmann, M.; Deng, M. Y., "Detection of *Escherichia coli* O157:H7 by Multiplex PCR," *Journal of Clinical Microbiology* **1995**, *33*, 2188-2191.
10. Jackson, M. P.; Neill, R. J.; O'Brien, A. D.; Holmes, R. K.; Newland, J. W., "Nucleotide sequence analysis and comparison of the structural genes for Shiga-like toxin I and Shiga-like toxin II encoded by bacteriophages from *Escherichia coli* 933," *FEMS Microbiology Letters* **1987**, *44*, 109-114.
11. Tzipori, S.; Gibson, R.; Montanaro, J., "Nature and Distribution of Mucosal Lesions Associated with Enteropathogenic and Enterohemorrhagic *Escherichia Coli* in Piglets and the Role of Plasmid-Mediated Factors," *Infection and Immunity* **1989**, *57*, 1142-1150.
12. Grabarek, Z.; Gergely, J., "Zero-Length Crosslinking Procedure with the Use of Active Esters," *Analytical Biochemistry* **1990**, *185*, 131-135.
13. Staros, J. V.; Wright, R. W.; Swingle, D. M., "Enhancement by N-Hydroxysulfosuccinimide of Water-Soluble Carbodiimide-Mediated Coupling Reactions," *Analytical Biochemistry* **1986**, *156*, 220-222.
14. Pascual, S.; Haddleton, D. M.; Heywood, D. M.; Khoshdel, E., "Investigation of the effects of various parameters on the synthesis of

oligopeptides in aqueous solution," *European Polymer Journal* **2003**, *39*, 1559-1565.

15. Black, C. B.; Huang, H. W.; Cowan, J. A., "Biological Coordination Chemistry of Magnesium, Sodium, and Potassium-Ions - Protein and Nucleotide-Binding Sites," *Coord. Chem. Rev.* **1994**, *135*, 165-202.

Chapter 5:
Initial Explorations into
Conjugating DNA to PPEs

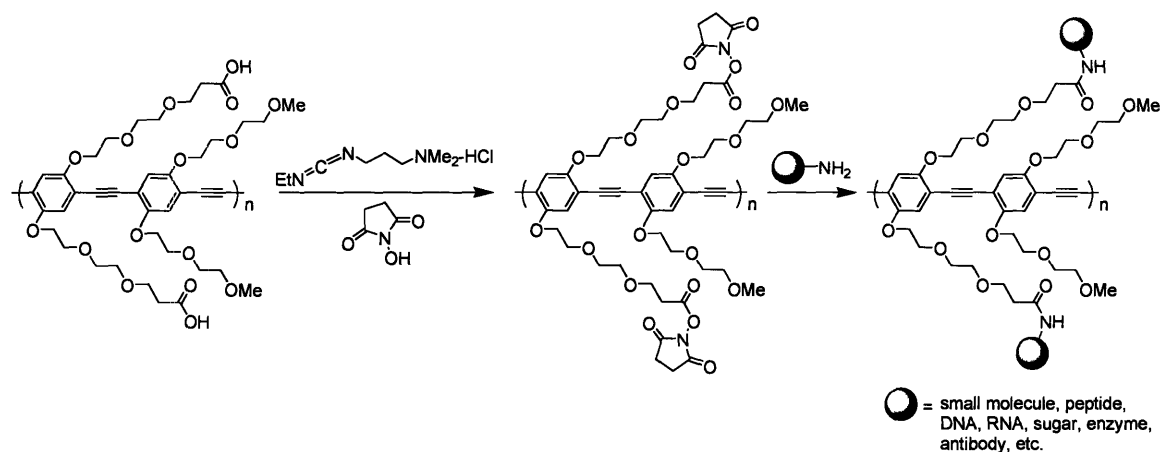
5.1 Introduction

The goal of this project is to ultimately bring together the three components described in the previous three chapters into a sensing platform: a PPE polymer, a DNA molecular beacon, and a dendritic quencher. One vital step is the ability to conjugate the molecular beacon to the PPE. Initial explorations towards this goal are outlined in this chapter.

5.2 Coupling DNA to Carboxylic Acid-PPEs

Preliminary studies were carried out using the carboxylic acid containing polymer **P-7** in order to take advantage of both established carboxylic acid-amine peptide coupling chemistry^{1, 2} and its use with PPEs.³ The polymer is first activated with *N*-(3-dimethylaminopropyl)-*N*-ethylcarbodiimide hydrochloride (EDAC) and *N*-hydroxysuccinimide (NHS), followed by the introduction of the amine-containing compound (Scheme 1). This could be a broad range of amines from small molecules to biological molecules such as DNA and antibodies.

Scheme 1 Initial activation of carboxylic acid groups with NHS and EDAC, followed by coupling of an amine-containing compound.



5.2.1 Determination of Extinction Coefficients for P-7 and EcmbT

The respective extinction coefficients of **P-7** and the Cy3 dye when bound to DNA were determined in order to calculate the extent of DNA conjugation. A stock solution of EcmbT was prepared with a concentration of 0.1 M, aliquots of which were added to 3000 μL P1 buffer (50 mM KCl, 20 mM Tris pH 7.6, and 10 mM MgCl_2) and the UV-Vis absorption spectra recorded (Figure 1A). The extinction coefficient of EcmbT at 548 nm, ϵ_{548} , was determined to be 154,140 $\text{M}^{-1} \text{cm}^{-1}$ (Figure 1B).

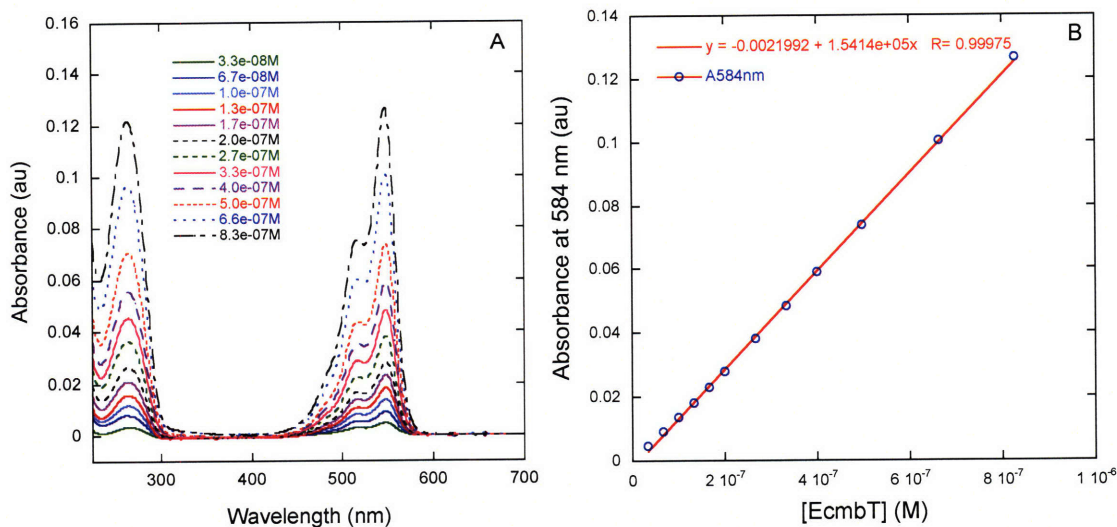


Figure 1 (A) Absorption spectra of aliquots of EcmbT added to P1 buffer. (B) Determination of ϵ_{548} for the Cy3 dye on EcmbT.

The extinction coefficient of **P-7** is readily calculated on a per moles of repeating units/L basis. This repeating unit extinction coefficient is then used to determine the number of Cy3 dyes present relative to the number of polymer repeat units in solution. A stock **P-7** solution was prepared with 0.411 mg in 1000 μL P1 buffer and aliquots were added to 3000 μL P1 buffer. The UV-Vis absorption spectra were recorded and a value of $24,740 \text{ M}^{-1} \text{ cm}^{-1}$ was obtained at 460 nm (Figure 2).

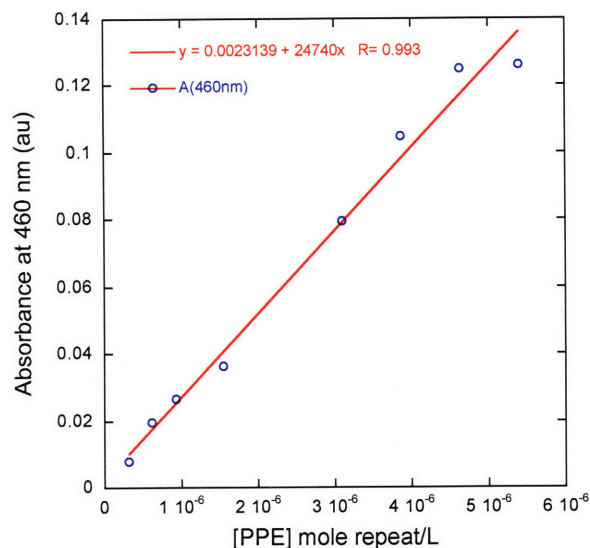
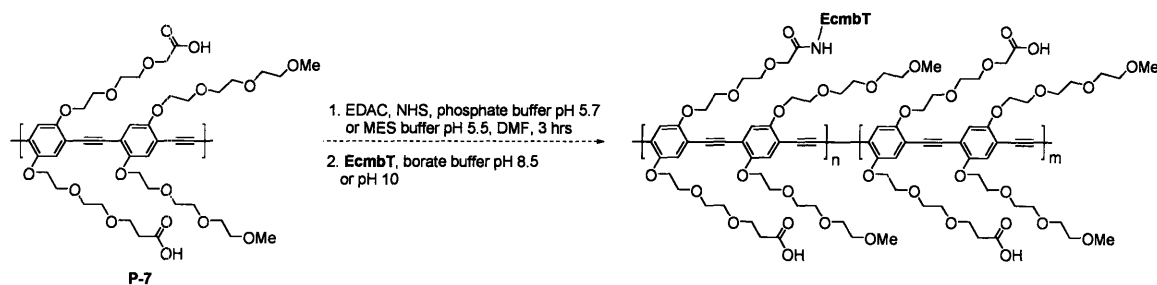


Figure 2 Determination of ϵ_{460} for P-7.

5.2.2 Coupling Conditions

Polymer P-7 was first activated with EDAC and NHS to form the succinimidyl ester, followed by the introduction of the amine-terminated EcmbT sequence (Scheme 2). There are several variables at play in the coupling reaction between the polymer and the molecular beacon: the solvents used for the activation and conjugation steps, the corresponding pH levels, the length of time for each step, the relative amounts of coupling agents and DNA used, as well as the purification technique used to remove excess DNA. Several of the reaction conditions used are listed in Table 1. In each of these cases, excess reagents were removed by dialysis, more of which will be discussed later.

Scheme 2 Conjugation of EcmBT to P-7.



The coupling time between the activated polymer and EcmBT was varied in trials 1 through 3. The importance of the length of coupling time was first investigated by coupling P-7 with EcmBT for 2, 3, and 20 hours, following a 3 hour activation time with EDAC/NHS in each case. The polymer (1 mg, 1 μmol), NHS (~3 eq), and EDAC (~3 eq) were first dissolved in 200 μL DMF and this solution was added to 1000 μL 0.1 M phosphate buffer pH 5.7 for activation. EcmBT (~4 eq) was subsequently added to the solution, followed by 5000 μL 0.1 M borate buffer pH 8.5. The half-life of hydrolysis for NHS esters at pH 7 is approximately 260 minutes, at pH 8 it is 50 minutes, and it is only 10 minutes at pH 8.6. The final pH of the solution was determined to be ~7, and for this reason the third reaction was run for 20 hours in an attempt to maximize the final yield. A more basic borate buffer with pH 10 was used in the coupling step for experiments 4 through 6, resulting in a final pH of ~8.5. The effect of the concentration of EDAC and its relative ratio to NHS was investigated in experiments 7 through 14 as well as the influence of the choice in activation buffer. In experiments 7 through 10, 0.1 M phosphate buffer pH 5.7 is used, while in experiments 11 through 14, 0.1 mM 4-morpholineethanesulfonic acid

(MES) buffer pH 5.5 is used. The effect of the activating and coupling steps on the polymer is investigated in experiments 8, 10, 12, and 14 with no DNA present. To elucidate whether non-specific binding occurs between the MB and P-7, two important controls are investigated in experiments 15 and 16 where no activating agents are present. After the allotted reaction time, the reaction mixtures were transferred to 10,000 molecular weight cut-off (MWCO) Snakeskin dialysis tubing and dialyzed against 1 L Millipore water and protected from the light. The water was changed regularly over two to four days.

Table 1 Experimental conditions that were explored using EDAC/NHS as activating agents and dialysis for purification.

Experiment	[EDAC] (eq)	[NHS] (eq)	DMF (μ L)	Activation Buffer ^o	Total Activation Volume (μ L)	Activation Time (hr)	[DNA] (eq)	Coupling Buffer ^o	Total Coupling Volume (μ L)	Coupling Time (hr)
1	3.4	3.1	200	A	1200	3	4.3	C	5000	2
2	3.2	3.3	200	A	1200	3	4.1	C	5000	3
3	3.4	3.4	200	A	1200	3	4.1	C	5000	20
4	3.5	3.7	200	A	1200	3	4.3	C	4600	0.5
5	3.5	3.5	200	A	1200	3	4.3	D	4600	1
6	3.5	3.3	200	A	1200	3	4.3	D	4600	2
7	200	50	0	A	1200	3	5	D	5000	1
8	200	50	0	A	1200	3	0	D	5000	1
9	20	50	135	A	1200	3	5	D	5000	1
10	20	50	135	A	1200	3	0	D	5000	1
11	200	50	0	B	1200	3	5	D	5000	1
12	200	50	0	B	1200	3	0	D	5000	1
13	20	50	135	B	1200	3	5	D	5000	1
14	20	50	135	B	1200	3	0	D	5000	1
15	0	0	50	A	300	4	48	D	1250	1
16	0	0	50	B	300	4	46	D	1250	1

^o A = 0.1 M phosphate buffer pH 5.7

B = 0.1 mM MES buffer pH 5.5

C = 0.1 M borate buffer pH 8.5

D = 0.1 M borate buffer pH 10

5.2.3 Determination of DNA Loading

For all the reactions listed in Table 1, the polymers were isolated, purified, and the UV-Vis absorbance and fluorescence spectra were collected. The latter was performed with direct excitation of both the dye at 540 nm and of the polymer only at 460 nm. Representative plots for experiments 7-9, 11, 13, 15, and 16 are shown in Figure 3.

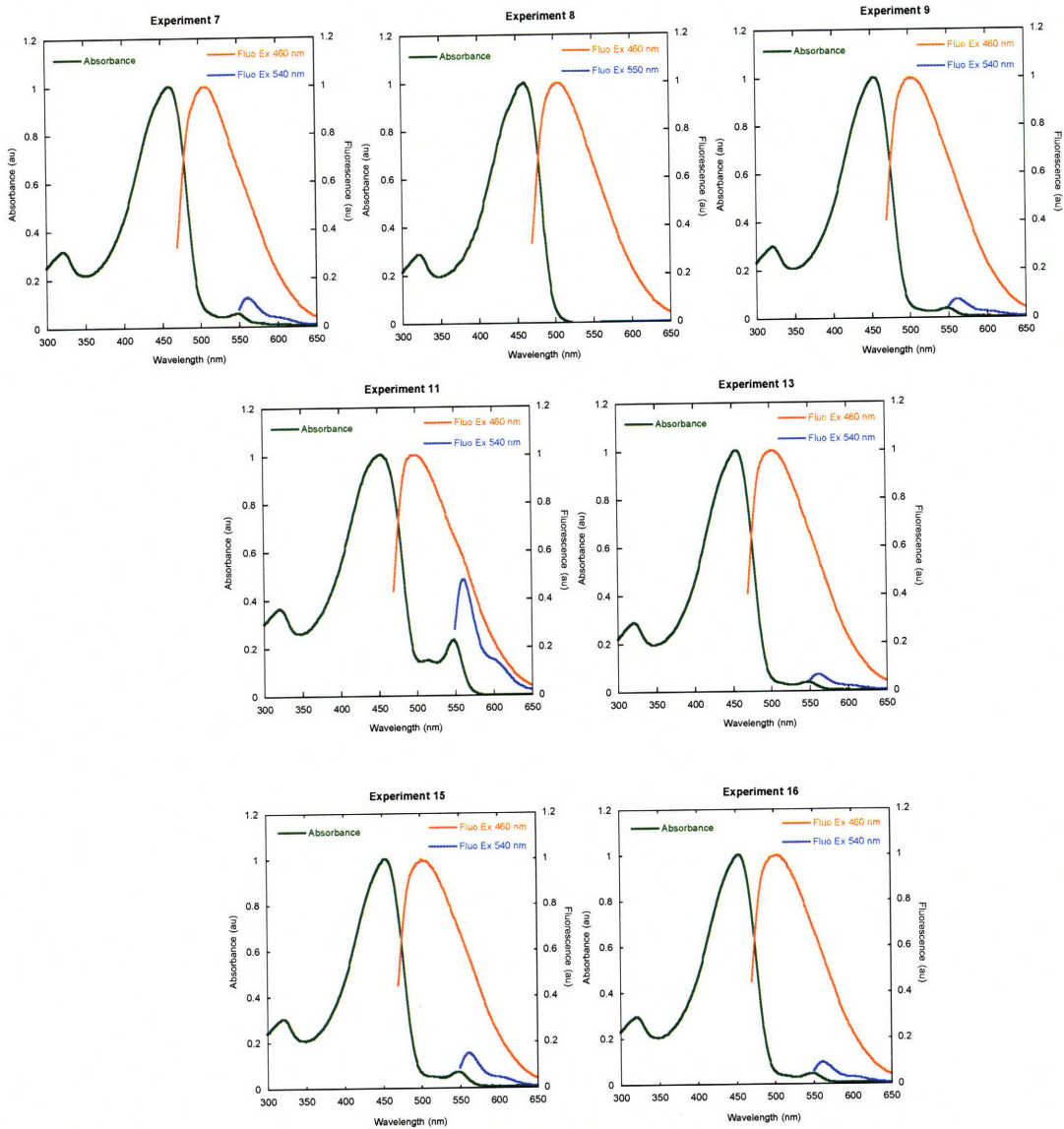


Figure 3 Absorbance and fluorescence spectra obtained for Experiments 7-9, 11, 13, 15, and 16, with excitation of the polymer at 460 nm and the dye at 540 nm.

The Cy3 dye attached to EcmbT can be clearly seen upon direct excitation in Experiments 7, 9, 11, 13, 15, and 16. From the absorbance spectra and the two extinction coefficients previously determined, the relative loading of the number of PPE repeat units for every Cy3 dye were calculated (Table 2). The most promising result was that one Cy3 dye is present for 39 PPE repeat units

(Expt. 11). This translates to 39 PPE repeat units for every strand of DNA. However, the results from control experiments 15 and 16 wherein no EDAC or NHS were added indicate unfortunately that EcmbT binds non-specifically to the polymer.

In summary, very little DNA appears to have been conjugated to **P-7**. Comparison of the loading values obtained in control experiments 15 and 16 indicate that the levels observed in the presence of activating agents is essentially the same as that observed from non-specific binding. One observation from the above series of reactions was that there is a sudden decrease in solubility of the polymer upon activation with EDAC/NHS. The polymer can be seen to precipitate out of solution upon the addition the coupling buffer. We suspect that the decreased solubility is due to the reduction in the number of solubilizing free carboxyl groups after activation with EDAC/NHS. Coupling conditions that will eliminate, or at least minimize, this drop in solubility are preferred. An additional problem is that prolonged dialysis does not remove the excess DNA, nor does switching to higher MWCO dialysis tubing or cassettes. A new purification technique was therefore required to ensure that only pure **P-7**/Ecmb conjugates are recovered and non-covalently bound DNA can be removed.

Table 2 Ratio of DNA to P-7 repeat units.

Experiment	PPE repeat unit/Cy3 Dye
1	220.25
2	235.52
3	234.76
4	174.11
5	174.60
6	189.50
7	152.33
9	194.51
11	39.45
13	196.64
15	90.34
16	143.43

Rather than use dialysis to remove excess DNA, C2 columns were adopted (Alltech, PN 207300, 412410). Using similar reaction conditions to those described above, P-7 dissolved in DMF was activated with 200 mM EDAC and 50 mM NHS in 0.1 mM MES buffer pH 5.5 for three hours, followed by the addition of 3.5 equivalents of EcmbT in either borate buffer at pH 8.5 or pH 10 for one hour. Parallel control reactions were performed without the presence of EDAC and NHS. The reaction mixtures were lyophilized, and then resuspended in 1 mL 25 mM phosphate buffer pH 7 for loading onto the C2 columns. The columns were flushed first with buffer, then with a 1:1 buffer to methanol mixture and finally with pure methanol. This protocol was developed based on the observation that pure DNA elutes in the buffer and buffer/methanol mixture, while P-7 was only observed to elute in the pure methanol flush. The fractions were concentrated and the UV-Vis absorbance and fluorescence

spectra recorded. Unfortunately, direct excitation of the dye at 550 nm generated fluorescence in the control samples that did *not* contain EDAC/NHS. This indicates that C2 columns are not able to separate excess DNA from **P-7**.

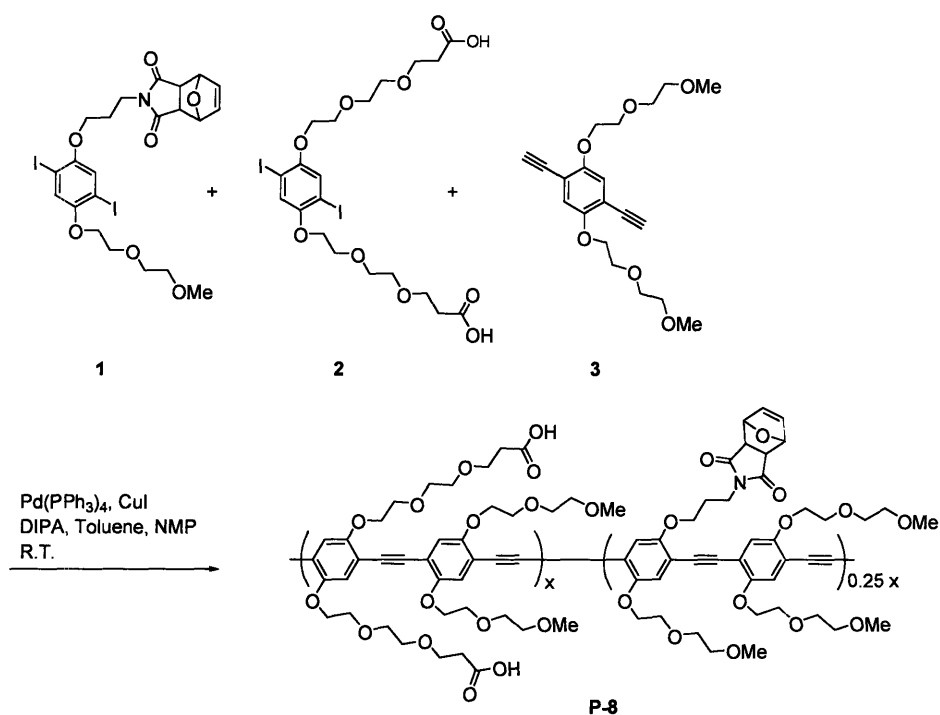
In the event that the dye was promoting the non-specific binding, the coupling reactions were carried out with the EcmbL, which is modified with only an amine at the 5' end, and the presence of DNA in isolated samples of **P-7** were monitored with the OliGreen® single stranded DNA stain (Invitrogen), one of the few commercially available ssDNA stains. These results were, however, inconclusive due to interference from the polymer absorption and emission at the wavelengths required for quantifying the OliGreen® stain. As a result, we decided to pursue an alternative approach.

5.3 A New Approach to Conjugating DNA to PPEs

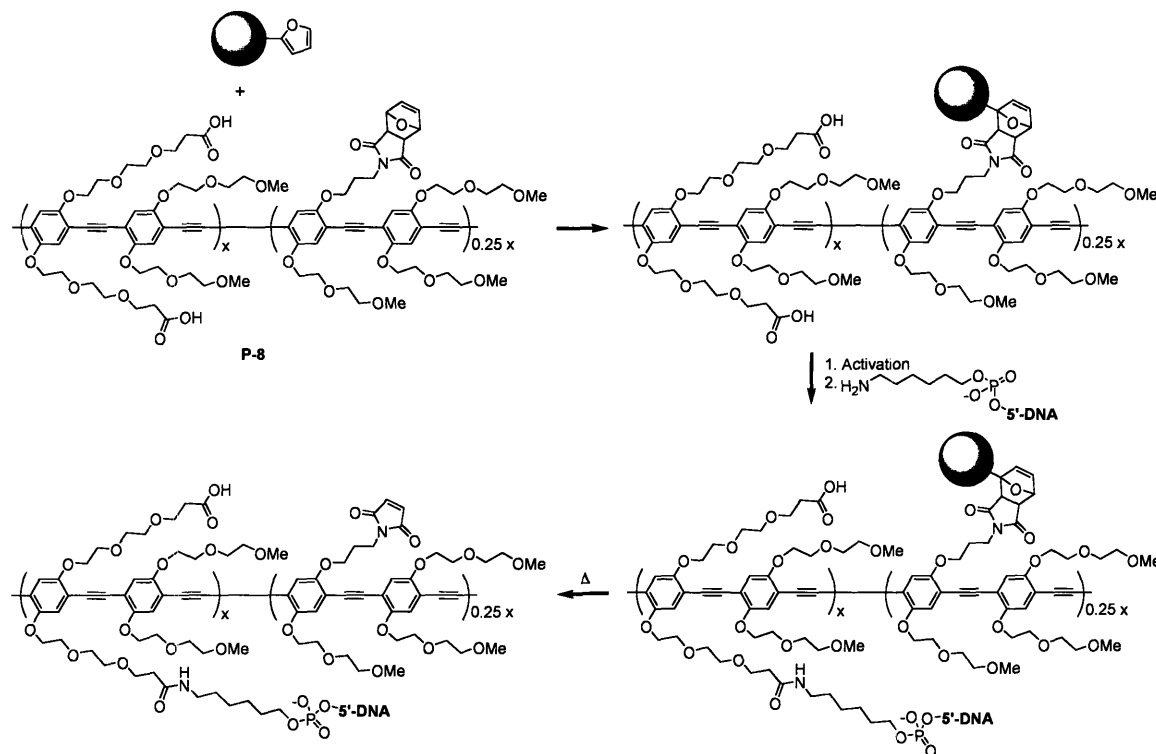
In an attempt to simplify purification of the PPE-DNA conjugates, a new system was devised. This approach incorporates the concepts outlined in Chapter 2 and a masked maleimide and carboxylic acid PPE, **P-8**, was prepared using conditions similar to those described in Scheme 2 in Chapter 2 (Scheme 3). This polymer is now equipped with two handles that can be manipulated; namely, the carboxylic acid and the maleimide group. The carboxylic acid remains the handle by which the DNA can be connected. The maleimide group will serve to immobilize the PPE to a solid support to facilitate purification. Beads modified to with pendent furan groups, which react with the maleimide in a Diels-

Alder reaction and anchor the polymer. Activation with EDAC and NHS is preceded by binding the polymer to the bead. This step is then followed by addition of the DNA strand. Purification would then require only a washing step, followed by removal of the polymer under gentle thermal retro Diels-Alder conditions (Scheme 4).

Scheme 3 Synthesis of P-8.



Scheme 4 Immobilization of **P-8** on a furan-bead, followed by DNA conjugation and removal of the DNA-P-8 conjugate under thermal conditions.

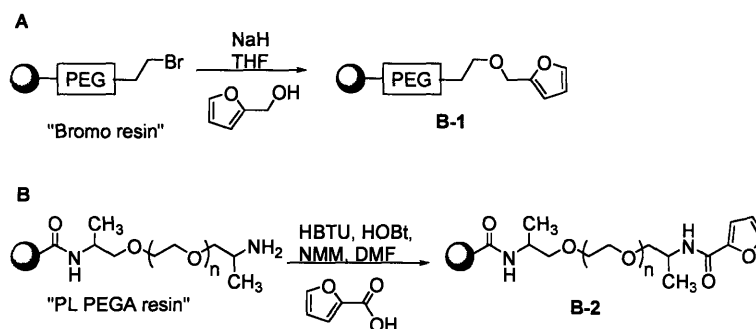


5.3.1 Preparation and Application of Furan-Containing Beads

Two types beads with different structures were initially investigated. One resin investigated was composed of low cross-link density polystyrene and low molecular weight polyethylene glycol (PEG) with terminal bromo groups (NovaSyn® TG bromo resin) was stirred with NaH in the presence of furfuryl alcohol (Scheme 5A).⁴ The other system was a PL-PEGA resin (Polymer Labs), composed of a polyamide/polyethylene glycol copolymer, and this system was activated with HBTU, HOBt, and *N*-methylmorpholine (NMM) in the presence of 2-furoic acid (Scheme 5B). The functionalization protocol was executed twice in

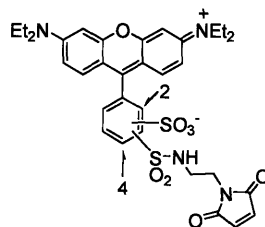
the case of the PL-PEGA resin. The beads were both initially swollen in the respective solvents used for the coupling experiments, THF in the first case and DMF in the second.

Scheme 5 Preparation of furan-containing beads.



As a test reaction, the resulting beads were then exposed to a DMF solution of the maleimide-functionalized dye, Rhodamine Red C2-maleimide (Scheme 6). Both resins were functionalized with the dye, while the unbound dyes are readily washed from the unfunctionalized resins. Heating at 60 °C released the dye from the beads into solution.

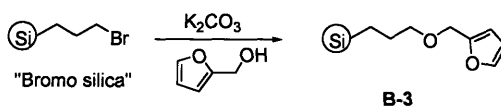
Scheme 6 Structure of Rhodamine Red C2 maleimide.



Beads **B-1** were also tested with polymer **P-8**. The swollen beads were stirred with **P-8** at 60 °C under an inert atmosphere to remove the furan mask from the polymer while preventing any potential oxidative degradation of the polymer. The beads effectively trapped all the polymer from solution, however, removal of the polymer from the beads proved difficult and required heating in excess of 100 °C. Even after this harsh treatment, the beads remained bright yellow indicating the presence of residual **P-8**.

An important issue that became apparent in the optimization of our reactions with the furan functionalized beads was the need to dry and then swell the beads when switching solvents. The bead reactions on the beads require different solvents. Binding of **P-8** is conducted in THF or DMF and the conjugation of DNA to **P-8** is performed in aqueous buffer. These changes in solvent affect the pore size of the bead and can trap compounds in the beads. For this reason, a silica bead, 4-bromopropyl functionalized silica gel (Aldrich), was modified under the mild conditions shown in Scheme 7 to yield a furan-containing silica bead. The beads were stirred in neat furfuryl alcohol in the presence of potassium carbonate base. These beads do not need to be swollen prior to use, nor will the pore size be affected by the choice of solvent.

Scheme 7 Preparation of a furan-containing silica bead.



The ability of furan modified silica beads, **B-3**, to bind and trap Rhodamine Red C2 maleimide in THF was tested. These beads trapped the dye turning a pale pink colour, while the unfunctionalized silica bead did not. This was followed by heating in MeOH at 70 °C to release the dye from the beads by a retro-Diels-Alder mechanism. The solvent was collected after heating and was also pink and fluoresced when excited with a black light (Figure 4)

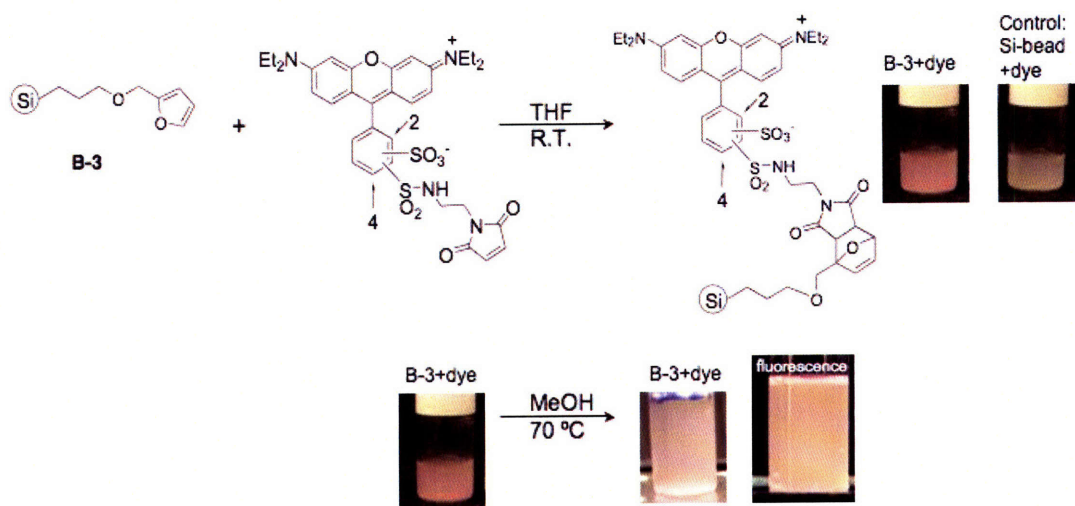


Figure 4 The binding and subsequent release of Rhodamine Red C2 maleimide from **B-3** by a retro-Diels-Alder mechanism.

Based upon the success with Rhodamine Red C2 maleimide, the performance of the furan functionalized silica bead with **P-8** was then tested (Figure 5). The beads and polymer were stirred in THF at 67 °C for 12 hours, and then stirred at room temperature for 8 hours. The beads were collected and thoroughly washed with THF. Beads **B-3** (15 mg, 20 nmol loading), removed the polymer (1 mg, 0.3 nmol) from solution resulting in yellow beads and a colourless

solution. Control experiments with bromo-silica beads did result in some capture of **P-8**, presumably through non-specific interactions, but the majority stayed in solution. The **B-3/P-8** beads were stirred in THF at 67 °C for 12 hours and filtered hot in an effort to release the polymer. Although some polymer was removed from the bead, it appears that most was retained. The persistence of the polymer binding is probably due to the low likelihood that all maleimide groups on a polymer strand would be released at the same time. In other words, while one may be released, another maleimide group at another location on the chain may still be bound to the bead. To prevent the reattachment of any maleimide groups on the polymer, excess *N*-propylmaleimide was added to block any furan groups on the beads. This did not appear to have the impact that was hoped, but further exploration into different maleimide containing compounds will elucidate those that will form more stable Diels-Alder adducts with the bead relative to the polymer. One solution to overcome the problem of irreversible polymer binding to **B-3** would be to prepare a polymer with only a small number of maleimide units along the backbone, or even perhaps incorporating maleimide only as end-caps to the polymer chain.

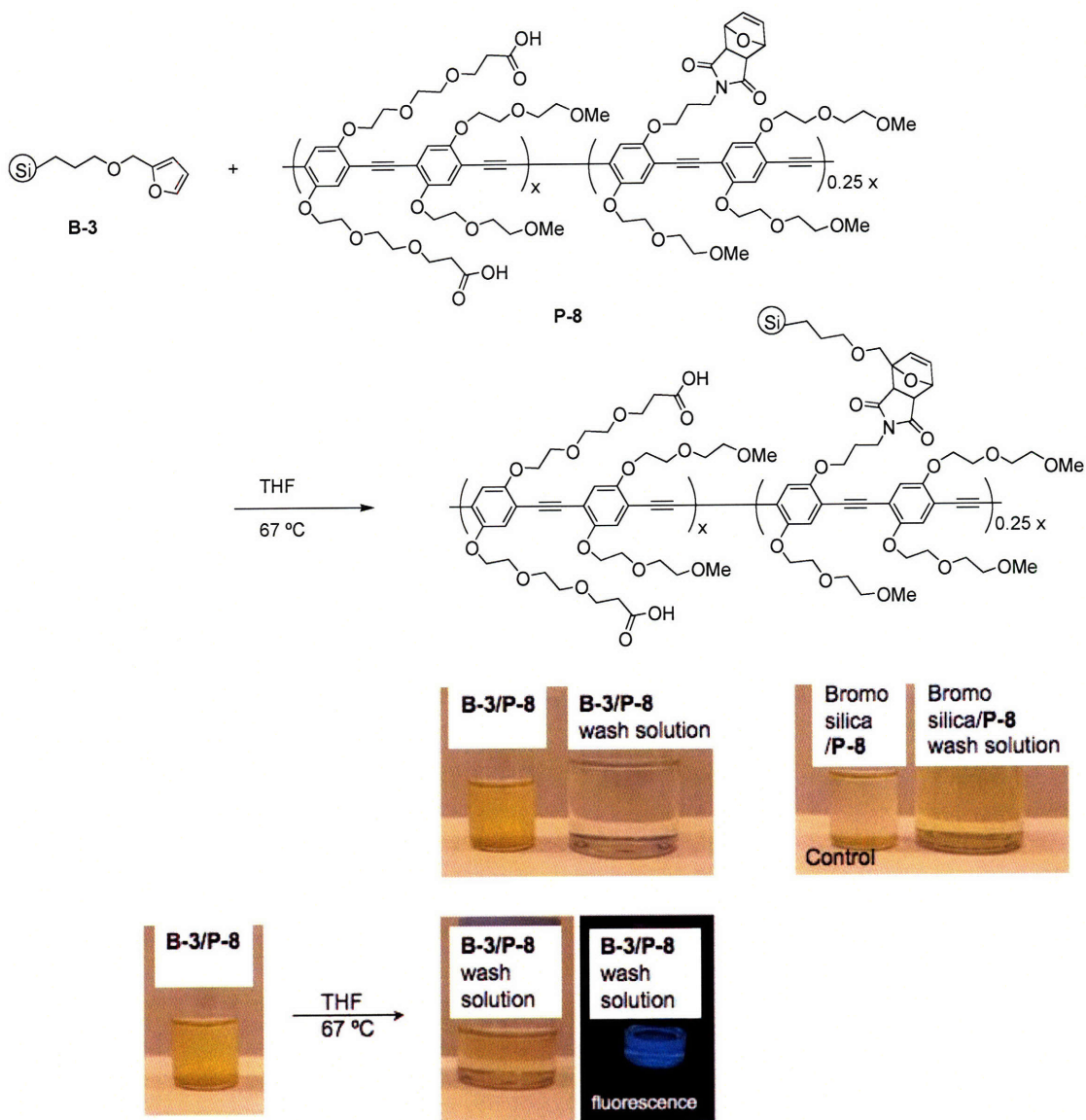


Figure 5 The binding and subsequent release of **P-8** maleimide from **B-3**. Heating the beads and **P-8** results in yellow beads and a colourless solution. In the presence of the unfunctionalized silica, labeled Bromo silica, **P-8** remains largely in solution. Heating the **B-3/P-8** beads releases the polymer into solution.

To characterize the surface chemistry on **B-3**, the beads were ground and pressed into KBr pellets^{5, 6} to be monitored by FTIR (Figure 6). The FTIR

spectrum of the beads, **B-3** and the unfunctionalized bromo-silica is depicted in Figure 6A. The FTIR spectrum of **P-8** is shown in Figure 6B and the spectrum for the control reaction of the unfunctionalized bromo-silica and **P-8** is given in Figure 6C. The sharp peaks associated with stretches of the $\text{-CH}_2\text{CH}_2\text{O-}$ units of the polymer at 1275, 1259, 1235, 1182, and 1126 cm^{-1} are not present when the bromo silica beads are stirred with the polymer, these peaks are clearly present in the beads resulting from the reaction of **B-3** and **P-7**.

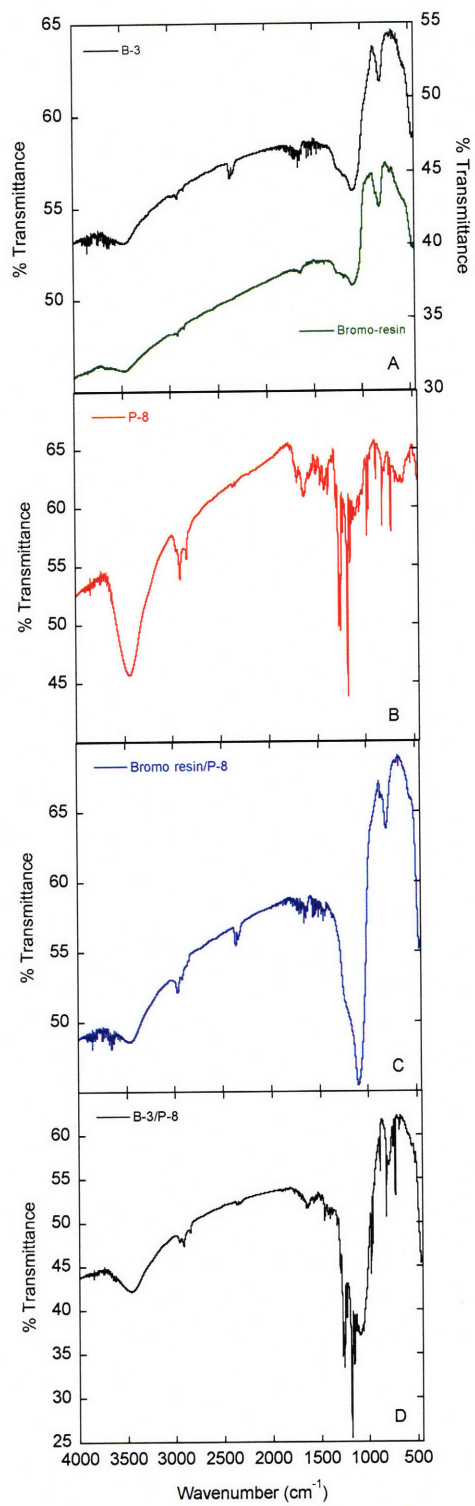


Figure 6 FTIR for **B-3** and **P-8** (KBr pellets). (A) Beads **B-3** (black) and the bromo silica (green); (B) Polymer **P-8**; (C) Result from control reaction of bromo-silica and **P-8**; (D) Result from reaction of **B-3** and **P-8**.

5.3.2 Interaction of EcmbT3 and B-3

Beads **B-3** were then exposed to EcmbT3 under the conditions required for coupling to **P-8** (HBTU, HOBt, DIPEA, DMF) to determine whether DNA would stick to the beads either by reacting with the surface of the silica beads or non-specifically, and to determine what conditions would be required to remove excess DNA. The solution and beads were stirred at room temperature overnight, then transferred to an efficiency column. The beads were first washed with DMF and then water. The fractions were collected and monitored by UV-Vis absorption. The vast majority of the DNA was removed in the first water wash. The beads were then rinsed with 20 mM tris buffer pH 7.4 and a second flush with water. Finally, a methanol wash was conducted and found to remove the last of the DNA from the beads.

5.3.3 Solid-phase Conjugation of EcmbT3 onto P-8

Polymer immobilized **B-3/P-8** beads were prepared and exposed to EcmbT3 both in the presence and absence of activating agents HBTU, HOBt, and DIPEA (Table 3) in DMF. This eliminates the problem of the activated polymer precipitating out of solution as encountered earlier. After four hours, the beads were washed in an efficiency column with DMF, water, Tris buffer, a second flush with water, and finally MeOH. The washes were monitored by UV-Vis absorption and fluorescence spectroscopy. Washing was continued until EcmbT3 could no longer be detected in the rinse. The **B-3/P-8/EcmbT3** beads were then heated for two hours at 67 °C in a 1:1 H₂O:DMF solution. The beads

were then centrifuged while still hot and the solution was decanted. The UV-Vis absorbance and fluorescence spectra of the final solutions were analyzed (Figure 7).

Table 3 Reaction matrix for the solid-phase conjugation of EcmbT3 to **P-8**. The equivalents listed are given relative to the polymer repeat unit, assuming 100 % loading of the polymer onto **B-3**.

Experiment	Amount of DNA	Amount of Activating Agents
1	10 eq	4 eq HBTU 4 eq HOBt 8 eq DIPEA
2	10 eq	—
3	—	—

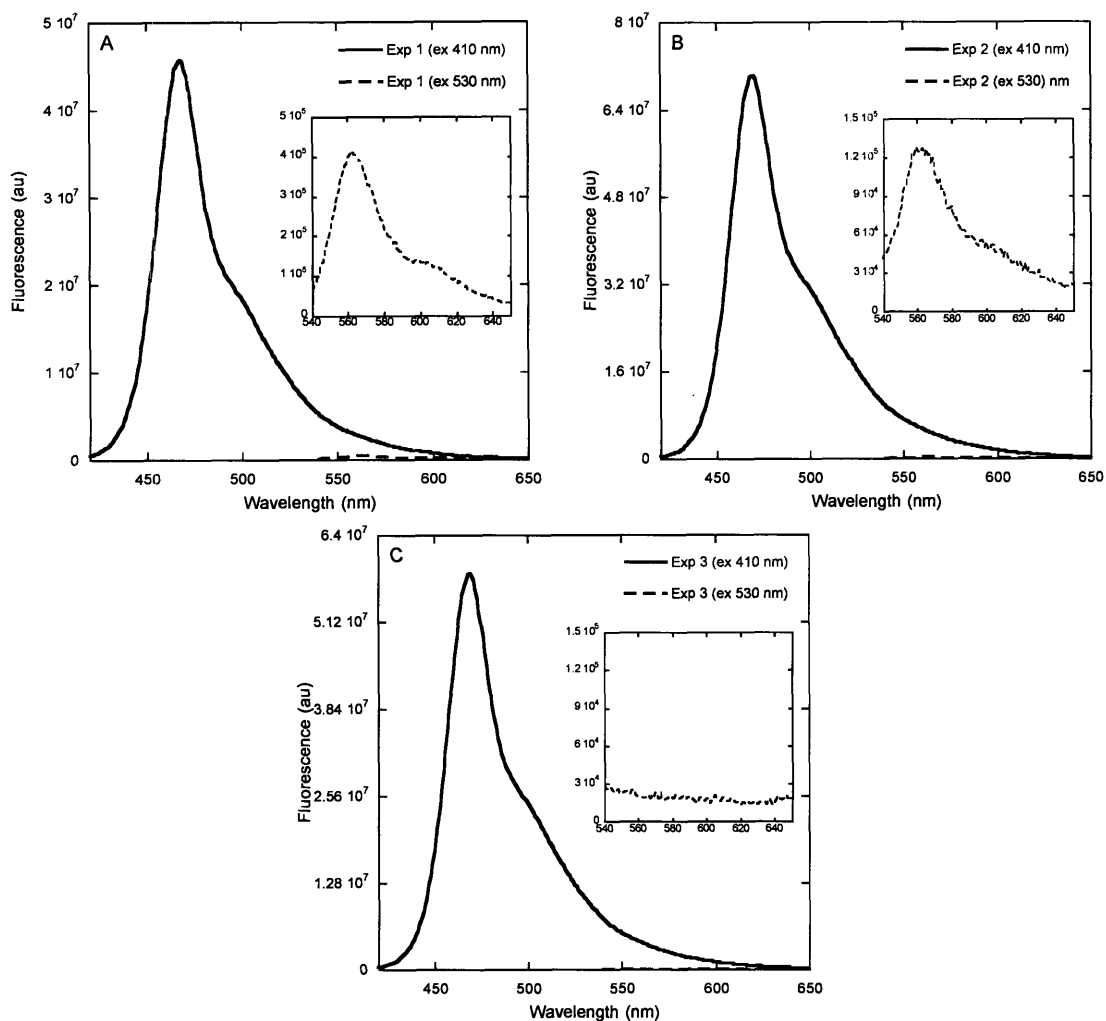


Figure 7 (A)-(C) Fluorescence results for Exp 1-3 with excitation of both the polymer at 410 nm and the dye at 530 nm. Inset: Dye fluorescence upon direct excitation at 530 nm.

Although the amount of DNA present in the solution of Expt. 1 is far greater than that in Expt. 2, there is, unfortunately, DNA present in the polymer solution from Expt. 2. This emphasizes the need to further develop a protocol for effective removal of excess DNA from silica bound PPEs. The use of surfactants or varying the pH of washes should be investigated in the future to optimize this process. Varying the activation and coupling conditions will also be useful in

optimizing the loading of DNA on the PPE, and may lead to conditions that reduce the non-specific binding of DNA to PPEs. The ability of proteins such as lysozyme, myoglobin and haemoglobin to bind non-specifically to carboxylic acid-PPEs has been encountered,⁷ and suggests that this may be an issue with biomolecules in general.

5.4 Conclusion

Initial explorations into conjugating DNA to PPEs were conducted. A new polymer was prepared containing two handles by which it can be manipulated. Amine containing compounds can be tethered to PPEs by reactions with pendent carboxylic acid groups. Furan, and potentially thiols, can be attached with the maleimide moiety.

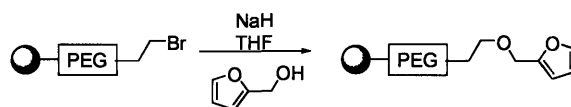
EDAC/NHS activation did not appear to be effective activating agents, and HBTU/HOBt coupling protocols were adopted. Three new furan-containing beads were prepared with the aim of improving purification of PPE-DNA conjugates, however an efficient and thorough protocol for removing excess DNA is still elusive.

Once an effective method for removing excess DNA is established, assembly of the DNA-PPE conjugate should be straightforward. The response of

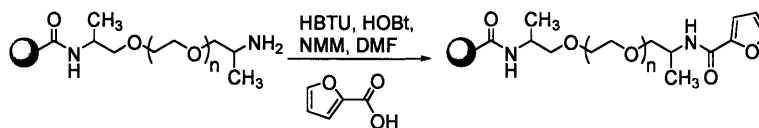
this system to *E. coli* targets will be important to establish and the information garnered will help in the final design of the sensor system.

5.5 Experimental

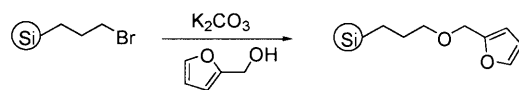
All DNA sequences were obtained from IDT DNA (Coralville, IA) purified by HPLC and used as received. DNA samples were re-suspended in Millipore water to have a final stock concentration of 1 nmol/ 10 μ L. UV/Vis spectra were recorded on an Agilent 8453 diode-array spectrophotometer and corrected for background signal with a solvent-filled cuvette. Emission spectra were acquired on a SPEX Fluorolog- τ 3 fluorometer (model FL-321, 450 W Xenon lamp) using right angle detection. The absorbance of all samples was kept to optical densities 0.1 au in order to minimize artifacts from reabsorption of emitted light. In section 5.3.1, beads were collected and washed with solvent in an efficiency column unless otherwise noted.



B-1: NovaSyn® TG bromo resin (0.2041 g, loading: 0.27 mmol/g) was stirred in 5 mL dry THF overnight to swell the beads. In a separate flask, furfuryl alcohol (25 μ L, 0.29 mmol) and NaH (60 % dispersion in oil, 0.0129 g NaH/oil, 0.32 mmol NaH) were stirred in 0.5 mL dry THF until bubbling ceased. This solution was then added to the bead solution. The beads were subjected to sequential washes with ~10 mL THF, MeOH, Hexanes, and THF.



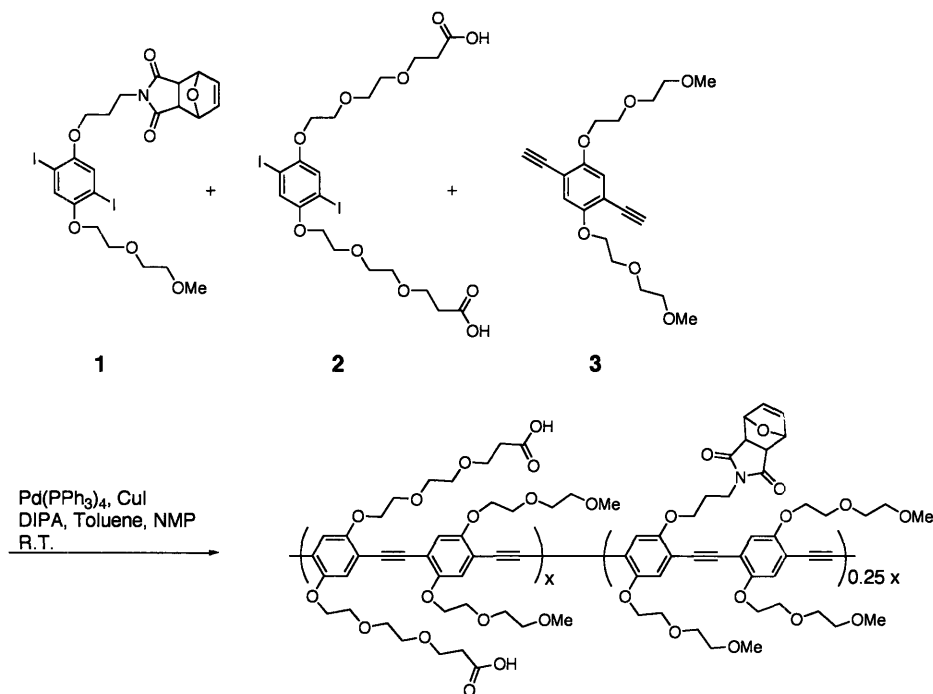
B-2: PL-PEGA methanol swollen resin (3.20 g \approx 0.4 g dry, loading: 0.4 mmol/g dry) were washed with \sim 200 mL DMF. The beads were gently stirred in 20 mL DMF by rocking with 2 furoic acid (0.0714 g, 0.51 mmol), HBTU (0.1836 g, 0.48 mmol), HOBT (0.0652 g, 0.48 mmol), and NMM (0.10 mL, 0.91 mmol) for 24 hours. The beads were collected, washed with \sim 200 mL DMF and transferred back to the vial and mixed for a second time with 2 furoic acid (0.0720 g, 0.51 mmol), HBTU (0.1866 g, 0.49 mmol), HOBT (0.0681 g, 0.50 mmol), and NMM (0.10 mL, 0.91 mmol) in 15 mL for 24 hours. The beads were again collected and washed by rocking the beads in 40 mL DMF for 2 hours, then every 24 hours for three days. Solvent was removed *in vacuo*.



B-3: 4-Bromopropyl-functionalized silica gel (0.2036 g, loading: 1.5 mmol/g) was stirred in 5 mL neat furfuryl alcohol with potassium carbonate (0.2144 g, 1.6 mmol) for 8 hours. The beads were then collected and sequentially washed in an efficiency column with dichloromethane, acetone, water, and acetone again. The solvent was removed *in vacuo*.

2: Compound **2** was prepared according to literature procedure^{3, 8} and was generously donated by Jessica Liao.

3: Compound **3** was prepared according to literature procedure.^{3, 8}



P-8: Monomers **1** (5.002 mg, 7.5 nmol), **2** (15.298 mg, 22.4 nmol), and **3** (11.075 mg, 30.6 nmol) were added to a 50 mL Schlenk flask. Under an inert atmosphere, catalytic amounts of Pd(PPh₃)₄ and CuI were added, followed by thoroughly degassed 1:4:5 DIPA:Toluene:NMP. The solution was stirred at room temperature for seven days. The polymer was precipitated in 100 mL EtOAc, and washed with water. The polymer transferred to the water layer and was dialyzed against MeOH in 7,000 MWCO dialysis tubing. The solution was then lyophilized to obtain a yellow powder.

5.6 References

1. Aslam, M.; Dent, A., *Bioconjugation: Protein Coupling Techniques for the Biomedical Sciences*. Macmillan: London, 1999.
2. Benoiton, N. L., *Chemistry of peptide synthesis*. Taylor & Francis/CRC Press: Boca Raton, 2006.
3. Wosnick, J. H.; Mello, C. M.; Swager, T. M., "Synthesis and Application of Poly(phenylene Ethynylene)s for Bioconjugation: A Conjugated Polymer-Based Fluorogenic Probe for Proteases," *J. Am. Chem. Soc.* **2005**, *127*, 3400-3405.
4. Martin-Matute, B.; Nevado, C.; Cardenas, D. J.; Echavarren, A. M., "Intramolecular reactions of alkynes with furans and electron rich arenes catalyzed by PtCl₂: The role of platinum carbenes as intermediates," *J. Am. Chem. Soc.* **2003**, *125*, 5757-5766.
5. Yucheng, W.; Lide, Z.; Guanghai, L.; Yong, Z.; Guangmin, S., "Preparation and optical properties of nanocomposites containing palladium within mesoporous silica via sol-gel chemistry," *J. Mater. Synth. Process.* **2002**, *10*, 175-182.
6. Onfroy, T.; Clet, G.; Houalla, M., "Quantitative IR characterization of the acidity of various oxide catalysts," *Microporous Mesoporous Mater.* **2005**, *82*, 99-104.
7. Kim, I. B.; Dunkhorst, A.; Bunz, U. H. F., "Nonspecific interactions of a carboxylate-substituted PPE with proteins. A cautionary tale for biosensor applications," *Langmuir* **2005**, *21*, 7985-7989.

8. Zheng, J.; Swager, T. M., "Poly(arylene ethynylene)s in chemosensing and biosensing," *Adv. Polym. Sci.* **2005**, *177*, 151-179.

EDUCATION

Ph.D., Organic Chemistry, September 2006

Massachusetts Institute of Technology, Cambridge, MA, USA

Thesis: Study Of Poly(Phenylene ethynylene)s, Dendritic Quenchers, And Molecular Beacons Towards The Application of A Poly(Phenylene ethynylene)-Based Biosensor

Advisor: Professor Timothy M. Swager

B.Sc., Honours Chemistry, First Class Honours, 2000

McGill University, Montréal, QC, Canada

Thesis: "Studies Towards Synthesis of Metal Directed Self-Assembly of DNA-Based Nanostructures"

Advisor: Professor Hanadi Sleiman

RESEARCH EXPERIENCE

2001-present Ph.D. Candidate, Massachusetts Institute of Technology

- › Designed and developed biosensors combining conducting polymers, DNA, and novel dendritic quenchers.
- › Synthesized conducting polymers for conjugating biomolecules in biosensing applications.
- › Developed new synthetic techniques for producing dendritic quenchers.
- › Investigated molecular beacon sequence properties for incorporation into biosensors.

1999-2000 Research Assistant, McGill University

- › Synthesized Ru, Pt, and Pd compounds for use in assembly of DNA architectures.
- › Gained expertise in inorganic synthetic techniques and DNA manipulation.

1998 Research Assistant, University of Ottawa

- › Explored "ship-in-a-bottle" syntheses for trapping metals in zeolites.

1997 Research Assistant, McGill University

- › Conducted NIR experiments for the non-invasive monitoring of disease in trees.

TEACHING AND RELATED EXPERIENCE

2002-2003 Chemistry Outreach Volunteer, Massachusetts Institute of Technology

- › Demonstrated science experiments for local grade school students.

2001-2002 Teaching Assistant, Massachusetts Institute of Technology

- › Lectured recitation for introductory organic and general chemistry courses.

2000-2001 Assistant to Immigration Officer, Canadian Embassy, Rabat, Morocco

- › Aided immigration officers in filing and granting of permanent visas.

2000-2001 Teacher and Private Tutor, Rabat American School, Rabat, Morocco

- › Instructed several high school courses, including chemistry and algebra.

1998-2000 Laboratory Assistant, McGill University, McGill University

- › Prepared and validated experiments for advanced analytical and physical undergraduate laboratory experiments.

AWARDS

- 2004 Best Poster Presentation – MPC Materials Day, MIT
- 2004 Best Poster Presentation – Fpi6 Conference, Cornell University
- 2002 T.A. Teaching Award, MIT
- 2001 MIT Graduate Student Award
- 2000 Dean's Honours List (4 years)
First Class Honours Award (4 years)
- 1999 NSERC Undergraduate Research Award
- 1998 NSERC Undergraduate Research Award
- 1997 Golden Key National Honour Society Member
- 1996 Esther Breuer Award for Excellence in Science
Excellence Awards in Mathematics, Chemistry, Physics, French

AFFILIATIONS

- American Chemical Society
- Materials Research Society
- Golden Key National Honour Society

PUBLICATIONS

- Bailey, G. C.; Swager, T. M. "Masked Michael Acceptors in Poly(phenyleneethynylene)s for Facile Conjugation." *Macromolecules*, **2006**, 39, 2815-2818.
- Bailey, G. C.; Swager, T. M. "Synthesis and properties of a masked maleimide-containing poly(phenyleneethynylene)." *Polymer Preprints*. **2004**, 45, 561-562.

PRESENTATIONS

- Bailey, G.C.; Swager, T. M. "Synthesis of Poly(phenyleneethynylene)s Containing Pendent Masked Michael Acceptors and Their Application into Biosensors." Materials Research Society Fall Meeting, Boston, MA, **2005**.
- Bailey, G. C.; Swager, T. M. "PPEs and Biosensors: A Tale of Two Conjugations." Materials Processing Center Materials Day, MIT, Cambridge, MA, **2004**.
- Bailey, G. C.; Swager, T. M. "Towards a PPE-Based Biosensor." American Chemical Society National Meeting, Philadelphia, PA, **2004**.
- Bailey, G. C.; Swager, T. M. "Conjugated Polymers for Biosensor Applications." NASA-NCI P.I. Meeting, Monterey, CA, **2004**.
- Bailey, G. C.; Swager, T. M. "Synthesis and Application of Pendent Maleimide Groups on Poly(*p*-phenyleneethynylene) Revealed During Post-Polymerization Deprotection." Fpi6, Cornell University, Ithaca, NY, **2004**.
- Bailey, G. C.; Swager, T. M. "Conjugated Polymers for Biosensor Applications." NASA-NCI P.I. Meeting, Chicago, IL, **2003**.
- Bailey, G. C.; Swager, T. M. "Binding Peptides and Antibodies to Conjugated Poly(*p*-phenyleneethynylene)." American Chemical Society National Meeting, New York, NY, **2003**.

Acknowledgments

When I first applied to MIT, it was with the intent to pursue a career as an inorganic chemist. An interest in polymers led me to sign up for a meeting with Professor Timothy Swager during visiting weekend. By the end of the meeting, my decision was made: I was going to MIT and I would join Professor Swager's group while switching to Organic. He was friendly and easy-going, and his passion for research was infectious. Tim was very supportive of my decision to defer my enrollment for one year while I traveled through Morocco and Europe. When I returned, I was granted the freedom to explore areas of research that were outside the general boundaries of the group, working with DNA and dendrimers, while still thinking about and focusing on PPEs and sensors. Tim is a wonderful advisor and has made my whole experience at MIT a positive one and I would like to thank him for all of his guidance, challenges, and words of encouragement.

My undergraduate supervisor, Professor Hanadi Sleiman, at McGill University, played an important role in my career. Her enthusiasm for research and encouragement convinced me to pursue my graduate degree in chemistry.

I would like to express deep gratitude to our collaborators, Drs. Charlene Mello and Romy Kirby, at the US Army Soldier Systems Center in Natick, MA. Without their guidance and advice, the work with molecular beacons would have been extremely challenging. Romy was always especially ready to answer questions on anything from buffers to dialysis and provide excellent insight on how to design a DNA experiment.

Dr. Robert Deans and Paul MacLean of Nomadics, Inc. were both very generous with their time in helping me with the Oligreen staining, and I thank them for it.

I would like to thank all of the excellent people I worked with in the DCIF: Jeff Simpson, Dave Bray, Li Li, Bob Kennedy, and Hongjun Pan. They were always ready to help, and were always a good source of departmental news.

One of the reasons that I loved coming to work everyday was the fact that I got to work with the best group members. Everyone was so helpful when I first joined the group from Kenichi Kuroda showing me how to properly stain a TLC plate, to Juan Zheng sharing her bench with me, and Jordan Wosnick teaching me the ropes of running reactions under inert atmosphere.

The overall tone of the lab was always cheerful with plenty of people to turn to either for funny stories or for help with chemistry: Alex Paraskos, Aimee Rose, JD Tovar, Phoebe Kwan, Jean Bouffard (thank you for all of the help with the GPC!), Jocelyn Nadeau, Evgueni Nesterov, Stefan Zahn, Dahui Zhao, Koji Miki, Kazunori Sugiyasu, Mark Taylor, Guy Joly, and Koushik Venkatesen. I would like to particularly thank Brad Holliday for all of his helpful discussions regarding job searches and career options.

Since Becky Bjork joined the ranks as Lab Manager, the lab has run like a well-oiled machine. Becky was always ready to help and was a great source for stories when chemistry was slow. I cannot thank her enough for helping with all the last minute orders and keeping the lab well stocked. Richard Lay and Kathy Sweeney were always a great help in dealing with the administrative side of chemistry. I would also like to thank Kathy for her help in proofing my thesis for typos!

My first year at MIT would not have been as smooth nor as happy without my classmate Chudi Ndubaku. He got us through countless study sessions and was my cheerleader throughout our time at MIT. I could always count on him whether I needed a laugh or help with the synthesis of a particular compound.

Sam Thomas had a significant impact on my experience at MIT. He was always ready with words of encouragement and was always available for discussions about chemistry. I especially want to thank him for all of his help with the fluorimeter, as well as his heir, Trisha Andrews.

Karen Martin has become a great friend and trusted advisor. She helped me get through the lows of graduate school and to see the light at the end of the tunnel. Her outlook on life always kept a smile on my face. And she always knew where we could get an excellent meal!

Andrew Satrijo and Anne McNeil were always ready for discussions about anything, whether chemistry related or not. Thank you, Anne, for your sympathetic ear as I finished writing up my thesis!

I want to thank the rest of my classmates in the Swager Group for their ready jokes and support: John Amara, Nate Vandesteeg, and Hyuna Kang.

In chemistry, we spend an extensive amount of time with our bench mates. Kenichi, Juan, and Jordan were instrumental in my learning my way around the lab and together we started the Biosensor Subgroup. A recent member of the "bio bay" was Ryo Takita and from our short overlap, I know he will have a great impact on the group. Over the last two years I spent endless

hours with Jessica Liao and Paul Kouwer. Paul's extensive knowledge of all things synthesis was a great resource and working with him was a pleasure given his easy-going nature and love of life. He was always there to cheer me on when chemistry was difficult. He and his wife Suzan have become great friends and I hope to see them in Calgary! Working with Jess was fantastic, and she always brought a breath of fresh air to the lab and a different approach to problems. She was always ready to help me discuss any research issues I might have had. I will miss working alongside her happy attitude, listening to her radio show, and living vicariously through her!

I would also like to thank Aurore Wery for her fabulous friendship and strength throughout all these years. Without Janine Mauzeroll, my years at McGill would not have been as interesting or as fun!

The people without whom this adventure would not have been possible are my family. Without their love, guidance, encouragement and support, this journey would have been extremely difficult.

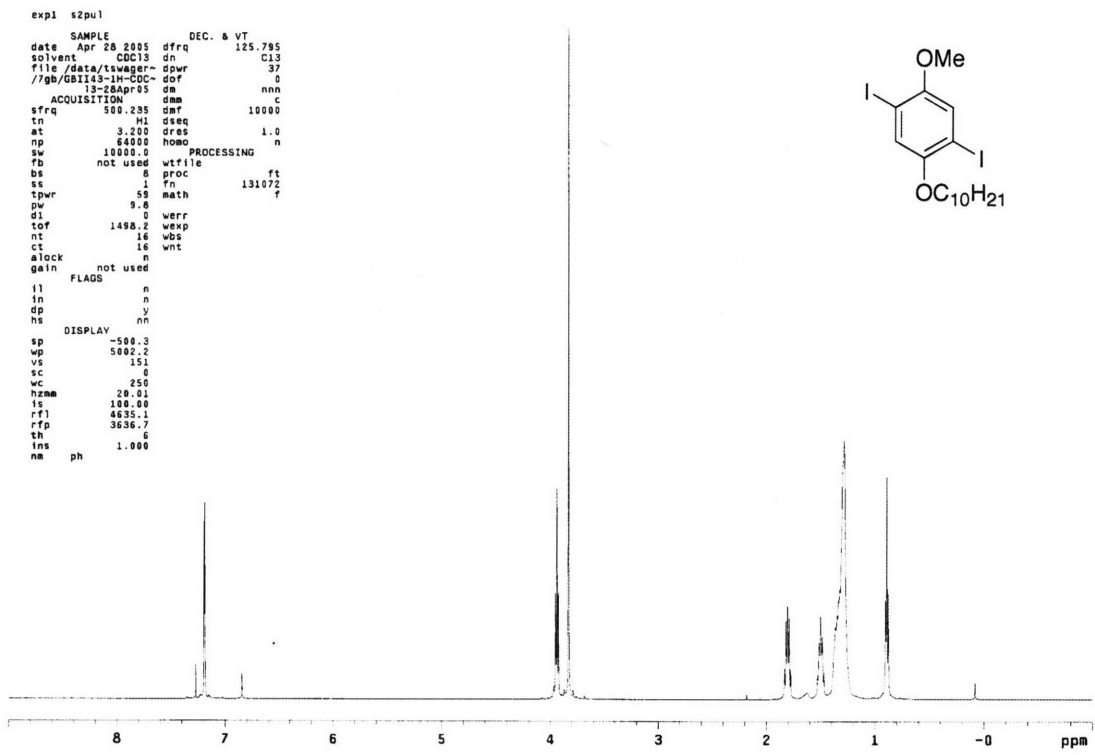
My grandparents, Zohra Bouhlal and Lillian and Wallace Bailey have taught me countless lessons that help guide me everyday.

My husband, Curtis, who joined me for the home stretch of this academic marathon, has been here for me as I finished my research at MIT. His support and love over these last three years, and his ability to make me laugh have helped lighten the load and make the time fly by. We started our lives together in Boston and I am so excited for us to continue our adventure in Calgary!

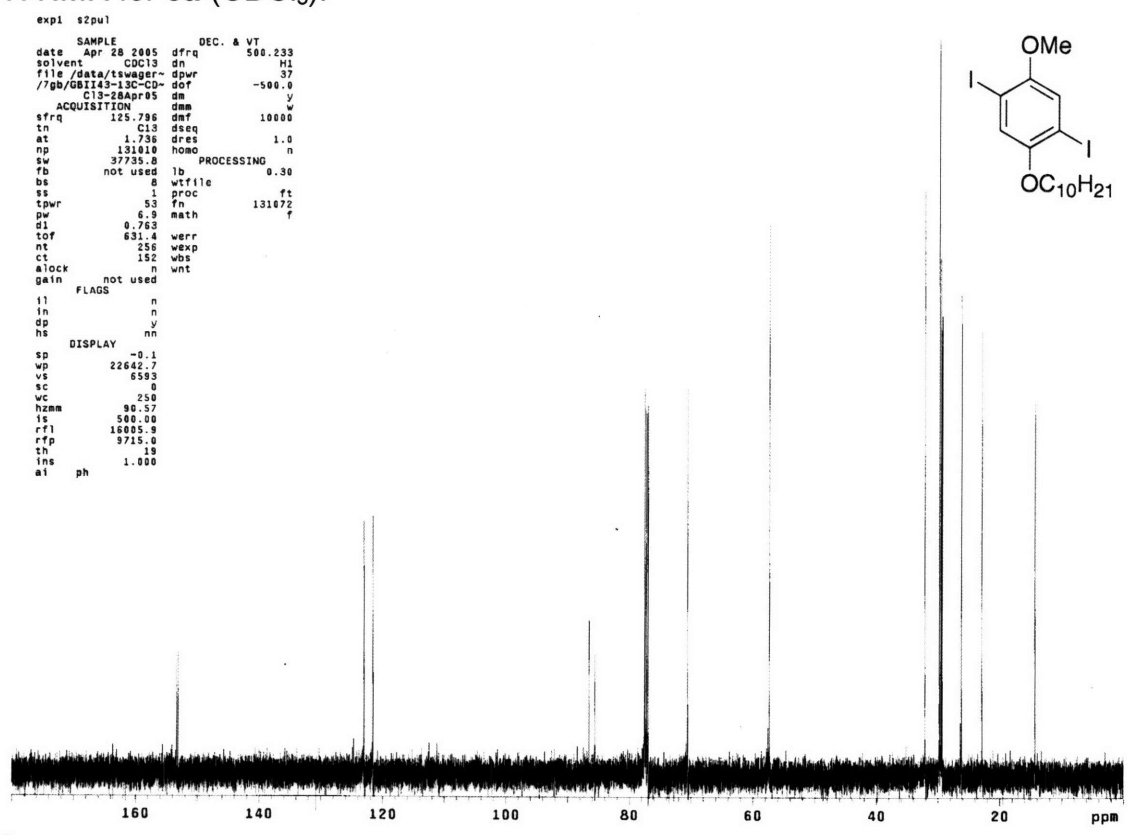
My sisters, Nawel and Soraya, were my first study partners. They have cheered me on, listened to countless chemistry stories, and were always ready to provide some comic relief.

My parents, Mark and Raja, are my foundation. They have taught me the importance of hard work while maintaining balance in life. They have instilled in me the principles and instincts to help me navigate through life, the drive to excel and succeed, and the confidence to know when to walk away. They have shown me the significance of goals, and by example, how to achieve them. They have taught me to appreciate life and to live it to the fullest. Their unlimited support and faith has helped me to reach for my dreams. For this, and for so much more, I am eternally grateful to them.

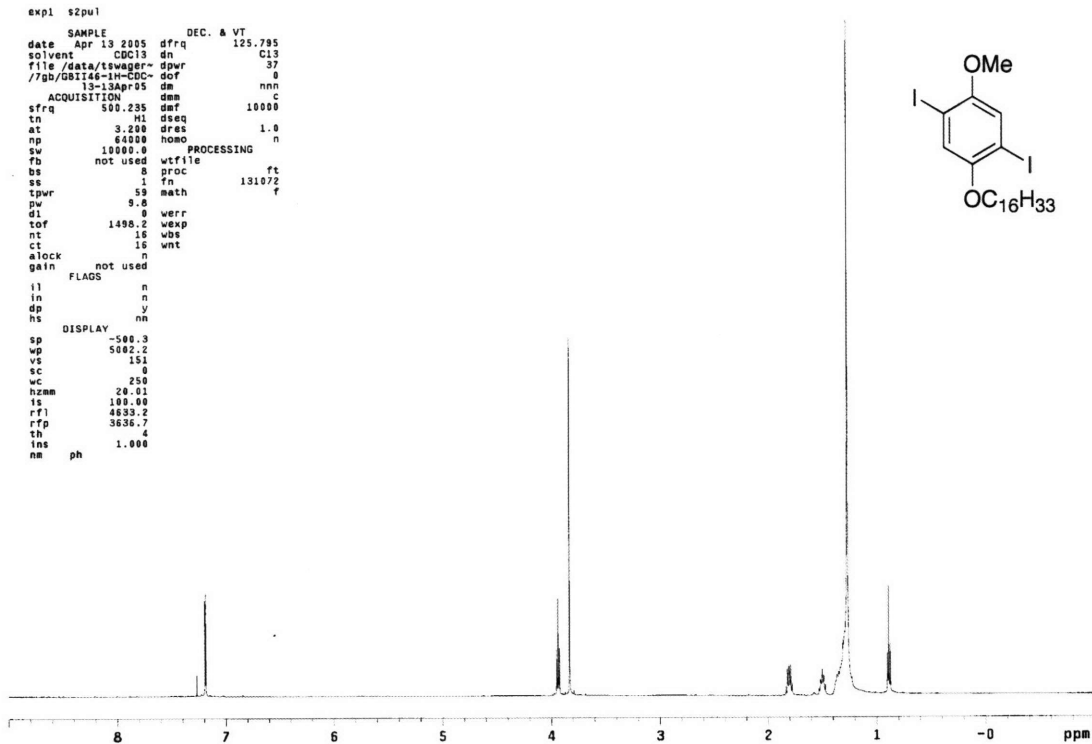
Appendix 1:
NMR Spectra for Chapter 2



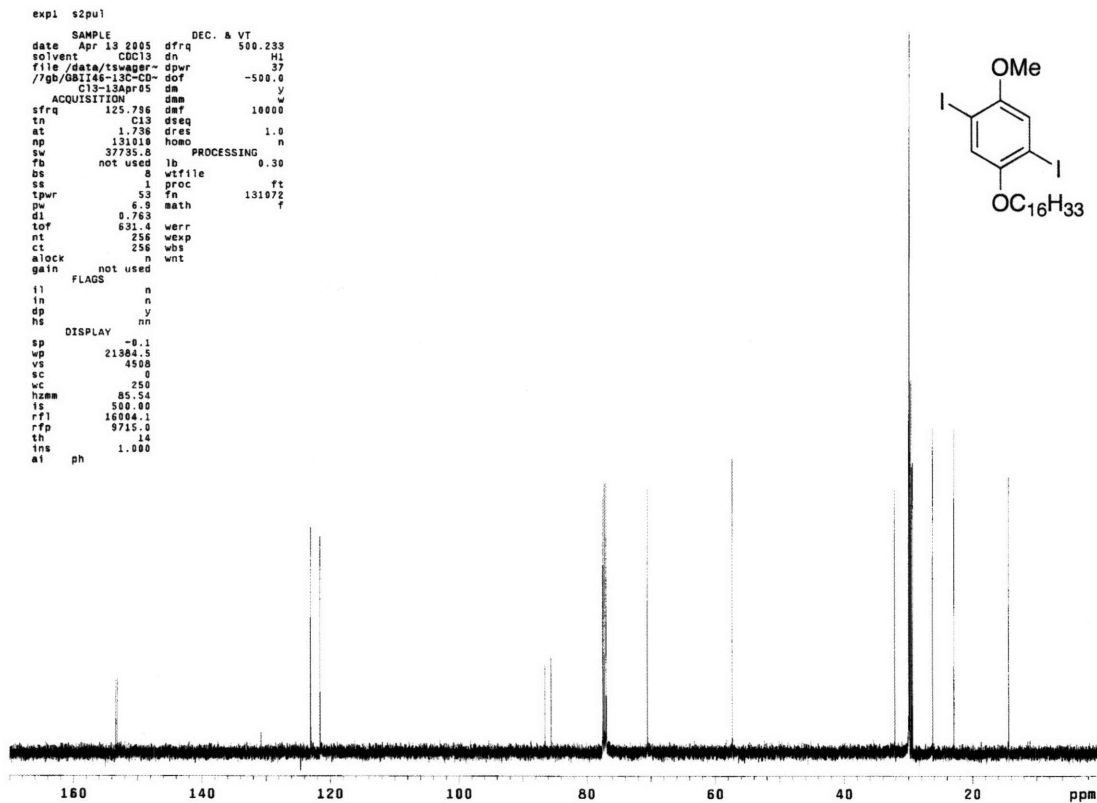
¹H NMR for 3a (CDCl₃).



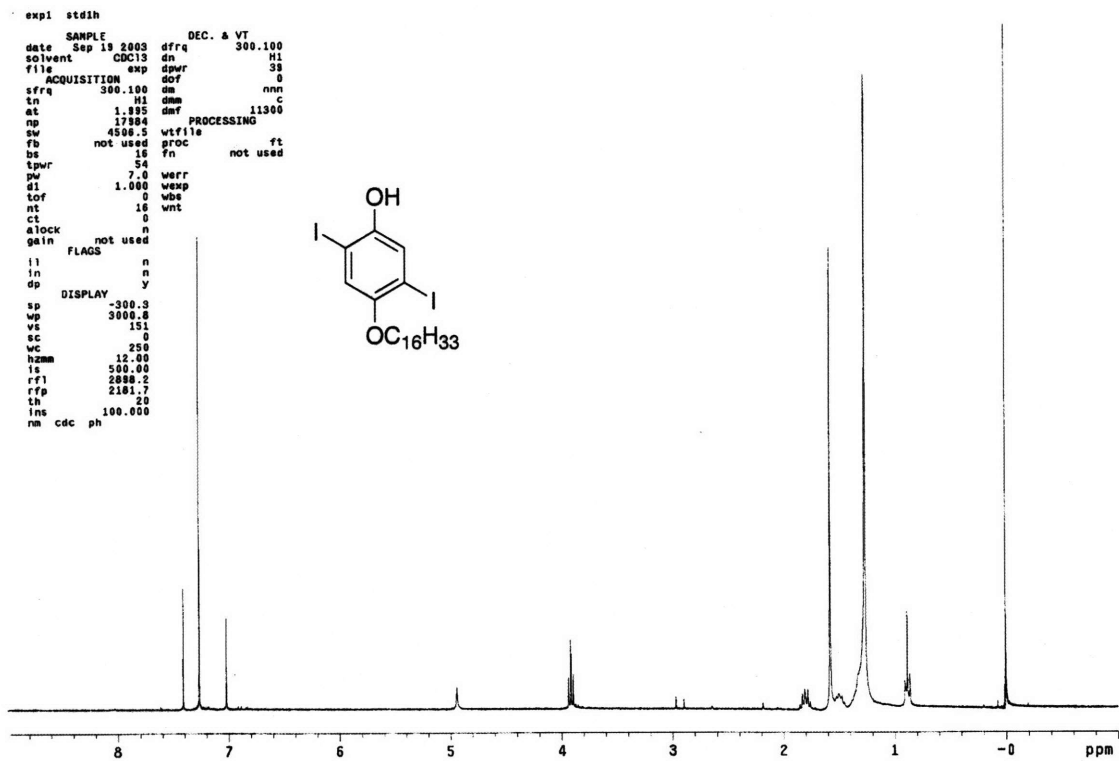
¹³C NMR for 3a (CDCl₃).



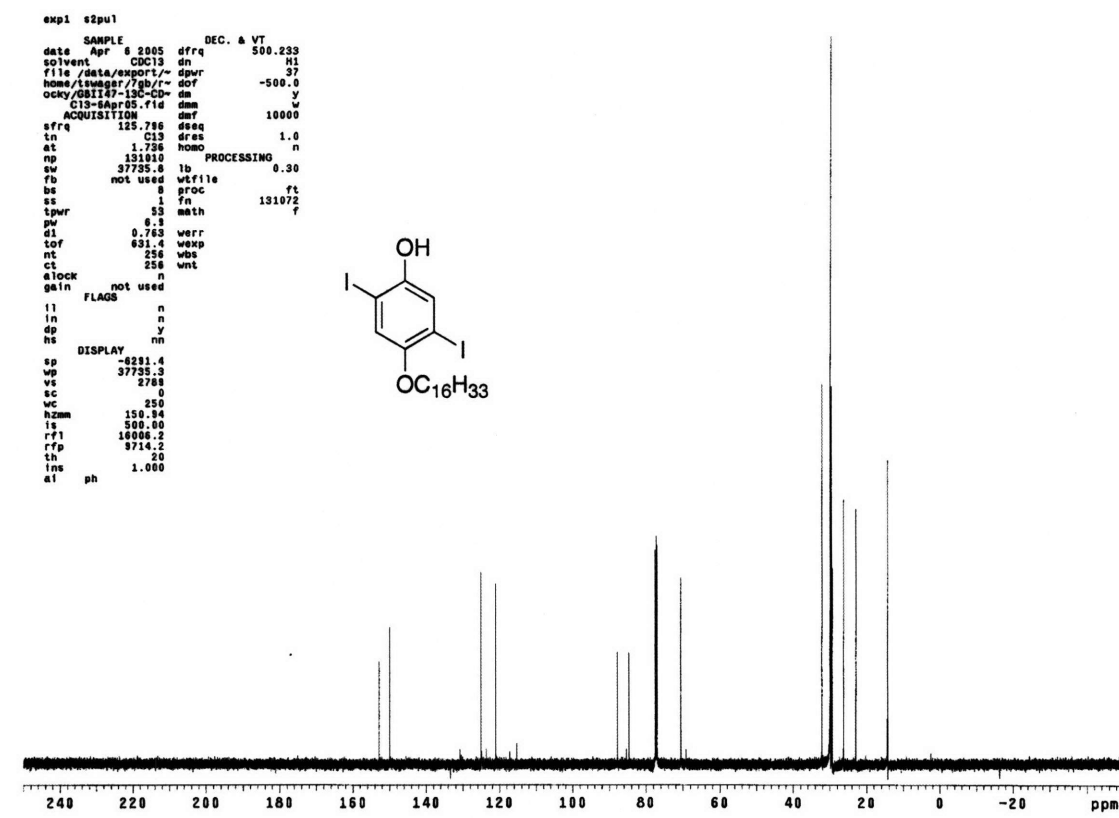
^1H NMR for **3b** (CDCl_3).



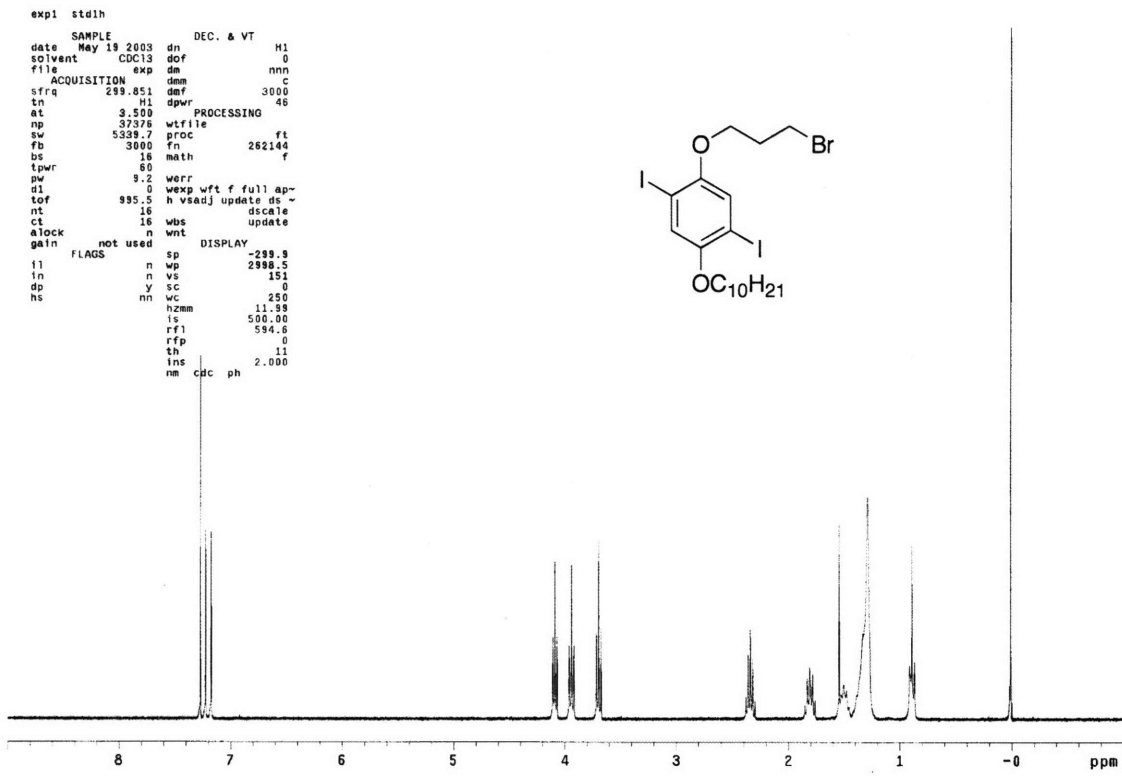
^{13}C NMR for **3b** (CDCl_3).



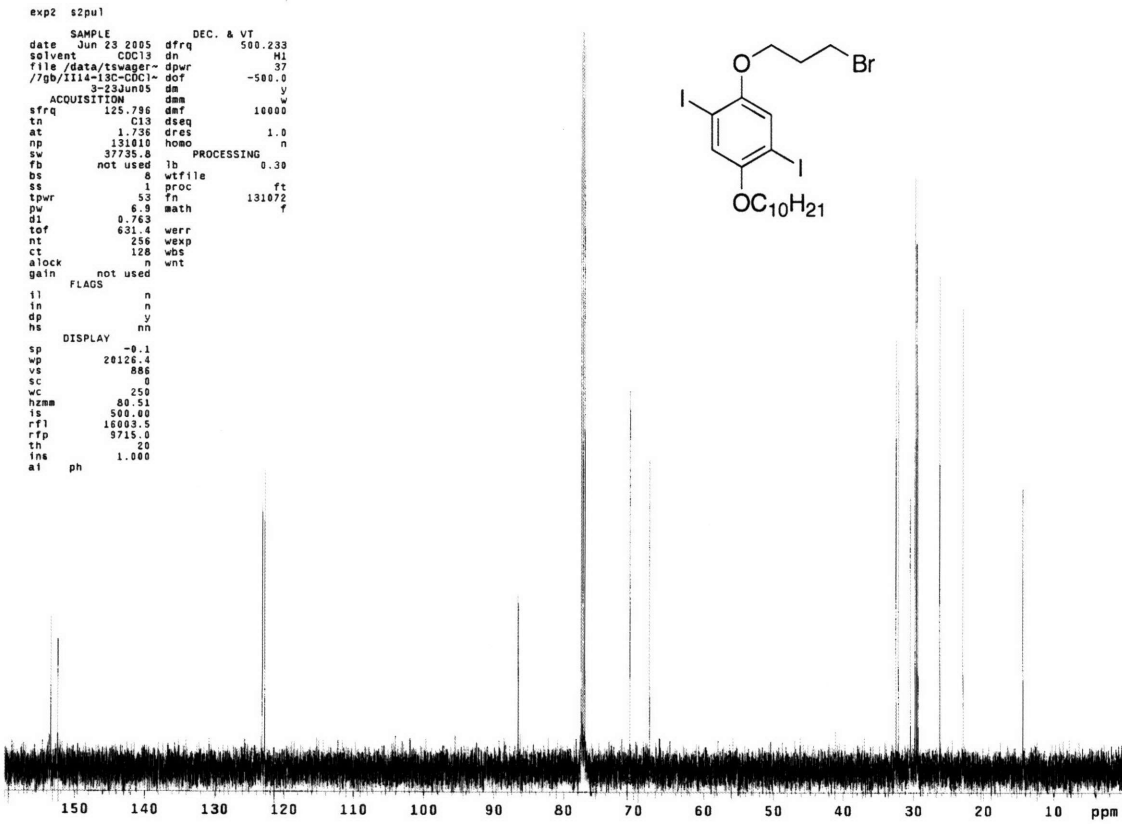
¹H NMR for **4b** (CDCl₃).



¹³C NMR for **4b** (CDCl₃).



¹H NMR for **5a** (CDCl₃).

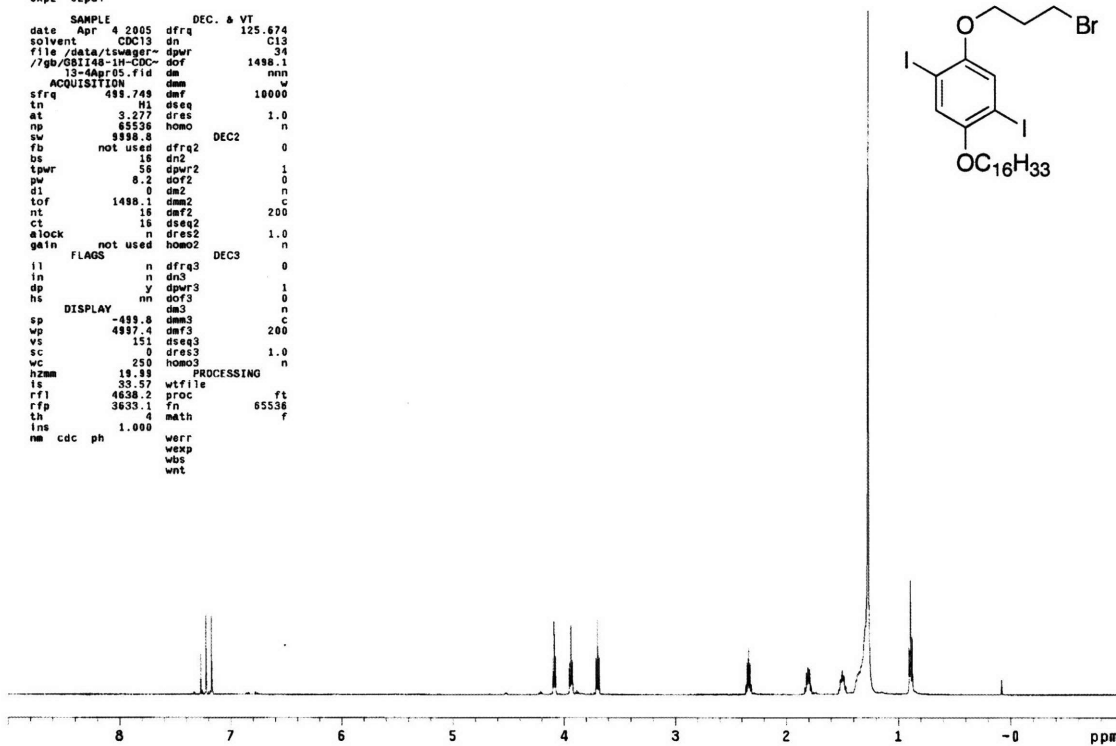


¹³C NMR for **5a** (CDCl₃).

```

exp2 s2pu1
SAMPLE
date Apr 4 2005 dfrq 125.674
solvent CDCl3 dn C13
file /data/lswager/dpwr 34
/7gb/GBI148-1H-CDCl3-dof 1498.1
13-Apr05.fid dm nnn
ACQUISITION dmm w
sfrq 499.749 dmf 10000
tn H1 dseq 1.0
at 3.277 dres n
np 65536 homo DEC2 0
sw 9998.8 dfrq2 0
fb not used dn2 1
bs 18 dpwr2 0
tpwr 56 dof2 0
d1 0 dm2 n
tof 1498.1 dmm2 C
nt 16 dmf2 200
ct 16 dseq2 1.0
alock n dres2 n
gain not used homo2 n
FLAGS DEC3 0
ll n dfrq3 0
ln n dnc 0
dp y dpwr3 1
hs nn dm3 0
DISPLAY dm3 C
sp -499.8 dmm3 200
wp 499.74 dmf3 0
vs 151 dseq3 1.0
sc 0 dres3 n
wc 250 homo3 n
hzmm 19.99 PROCESSING
ls 39.57 wfile ft
rfi 4638.2 proc 65536
rfp 3633.1 fn
th 4 math f
ins cdc ph werr
nm wexp
wbs
wnt

```

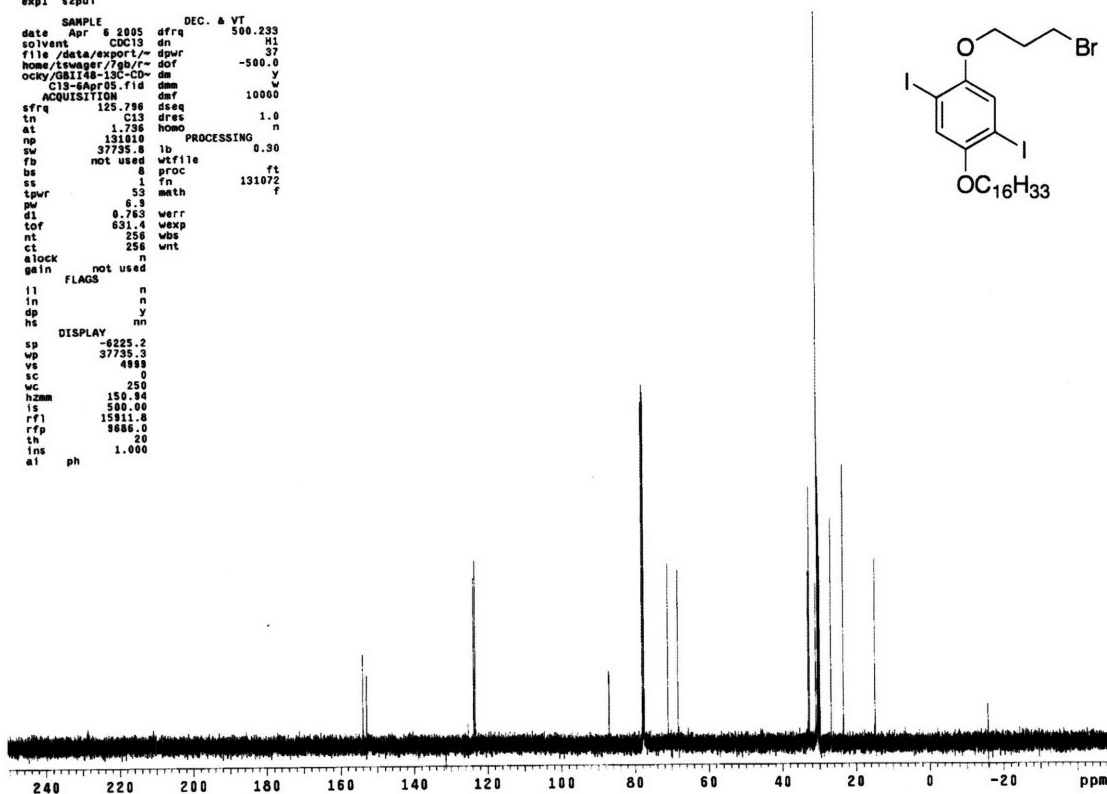


¹H NMR for **5b** (CDCl₃).

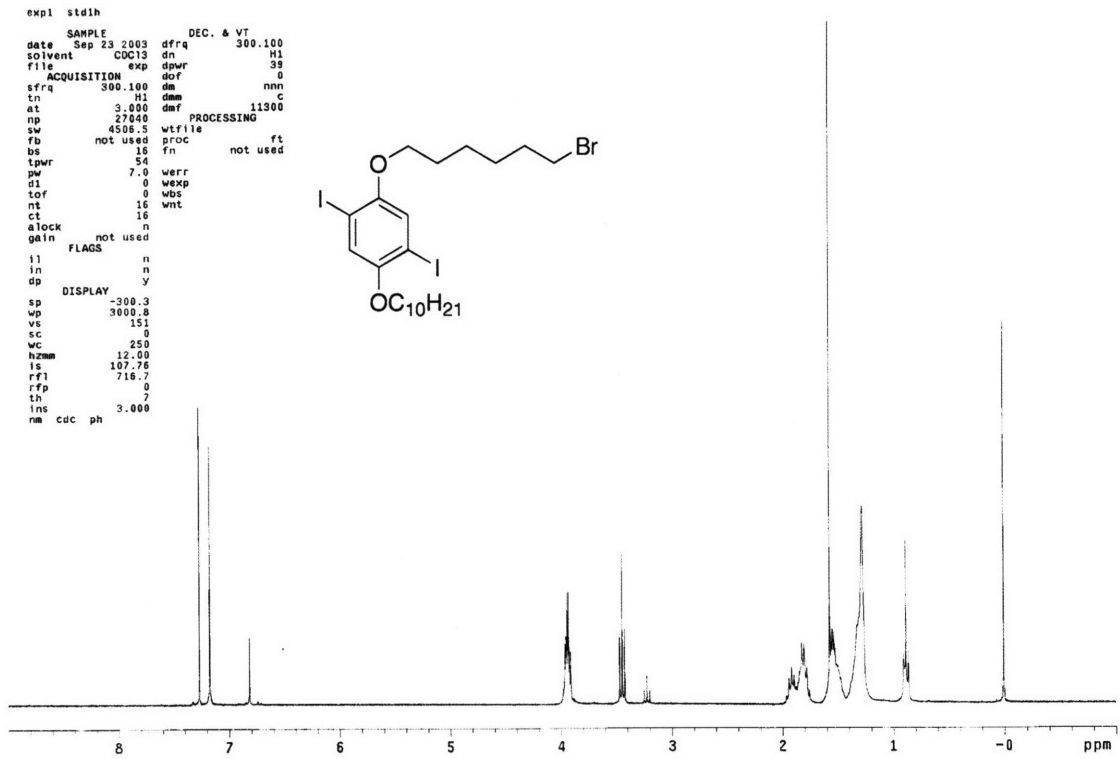
```

exp1 s2pu1
SAMPLE
date Apr 6 2005 dfrq 500.233
solvent CDCl3 dn H1
file /data/export/~dpwr 37
homs/lswager/7gb/~dof -500.0
OCR/GBI148-13C-CDCl3-dm w
C13-6Apr05.fid dmm W
ACQUISITION dmf 10000
sfrq 125.796 dseq 1.0
tn C13 dres n
at 1.796 homo PROCESSING
np 131010 lb 0.30
sw 37735.8 wfile ft
fb not used wfn 131072
bs 8 proc f
ss 1 fn
tpwr 53 math
pw 6.9
d1 0.763 werr
tof 631.4 wexp
nt 256 wbs
ct 256 wnt
alock n
gain not used
FLAGS
ll n
ln n
dp y
hs nn
DISPLAY
sp -6225.2
wp 37735.3
vs 4998
sc 0
wc 250
hzmm 150.94
ls 500.00
rfi 15911.8
rfp 3686.0
th 20
ins ph 1.000
at

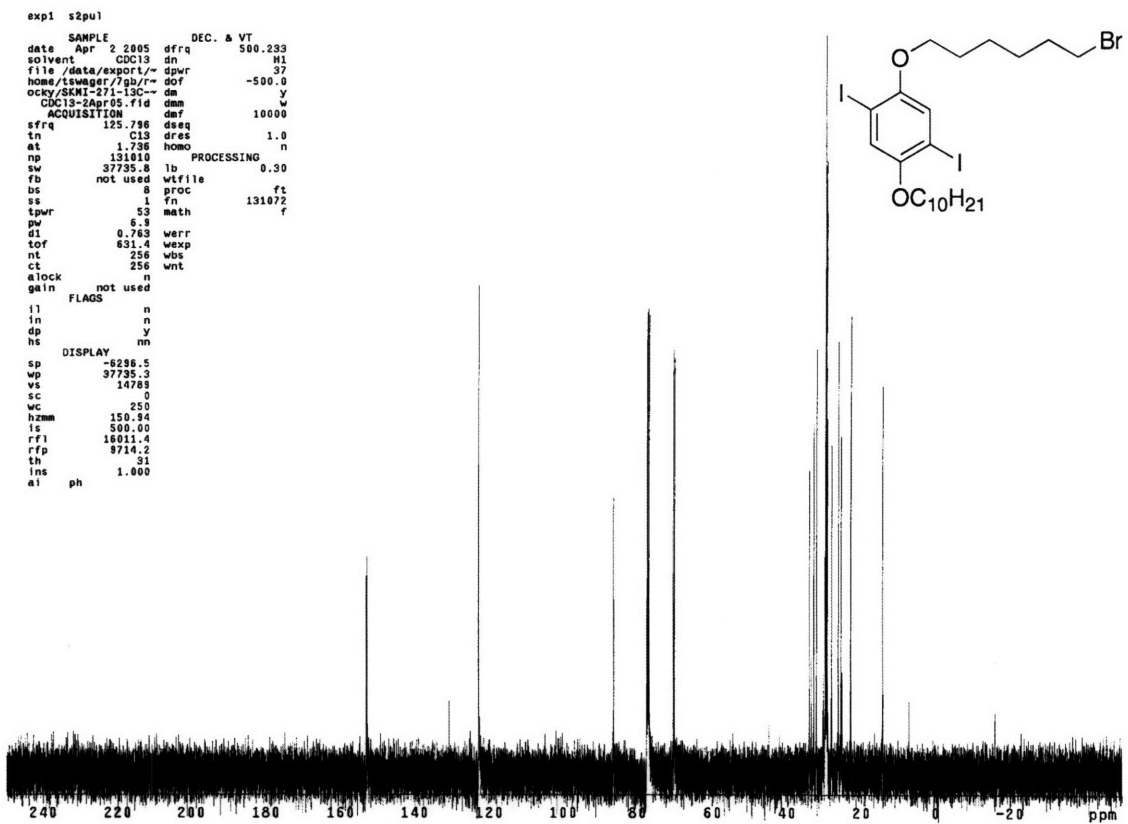
```



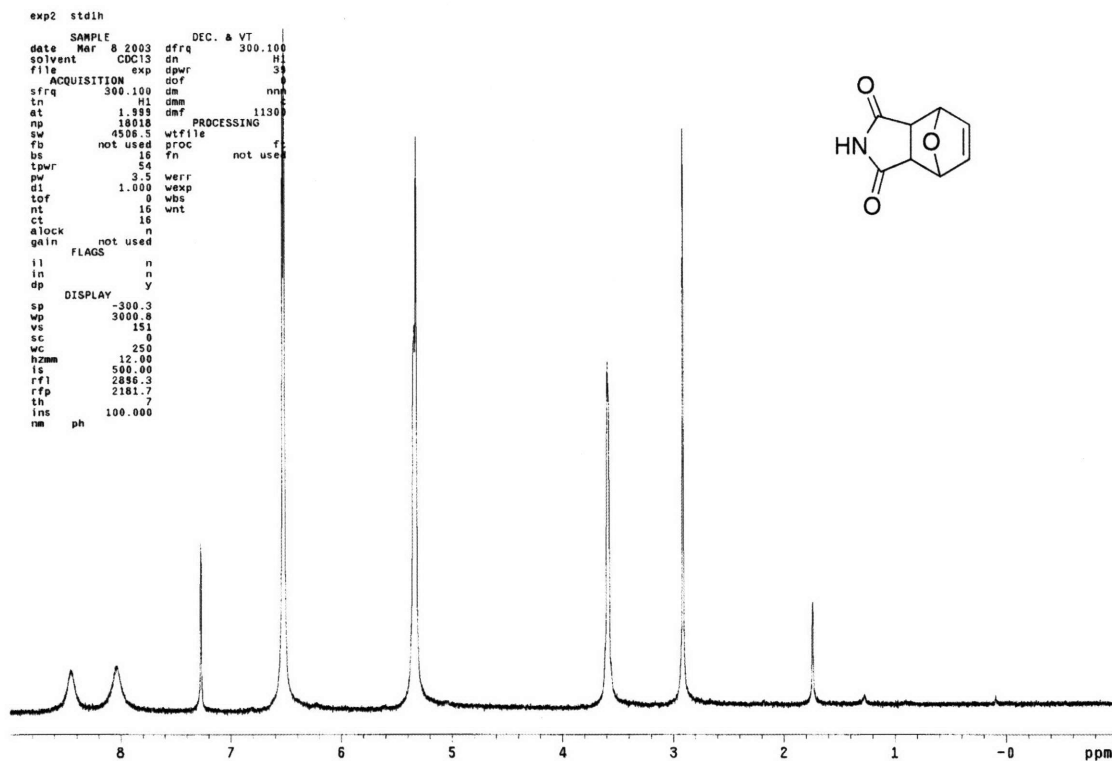
¹³C NMR for **5b** (CDCl₃).



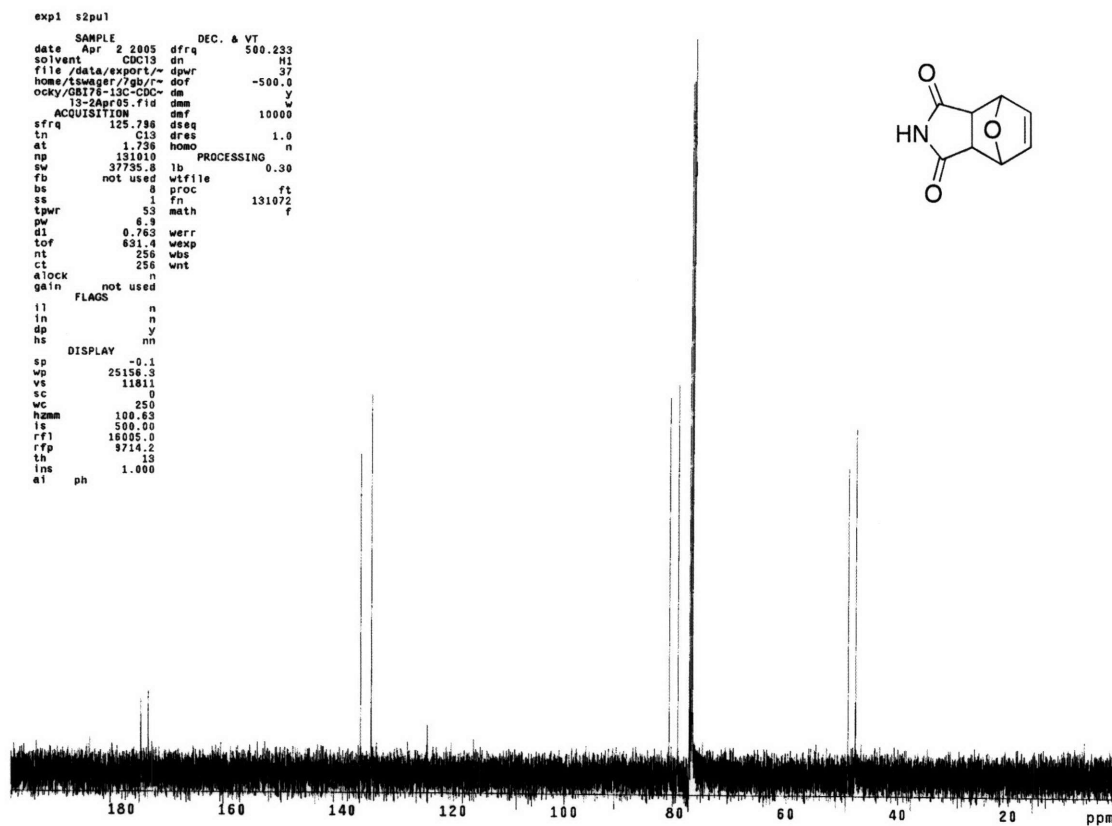
^1H NMR for **5c** (CDCl_3).



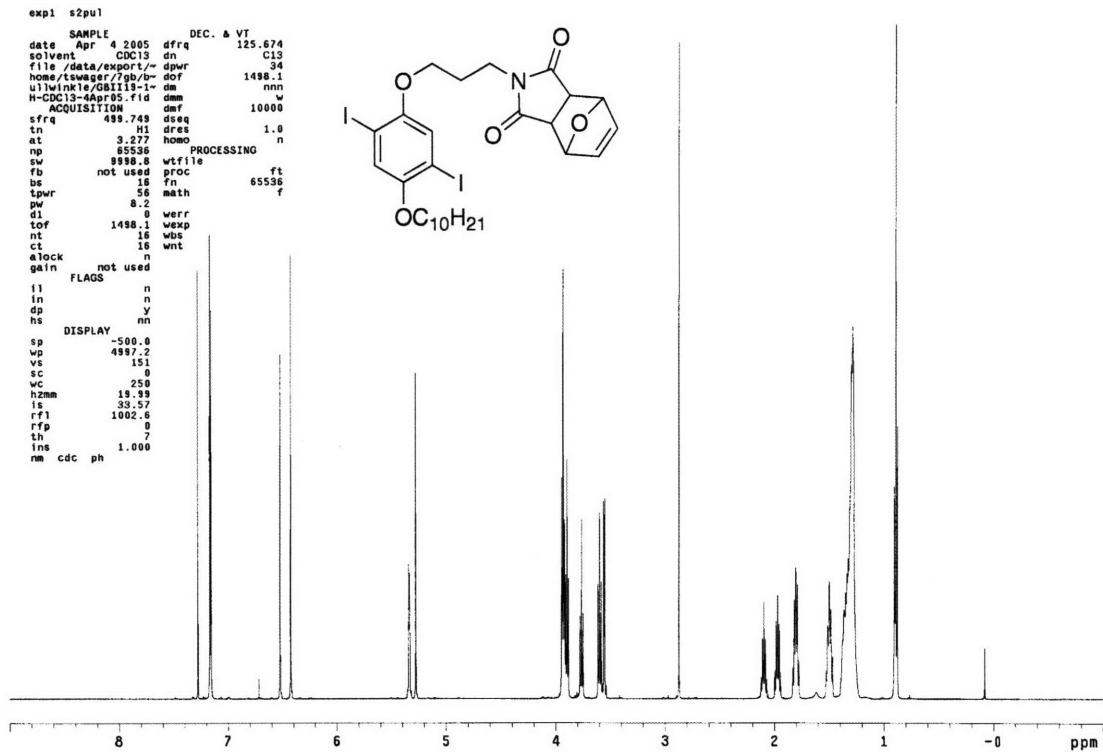
^{13}C NMR for **5c** (CDCl_3).



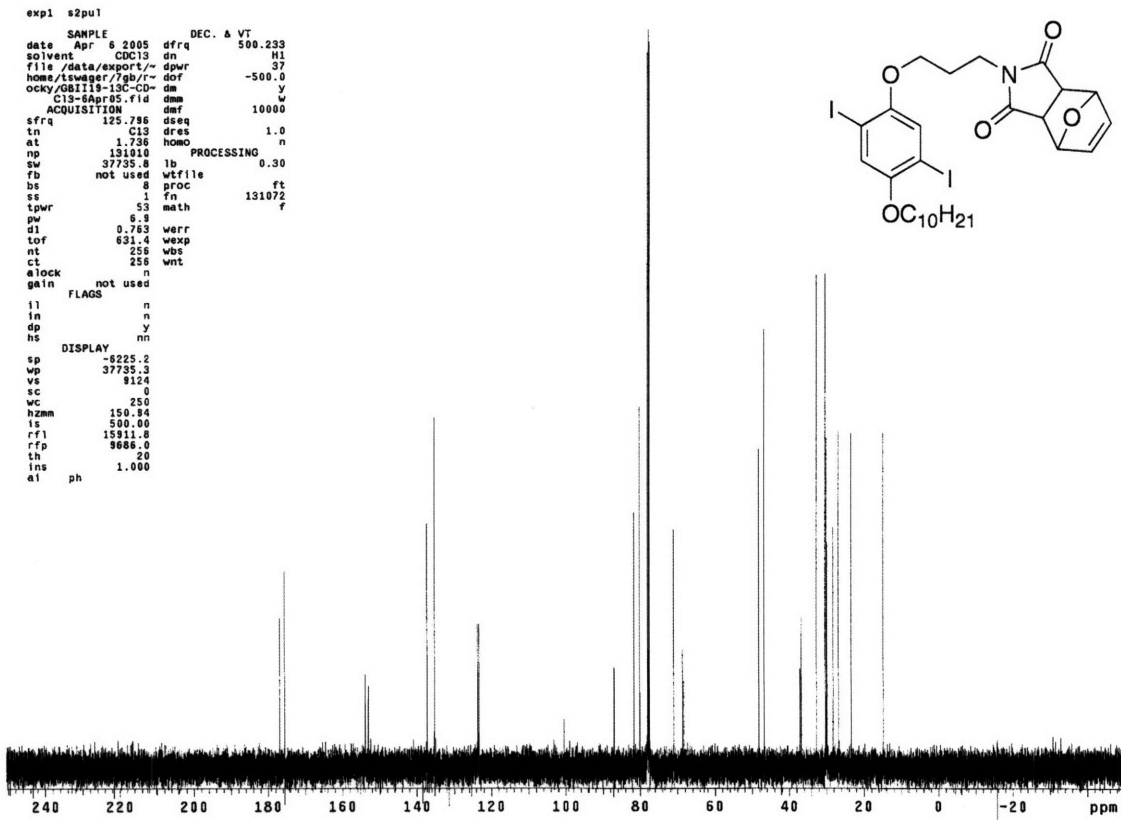
^1H NMR for 6 (CDCl_3).



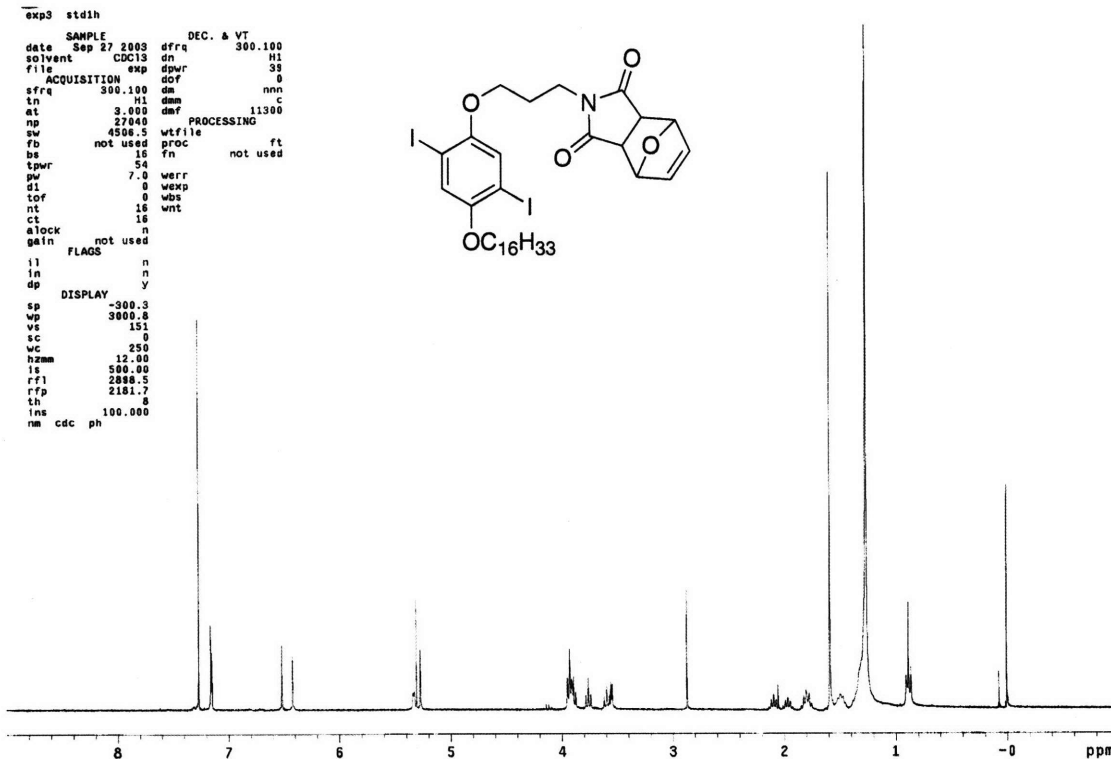
^{13}C NMR for 6 (CDCl_3).



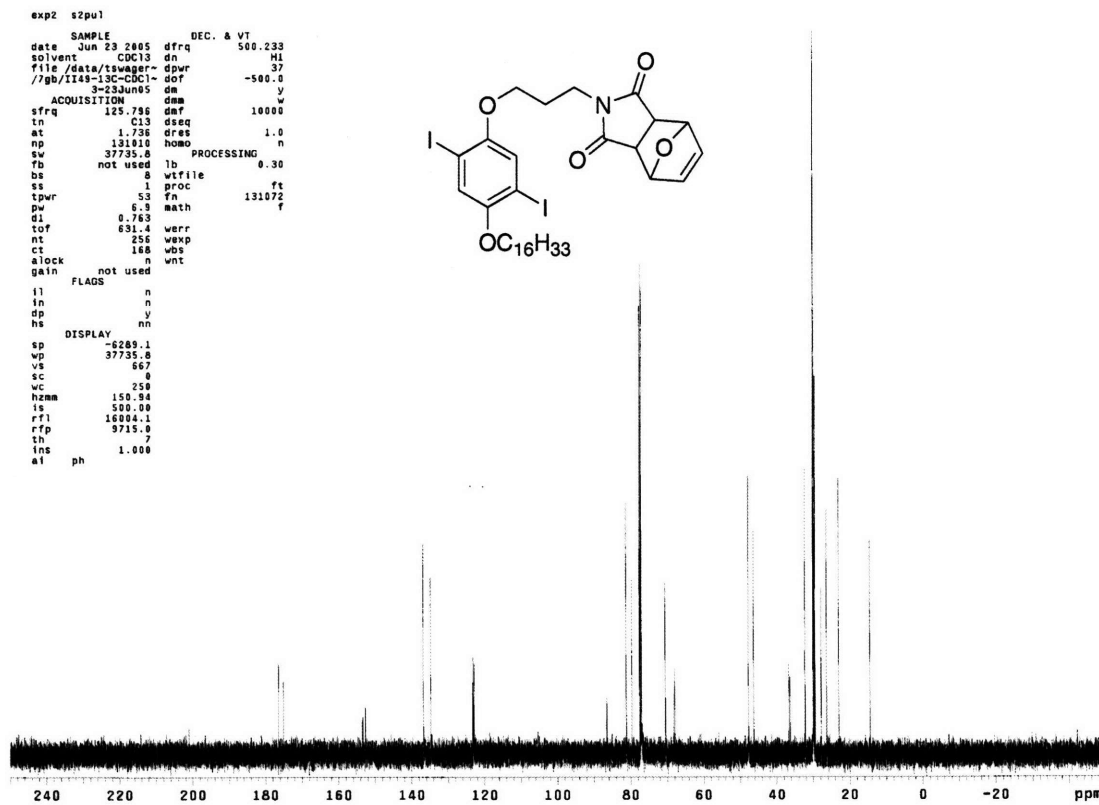
¹H NMR for **7a** (CDCl₃).



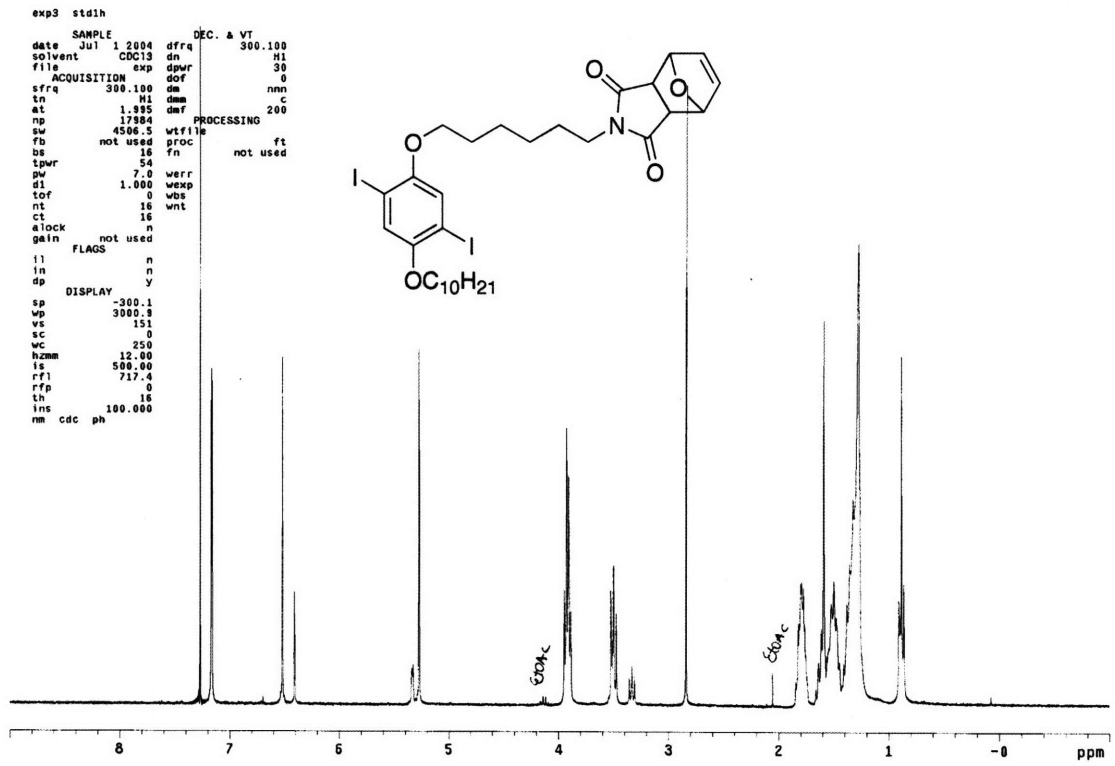
¹³C NMR for **7a** (CDCl₃).



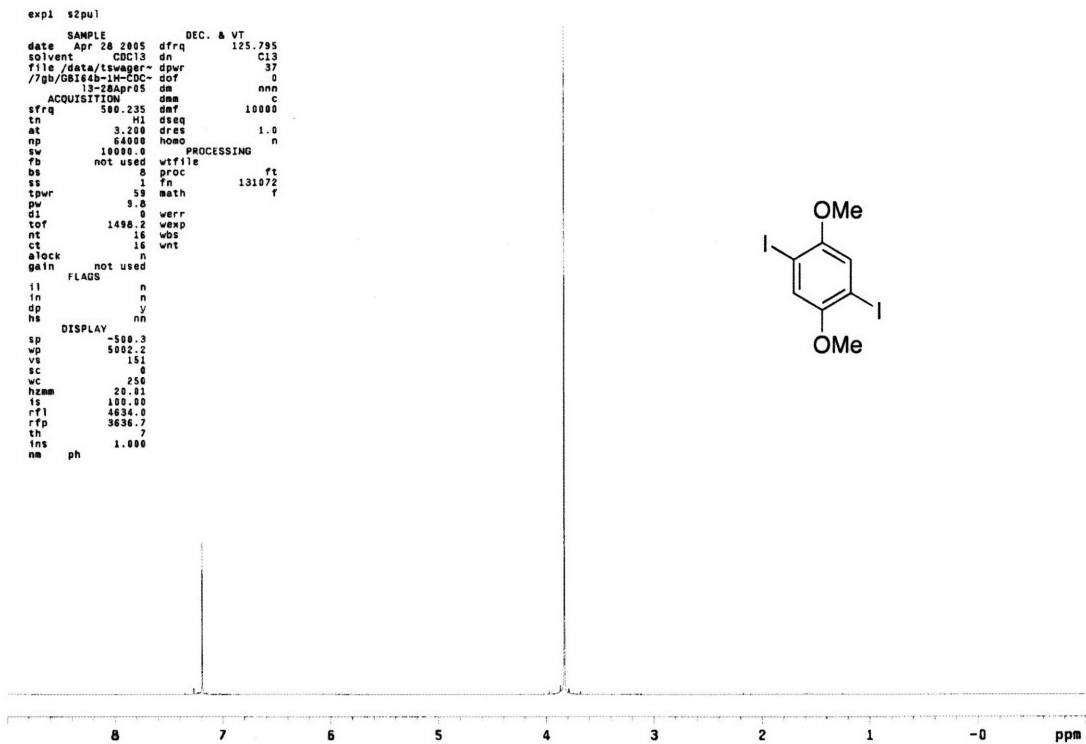
¹H NMR for **7b** (CDCl₃).



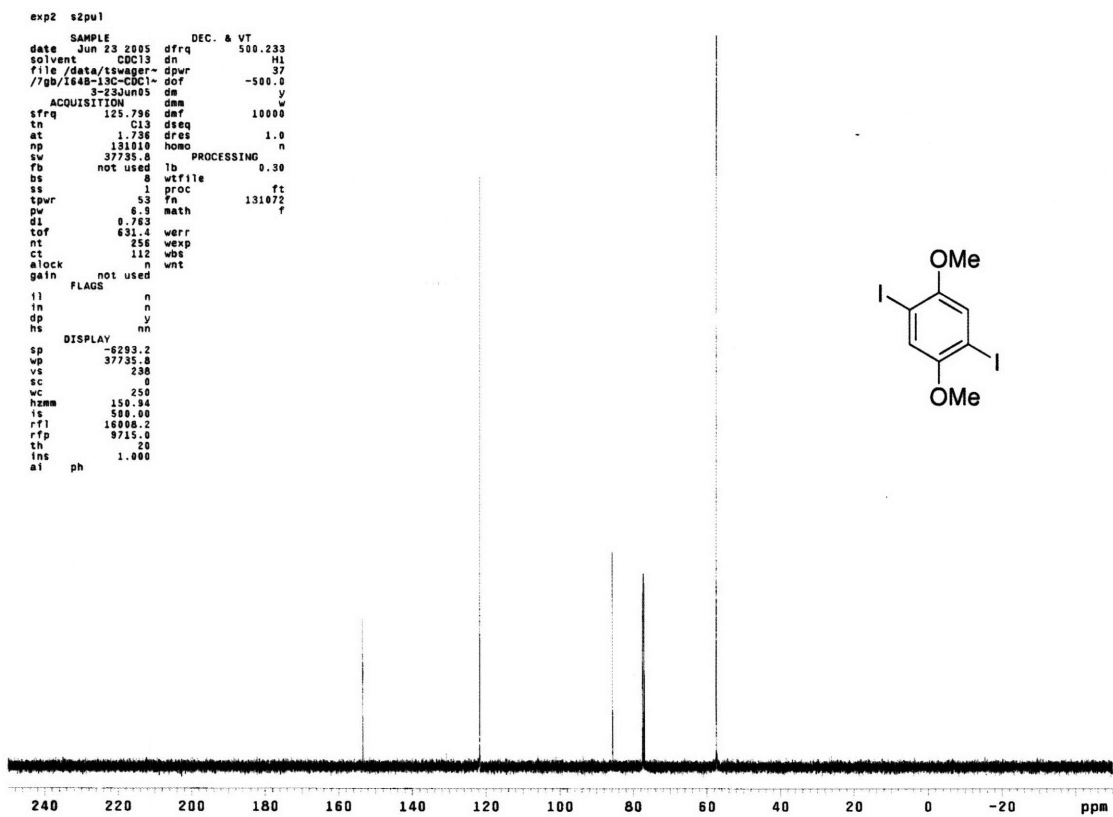
¹³C NMR for **7b** (CDCl₃).



¹H NMR for **7c** (CDCl₃).

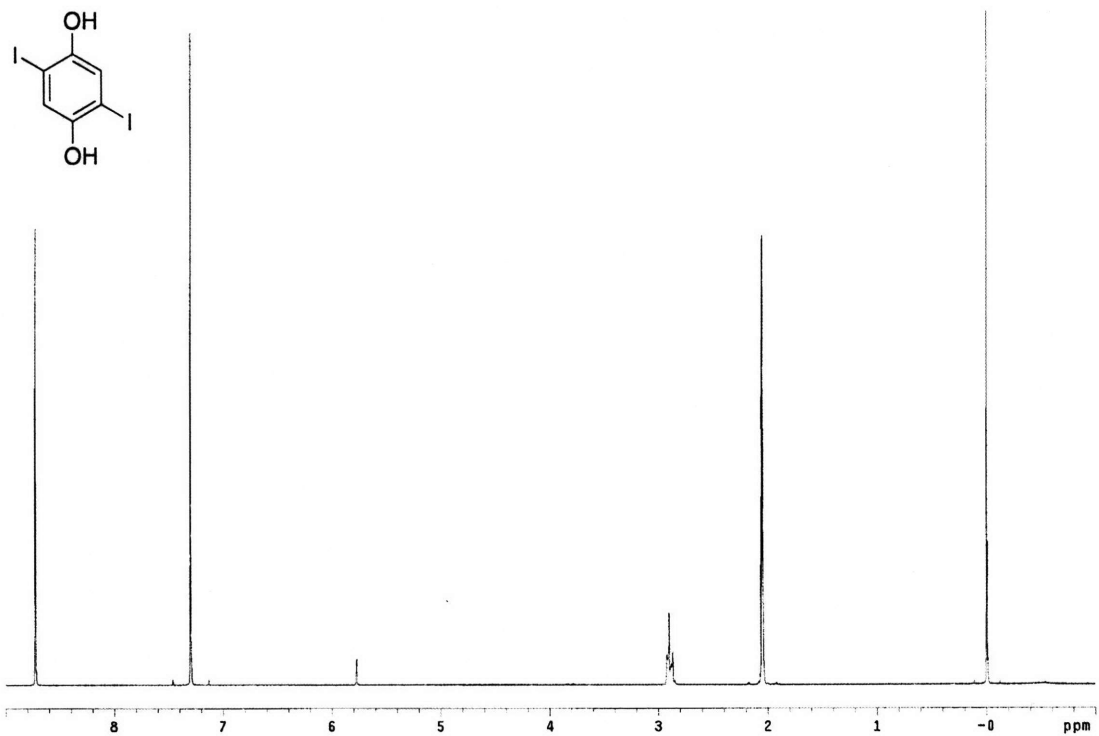


^1H NMR for **8** (CDCl_3).



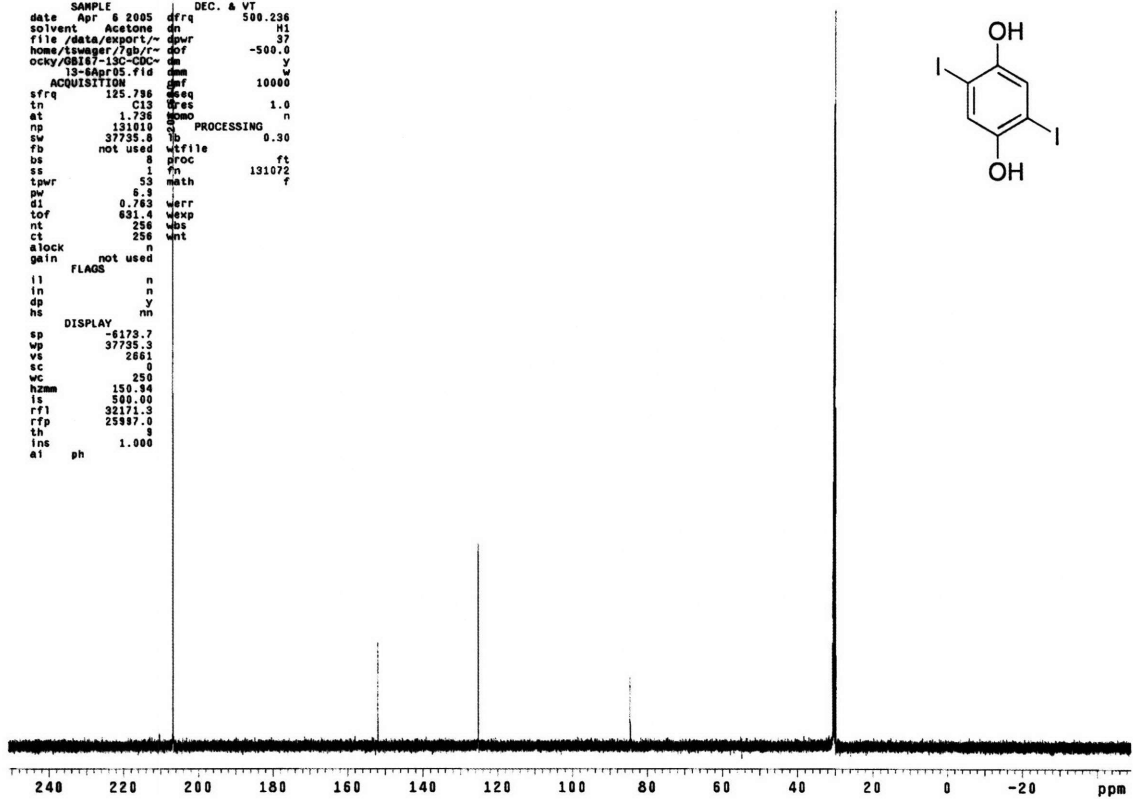
^{13}C NMR for **8** (CDCl_3).

Pulse Sequence: s2pu1

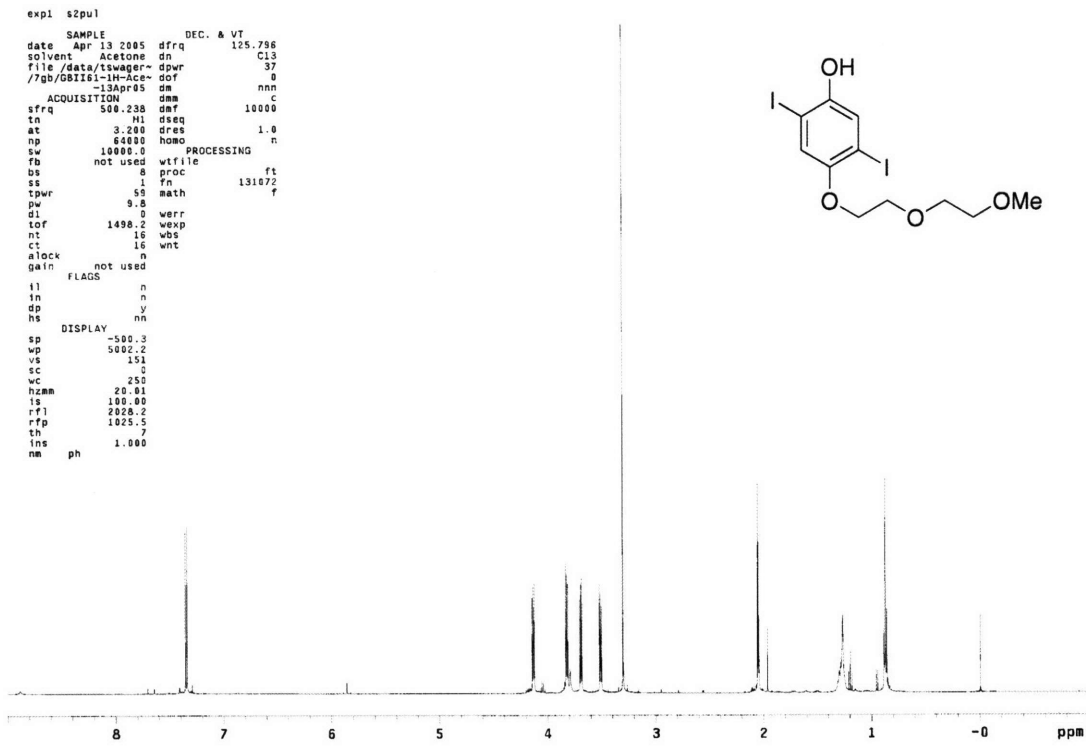


^1H NMR for **9** (Acetone- d_6).

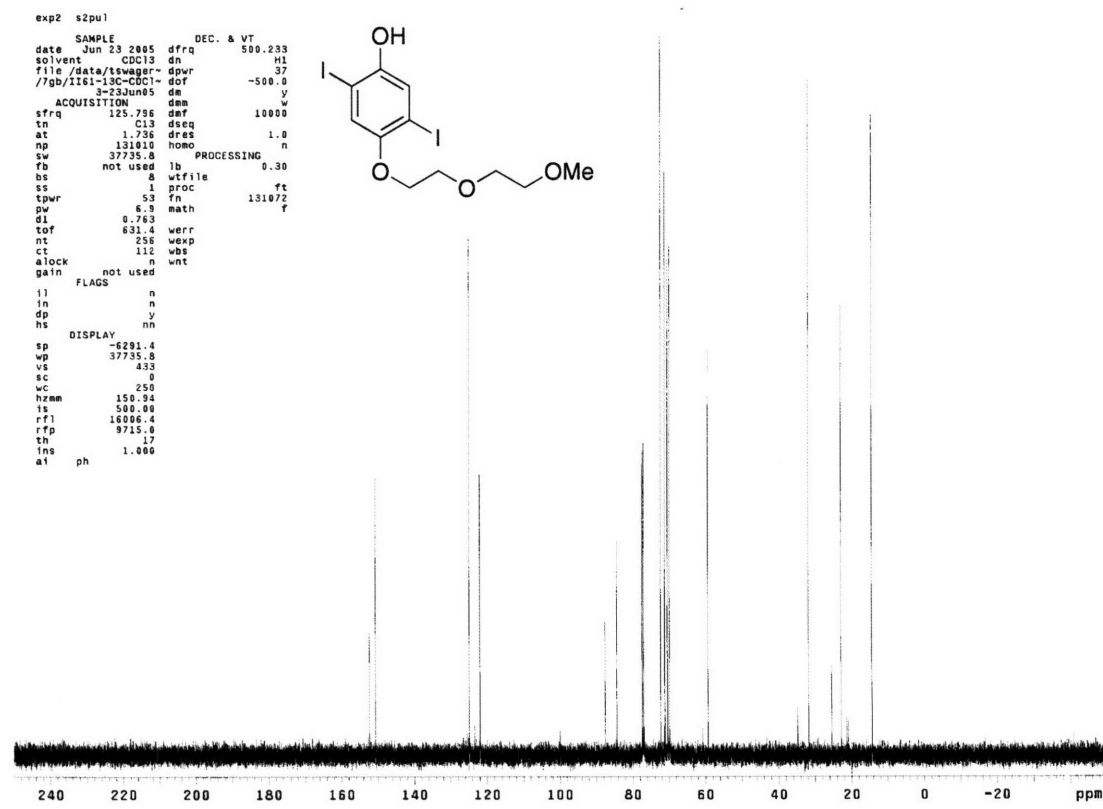
```
exp1 s2pu1
SAMPLE DEC. & VT
date Apr 6 2005 dfrq 500.236
solvent Acetone dn M1
file /data/export/~ dpwr 37
home/rtusergar/7gd/r~ dpr -500.0
ocky/08167-13C-CDC- dm y
13-Apr05.fid dnm w
ACQUISITION dnf 10000
sfrq 125.786 deeq 1.0
in C13 pres n
at 1.736 homo n
np 131010 p PROCESSING n
sw 37735.0 lb 0.30
fb not used wfile
bs 0 proc ft
ss 1 fn 131072 f
tpwr 53 math
pw 6.3 i
d1 0.763 werr
tof 631.4 wexp
nt 256 wds
ct 256 wnt
alock not used n
gain FLAGS
l) n
ln n
dp y
hs nn
DISPLAY
sp -6173.7
wp 37735.3
vs 2661
sc 0
wc 250
hzmm 150.34
ls 500.00
rfl 32171.3
rfp 25997.0
ln 3
ins 1.000
a1 ph
```



^{13}C NMR for **9** (CDCl_3).



¹H NMR for 10a (Acetone-d₆).

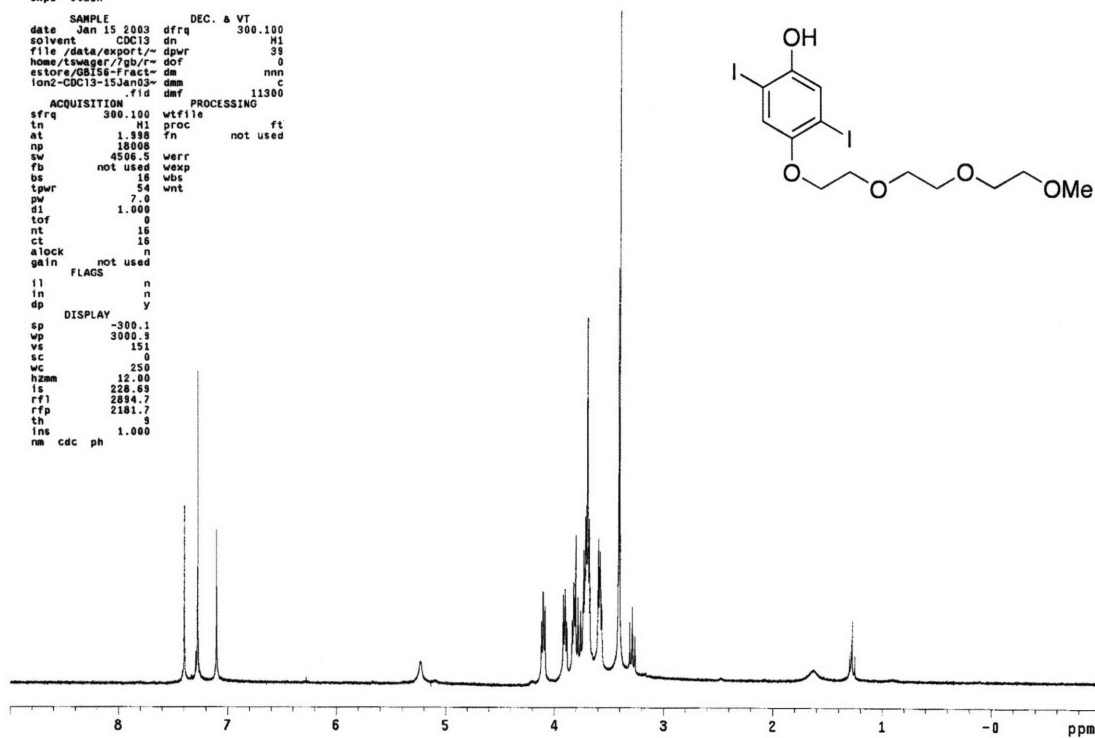
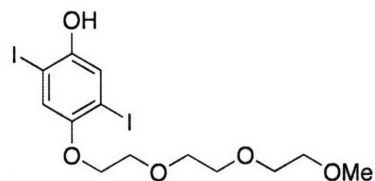


¹³C NMR for 10a (CDCl₃).

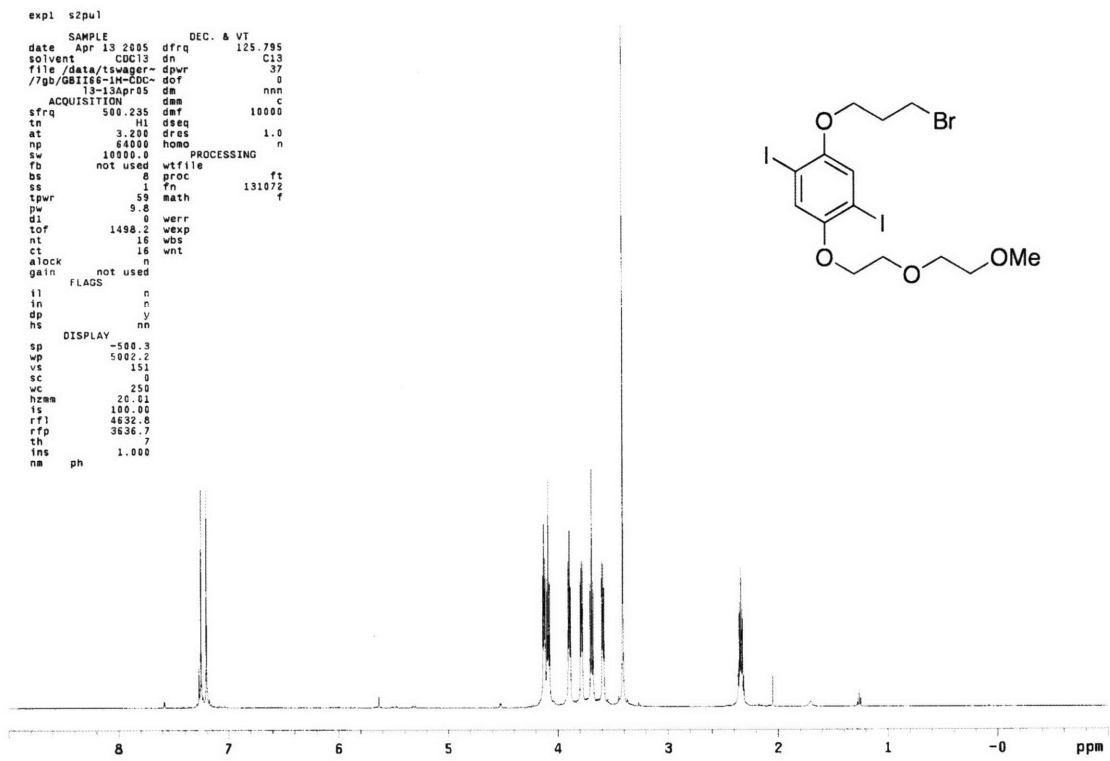
```

expl stdih
SAMPLE DEC. & VT
date Jan 15 2003 dfrq 300.100
solvent CDCl3 dn H1
file /data/export/~ dpwr 39
home/tswager/3g/r- dof 0
estore/GB156-Fract- dm nnn C
ion2-CDCl3-15Jan03- dmm 11300
      .f1a dmf
ACQUISITION PROCESSING
sfrq 300.100 wtfile
in H1 proc ft
at 1.398 fn not used
np 18008
sw 4598.5 werr
fb not used wexp
bs 16 wbc
tpwr 54 wnt
pw 7.0
d1 1.000
tof 0
nt 16
ct 16
elock n
gain not used
FLAGS
f1 n
in n
dp y
DISPLAY
sp -300.1
wp 3000.3
vs 151
sc 0
wc 250
hzam 12.00
ls 228.69
rf1 2284.7
rfp 2181.7
th 9
ins
nm cdc ph

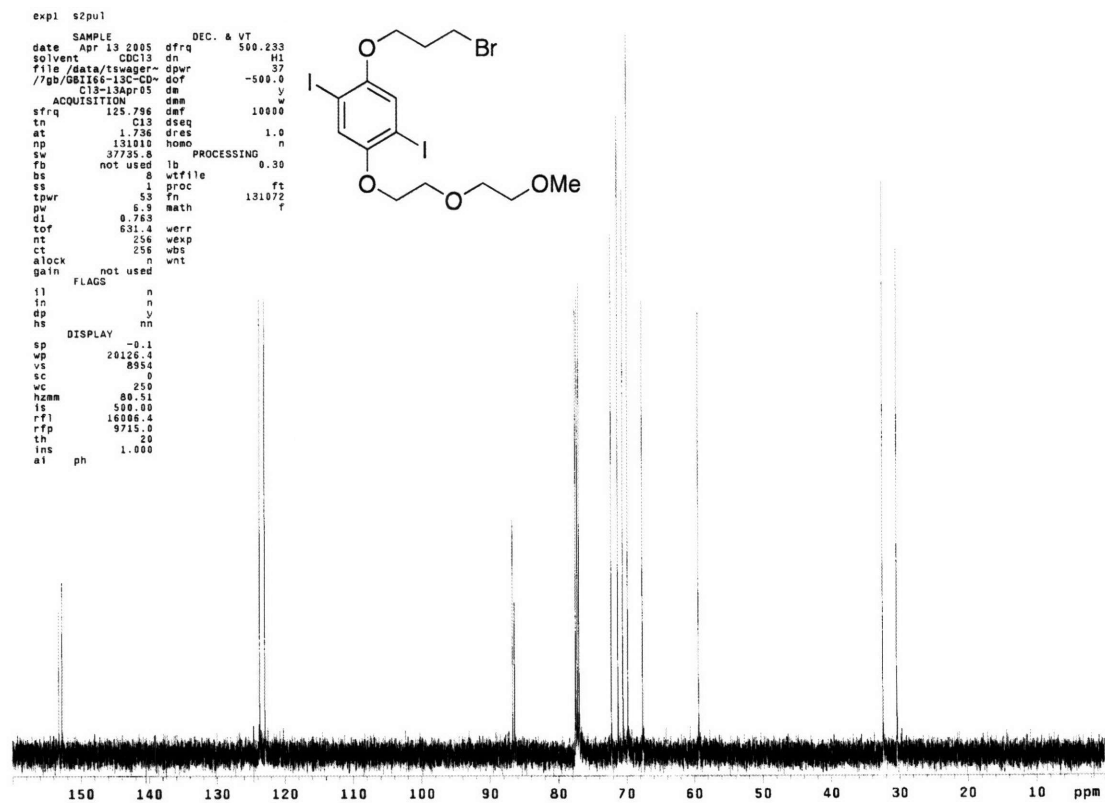
```



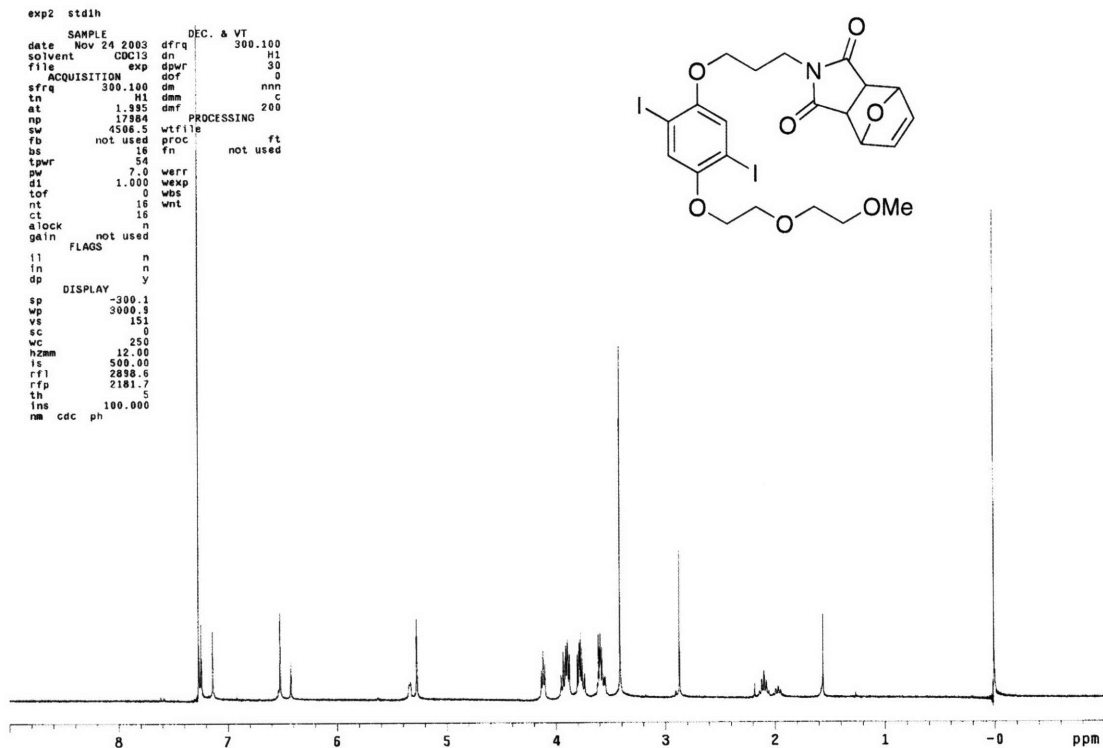
^1H NMR for **10b** (CDCl_3).



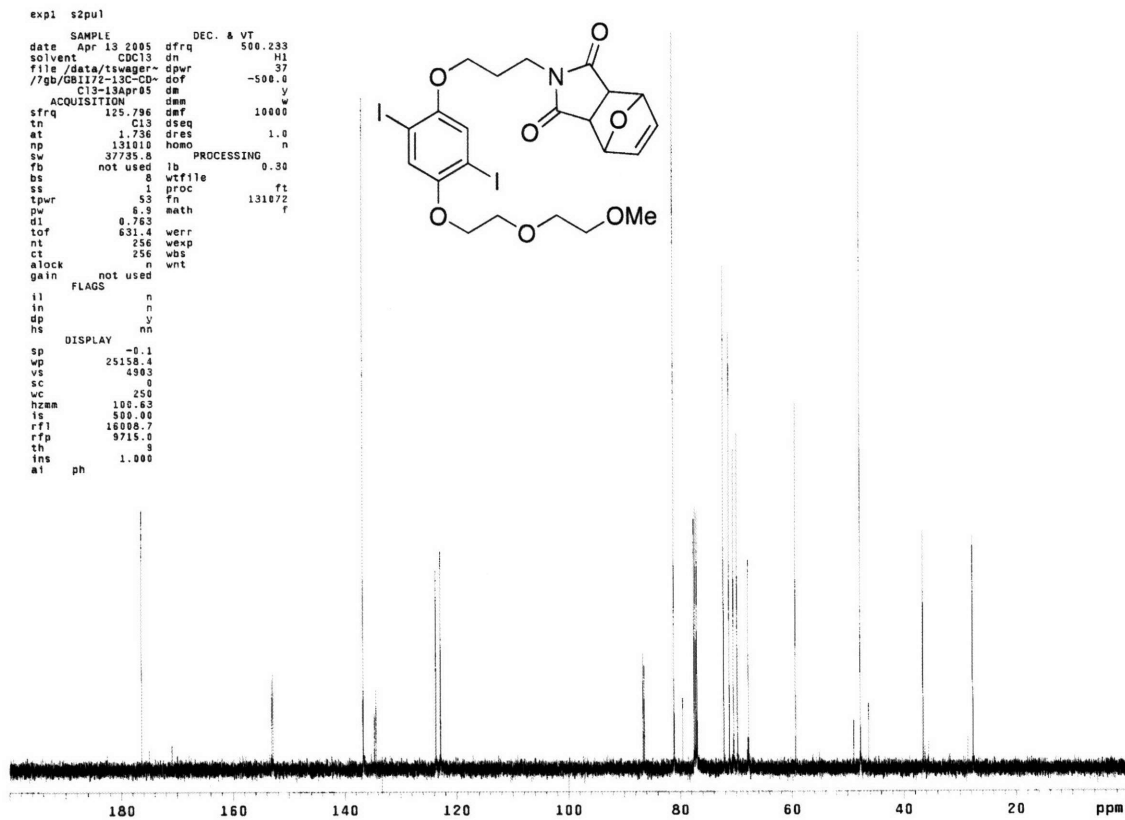
^1H NMR for **11a** (CDCl_3).



^{13}C NMR for **11a** (CDCl_3).



^1H NMR for **12a** (CDCl_3).

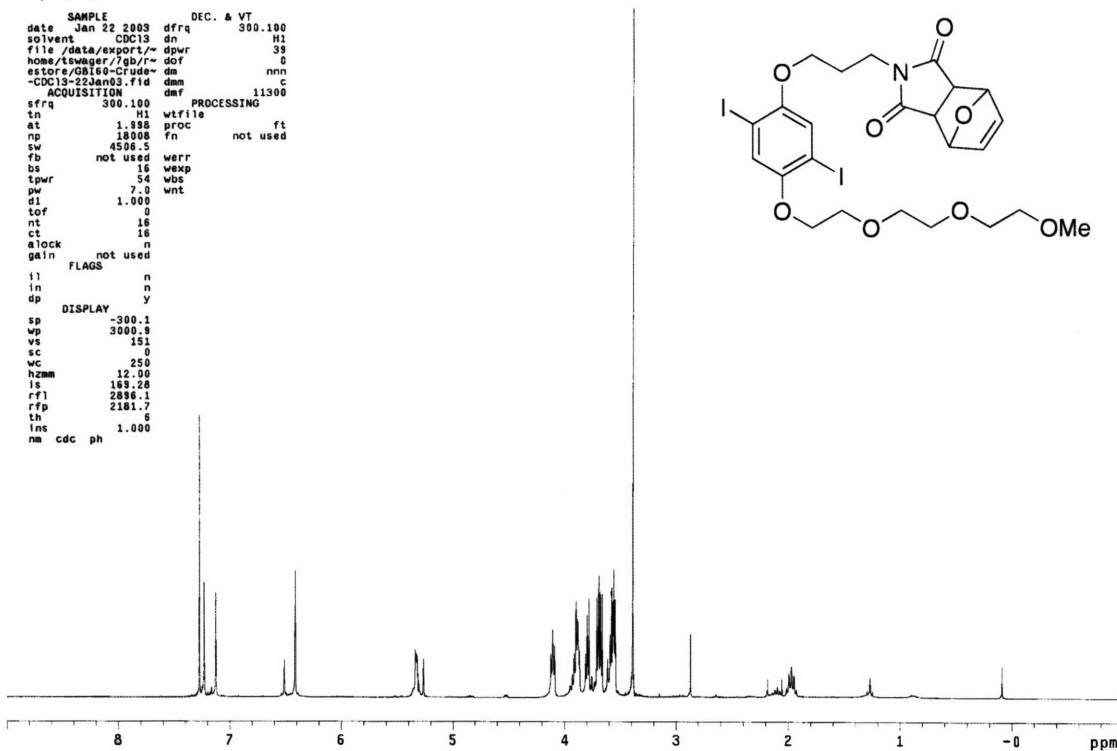
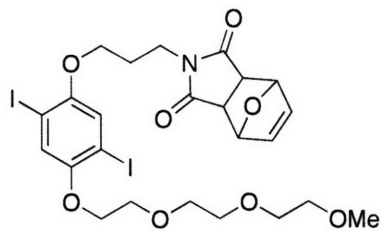


^{13}C NMR for **12a** (CDCl_3).

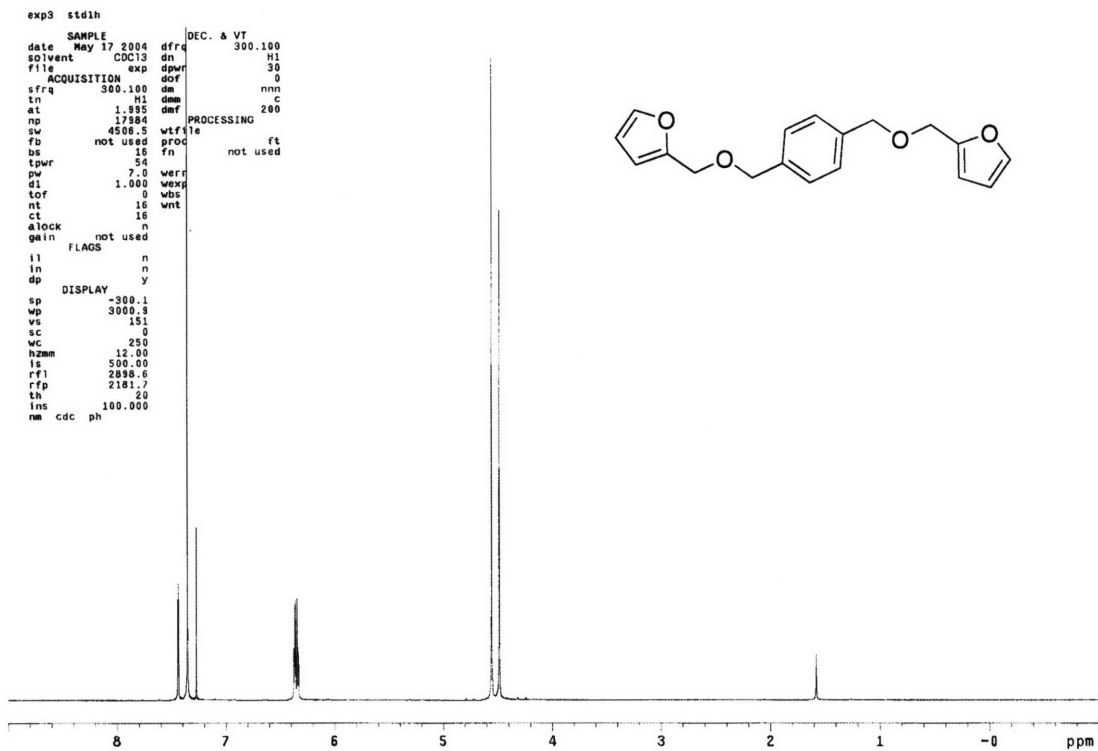
```

exp1 stdih
SAMPLE DEC. & VT
date Jan 22 2003 dfrq 300.100
solvent CDCl3 dn H1
file /data/export/~dpwr 39
name/tswager/7gb7~ dof 0
estore/G8160-Crude~ dm nnn
-CDCl3-22Jan03.fid dnm c
ACQUISITION dmf 11300
sfrq 300.100 PROCESSING
tn H1 wtfile
at 1.388 proc ft
np 18008 fn not used
sw 4508.5
fb not used warr
bs 16 wexp
tpwr 54 wbs
pw 7.0 wnt
d1 1.000
tof 0
nt 16
ct 16
alock n
gain not used
FLAGS
il n
in n
dp y
DISPLAY
sp -300.1
wp 3000.9
vs 151
sc 0
wc 250
hzmm 12.00
ls 169.28
rf1 2896.1
rfp 2181.7
th 6
lrs cdc ph
nm 1.000

```



¹H NMR for **12b** (CDCl₃).

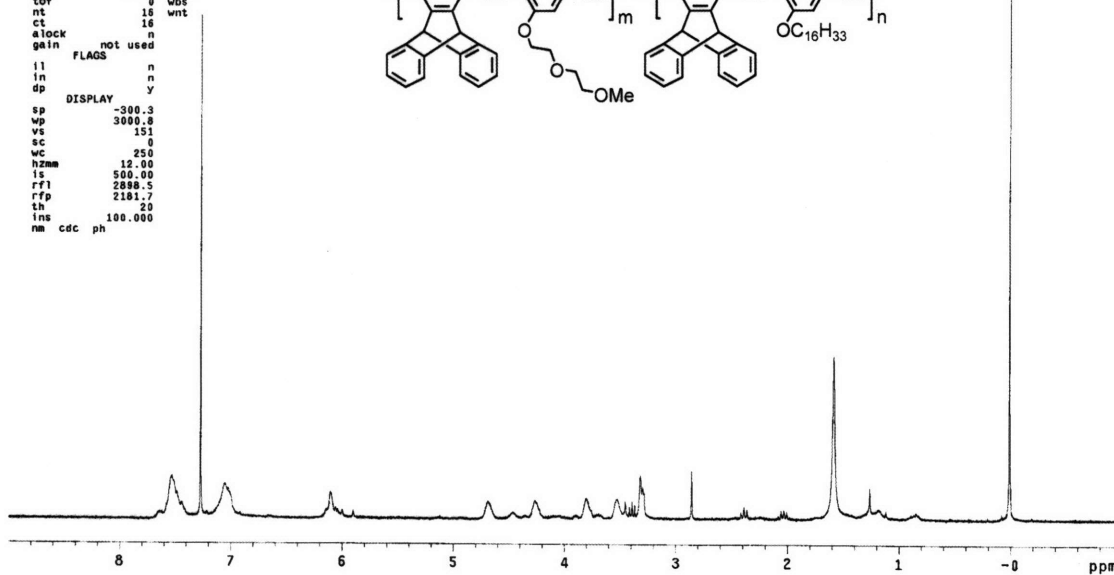
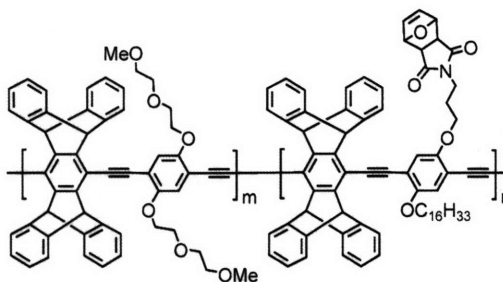


¹H NMR for **16** (CDCl₃).

```

expt std1h
SAMPLE DEC. & VT
date Jul 18 2003 dfrq 300.100
solvent CDCl3 dn H1
file exp dpwr 39
ACQUISITION dof 0
sfrq 300.100 dn nnn
ln H1 dm C
et 1.395 dmf 11300
np 17984
sw 4506.5 wtf1le
fb not used proc ft
bs 16 fn not used
tpwr 54
pw 7.0 werr
d1 1.000 wekp
tof 0 wbs
nt 16 wnt
ct 16
alock n
gain not used
FLAGS n
il n
in n
dp y
DISPLAY
sp -300.3
np 3000.8
vs 151
sc 0
vc 250
hzmm 12.00
ls 500.00
rf1 2886.5
rfp 2181.7
th 20
lms 100.000
nm cdc ph

```



^1H NMR for P-2 (CDCl_3).

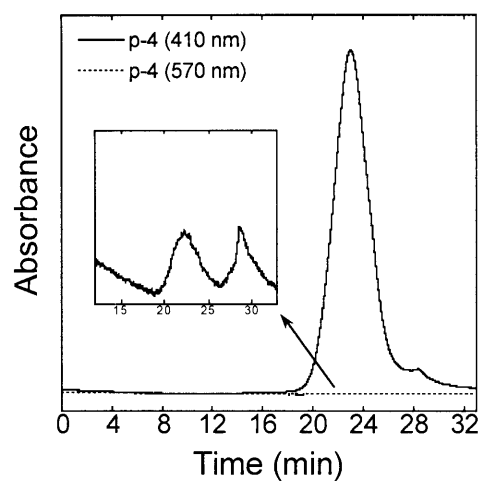
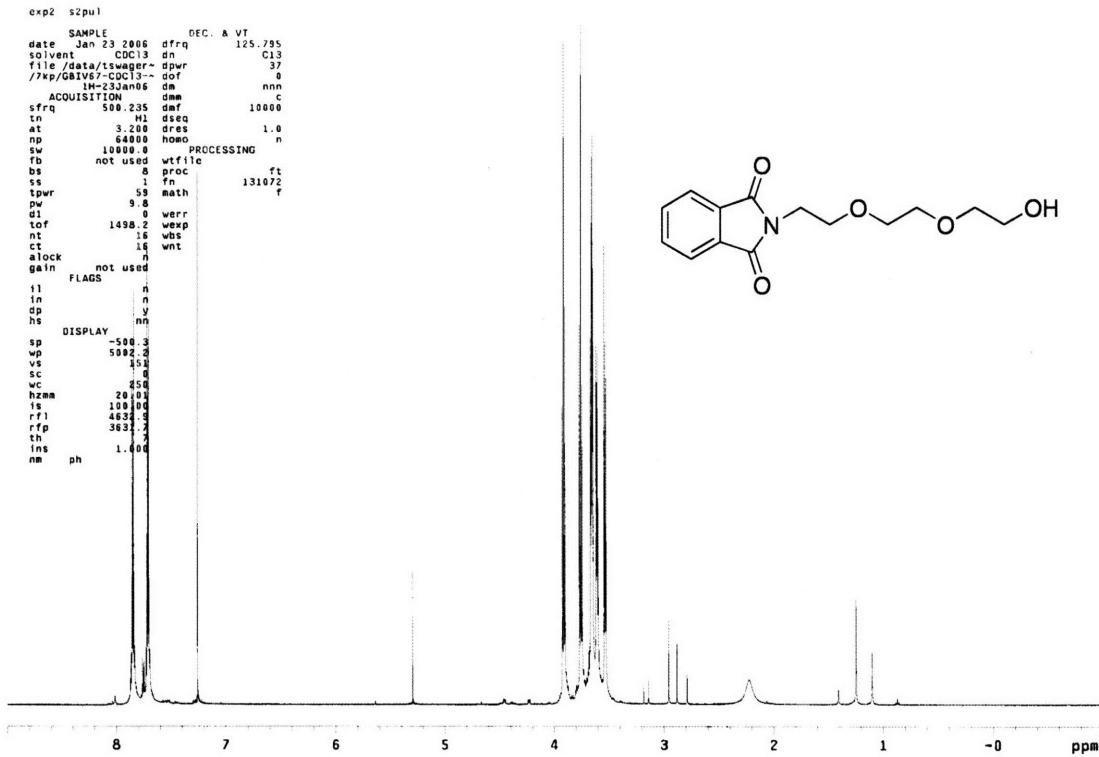
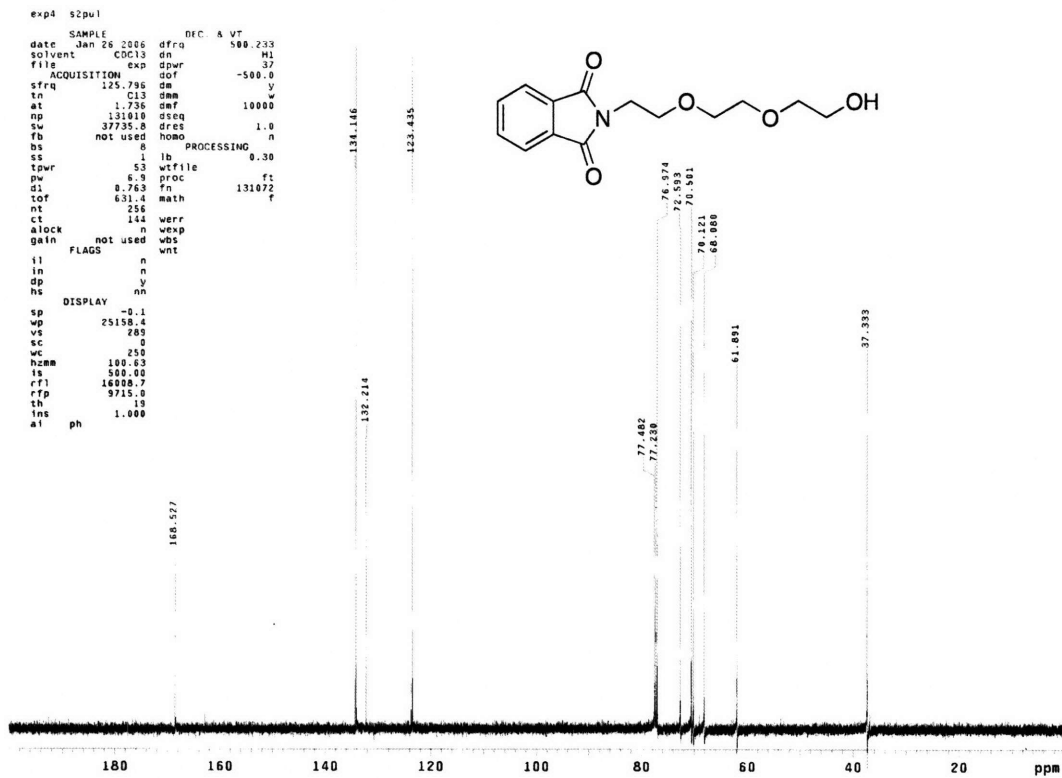


Figure A1. GPC trace obtained for polymer P-4, monitoring at 410 nm and 570 nm. Absorption at 570 kept to scale with that at 410. Inset: Monitoring at 570 nm, bound dye elutes at 23 min, while free dye elutes at about 30 min. Absorption at 570 nm is weaker due to a lower concentration of the dye relative to the polymer.

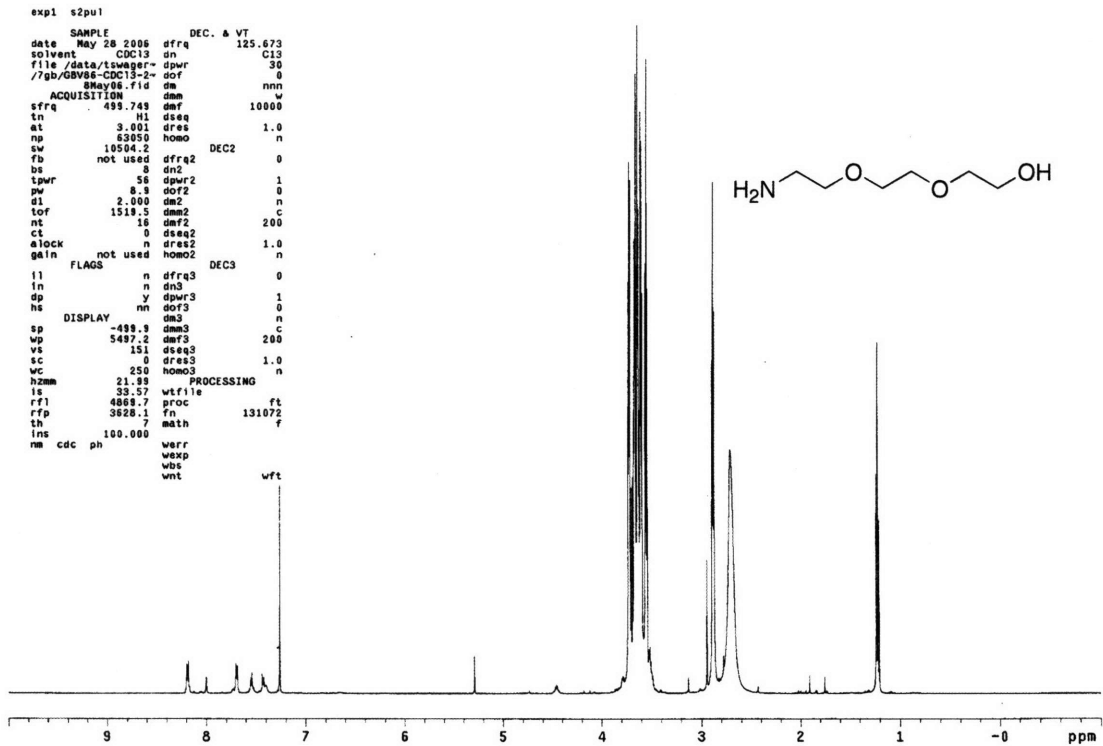
Appendix 2:
NMR Spectra for Chapter 3



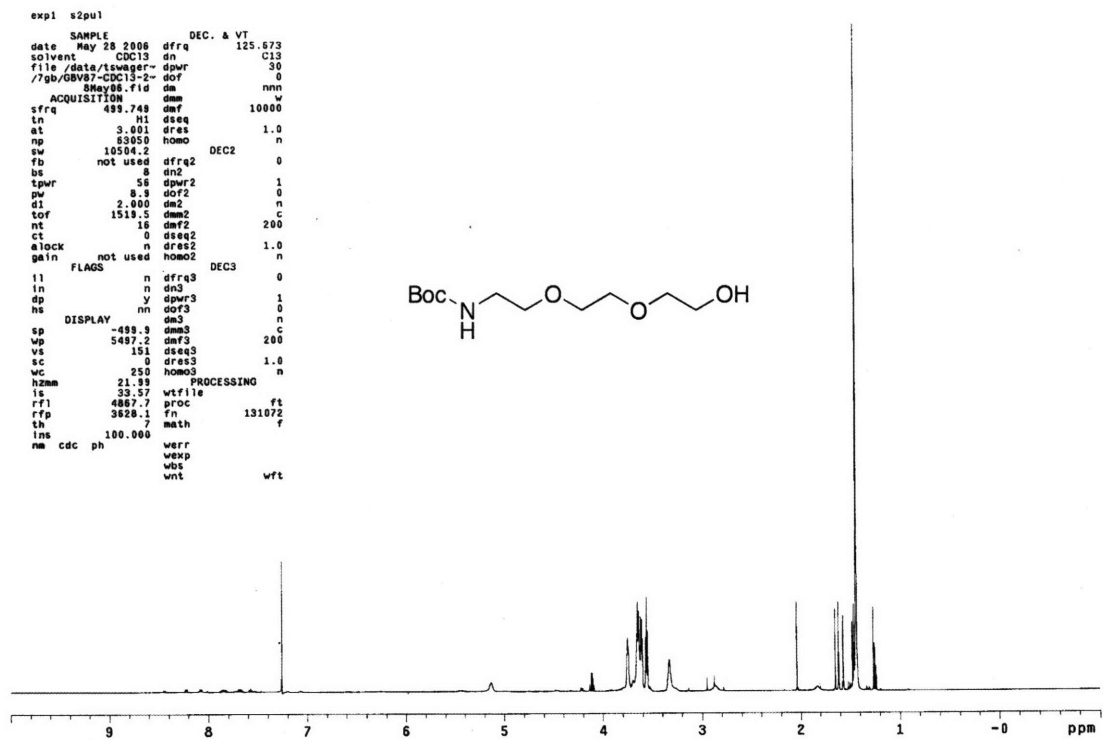
^1H NMR for 1 (CDCl_3).



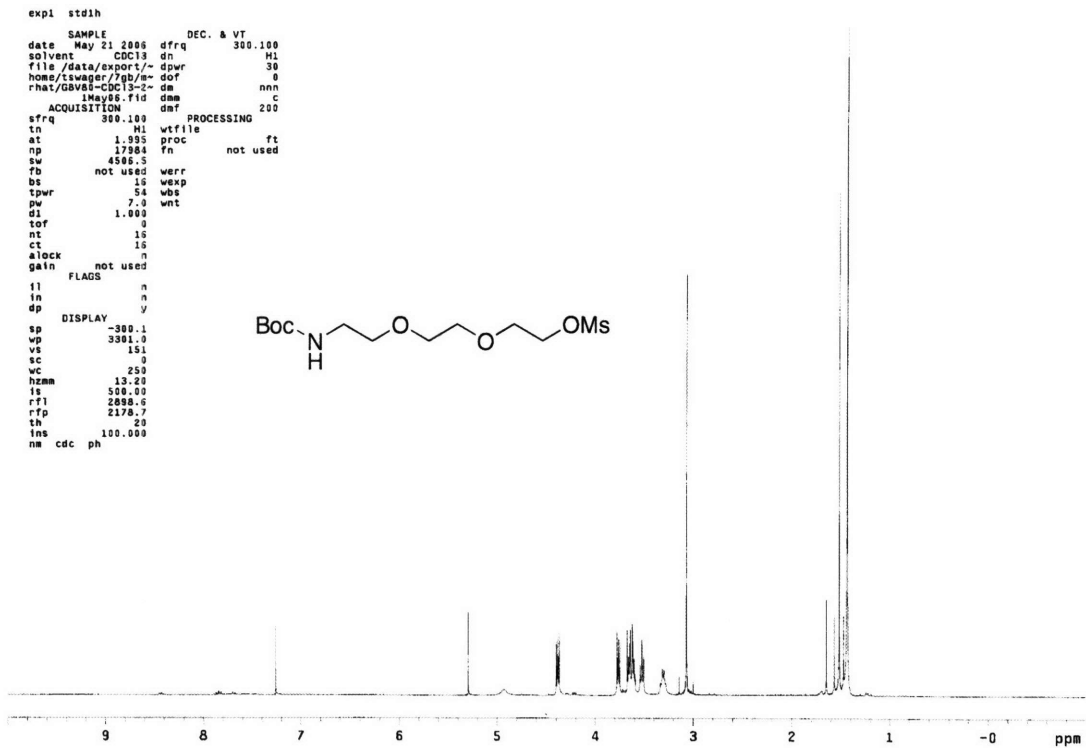
^{13}C NMR for 1 (CDCl_3).



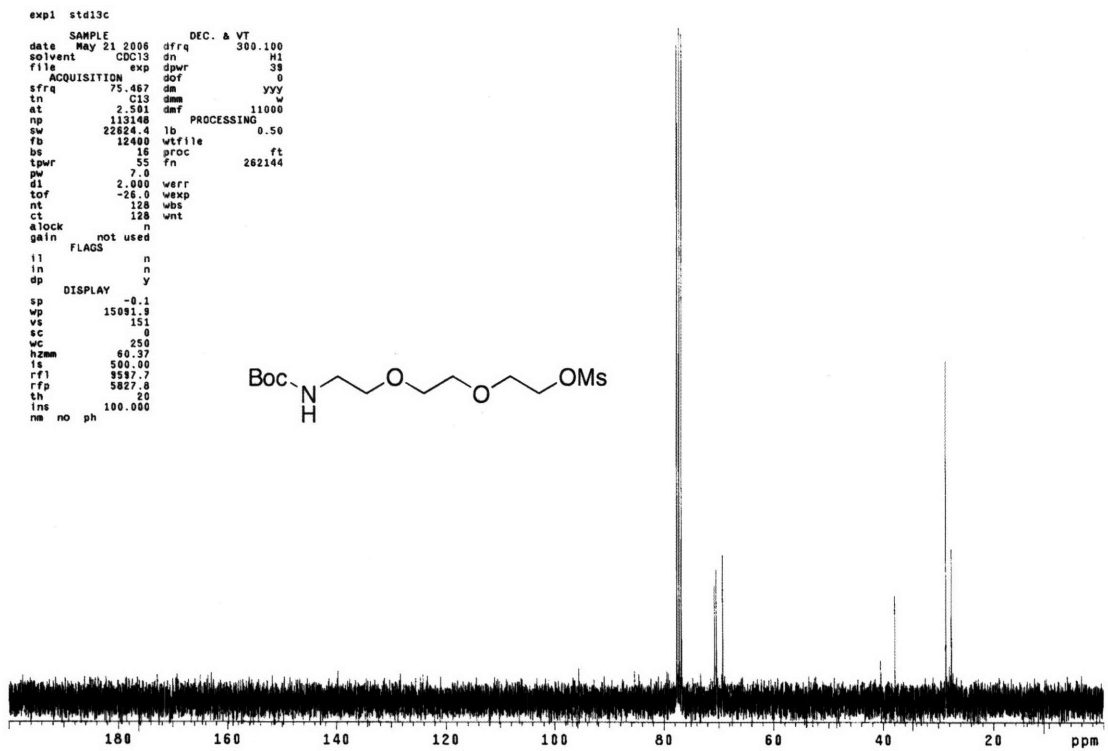
¹H NMR for **2** (CDCl₃).



¹H NMR for **3** (CDCl₃).



^1H NMR for 4 (CDCl_3).

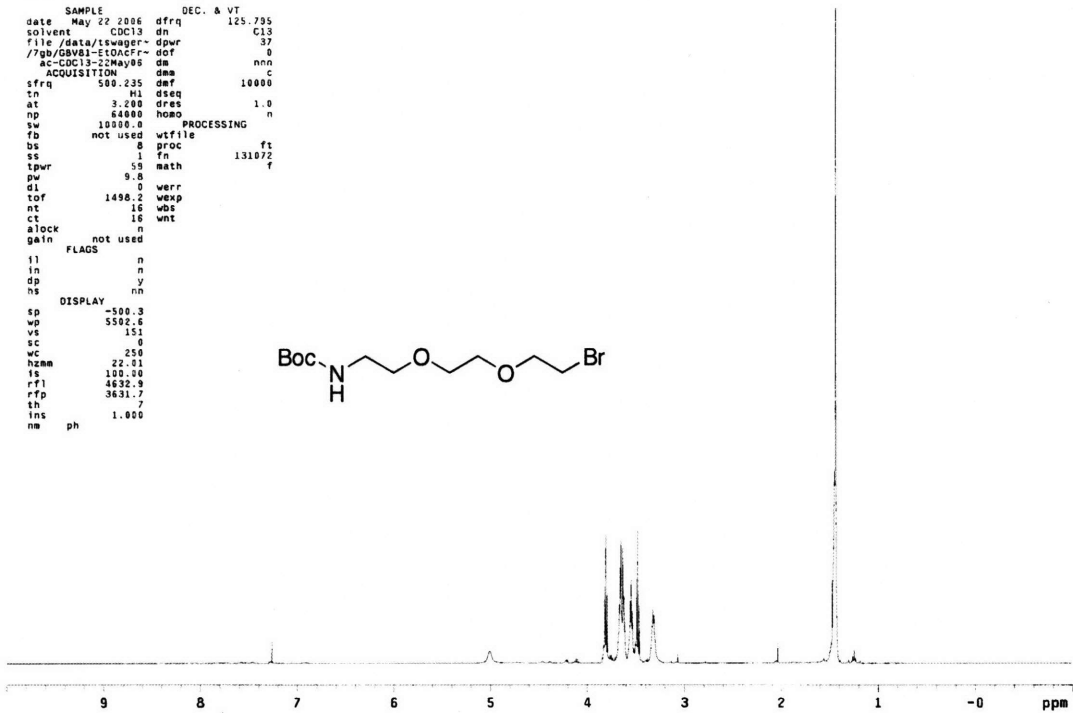
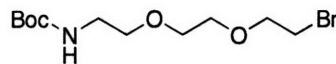


^{13}C NMR for 4 (CDCl_3).

```

expt s2pu1
SAMPLE DEC. & VT
date May 22 2006 dfrq 125.795
solvent CDCl3 dn C13
file /data/tswager-dpwr 37
/7qb/GBV81-ETOAcFr-dof 0
AC-C13-20May06 dm nno
ACQUISITION dnm 10000
sfrq 500.235 dmf
tn H1 dseq
at 3.200 dres 1.0
np 64000 homo n
sw 10000.0 PROCESSING
fb not used wtf file ft
bs 0 proc 131072
ss 1 fn
tpwr 59 math f
pw 9.8
d1 0 werr
tof 1498.2 wexp
nt 16 wbs
ct 16 wnt
alock n
gain not used
FLAGS
il n
in n
dp y
hs nn
DISPLAY
sp -500.3
wp 5502.6
vs 151
sc 0
wc 258
hzmm 22.01
ls 100.00
rf1 4632.9
rfp 3631.7
th 8
lms 1.000
na ph

```

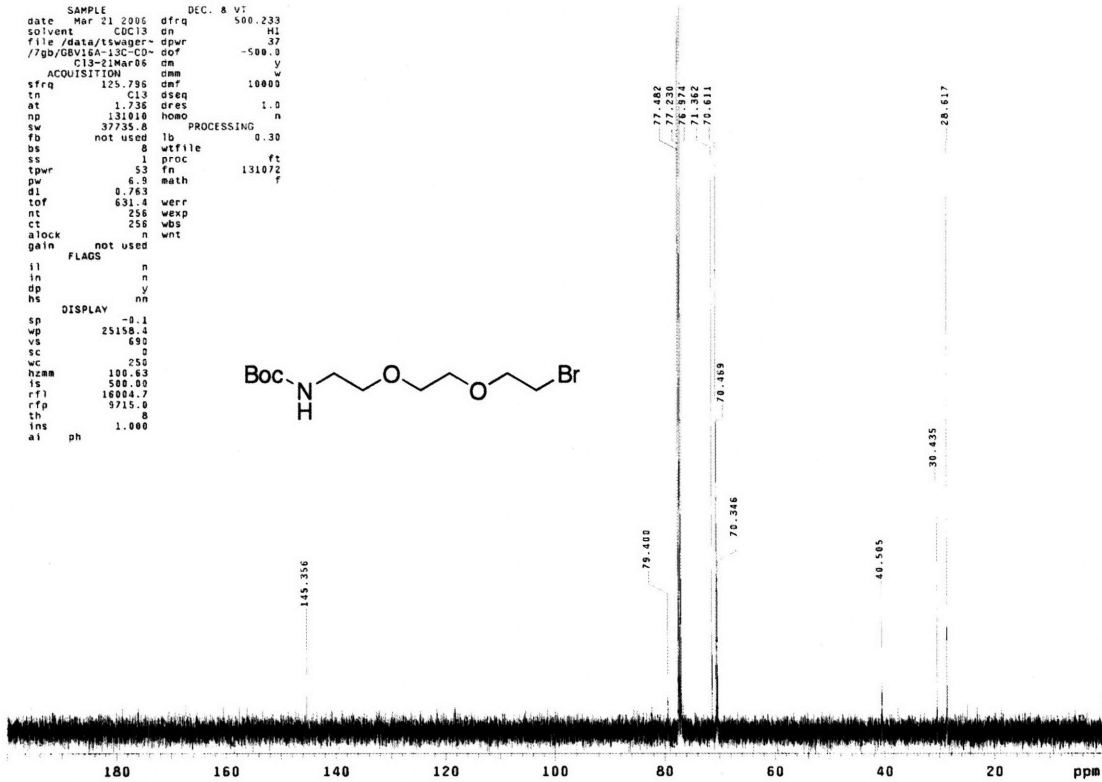
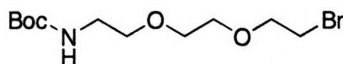


¹H NMR for **5** (CDCl₃).

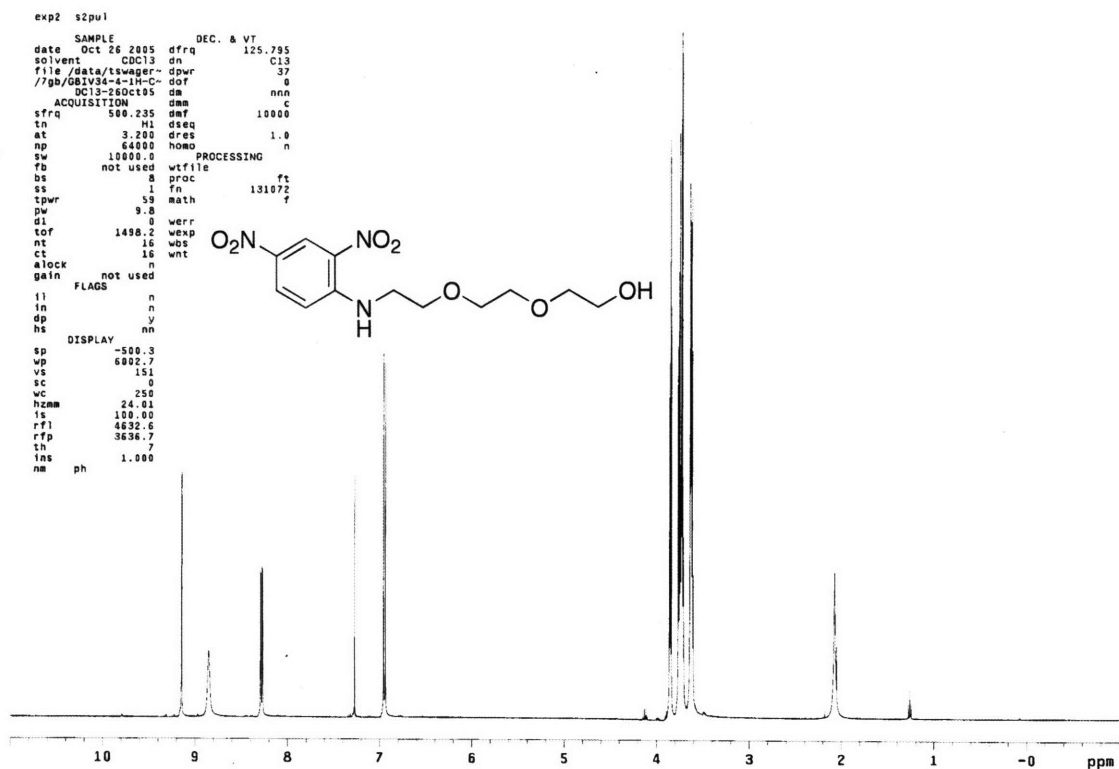
```

expt s2pu1
SAMPLE DEC. & VT
date Mar 21 2006 dfrq 500.233
solvent CDCl3 dn H1
file /data/tswager-dpwr 37
/7qb/GBV16A-13C-CD- dof -500.0
AC-C13-21Mar06 dm y
ACQUISITION dnm 10000
sfrq 125.795 dmf
tn C13 dseq
at 1.736 dres 1.0
np 131010 homo n
sw 37735.8 PROCESSING
fb not used lb 0.30
bs 0 wtf file ft
ss 1 proc 131072
tpwr 53 fn
pw 6.9 math f
d1 0.763
tof 631.4 werr
nt 256 wexp
ct 258 wbs
alock n wnt
gain not used
FLAGS
il n
in n
dp y
hs nn
DISPLAY
sp -0.1
wp 25158.4
vs 690
sc 0
wc 256
hzmm 100.83
ls 500.00
rf1 16004.7
rfp 9715.0
th 8
lms 1.000
na ph

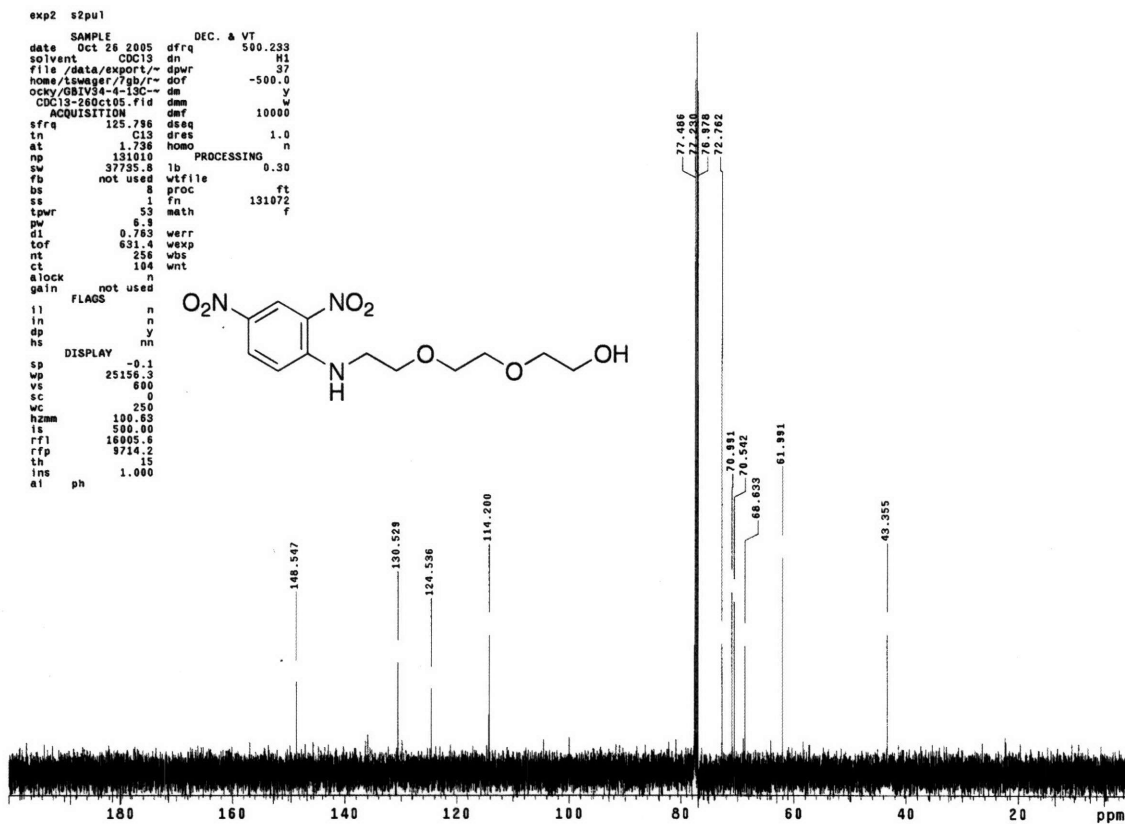
```



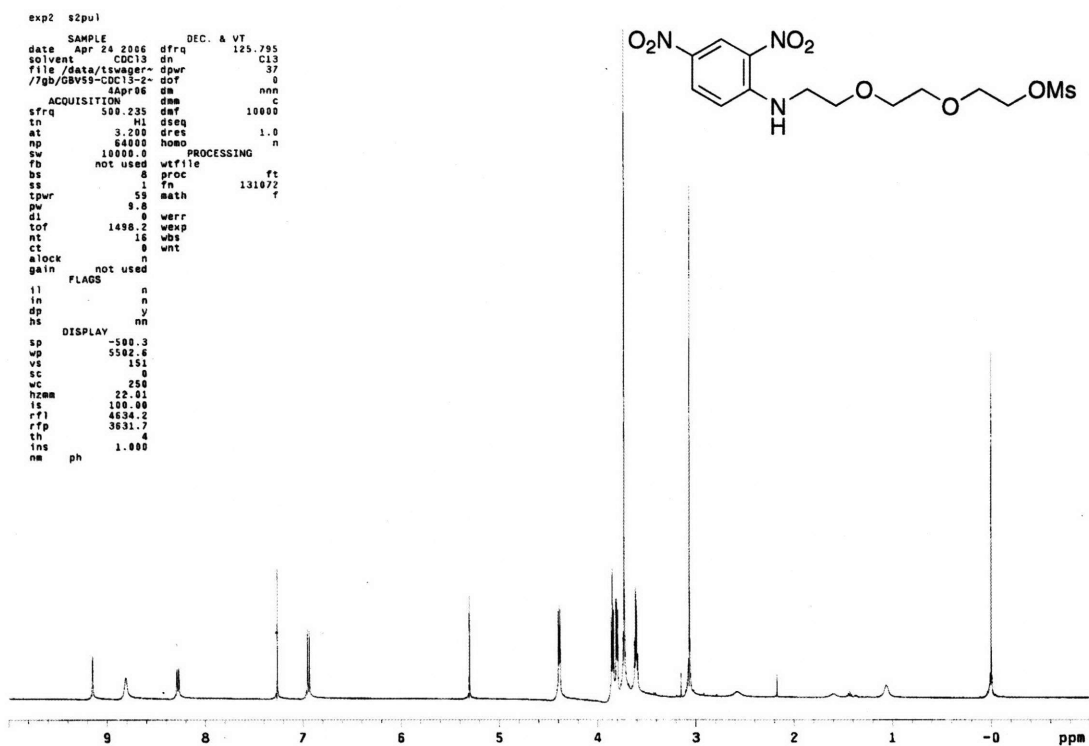
¹³C NMR for **5** (CDCl₃).



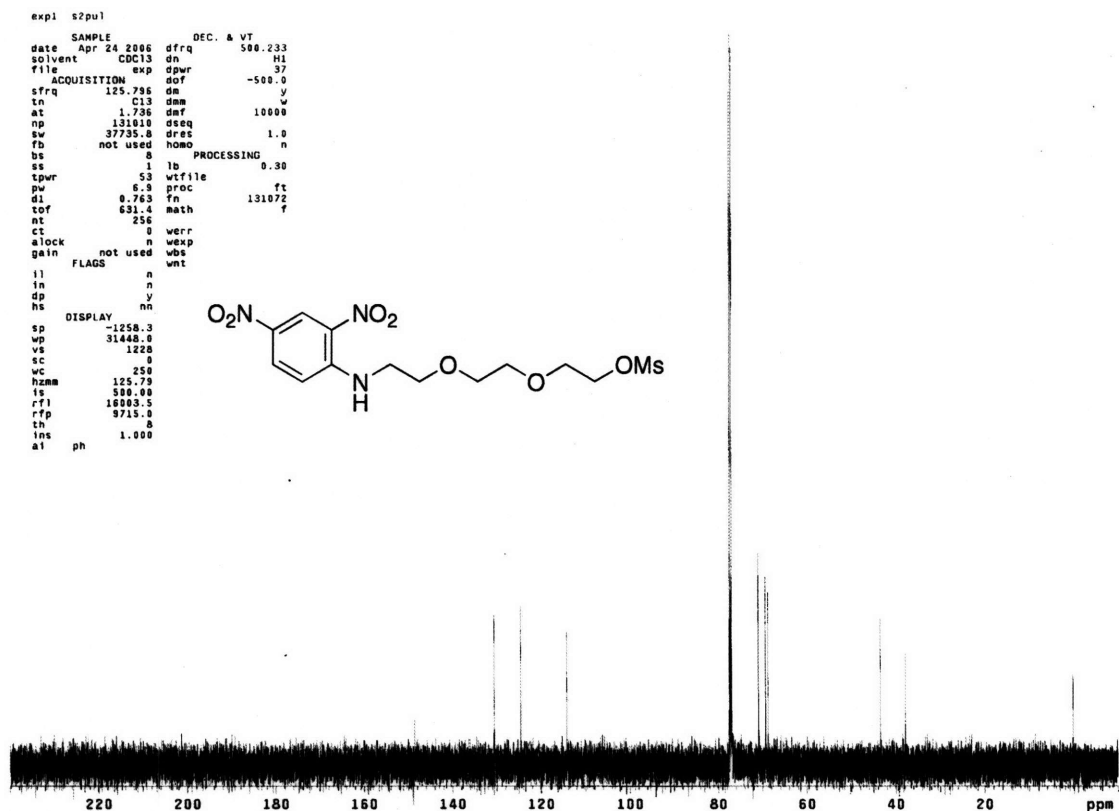
^1H NMR for 6 (CDCl_3).



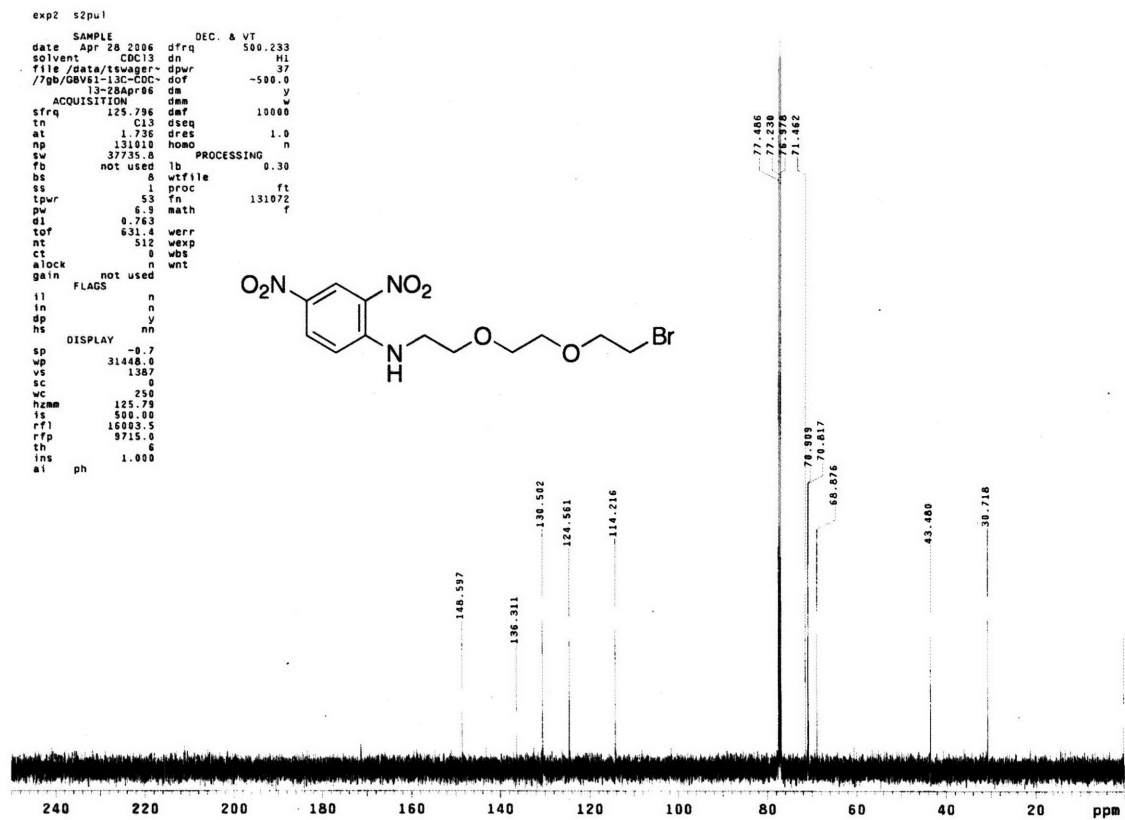
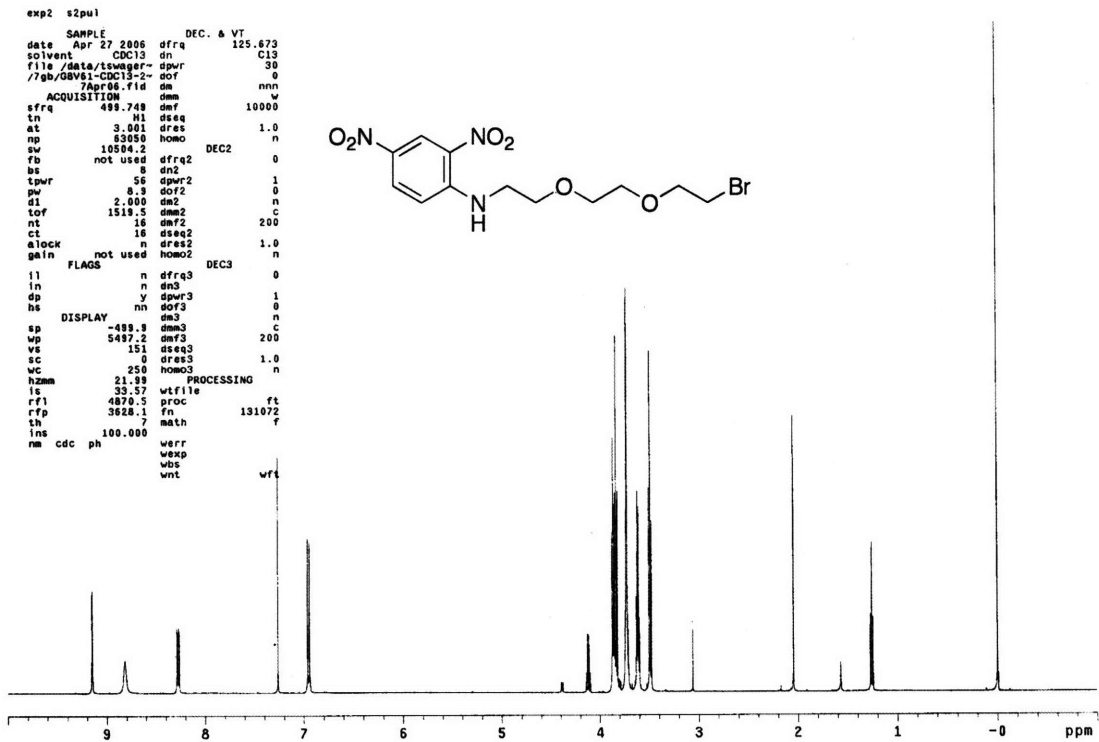
^{13}C NMR for 6 (CDCl_3).

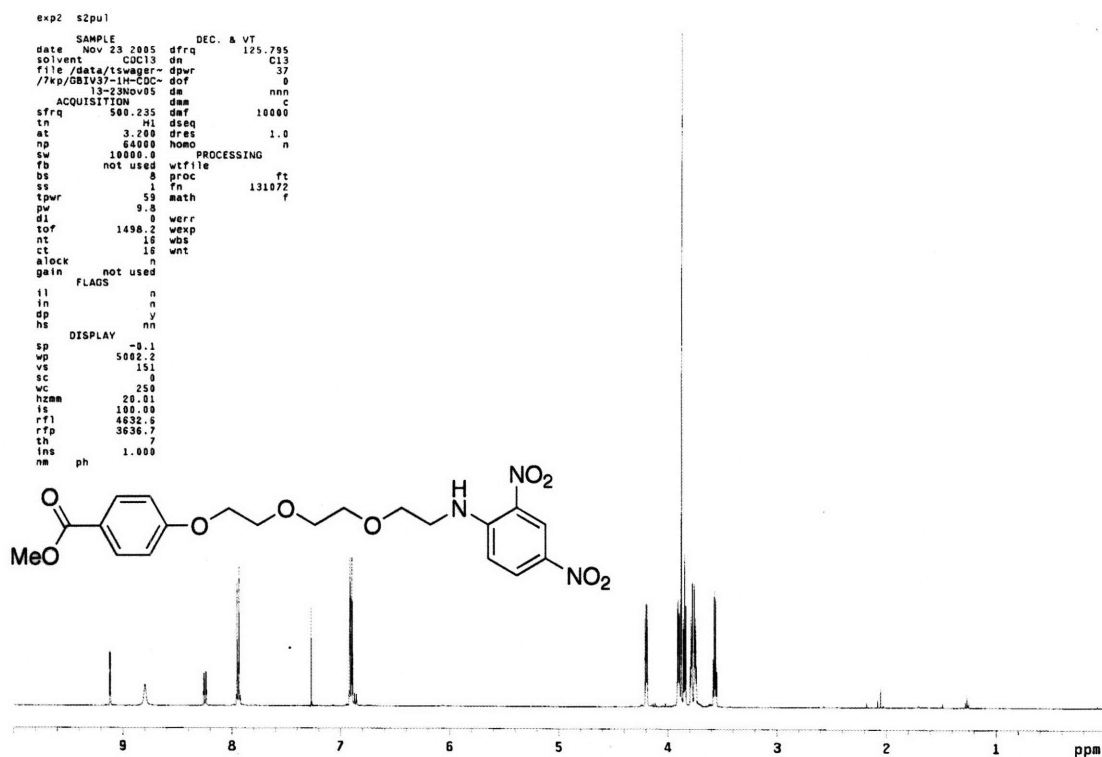


¹H NMR for 7 (CDCl₃).

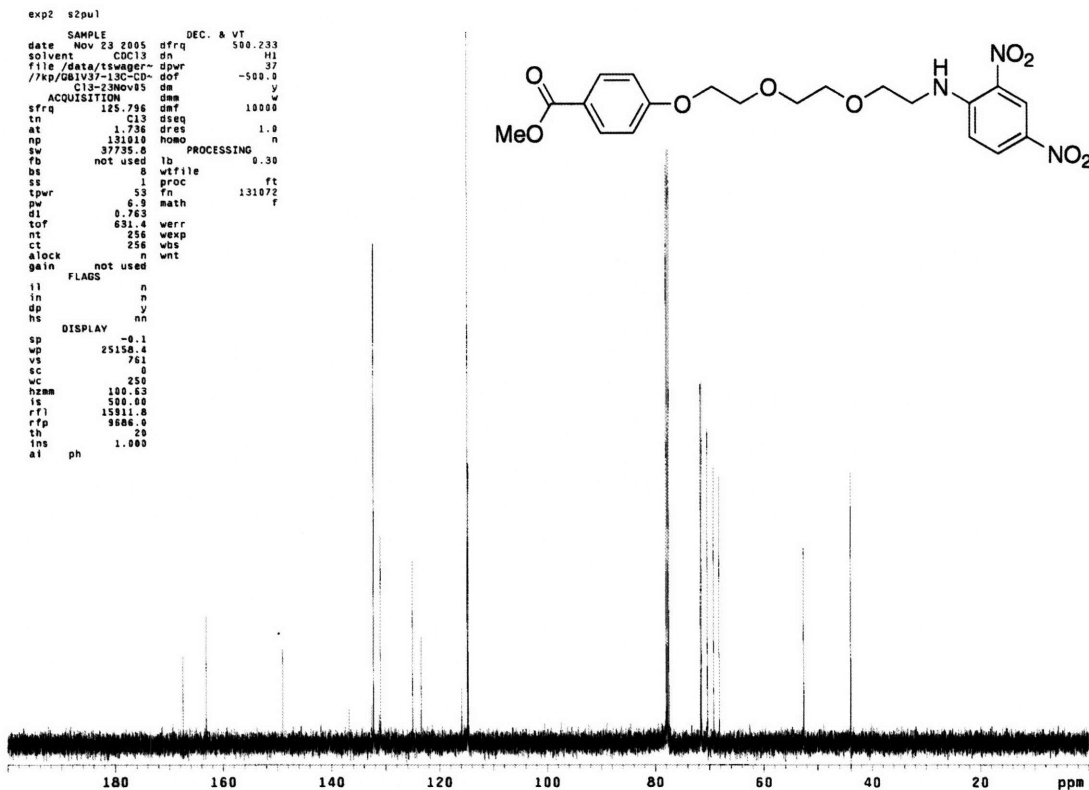


¹³C NMR for 7 (CDCl₃).





¹H NMR for 9 (CDCl₃).

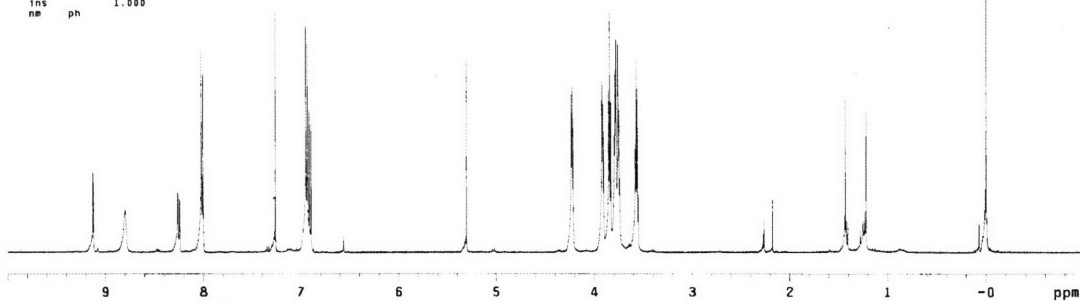
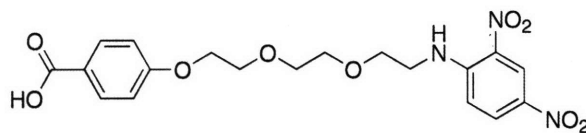


¹³C NMR for 9 (CDCl₃).

```

exp2 s2pul
SAMPLE
date Mar 29 2006 DEC. & VT 125.795
solvent CDC13 dn C13
file /data/tswager~ dpwr 37
//7gb/SBV24-IN=CDC13 dof 0
3-BadShim-29Mar06 dm nnn
ACQUISITION dmm 10000
sfrq 500.235 dmf 10000
tn H1 dseq 1.0
at 3.200 dres 1.0
np 64000 homo n
sw 10000.0 PROCESSING n
fb not used wtf1le ft
bs 0 proc 131072
ss 1 fn 131072
tpwr 9.8 math f
d1 0 werr
tof 1498.2 wexp
nt 16 wbs
ct 16 wnt
alock n
gain not used
FLAGS n
il n
in n
dp y
hs nn
DISPLAY
sp -500.3
wp 5507.4
vs 151
sc 0
wc 250
hzm 22.01
ls 100.00
rf1 4823.2
rfd 3631.7
sh 5
lms 1.000
nm ph

```

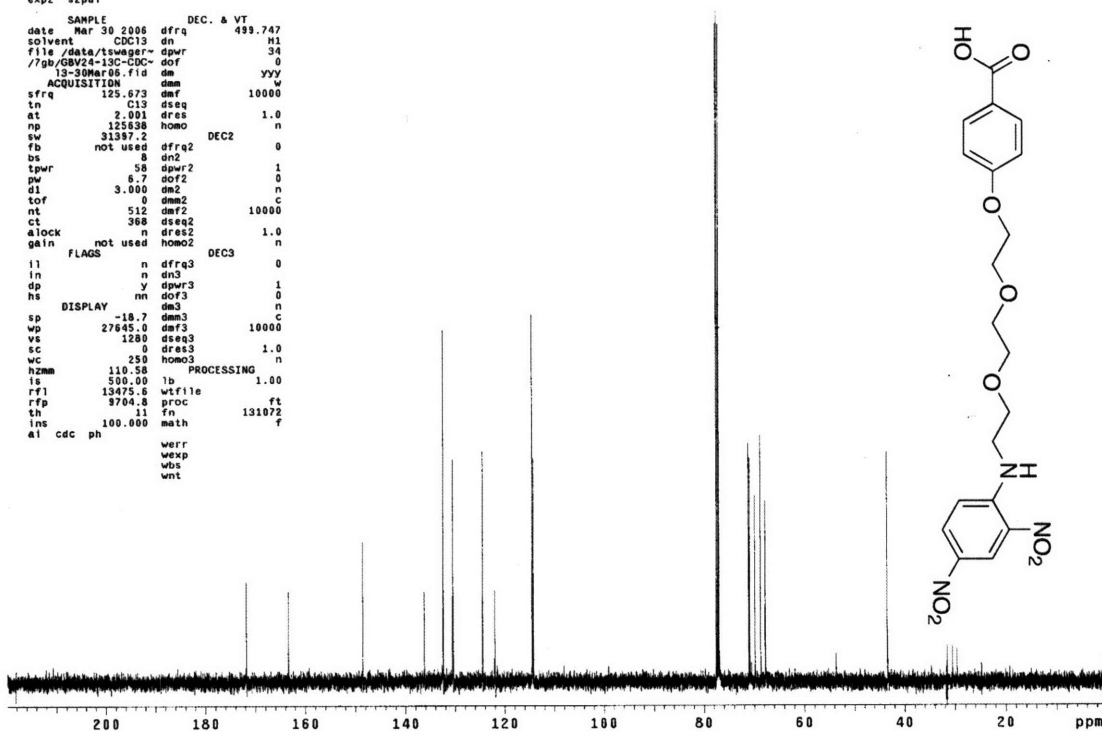
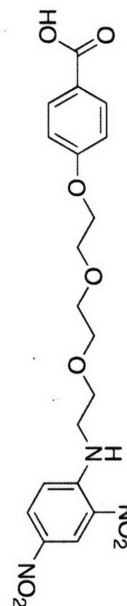


¹H NMR for **10** or **G0** (CDCl₃).

```

exp2 s2pul
SAMPLE
date Mar 30 2006 DEC. & VT 499.747
solvent CDC13 dn H1
file /data/tswager~ dpwr 34
//7gb/SBV24-13C=CDC- dof 0
13-30Mar06.fid dm yyy
ACQUISITION dmm 10000
sfrq 125.673 dmf 10000
tn C13 dseq 1.0
at 2.001 dres 1.0
np 125000 homo n
sw 31397.2 DEC2 0
fb not used dfrq2 0
bs 8 dnt 1
tpwr 58 dpwr2 1
pw 8.7 dof2 0
d1 3.000 dm2 n
tof 0 dmm2 c
nt 512 dmf2 10000
ct 368 dseq2 1.0
alock n dres2 1.0
gain not used homo2 n
FLAGS n dfrq3 0
il n dn3 1
in n dn3 1
dp y dpwr3 1
hs nn dof3 0
DISPLAY dm3 n
sp -18.7 dmm3 c
wp 27645.0 dmf3 10000
vs 1280 dseq3 1.0
sc 0 dres3 n
wc 250 homo3 n
hzm 110.58 PROCESSING 1.00
ls 500.00 lb 1.00
rf1 13475.6 wtf1le ft
rfd 9704.8 proc 131072
sh 1 fn 131072
lms 100.000 math f
al cdc ph
werr
wexp
wbs
wnt

```

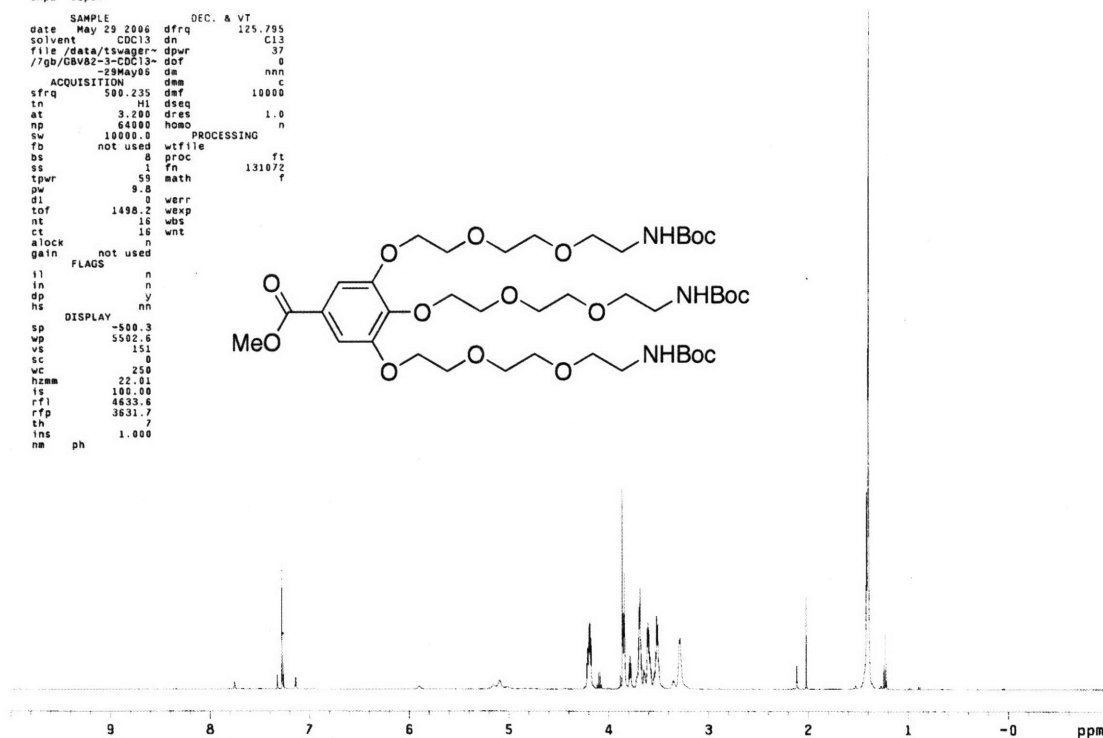
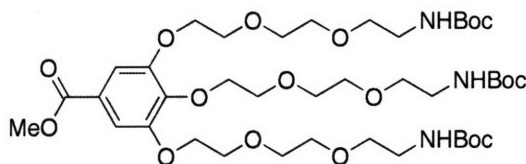


¹³C NMR for **10** or **G0** (CDCl₃).

```

exp2 s2pu1
SAMPLE DEC. & VT
date May 29 2006 dfrq 125.795
solvent CDCl3 dn C13
file /data/tswager- dpwr 37
//gb/GBV82-3-CDCl3- dof 0
-29May06 dm nnn
ACQUISITION ddm C
sfrq 509.235 def 10000
tn H1 dseq
at 3.200 dres 1.0
np 6400 homo n
sw 10000.0 PROCESSING
fb not used wfile ft
bs 8 proc 131072
ss 1 fn f
tpwr 53 math
pw 8.8 werr
d1 0 wexp
tof 1498.2 wbs
nt 16 wnt
ct 16 wnt
alock not used
gain not used
FLAGS
il n
in n
dp y
hs nn
DISPLAY
sp -500.3
wp 5502.6
vs 151
sc 0
wc 250
hzam 22.01
ls 100.00
rfi 4633.6
rfp 3631.7
th 7
ins 1.000
na ph

```

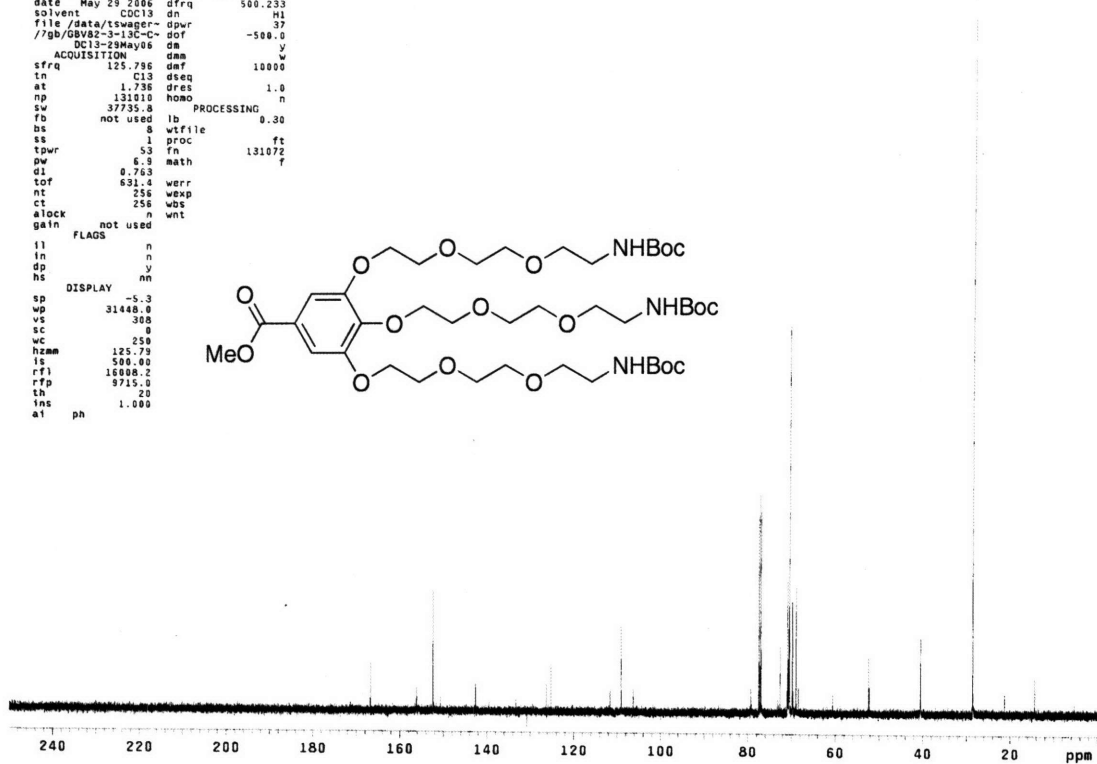
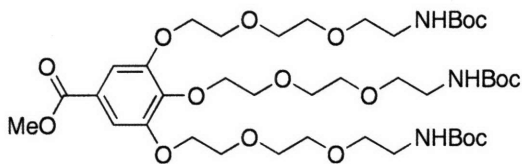


¹H NMR for 11 (CDCl₃).

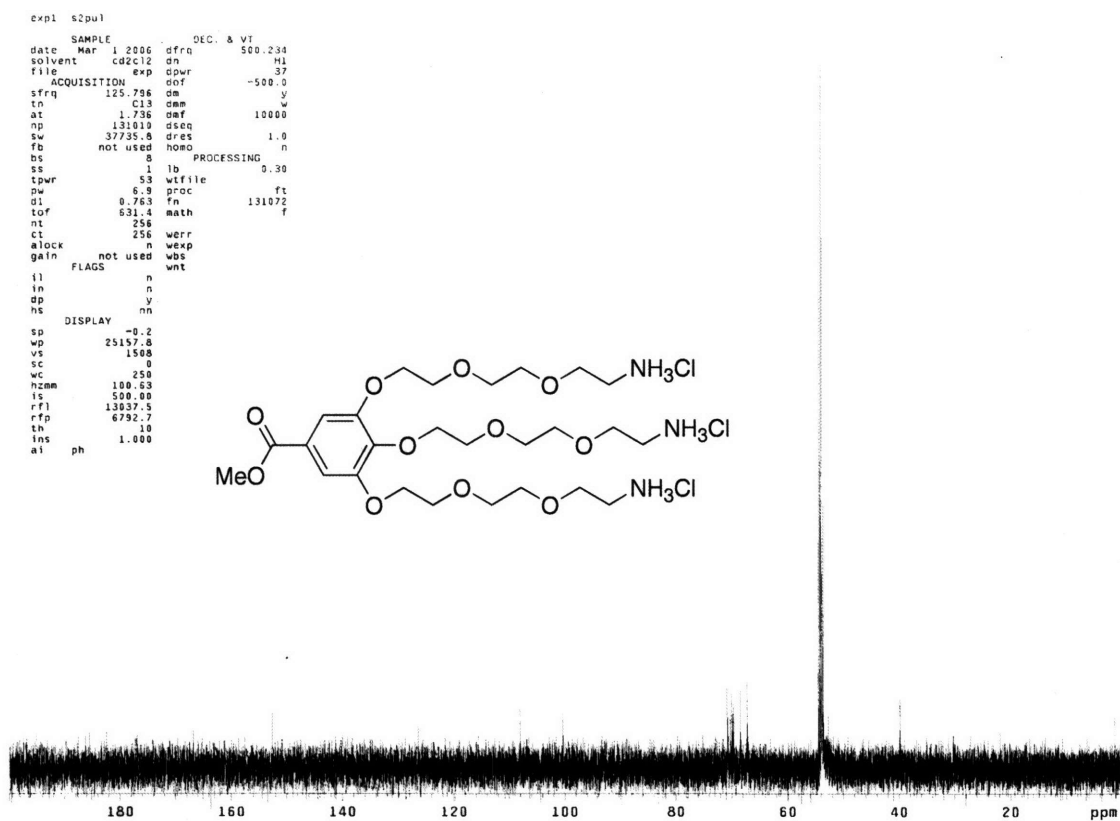
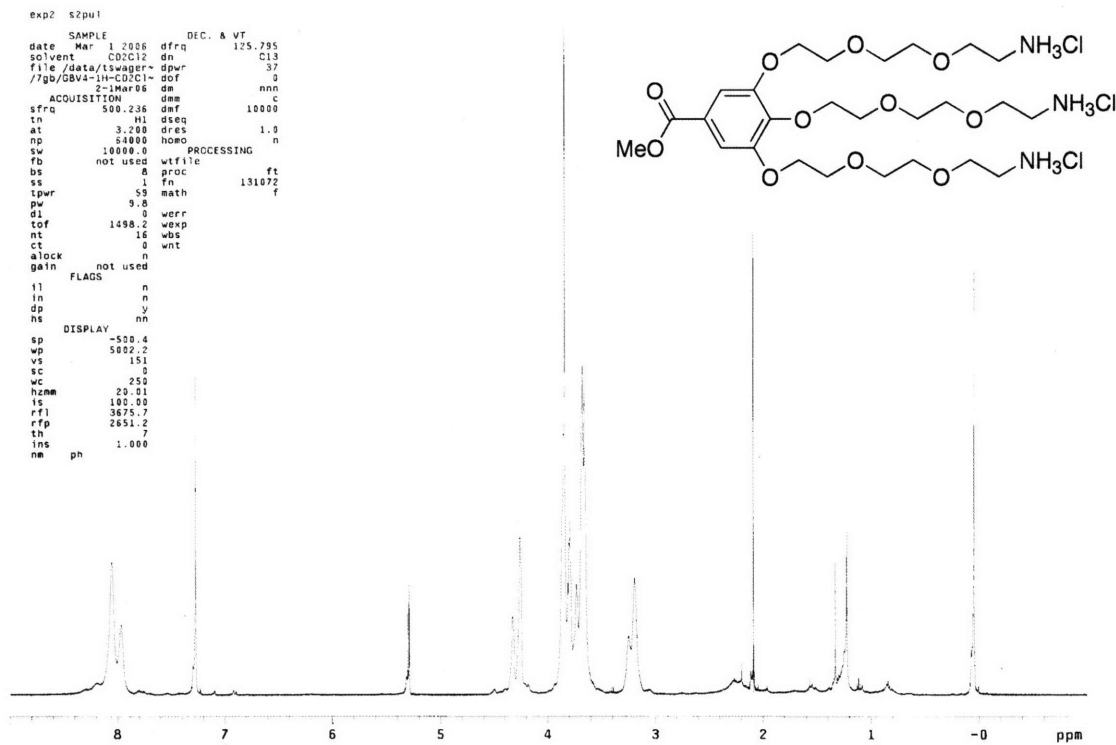
```

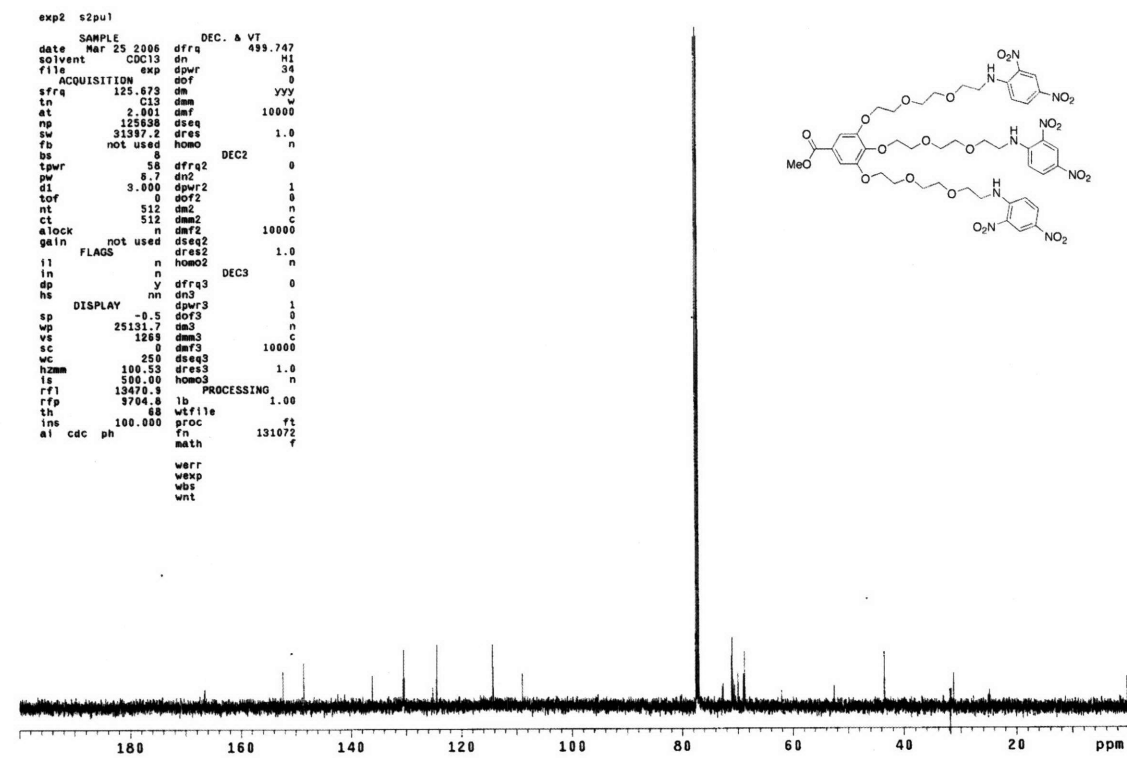
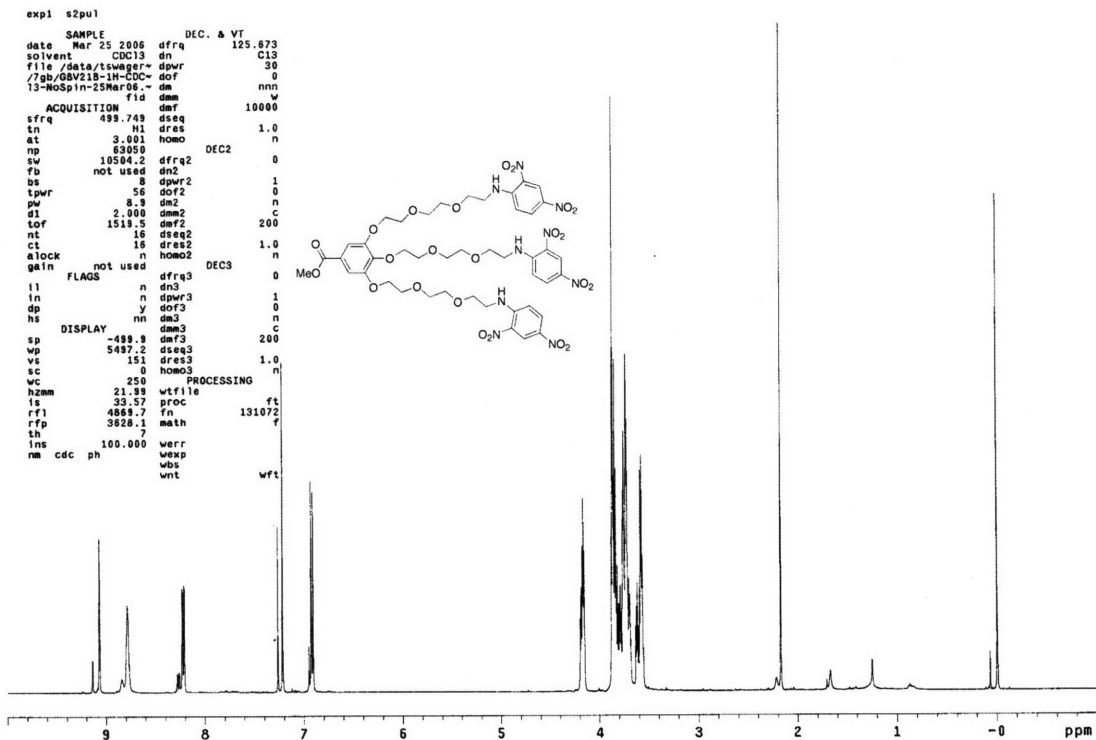
exp2 s2pu1
SAMPLE DEC. & VT
date May 29 2006 dfrq 125.796
solvent CDCl3 dn H1
file /data/tswager- dpwr 37
//gb/GBV82-3-13C- dof -500.0
CDCl3-29May06 dm y
ACQUISITION ddm w
sfrq 125.796 def 10000
tn C13 dseq
at 1.736 dres 1.0
np 131010 homo n
sw 37735.8 PROCESSING
fb not used lb 0.30
bs 8 wfile ft
ss 1 proc 131072
tpwr 53 math
pw 6.8 werr
d1 0.763 wexp
tof 631.4 wbs
nt 256 wnt
ct 256 wnt
alock not used
gain not used
FLAGS
il n
in n
dp y
hs nn
DISPLAY
sp -5.3
wp 31448.0
vs 300
sc 0
wc 250
hzam 125.79
ls 500.00
rfi 16000.2
rfp 9715.0
th 20
ins 1.000
a1 ph

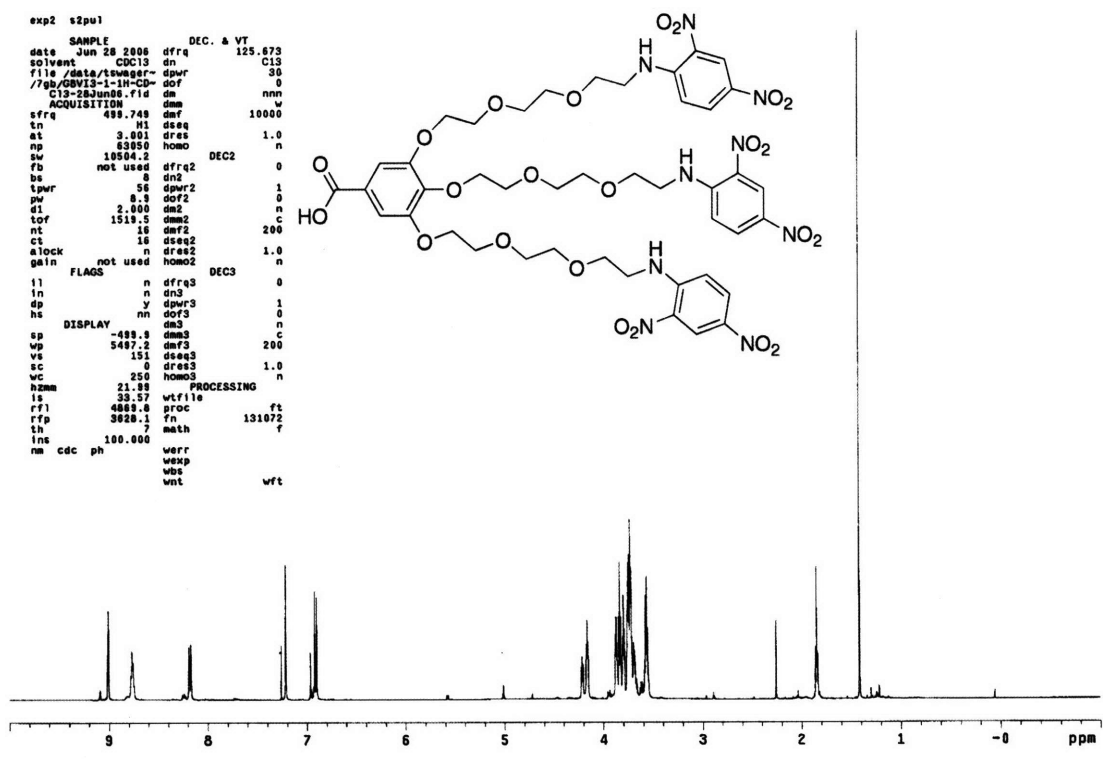
```



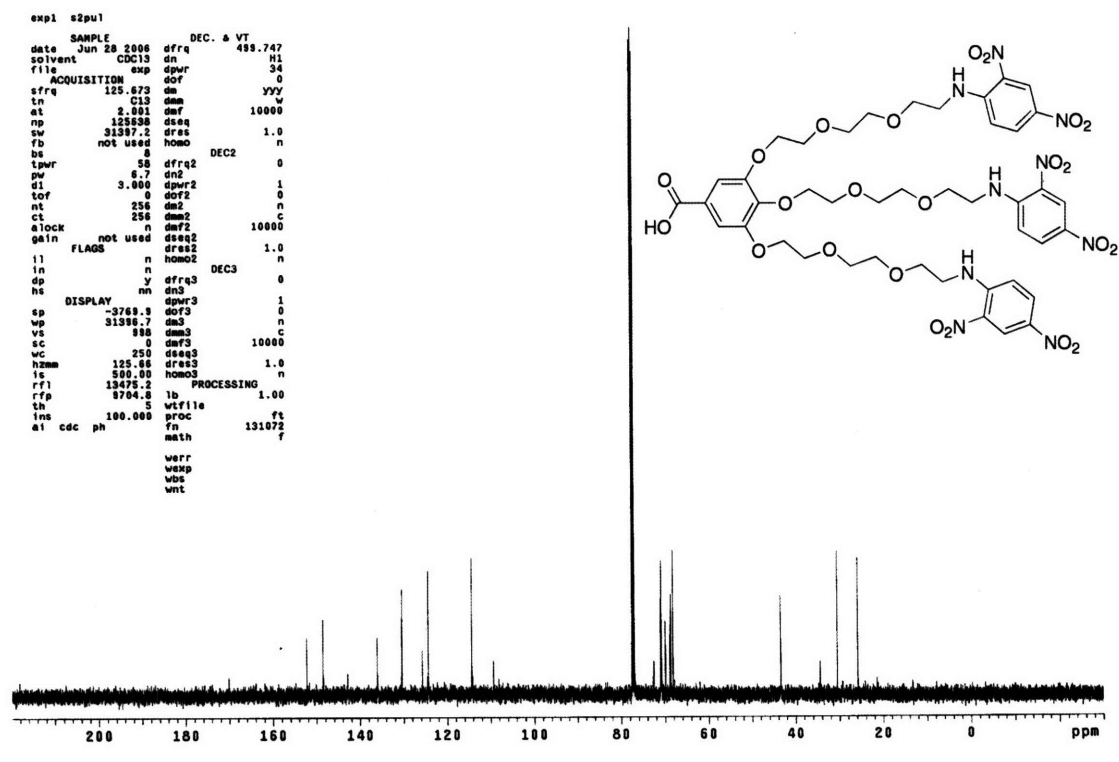
¹³C NMR for 11 (CDCl₃).







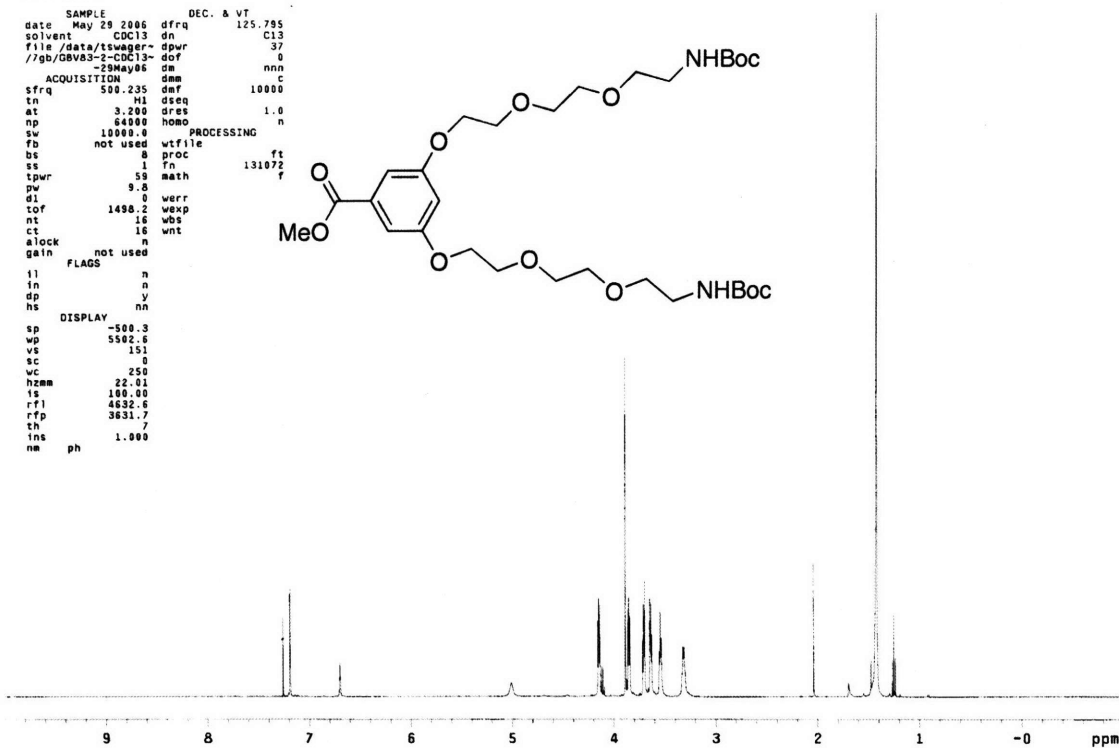
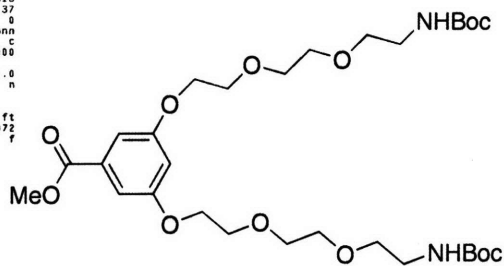
¹H NMR for **14** or **G13** (CD₂Cl₂).



¹³C NMR for **14** or **G13** (CD₂Cl₂).

exp2 s2pu1

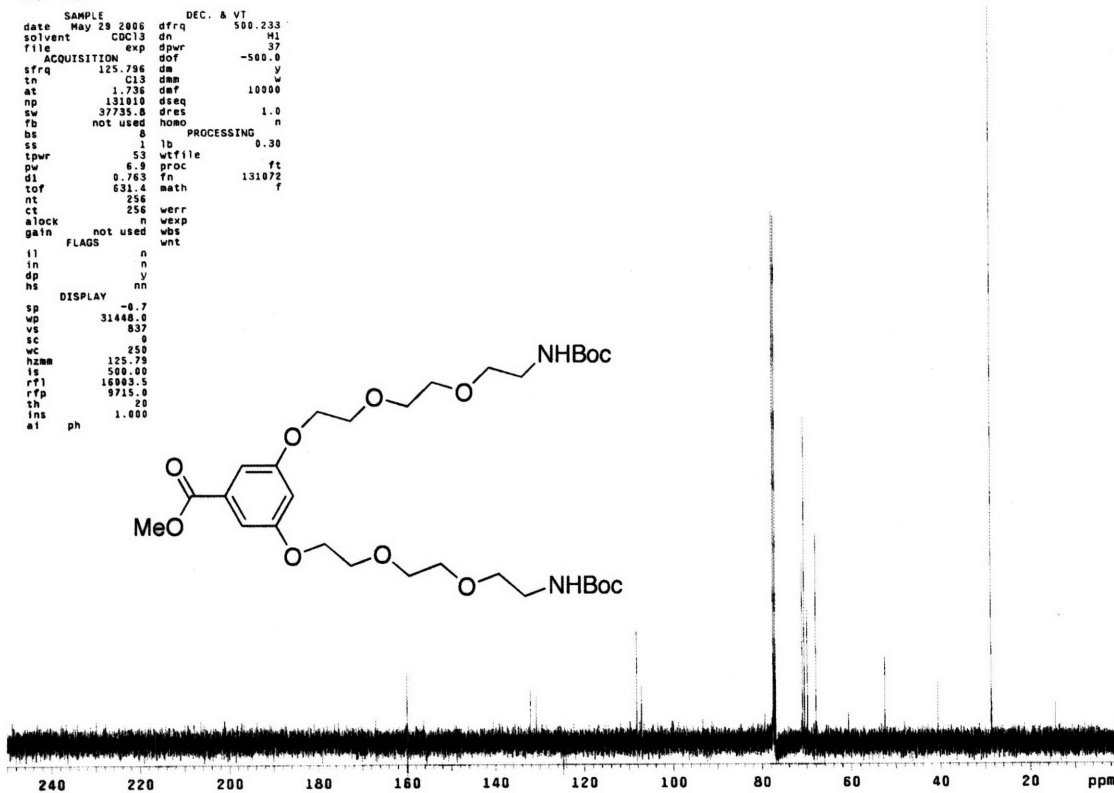
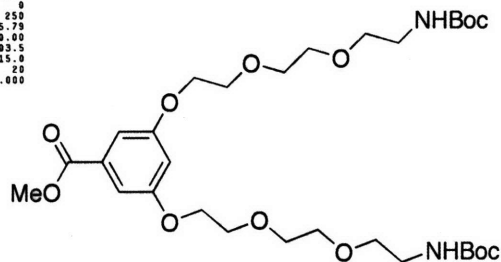
```
SAMPLE DEC. & VT
date May 29 2006 dfrq 125.795
solvent CDCl3 dn C13
file /data/tswager- dpwr 37
//gb/GBW83-2-CDCl3- dof 0
ACQUISITION dmm nnn
sfrq 500.235 dmf 10000
tn H1 dseq 1.0
at 3.200 dres 1.0
np 84800 homo n
sw 10980.9
fb not used
bs 8 proc
ss 1 fn 131072
tpwr 59 math f
pw 9.8
d1 0 werr
tof 1498.2 wexp
nt 16 wbs
ct 16 wnt
alock n
gain not used
FLAGS n
il n
in n
dp y
hs nn
DISPLAY
sp -500.3
wp 5502.6
vs 151
sc 0
wc 250
hzmm 22.01
ls 100.00
rf1 4882.6
rfp 3831.7
th
ins 1.000
ne ph
```



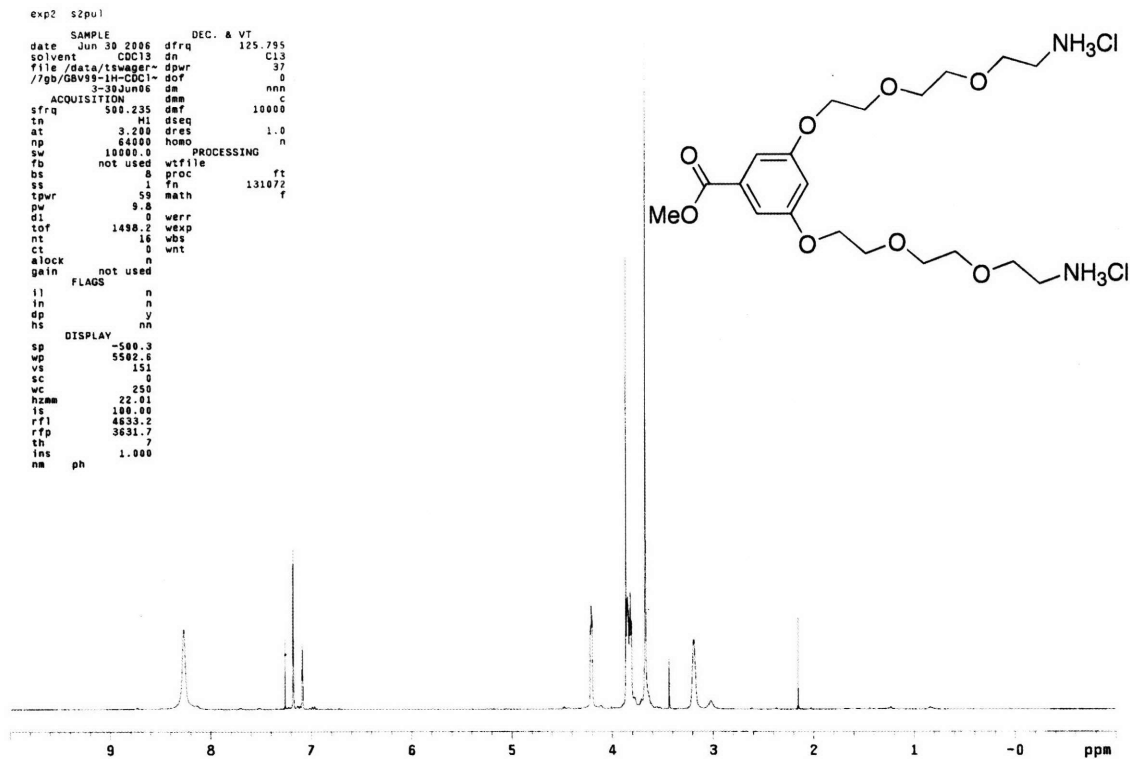
¹H NMR for 15 (CDCl₃).

exp1 s2pu1

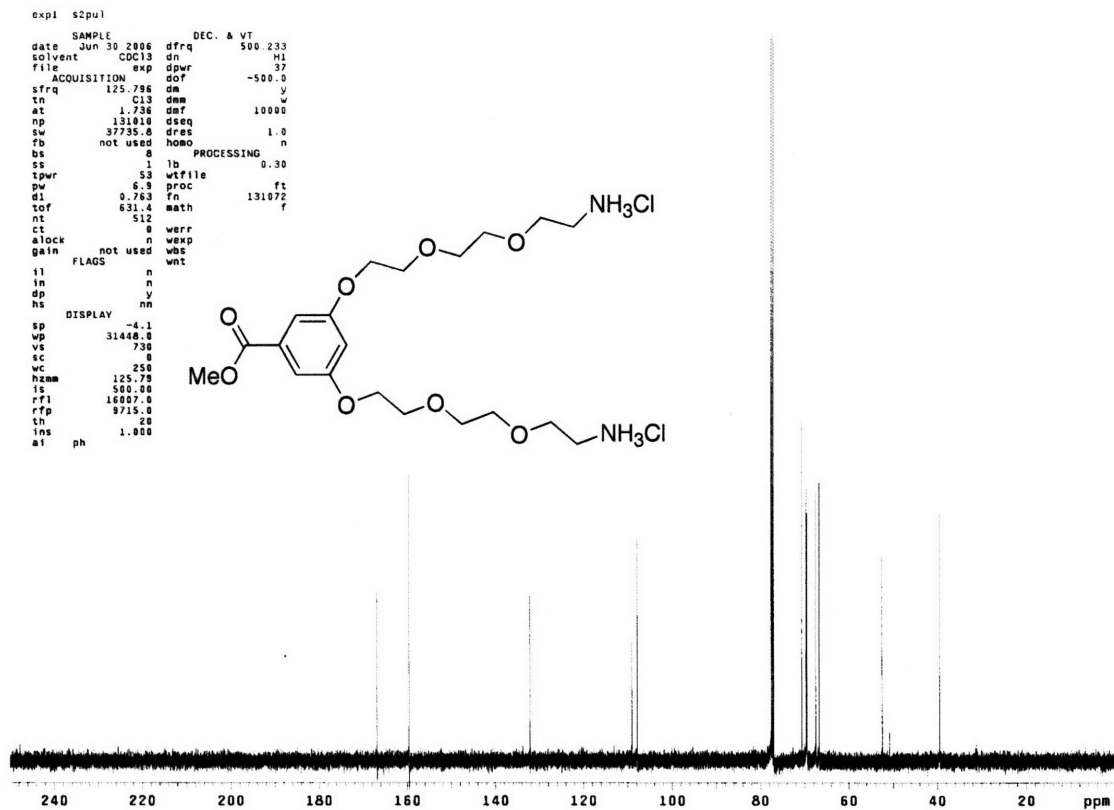
```
SAMPLE DEC. & VT
date May 29 2006 dfrq 125.796
solvent CDCl3 dn M1
file /data/tswager- exp dpwr -500.0
ACQUISITION dof y
sfrq 125.796 da y
tn C13 dmm 10000
at 1.736 dmf 10000
np 131010 dseq 1.0
sw 37735.8 dres 1.0
fb not used homo n
bs 8
ss 1 lb 0.30
tpwr 53 wfile
pw 6.9 proc ft
d1 0.763 fn 131072
tof 631.4 math f
nt 256 werr
ct 256 wexp
alock n
gain not used wbs
gain not used wnt
FLAGS n
il n
in n
dp y
hs nn
DISPLAY
sp -0.7
wp 31448.0
vs 837
sc 0
wc 250
hzmm 125.79
ls 500.00
rf1 10983.5
rfp 9715.0
th 20
ins 1.000
at ph
```



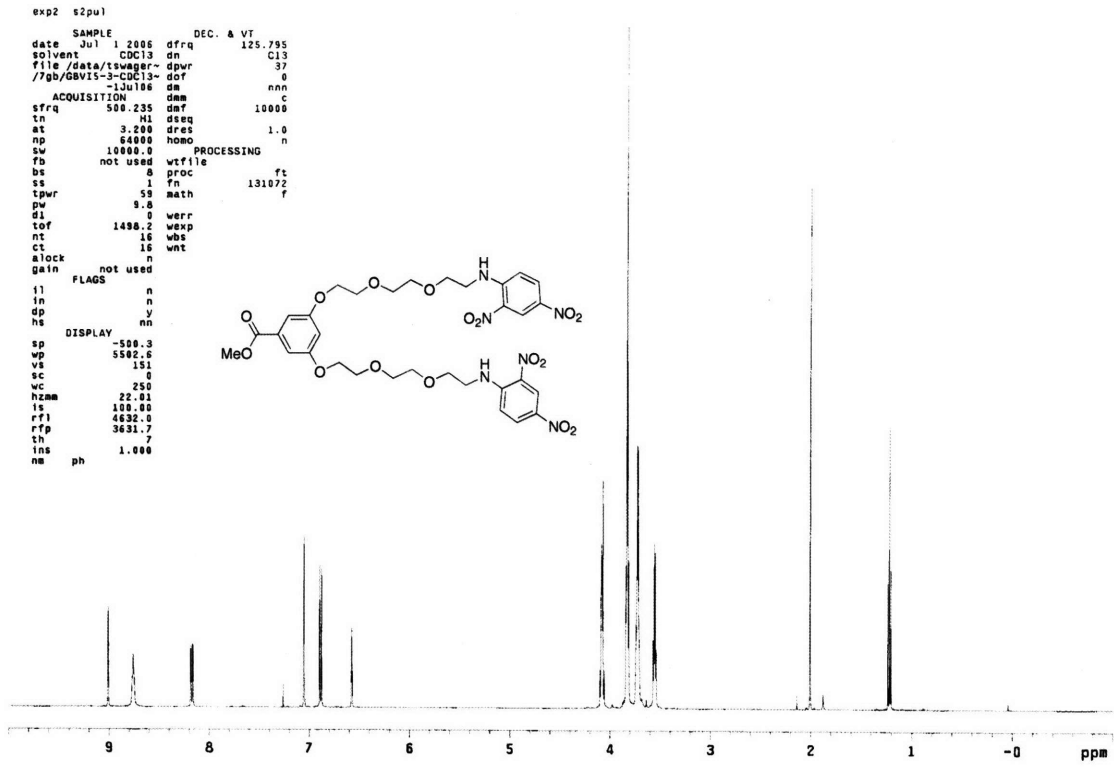
¹³C NMR for 15 (CDCl₃).



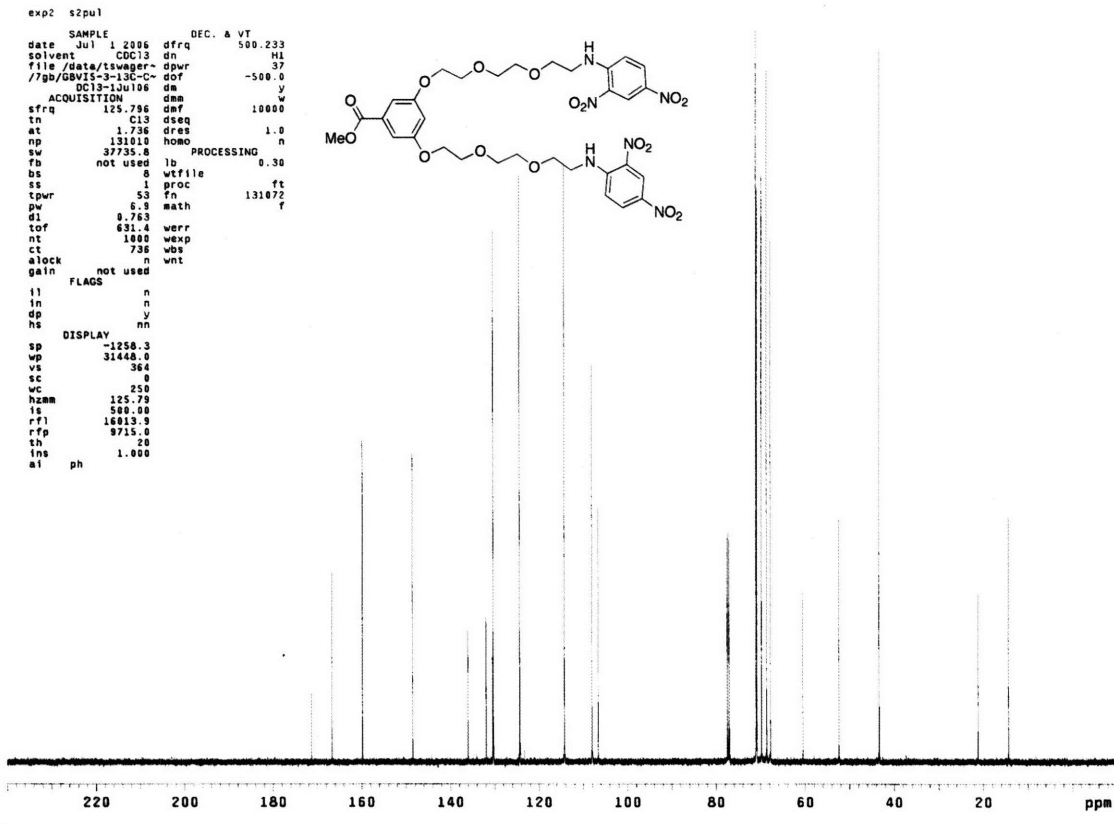
^1H NMR for **16** (CDCl_3).



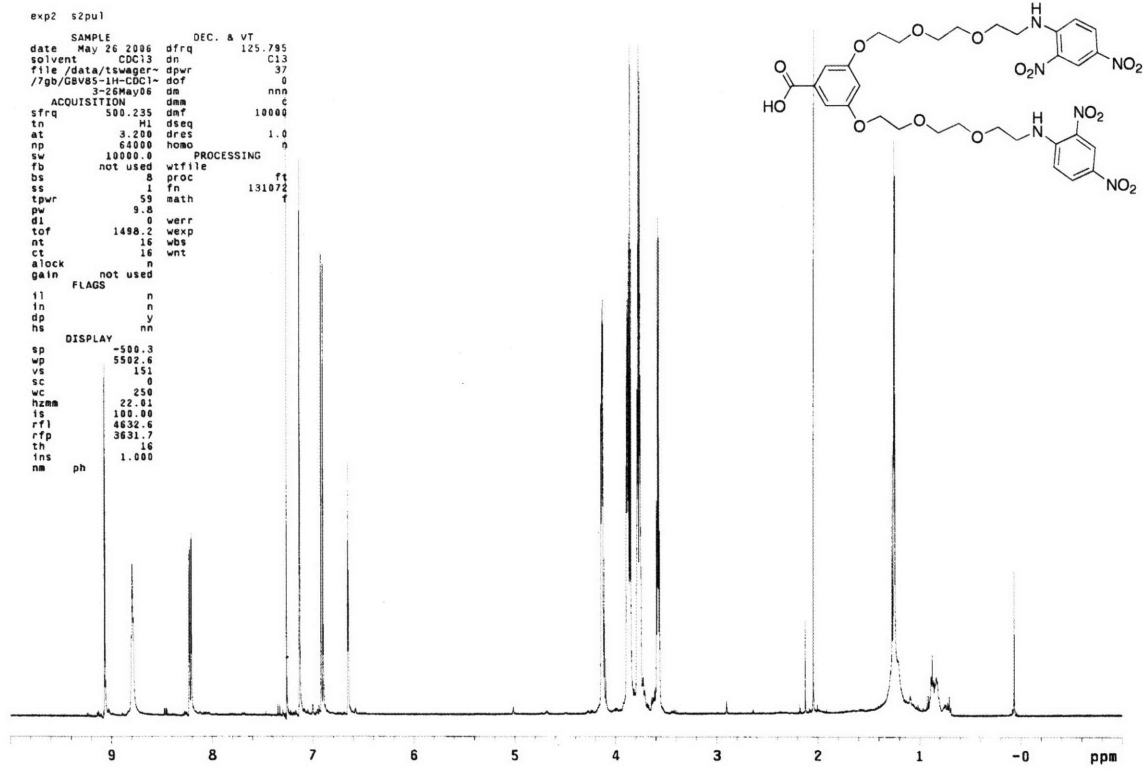
^{13}C NMR for **16** (CDCl_3).



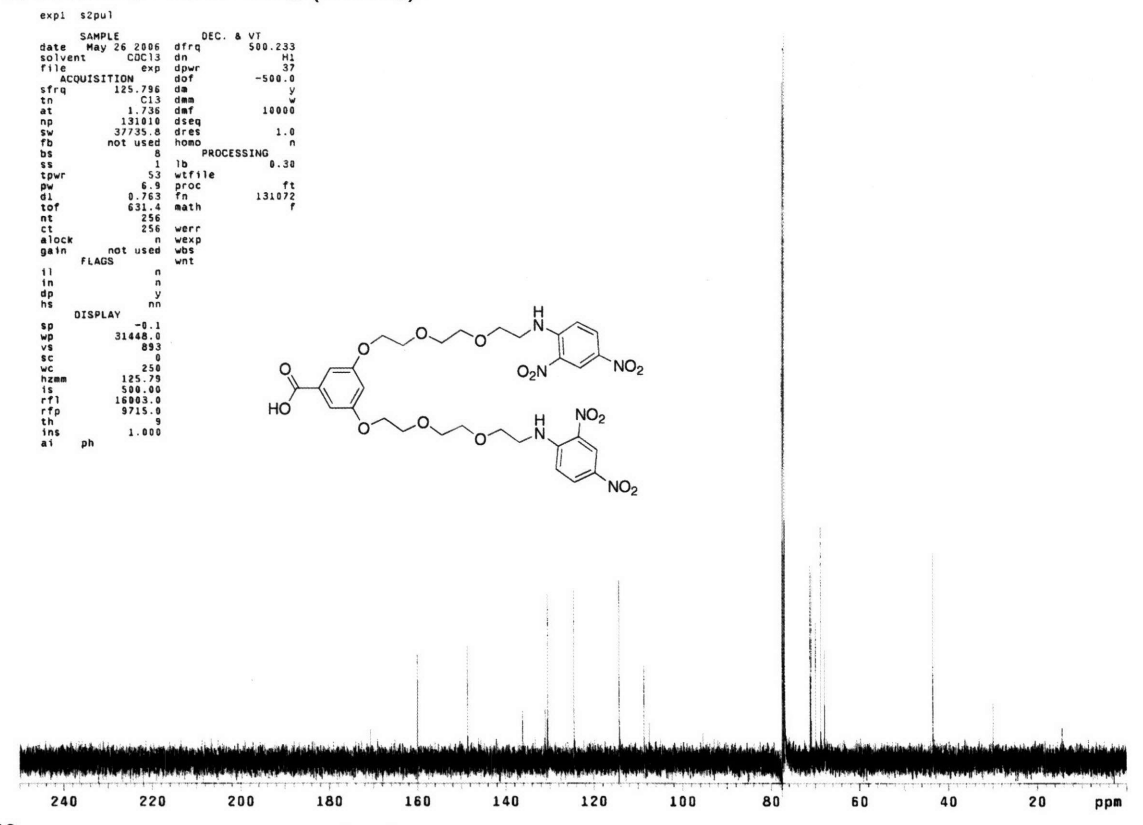
¹H NMR for 17 (CDCl₃).



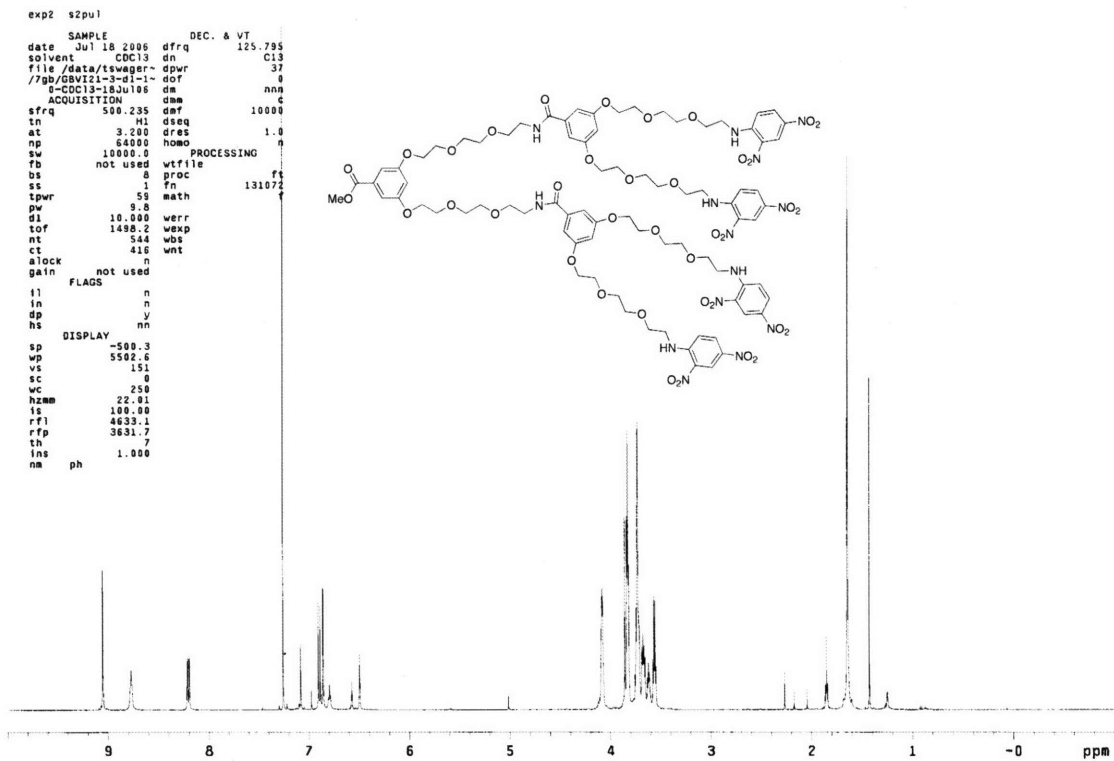
¹³C NMR for 17 (CDCl₃).



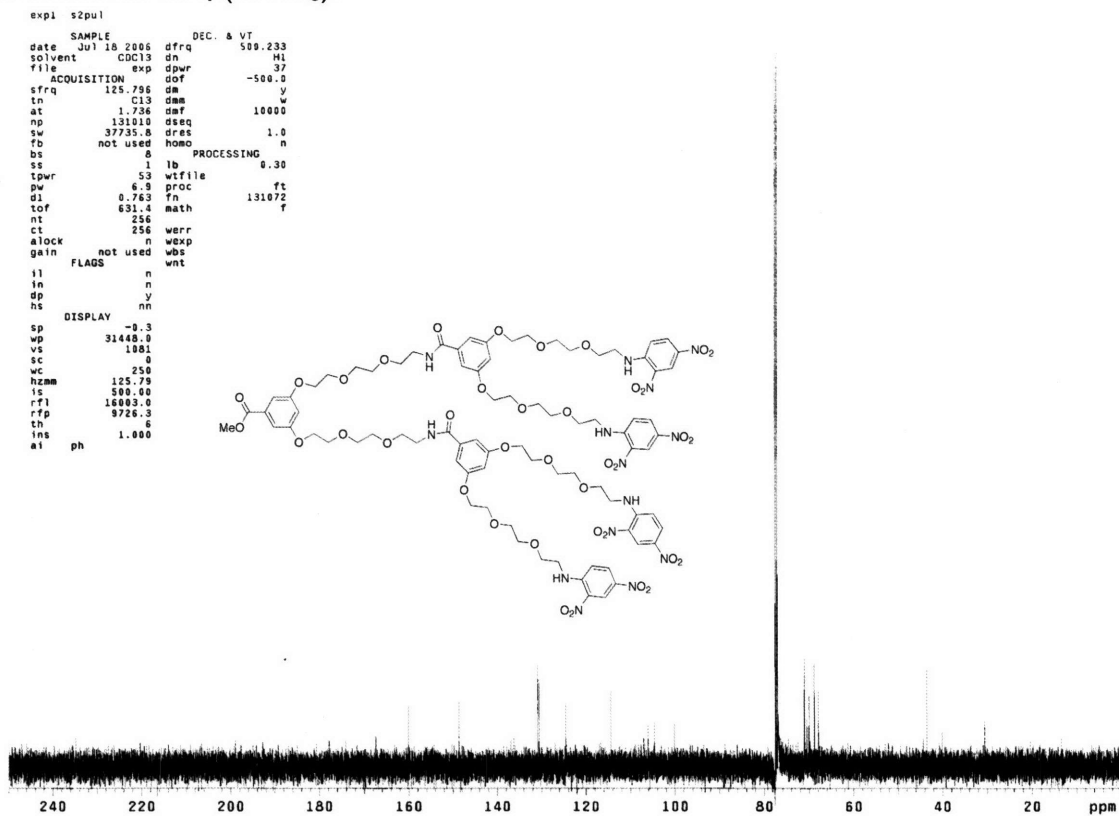
¹H NMR for **18** or **G1₂** (CDCl₃).



¹³C NMR for **18** or **G1₂** (CDCl₃).



^1H NMR for **G₂₄** (CDCl_3).



^{13}C NMR for **G₂₄** (CDCl_3).